Model Based Study on the Dynamics of Coral Reef Ecosystem with Special Emphasis in Disease and its Control

Thesis
submitted for the award of the degree of

Doctor of Philosophy
in Science

by
Buddhadev Ranjit

Under the supervision of
Dr. Santosh Biswas

Centre for Mathematical Biology and Ecology
Department of Mathematics
Jadavpur University
Kolkata-700032, India
July, 2025

Declaration

I, Buddhadev Ranjit, hereby declare that this thesis is the result of my original research conducted after my Ph.D. registration at Jadavpur University. It has not been submitted previously for any degree, diploma, or academic credential.

Buddhadev Ranjit, 01/07/2025

Buddhadev Ranjit

যাদবপুর বিশ্ববিদ্যালয়

FACULTY OF SCIENCE
DEPARTMENT OF MATHEMATICS

JADAVPUR UNIVERSITY
Kolkata-700 032, India
Telephone : 91 (33) 2414 6717

CERTIFICATE FROM THE SUPERVISOR

This is to certify that the thesis entitled " **Model Based Study on the Dynamics of Coral Reef Ecosystem with Special Emphasis in Disease and its Control** " Submitted by Buddhadev Ranjit who got his name registered on 12th October 2020 (Registration No. SMATH1202920, Index No. 29/20/MATHS./27) for the award of Ph. D. (Science) Degree of Jadavpur University, is absolutely based upon his own work under the supervision of Dr. Santosh Biswas and that neither this thesis nor any part of it has been submitted for either any degree / diploma or any other academic award anywhere before.

01.07.25

.....

Dr. Santosh Biswas
Associate Professor
Department of Mathematics
Jadavpur University
188, Raja S.C Mullick Road,
Kolkata – 700032, India

Dr. Santosh Biswas
Associate Professor
Department of Mathematics
Jadavpur University
Kolkata – 700 032, West Bengal

This thesis is dedicated to my parents

Kanailal Ranjit & Sumitra Ranjit

Acknowledgement

I express my deepest gratitude to my Ph.D. supervisor, Dr. Santosh Biswas (Department of Mathematics, Jadavpur University), Prof. Joydev Chattopadhyay (Agricultural and Ecological Research Unit, ISI, Kolkata), and Dr. Joydeb Bhattacharyya (Department of Mathematics, Karimpur Pannadevi College) for their invaluable mentorship. Their unwavering dedication to mathematics, disciplined work ethic, and profound guidance have been a source of inspiration since the inception of my research. Their insightful advice, meticulous review of complex concepts, and constant support—both academically and personally—were instrumental in shaping this thesis.

I extend my sincere appreciation to my RAC expert, Prof. Nandadulal Bairagi, for his steadfast encouragement in my research endeavors. I am also deeply grateful to the Center for Mathematical Biology and Ecology, Department of Mathematics, Jadavpur University, the Bio-Mathematical Society of India, and my esteemed teachers at Jadavpur University for their intellectual guidance and encouragement. Additionally, I acknowledge the Council of Scientific and Industrial Research (CSIR), Government of India, for its generous financial support through a Research Fellowship, which has been crucial in facilitating my research.

I am thankful to Arnab Chattopadhyay, Dr. Arindam Mandal, Amit Samadder, Sujit Halder, Dr. Sudip Samanta, and Dr. Santanu Biswas for their invaluable assistance. My heartfelt appreciation also goes to my fellow researchers and collaborators Dr. Mrinmoy Sardar, Dr. Saddam Mollah, Purnendu Sardar, Raktim Kar, Sudipta Panda, Richik Bandyopadhyay, Kaushik Kayal, Sagar Karmakar and Md Kausar Sk whose support and encouragement have been indispensable.

Furthermore, I extend my gratitude to everyone who has contributed to my journey, even if not mentioned individually. Finally, my deepest thanks go to my wife, Jaysree Kayal, whose unwavering support and patience have been the cornerstone of my progress. Her belief in me has transformed my journey from uncertainty to achievement.

Contents

1 Introduction

1.1 Introduction and Overview

Coral reefs are vital to both global biodiversity [1–3] and economies [4–6], often referred to as "the rainforests of the sea" due to their crucial role in supporting diverse ecosystems [7, 8]. These ecosystems are among the most biologically diverse on Earth, despite covering less than 1% of the ocean floor [9–11]. Coral reefs support approximately 25% of all marine species, including fish, mollusks, crustaceans, and both vertebrates and invertebrates [1, 12–15]. As such, they are critical habitats that contribute to global biodiversity. Economically, coral reefs are invaluable assets, directly benefiting over 100 countries, especially in tropical regions. They are central to industries such as tourism, fisheries, and coastal protection, generating an estimated 375 billion annually in goods and services [16–20]. Coral reefs attract millions of tourists each year, who visit for activities like snorkeling and diving. They also sustain fisheries that provide food and livelihoods for millions of people and protect coastlines from erosion and storm damage [21–23]. Additionally, coral reefs play a role in carbon sequestration and hold potential for future medical discoveries, further emphasizing their economic importance [24–26]. The conservation of coral reefs is essential for preserving both ecological balance and economic stability. Given their critical role, our focus on developing a mathematical model for understanding and protecting coral reefs is of utmost importance.

1.2 Coral Reefs and Associated Biology

Corals are marine invertebrates that belong to the class *Anthozoa* of the *phylum Cnidaria*. These stationary organisms, commonly known as polyps, depend on a symbiotic relationship with tiny algae called zooxanthellae, a type of phytoplankton. Zooxanthellae live within the coral's tissue, exchanging nutrients and essential molecules to sustain both organisms. In addition to this symbiosis, corals feed on zooplankton [27–30]. Their tentacles, equipped with stinging cells called cnidocytes, capture and immobilizeprey [31, 32]. The tentacles then guide the zooplankton to the coral's mouth, where it is ingested and digested in the gastrovascular cavity [33]. Coral reefs are formed by thousands of polyps clustering together, creating ecosystems that are among the most diverse on Earth. Found in shallow, warm waters of tropical and subtropical regions, coral reefs provide habitats for a vast array of marine species, fostering biodiversity and ecological stability. Beyond corals, other organisms such as macroalgae and turf algae interact with the reef environment. In healthy ecosystems, corals typically dominate. However, disturbances like overfishing, pollution, and climate change can upset this balance, allowing macroalgae and turf algae to overgrow and compete with corals for space, light, and nutrients. This competition disrupts the delicate equilibrium of reef ecosystems, reducing coral cover and biodiversity.

- **Macroalgae:** Macroalgae, commonly known as seaweeds, are multicellular autotrophs classified into three groups based on their color: green (*Chlorophyta*), red (*Rhodophyta*), and brown (*Phaeophyta*). They play a crucial role in marine ecosystems by supporting benthic animal communities and serving as bioindicators for water quality. Seaweed farming involves harvesting wild seaweeds or cultivating them in onshore and nearshore environments, but onshore cultivation often conflicts with other coastal activities. Offshore cultivation has been explored as a sustainable alternative for biofuel and feed production, requiring careful selection of species and site conditions. With a global market value of approximately USD 6 billion, around 10 species are intensively cultivated, with Saccharina Japonica being the most dominant, followed by Kappaphycus alvarezii and several others.

- **Turf algae:** Turf algae are dense, filamentous, and short-growing algae that form a mat-like layer over hard substrates in marine environments. They are a mixed assemblage of small algal species, including filamentous red, green, and brown algae, as well as cyanobacteria. Turf algae play an important ecological role by providing habitat and food for various marine organisms, but they can also compete with corals for space and resources. Their overgrowth is often associated with environmental disturbances such as nutrient enrichment, overfishing, and coral degradation. In degraded reef systems, turf algae can dominate, hindering coral recovery and altering ecosystem dynamics.

- **Phytoplankton:** Phytoplankton are microscopic, photosynthetic organisms that drift in aquatic environments, forming the base of the marine and freshwater food web. They include a diverse group of organisms such as cyanobacteria, diatoms, dinoflagellates, and green algae. As primary producers, they convert sunlight into energy through photosynthesis, producing oxygen and supporting marine life. Their abundance and composition are influenced by factors like light, nutrients, temperature, and water movement. Phytoplankton play a crucial role in global carbon cycling and are key indicators of water quality and ecosystem health.

- **Zooplankton:** Zooplankton are small, heterotrophic organisms that drift in aquatic environments and serve as a crucial link in the marine and freshwater food web. They include a diverse range of animals such as protozoans, crustaceans (e.g., copepods and krill), and the larval stages of fish and invertebrates. Zooplankton primarily feed on phytoplankton and other microscopic organisms, transferring energy up the food chain to larger predators. Their distribution and abundance are influenced by environmental factors such as temperature, salinity, and nutrient availability. Zooplankton play a vital role in nutrient cycling, carbon sequestration, and maintaining ecosystem balance.

1.3 Threats on Coral Reefs Ecosystem

Coral reef ecosystems, among the most biologically diverse habitats on Earth, are increasingly threatened by a range of interlinked factors, primarily driven by human activities and environmental changes [16, 34–40]. Climate change is one of the most significant threats, manifesting through rising sea temperatures, ocean acidification, and coral bleaching [41–49]. As global temperatures rise due to greenhouse gas emissions [50–52], coral bleaching occurs when corals expel the symbiotic algae (*zooxanthellae*) that provide energy and vibrant coloration [53]. This leaves corals weakened, white, and vulnerable to disease. Ocean acidification, caused by the absorption of excess atmospheric CO_2, further exacerbates the problem by reducing the availability of calcium carbonate needed for corals to build and maintain their skeletons, hindering reef growth and resilience [54–56]. In addition to climate change, pollution poses a serious threat to coral reefs [57–59]. Agricultural runoff introduces excess nutrients into marine environments, promoting algal blooms that outcompete corals for sunlight and oxygen [60–65]. Sedimentation from deforestation, mining, and coastal development smothers reefs and reduces light penetration, which is vital for photosynthesis [66, 67]. Furthermore, marine debris, especially plastics, physically damages coral structures and introduces toxins that harm marine organisms [68–72]. Overfishing and unsustainable practices compound these challenges by disrupting the ecological balance of reef ecosystems [57, 73–75]. The depletion of herbivorous fish, such as

parrotfish and sea urchins, allows algae to overgrow, smothering coral colonies [76–79]. Destructive fishing methods, including dynamite and cyanide fishing, physically damage coral structures and decimate populations of reef-dependent species [80, 81]. Coastal development amplifies these threats, as land reclamation, dredging, and construction increase sedimentation and pollution in reef areas [82–84]. Human activities related to tourism, such as careless anchoring, snorkeling, and diving, contribute to physical damage that breaks coral structures and disrupts habitats [85, 86]. The introduction of invasive species further jeopardizes coral reefs [87–90]. Predators like the crown-of-thorns starfish (*Acanthaster planci*) can decimate coral populations when their numbers are unchecked, often due to the absence of natural predators and human disruptions to the ecosystem [57, 91]. Natural events, such as hurricanes and cyclones, can physically destroy reefs, but their frequency and intensity are increasing due to climate change, leading to greater damage over time [57, 92–94].

Finally, coral disease plays a crucial role as one of the most significant threats to the survival of coral reefs on Earth [95–97]. Coral disease is an abnormal condition of coral reefs that interrupts organism function linked with specific symptoms and signs. White Plague Disease (WPD), White Band Disease (WBD), and Black Band Disease (BBD) are among the most significant diseases impacting coral reef ecosystems, as highlighted by various studies [98–106]. The spread of these diseases is driven by diverse microbial communities that damage coral tissues, disrupt the symbiotic relationship between corals and their *zooxanthellae* (photosynthetic algae critical for coral metabolism), create unfavorable chemical environments, and ultimately contribute to coral bleaching [103, 105, 107–110].

The spread of diseases in coral reefs occurs through two main mechanisms: direct and indirect transmission [111, 112]. Direct transmission involves physical contact between infected and healthy corals, though this is less common due to the immobile nature of corals. Conversely, indirect transmission, particularly through pathogens (bacteria, viruses, fungi, and protozoa, etc), is a more efficient method in coral reef outbreaks. Ocean currents are instrumental in this process, enabling free-living pathogens to travel across vast ocean distances [113]. This indirect form of pathogen transfer is known as waterborne transmission [114]. A more critical pathway, however, is vector-borne transmission, where pathogens are carried from infected corals to healthy ones by corallivores such as fireworms, snails, and especially various reef fish, significantly enhancing the spread of infections [115–119]. Key groups of coral disease pathogens include:

- **Bacteria:** Bacteria are single-celled microorganisms belonging to the domain (*Bacteria*), characterized by their simple cell structure without a nucleus. They are found in various environments, including marine ecosystems, where they play essential roles in nutrient cycling, symbiosis, and decomposition. While some bacteria are beneficial, others can be pathogenic and contribute to coral diseases. Common bacterial coral diseases include White Band Disease (WBD), Black Band Disease (BBD),

Yellow Band Disease (YBD), and White Plague (WPD). These diseases can lead to coral tissue loss, reduced growth, and ecosystem imbalances, often exacerbated by environmental stressors such as pollution and climate change.

- **Fungi:** Fungi are diverse group of eukaryotic microorganisms that include yeasts, molds, and filamentous fungi, playing essential roles in decomposition, nutrient cycling, and symbiotic relationships in various ecosystems. They reproduce through spores and can thrive in a wide range of environments, including marine habitats. While some fungi are beneficial, others can act as pathogens, causing diseases in plants, animals, and corals. In coral ecosystems, Aspergillosis, caused by the fungus Aspergillus sydowii, is a well-known disease that primarily affects sea fan corals (*Gorgonia spp.*), leading to tissue loss and necrosis. Environmental stressors such as pollution and climate change can increase fungal infections, further threatening coral health and reef stability.

- **Viruses:** Viruses are microscopic infectious agents that consist of genetic material (DNA or RNA) enclosed in a protein coat, requiring a host cell to replicate. They infect a wide range of organisms, including bacteria, plants, animals, and marine life. In coral ecosystems, viruses can contribute to coral diseases by targeting symbiotic algae (Symbiodiniaceae) or coral tissues, leading to stress and bleaching. One known viral-associated coral disease is White Plague, which has been linked to bacterial and potential viral pathogens, causing rapid tissue loss in corals. Environmental stressors such as rising sea temperatures and pollution can exacerbate viral infections, further threatening coral reef health.

- **Protozoa:** Protozoa are single-celled, eukaryotic microorganisms that exhibit animal-like behavior, such as movement and predation. They are found in diverse environments, including marine ecosystems, where they play essential roles in nutrient cycling and as part of the food web. While many protozoa are beneficial, some can act as pathogens, causing diseases in corals and other marine organisms. One such disease is Brown Band Disease (BrB), associated with protozoan parasites like Helicostoma nonatum, which consume coral tissue and symbiotic algae, leading to coral degradation. Environmental stressors such as temperature fluctuations and pollution can increase protozoan infections, further impacting coral reef health.

- **Cyanobacteria:** Cyanobacteria, also known as blue-green algae, are photosynthetic prokaryotic microorganisms that play a crucial role in marine and freshwater ecosystems. They contribute to primary production, nitrogen fixation, and microbial interactions in coral reef environments. However, under certain conditions such as nutrient enrichment and rising sea temperatures, cyanobacteria can proliferate excessively, leading to harmful effects on corals. One such disease is Black Band Dis-

ease (BBD), caused by a microbial consortium dominated by cyanobacteria such as *Phormidium corallyticum*, which forms dark bands on coral surfaces and degrades tissue. Environmental stressors like pollution and climate change can further promote cyanobacterial growth, exacerbating coral reef degradation.

1.4 Delay in Coral Reefs Ecosystem

Delay refers to the time lag between an action or event and its observable effect within a system. In ecological contexts, delays capture the non-instantaneous responses of organisms or processes, such as population growth, recovery, or interactions. These delays are essential for understanding dynamic systems, as they significantly influence stability, resilience, and the effectiveness of interventions. Without accounting for these time lags, models and management strategies risk oversimplifying complex natural processes and overlooking critical aspects of ecosystem dynamics.

Delays can be categorized into two primary types: continuous delays and discrete delays. Continuous delays occur when the effect of past states influences the current state over a range of time. These are typically modeled using distributed delay kernels, such as gamma distributions, to provide a more realistic representation of gradual effects. For example, habitat restoration or changes in predator-prey dynamics often follow a continuous delay pattern. In contrast, discrete delays involve fixed time lags where a specific past state directly affects the present, such as the immediate but delayed impact of a disturbance or the onset of disease symptoms. Both types are crucial for capturing the complexities of ecological systems.

In the context of coral reef ecosystems, delays play a pivotal role in understanding and managing the intricate processes that sustain these environments. Coral reefs face numerous stressors, including climate change, disease outbreaks, and predator-prey imbalances. Delays reflect the inherent time lags in ecological responses, such as coral recovery after disturbances, the delayed adjustments of predator populations to changes in prey availability, or the incubation periods of diseases. Incorporating these delays into models helps to predict more realistic recovery timelines and understand the long-term impacts of interventions.

Blackwood et al. [120] demonstrated the importance of delays in coral-algal interactions on Caribbean reefs. They highlighted the delayed response of parrotfish populations to changes in coral habitat complexity. Although these delays did not alter the stability of equilibria, they significantly reshaped the basins of attraction, affecting the likelihood of recovery to a coral-dominated state. This emphasizes the need for considering transient dynamics in reef management, as interventions might require accounting for delayed ecological effects to ensure success. Similarly, Dela Cruz et al. [121] examined predator-prey dynamics involving Crown-of-Thorns Starfish (COTS) and coral species. They empha-

sized how lags in coral recovery and predator population responses to human interventions critically impact the effectiveness of COTS management. By incorporating delays, their model provided more accurate recovery timelines, enabling better planning and conservation strategies. Bhattacharyya et al. [122] explored delays in coral diseases, such as Black Band Disease (BBD). Their research identified two critical delays: the incubation period of pathogens in corals and the recovery time of algal turf following grazing by herbivores. These delays play a crucial role in determining ecosystem stability. Crossing certain thresholds can lead to regime shifts, such as oscillatory behavior or transitions to algae-dominated states. Their findings stress the importance of timely interventions to prevent long-term damage to coral reefs. Together, these studies highlight that delays are not just technical details but fundamental aspects of coral reef dynamics. Ignoring them can lead to unrealistic predictions and ineffective strategies. By capturing the delayed responses of key processes, researchers and managers can better understand the resilience and recovery potential of coral reefs, ultimately guiding more effective interventions to preserve these vital ecosystems amidst increasing environmental stressors.

1.5 Literature Review and Motivation

Coral reefs, as one of the most diverse and essential marine ecosystems, provide critical services, including biodiversity preservation, food security, and coastal protection. However, these ecosystems are increasingly threatened by various factor such as biotic (diseases, overfishing, competition with macroalgae, etc.) and abiotic (rising sea temperatures, ocean acidification, pollution, etc.) factors, which play a pivotal role in reef degradation. To comprehend the impacts of these factors comprehensively, developing a mathematical model of coral reef dynamics is essential. Mathematical models are valuable tools for gaining deeper insights into the underlying dynamics of observed coral communities while also assessing the potential effects of stressors and the effectiveness of management strategies aimed at ensuring coral survival and resilience. To understand and address this problem, Mumby et al. [123] first developed a mathematical model in 2007, using a system of ordinary differential equations (ODEs) to explore the interactions between corals, macroalgae, and algal turfs. In this paper authors assumed that the seabed was entirely covered by these three components and analyzed how grazing intensity, primarily by herbivorous fish like parrotfish, influenced the stability of coral reef ecosystems. The key objective of the study was to determine whether algae-dominated reefs represented an alternative stable state and to identify the thresholds for coral recovery. A critical finding was the phenomenon of hysteresis, where the transition from coral to algae dominance occurred at a lower threshold of grazing intensity than the threshold required for recovery. This result highlighted the significant ecological feedbacks between grazing intensity and coral resilience, indicating that recovering degraded reefs required much higher management efforts compared

to maintaining healthy coral cover. In 2012, the model was extended by Blackwood et al. [124] they introduced the explicit dynamics of herbivorous fish populations, such as parrotfish, into the system. This work moved beyond the static assumption of fixed grazing rates by incorporating population dynamics, including the effects of fishing pressure and natural mortality. By coupling grazer abundance with coral recovery, the model allowed researchers to study how feedbacks between coral habitat and grazer populations influenced reef resilience. Two distinct recovery scenarios were identified: (1) severely damaged reef structures where physical habitat loss limited parrotfish recruitment, and (2) structurally intact but coral-depleted reefs, where algae dominated due to reduced grazing or bleaching events. The study emphasized that recovery efforts needed to address both fishing pressure and other restoration strategies, particularly in regions with significant physical damage. It showed that reducing fishing alone might be insufficient for severely degraded systems and that coupled efforts were essential for resilience. Building upon these foundations, Blackwood et al. [125] in 2018, revisited and refined the coral-algae interaction model, further exploring the concept of alternative stable states in the presence of multiple stressors. This study incorporated external factors such as ocean acidification, rising sea temperatures, and hurricane-induced damage, making the model more comprehensive and applicable to real-world conditions. They expanded the model to include additional interactions, such as competition with sponges, recruitment dynamics, and external coral and algae inputs. They analyzed the bifurcation behavior of the system, identifying the critical grazing thresholds that determined whether a reef would remain in a coral-dominated state or transition to algae dominance. This findings underscored the importance of localized management strategies, tailored to specific reef conditions and stressors. For instance, reefs subjected to overfishing might benefit from targeted fishing regulations, while those affected by bleaching events might require coral transplantation or other restoration techniques. Several studies [121, 126–129] have expanded on [123], describing the dynamics of coral reef ecosystems and their interactions with various factors such as rising sea surface temperatures, destructive fishing, and more.

Among the various factors contributing to coral reef degradation, coral disease is one of the most severe. It is an abnormal condition that disrupts the functions of coral organisms, often presenting with distinct symptoms and signs. The first recorded coral disease, Black Band Disease (BBD), was observed by Antonious in 1973 [130], with additional diseases identified in subsequent studies [131–133]. Coral diseases spread through two primary pathways: contagious transmission (direct contact) and non-contagious transmission (pathogen-mediated) [112, 134, 135]. To better understand coral disease dynamics, many scientists have conducted field experiments and case studies [37, 136–142]. Bhattacharyya et al. in [122], was the first to introduce a mathematical model using ordinary differential equation on coral disease, extending the framework presented in [124]. This model categorized coral populations into two subclasses: susceptible and infected. In this

study, the authors focused on understanding the impact of Black Band Disease (BBD) on coral reefs using an eco-epidemiological model. They examines how BBD transmission pathways (both contagious and non-contagious), reduced herbivory, and macroalgal growth contribute to coral decline and phase shifts in reef ecosystems. The findings reveal that low coral recruitment, high macroalgal immigration, and decreased herbivory can drive irreversible shifts from coral-dominated to macroalgae-dominated reefs. Furthermore, the model demonstrates that when BBD transmission surpasses a critical threshold, it triggers significant coral loss through bifurcations, including transcritical, saddle-node, and Hopf bifurcations. These results emphasized that managing herbivore populations and controlling macroalgal spread are essential for maintaining coral reef resilience. Bhattacharyya et al. introduced another mathematical model [143] using an ordinary differential equation (ODE) system, expanding on the framework presented in [122–124, 144]. This extended model incorporates pathogen growth rate as a state variable, allowing for a more comprehensive analysis of disease dynamics in coral reef ecosystems. The primary objective of this study is to investigate the impact of macroalgal allelopathy and pathogen-mediated disease transmission on coral reefs using an eco-epidemiological model. Their study explores how macroalgae contribute to pathogen proliferation, affecting disease transmission and coral resilience. They observed that increased macroalgal toxicity and pathogen growth can lead to severe coral decline, whereas higher herbivore grazing plays a crucial role in maintaining reef stability and resilience.

Several studies [145–147] have explored the recovery of coral an infected state to a susceptible state. These experimentals studying collectively suggest that coral recovery is influenced by lesion size, environmental conditions, immune responses, and initial colony health. Corals transition from an infected state back to a susceptible state through a multiphase healing process, including wound sealing, immune activation, tissue proliferation, and recolonization by symbiotic algae. Immune responses, such as upregulation of Toll-like receptor pathways and antimicrobial peptides, prevent bacterial infections, allowing corals to restore their microbial homeostasis and regenerate tissues. The studies also emphasize the role of environmental factors, with higher regeneration rates observed in less stressed habitats, while chronic stressors like pollution and high turbidity hinder recovery. This recovery phenomenon, we introduced in **Chapter** 2, coral disease mathematical model which extension of [122] and also described the effect of recovery rate on coral disease dynamics. The study of ecological models frequently emphasizes their long-term behavior; however, there is growing acknowledgment of the significance of understanding transient dynamics. For this reason we introduced a delay differential equation in **Chapter** 3, and developed a mathematical model to study the dynamical behaviour of coral disease and recovery rate. Disease spreads into corals not only through contagious and non-contagious ways but also through the consumption of zooplankton by susceptible corals [112, 148]. In a tank-based experiment [136], researchers demonstrated that zooplankton

can act as a vector for white band disease (WBD) in the endangered coral species *Acropora cervicornis*. This study found that zooplankton exposed to disease-causing pathogens were capable of transmitting WBD to healthy corals in controlled conditions. Since corals feed on zooplankton as part of their natural diet, the ingestion of pathogen-carrying zooplankton allows bacteria to enter coral tissues, facilitating disease transmission. Identifying this gape and being motivated by this, we devoloped a mathematical work in **Chapter** 4, and described the impact of zooplankton mediated disease out-break in coral reefs ecosystem. In addition to these factors, fish also play a crucial role in spreading disease among coral reef populations. Many experimental studies [117, 149, 150] show that disease spreads among coral populations by fish predation. In [149] authors examined the role of coral predators (corallivores) in influencing coral disease dynamics, a factor often overlooked in coral disease research. This study synthesizes data from 65 studies across 26 ecoregions, demonstrating that corallivores can facilitate disease by breaking through coral tissue, acting as disease vectors, or serving as pathogen reservoirs. This observational studies found strong positive correlations between corallivore abundance and disease prevalence, while experiments confirmed that corallivores could transmit pathogens and influence disease progression. Also finding this gap and being motivated by the work [149], we developed a mathematical model in **Chapter** 5, to describe the impact of fish predation on coral disease dynamics, which is an extension of the model [143].

1.6 Orientation

The thesis has been organized in the following manner: In **Chapter** 2, we developed a mathematical model to analyze the dynamics of coral disease transmission and recovery, focusing on the interactions between infected and susceptible coral colonies. The study examines how disease spreads through waterborne pathogens and how environmental factors, such as macroalgae overgrowth and fish grazing, influence coral health. The key finding of the research is the identification of a tri-stability region, where different stable states of the coral reef ecosystem can coexist. The model reveals that the interplay between disease transmission rate (λ) and recovery rate (ω) plays a crucial role in determining coral resilience. The study also highlights the importance of fish grazing (g) in controlling macroalgae, which indirectly supports coral recovery. These insights provide a deeper understanding of coral reef ecosystem dynamics and offer guidance for conservation and management strategies. In **Chapter** 3, we investigate the impact of incubation time delay on coral reef ecosystems affected by coral disease. For this study, we propose a mathematical model incorporating time delay to analyze the stability of coral populations and the dynamics of disease transmission. Key findings indicate that incubation delay can destabilize the system, leading to oscillatory behavior in coral populations. The model demonstrates that a critical delay threshold exists, beyond which the system undergoes a

Hopf-bifurcation, resulting in periodic fluctuations in coral and macroalgae populations. Numerical simulations validate these theoretical predictions and highlight how varying disease transmission rates influence coral health. The study also shows that increasing the rate at which infected coral recovers to a healthy state can mitigate oscillations and reduce disease spread. Furthermore, the research emphasizes the role of environmental and ecological factors in shaping coral reef dynamics. The findings provide insights into the resilience of coral ecosystems and inform strategies for reef conservation. In **Chapter** 4, we discusse and analyze the role of zooplankton in the transmission of White Band Disease (WBD) in coral reef ecosystems. For this study, we consider a five-dimensional non-linear eco-epidemiological model to investigate both contagious and non-contagious pathways of disease transmission. Key findings suggest that zooplankton-mediated transmission is more harmful to corals compared to other modes, while infected coral-to-coral transmission is the least detrimental. The study also identifies a Hopf bifurcation occurring when disease transmission rates exceed a critical threshold, leading to oscillatory coral population dynamics. Increased mutualism between phytoplankton and susceptible corals is found to aid coral recovery. Numerical simulations validate these analytical results, demonstrating different equilibrium and stability scenarios. The study provides crucial insights into coral disease dynamics, emphasizing the need for conservation efforts that consider multiple transmission pathways. In **Chapter** 5, we investigate the intricate relationship between fish predation and coral disease dynamics using a mathematical modeling approach. This study investigates the impact of fish grazing on coral health, the spread of diseases, and competition with macroalgae within coral reef ecosystems. This study finds that fish predation plays a dual role—while it can facilitate disease transmission by spreading pathogens, it also suppresses macroalgae, which competes with corals for space. The analysis reveals that coral survival depends on a delicate balance of fish predation, where both extremely low and high predation levels can protect corals from disease outbreaks. The study also identifies a tipping point where increasing fish predation shifts the ecosystem from a disease-dominated state to a healthier one. Additionally, the work shows that disease severity (virulence) and disease transmission rates interact with predation levels, influencing coral persistence. These findings underscore the necessity of incorporating biotic interactions into coral reef conservation strategies, particularly in the context of overfishing and habitat degradation. Finally, the thesis ends with the conclusion and future direction in **Chapter** 6.

1.7 Some Basic Mathematical Definitions and Theorems

This section introduces the essential mathematical concepts and analytical tools used to study the behavior of dynamical systems. These foundational definitions and theorems will serve as the basis for examining the different models presented throughout this thesis.

1.7.1 Nonlinear System

A dynamical system characterizes how certain variables or states change over time, guided by specific rules that govern their temporal evolution. In essence, it provides a mathematical model for capturing the progression of a system's behavior. Analyzing such systems especially those exhibiting continuous and nonlinear dynamics requires the use of differential equations. These equations allow us to formally describe the interplay between variables and their rates of change, offering insights into the system's behavior and long-term evolution. A general form of a nonlinear dynamical system is given by:

$$\frac{dy(t)}{dt} = f(y(t)), \tag{1.1}$$

where f is a nonlinear, vector-valued function whose components act on the respective elements of the state vector.

$$y(t) = [y_1, y_2, ..., y_r]^T. \tag{1.2}$$

In a dynamical system, the components of the state vector y_i $(i = 1, 2, ..., r)$; evolve over time, capturing the temporal behavior fundamental to the system's dynamics. To mathematically represent such systems, one can utilize a range of differential equation frameworks, including ordinary differential equations (ODEs), delay differential equations (DDEs), stochastic differential equations (SDEs), and others.

1.7.2 Non-negativity

The non-negativity of solutions to the system (1.1) ensures that, for nonnegative initial conditions, the state variables remain nonnegative for all finite time t. This property reinforces the reliability and interpretability of the model's predictions. A subset $\Lambda \subset \mathbb{R}^r_{+,0}$ is defined as a *Non-negativity invariant set* if

$$\Lambda = \{y \in \mathbb{R}^r_{+,0} : y_i \geq 0\}, \tag{1.3}$$

where $y(0) = y_0 \in \Lambda$ implies $y(t, y_0) \in \Lambda$ for all $t \geq 0$.

1.7.3 Existence and Uniqueness Theorem

Theorem 1.1 *Assume that $f \in C^1(A)$, where A is an open subset of $\mathbb{R}^r_+$ containing the point y_0. Then, there exists a real number $L > 0$ such that the dynamical system (1.1) with initial condition $y(0) = y_0$ admits a unique solution on the interval $[-L, L]$.*

1.7.4 Boundedness and Uniform Persistent

From a biological perspective, the boundedness of the system implies that the population cannot grow without limit or tend toward infinity. Conversely, to analyze the system's long-term dynamics, it is essential to examine the property of uniform persistence.

Definition 1.2 *The nonlinear dynamical system* (1.1) *is considered bounded if there exists a real constant* $L > 0$ *such that every solution* $y(t)$ *of the system satisfies* $\limsup_{t\to\infty} y(t) \leq L$.

Definition 1.3 *The nonlinear dynamical system* (1.1) *is said to exhibit uniform persistence if every solution* $y(t)$ *satisfies* $\liminf_{t\to\infty} y(t) > 0$.

1.7.5 Equilibrium Point

An equilibrium point of a dynamical system is a constant solution that does not change with time and arises from the system's differential equations. It is also commonly referred to as a singular point, fixed point, or stationary point.

Definition 1.4 *A point* y_1 *is defined as an equilibrium point of the system* (1.1) *if it satisfies* $\frac{dy}{dt}\big|_{y=y_1} = f(y_1) = 0$.

1.7.6 Local Stability

The next section provides a comprehensive overview of stability analysis, a fundamental concept with wide-ranging applications across numerous areas of applied mathematics.

Definition 1.5 *A fixed point* y_1 *of the system* (1.1) *is said to be locally stable if, for every* $\varepsilon > 0$*, there exists a* $\delta > 0$ *such that any solution* $y(t)$ *of the system with initial condition* $y(0) = y_0$*, satisfying* $\|y_0 - y_1\| \leq \delta$*, also satisfies* $\|y(t) - y_1\| < \varepsilon$ *for all* $t \geq 0$*, where* $\|\cdot\|$ *denotes the Euclidean norm.*

Definition 1.6 *A fixed point* y_1 *of the system* (1.1) *is said to be locally asymptotically stable if it is locally stable and there exists a constant* $\mu > 0$ *such that for any initial condition* $y(0) = y_0$ *with* $\|y_0 - y_1\| < \mu$*, the solution* $y(t)$ *satisfies* $\lim_{t\to\infty} \|y(t) - y_1\| = 0$.

Definition 1.7 *A fixed point* y_1 *of the system* (1.1) *is considered unstable if it does not satisfy the conditions for stability.*

1.7.7 Routh-Hurwitz Criteria

Assume that B is a square matrix and I_r denotes the identity matrix of order r. Let $p_i \in \mathbb{R}$ for $i = 1, 2, \ldots, r$, with $p_r \neq 0$. Then, the characteristic polynomial of the matrix B is defined as

$$B(\lambda) = det(B - \lambda I_r) = \lambda^r + p_1\lambda^{r-1} + p_2\lambda^{r-2} + \ldots\ldots + p_{r-1}\lambda + p_r. \tag{1.4}$$

The eigenvalues of the matrix B are all negative or possess negative real parts if and only if

$$B_s = \begin{vmatrix} p_1 & p_3 & p_5 & ..... & 0 \\ 1 & p_2 & p_4 & ..... & 0 \\ 0 & p_1 & p_3 & ..... & 0 \\ . & . & . & ..... & . \\ . & . & . & ..... & . \\ 0 & 0 & 0 & ..... & p_s \end{vmatrix} > 0, \quad \text{for s = 1, 2, 3,.....r.}$$

Followings are the Routh-Hurwitz criteria for $r = 2,\ 3$ and 4.

$$\text{For } r = 2 \ : \ p_1 > 0,\ p_2 > 0.$$

$$\text{For } r = 3 \ : \ p_1 > 0,\ p_3 > 0,\ p_1 p_2 - p_3 > 0.$$

$$\text{For } r = 4 \ : \ p_1 > 0,\ p_3 > 0,\ p_4 > 0,\ (p_1 p_2 - p_3) p_3 - p_1^2 p_4 > 0.$$

1.7.8 Bifurcation Theory

In mathematics, bifurcation theory explores how the qualitative behavior of a system evolves as parameters are varied. It focuses on identifying critical parameter values at which the system undergoes transitions between distinct states or dynamic regimes. Typically applied to nonlinear systems—such as those described by differential equations—bifurcation theory analyzes how even minor changes in parameters can result in significant shifts in the system's overall behavior.

- **Transcritical Bifurcation** A transcritical bifurcation is a particular type of bifurcation observed in dynamical systems when a parameter attains a critical threshold. This bifurcation is characterized by the exchange of stability between two equilibrium (or fixed) points. The term "transcritical" reflects the fact that these equilibria intersect and swap their stability properties. As the control parameter is varied, the system undergoes a qualitative shift in behavior, with the stability of the involved equilibrium points reversing accordingly.

Let us assume that

$$\frac{dy}{dt} = f(y, \mu) \tag{1.5}$$

is a system of ordinary differential equations, where $y \in \mathbb{R}^r_+$ and $\mu \in \mathbb{R}$. Suppose that the system (1.5) admits an equilibrium point denoted by y_0.

Theorem 1.8 *(Sotomayor's theorem [151]). Assume that* $f(y_0, \mu_0) = 0$*, and let* $\Gamma \equiv D_y f(y_0, \mu_0)$ *be a* $p \times r$ *matrix representing the Jacobian of* f *evaluated at* (y_0, μ_0)*. Suppose* Γ *has a simple eigenvalue* $\lambda = 0$ *with associated eigenvector* w*, and that the transpose* Γ^T *possesses a corresponding eigenvector* u *for the same eigenvalue* $\lambda = 0$*. If the following conditions are satisfied:*

$$u^T \Gamma(y_0;\ \mu_0) = 0; \quad u^T [D\Gamma(y_0;\ \mu_0)w] \neq 0; \quad u^T [D^2\Gamma(y_0;\ \mu_0)(w,\ w)] \neq 0,$$

then the system undergoes a transcritical bifurcation at the equilibrium point y_0 *as the parameter* μ *crosses the critical value* $\mu = \mu_0$*.*

- **Hopf Bifurcation** Named after the mathematician Eberhard Hopf, the Hopf bifurcation is a fundamental concept in dynamical systems theory, particularly in the context of ordinary differential equations. It describes a scenario in which a system undergoes a qualitative change in behavior as a parameter reaches a critical threshold, leading to the emergence of a stable limit cycle. Specifically, a Hopf bifurcation occurs when a previously stable equilibrium point becomes unstable, and a periodic solution (limit cycle) is born as the control parameter varies.

Theorem 1.9 *Let*

$$\frac{dy}{dt} = f(y,\ \phi) \tag{1.6}$$

be a system of continuously differentiable equations defined on $\mathbb{R}^r_+$*, with* $\phi \in \mathbb{R}$ *representing a system parameter. Suppose the Jacobian matrix evaluated at the equilibrium point* E *possesses a pair of complex conjugate eigenvalues.*

$$\mu = c(\phi) \pm id(\phi), (where\ c,\ d \in \mathbb{R})$$

At a critical parameter value $\phi = \phi_1$*, the complex conjugate eigenvalues become purely imaginary, i.e.,* $[Re(\mu)]_{\phi=\phi_1} = 0$*.*
The eigenvalues cross the imaginary axis if the transversality condition is satisfied, namely,

$$\left[\frac{dRe(\mu)}{d\phi}\right]_{\phi=\phi_1} \neq 0.$$

Consequently, the system (1.6) *undergoes a Hopf bifurcation at the critical parameter value* $\phi = \phi_1$ *in the neighborhood of the equilibrium point* E*. The parameter* ϕ *is referred to as the bifurcation parameter, while* ϕ_1 *is known as the bifurcation point.*

2

Coral Disease and Recovery Dynamics: A Mathematical Model Apporach

2.1 Introduction

Coral reefs, although occupying less than 1% of the ocean floor, support approximately 25% of marine biodiversity, making them among the most ecologically rich and economically significant ecosystems globally. They provide critical habitat, feeding, and breeding grounds for numerous marine organisms, while also offering substantial economic benefits through fisheries, tourism, and shoreline protection. The intricate three-dimensional structures of reefs act as natural barriers, mitigating coastal erosion and storm damage. As such, the protection and sustainable management of coral reefs are essential to global ecological balance and economic stability. However, these vital ecosystems are increasingly endangered by a combination of anthropogenic and natural stressors. Activities such as overfishing, pollution, habitat destruction, and unregulated coastal development have contributed significantly to reef degradation. Compounding these impacts, climate change has emerged as a dominant threat, with rising sea surface temperatures triggering mass coral bleaching and ocean acidification undermining reef structural integrity. These stressors compromise coral health and resilience, creating favorable conditions for the emergence and proliferation of coral diseases. Coral diseases have become a leading cause of reef decline, with multiple syndromes identified over recent decades. Diseases such as Black Band Disease (first recorded by A. Antonius in 1973), White Band Disease, Yellow

Band Disease, White Pox Disease, Aspergillosis, and Brown Band Disease are associated with distinct pathogenic organisms and environmental triggers. These diseases manifest through various symptoms, including tissue necrosis, discoloration, and skeletal exposure, often leading to partial or total colony mortality. For example, Black Band Disease is driven by a complex microbial mat dominated by cyanobacteria and sulfur-cycling bacteria, while Aspergillosis is caused by fungal pathogens affecting gorgonian sea fans. Pathogen transmission occurs through multiple routes: direct contact between infected and healthy colonies, waterborne dispersal via ocean currents, and biological vectors such as fish, invertebrates, and suspended sediments. Infected colonies function as continuous reservoirs, releasing pathogens that spread to nearby susceptible corals. Elevated sea temperatures and nutrient enrichment further intensify disease outbreaks by weakening coral immune responses and promoting microbial imbalances. Given the diversity in microbial communities associated with different diseases, understanding the specific interactions between hosts, pathogens, and environmental factors is crucial for managing disease spread. Despite these challenges, coral recovery remains possible through a combination of internal and external mechanisms. Biologically, corals can initiate immune responses and produce antimicrobial substances to combat pathogens [146]. Recovery is supported by energy from symbiotic *zooxanthellae*, which may be replaced by thermally tolerant strains after bleaching events [152, 153]. Ecological support, including herbivorous fish that control algal overgrowth, improves the environment for regeneration [154]. Moreover, connectivity with nearby healthy reefs can facilitate the exchange of beneficial microbes and genetic material, enhancing resistance and recovery potential [155]. In severely degraded reef systems, active interventions such as coral nurseries, transplantation, and microbial therapies (e.g., probiotics or amoxicillin treatments) have shown promising results in controlling disease and aiding recovery. When integrated with broader conservation strategies including marine protected areas, sustainable resource management, and water quality improvements these measures contribute to a holistic framework for reef restoration. This study aims to develop and analyze a mathematical framework that captures the key features of coral disease and recovery dynamics. The results will inform targeted management and intervention strategies, ultimately contributing to the preservation of coral reef ecosystems in an era of accelerating environmental change.

2.2 Model Formulation

We examine the temporal evolution of spatial occupation among foundational benthic functional groups, namely corals $C(t)$, macroalgae $M(t)$, and turf algae $T(t)$, within reef ecosystems. Corals are subject to competitive overgrowth by macroalgae at a rate a, while turf algae are similarly displaced by macroalgal expansion at a rate γ. Following mortality events affecting either corals or macroalgae, turf algae rapidly exploit the liberated sub-

strate, exhibiting opportunistic colonization behavior. Coral recruitment and subsequent growth are facilitated by settlement on turf-dominated substrates, governed by a rate r. Both macroalgae and coral populations are subject to intrinsic mortality, parameterized by v and d, respectively. Furthermore, herbivorous fish exert top-down control on macroalgae through grazing, thereby creating spatial vacancies that are subsequently colonized by turf algae; the maximal rate of such grazing activity is represented by g. Based on these biotic interactions and ecological feedback mechanisms, we formulate a system of nonlinear coupled differential equations to encapsulate the dynamic interplay among these benthic assemblages. This modeling framework aligns with established approaches in the literature (cf. [123, 124, 126, 129, 156–158]), providing a quantitative foundation for understanding coral reef regime shifts and resilience dynamics.

$$\begin{aligned} \frac{dM}{dt} &= aMC - g\frac{M}{M+T} + \gamma MT - vM, \\ \frac{dC}{dt} &= rCT - aMC - dC, \\ \frac{dT}{dt} &= g\frac{M}{M+T} + vM + dC - (\gamma M + rC)T, \end{aligned} \tag{2.1}$$

where $M+C+T=1$.

Coral disease poses a profound threat to the integrity and persistence of reef ecosystems, contributing significantly to coral mortality and the erosion of biodiversity. Like other organisms, corals are vulnerable to pathogenic infections, with outbreaks frequently exacerbated by environmental perturbations such as elevated sea surface temperatures, nutrient enrichment, pollution, and ocean acidification. These stressors can compromise coral immune defenses and disrupt microbial homeostasis, enabling opportunistic pathogens to initiate infections. Pathogenic agents residing in the water column, sediments, or reef surfaces can infiltrate coral tissues via multiple transmission routes [112]. Once established, infections propagate efficiently through coral populations, modifying the host-associated microbiome and fostering conditions conducive to further disease proliferation. Despite the ecological urgency, relatively few mathematical models have been constructed to rigorously investigate coral disease dynamics [110, 122, 143]. In modeling the infection process, two principal mechanisms are recognized: direct (contagious) transmission and indirect (environmentally mediated) transmission. Let $C_S(t)$ and $C_I(t)$ represent the densities of susceptible and infected corals at time t, respectively, such that $C_S + C_I = C$. For analytical tractability, we consider a simplified scenario in which disease propagation occurs exclusively through direct (contagious) transmission. In this framework, infected coral colonies (C_I) disseminate pathogens into the surrounding water, thereby infecting adjacent susceptible colonies (C_S) via contact-mediated transmission. This interaction adheres to a mass-action formulation, with the infection rate expressed as $\lambda C_S C_I$, where λ is the disease

transmission rate through contagious way. Infected corals experience elevated mortality, represented by the additional death rate e. However, recovery mechanisms such as lesion healing and sloughing of diseased tissue permit infected colonies to revert to a susceptible state. This recovery process is modeled as a transition from C_I to C_S at a rate ω, under the assumption that immunity is not retained post-recovery. Integrating these assumptions, the disease extended reef dynamics can be described by the following system of nonlinear differential equations:

$$\begin{aligned}
\frac{dM}{dt} &= aM(C_S+C_I) - \frac{gM}{M+T} + \gamma MT - vM, \\
\frac{dC_S}{dt} &= rTC_S - aMC_S - dC_S - \lambda C_S C_I + \omega C_I, \\
\frac{dC_I}{dt} &= \lambda C_S C_I - aMC_I - (d+e)C_I - \omega C_I, \\
\frac{dT}{dt} &= \frac{gM}{M+T} + vM + d(C_S+C_I) + eC_I - \gamma MT - rTC_S.
\end{aligned} \tag{2.2}$$

Without any loss of generality, we assume that $M+T+C_S+C_I = 1$ then from model (2.2) we obtained

$$\begin{aligned}
\frac{dM}{dt} &= aM(C_S+C_I) - \frac{gM}{1-C_S-C_I} + \gamma M(1-M-C_S-C_I) - vM \equiv F_1, \\
\frac{dC_S}{dt} &= rC_S(1-M-C_S-C_I) - aMC_S - dC_S - \lambda C_S C_I + \omega C_I \equiv F_2, \\
\frac{dC_I}{dt} &= \lambda C_S C_I - aMC_I - (d+e)C_I - \omega C_I \equiv F_3.
\end{aligned} \tag{2.3}$$

To analyze model (2.3), we consider positive initial conditions: $M(0) > 0$, $C_S(0) > 0$ and $C_I(0) > 0$.

2.3 Results

2.3.1 Positivity

As the state variables of the system (2.3) correspond to population densities, the concept of positivity indicates that populations never reach zero and consistently endure.

Theorem 2.1 *Given positive values, each solution to our system (2.3) is not only exists but also unique in the interval* $[0,\infty)$*, ensuring that* $M(t) > 0$, $C_S(t) > 0$, $C_I(t) > 0$, $\forall\, t > 0$.

Proof: Let $H = (M,\, C_S,\, C_I)^T$ and $G(H) = [G_1,\, G_2,\, G_3]^T$. Consequently, the system (2.3) can be represented as:

$$\dot{H} = G(H),$$

where $G : R_+ \to R_+^3$ and $H(0) = H_0 \in R_+^3$, with $G_i \in R^\infty(R_+)$, for $i = 1,2,3$. The vector function G is completely continuous and locally Lipschitzian concerning the variables $(M,\ C_S,\ C_I)$ in $G = [M(t),\ C_S(t),\ C_I(t)]$; $M > 0, C_S > 0$ and $C_I > 0$. Utilizing the lemma from [163], we can assert that any solution $(M,\ C_S,\ C_I,)$ of the system (2.3) with positive initial values exits and is unique in the interval $[0,T]$, $\forall\ t > 0$. Where T is a finite positive real number.

2.3.2 Stability and Bifurcation Analysis

2.3.2.1 Existence of Equilibrium Points

The system (2.3) has four different equilibrium points, which are described as follows:

i. Coral free equilibrium $E_1 = \left(1 - \frac{g+v}{\gamma}, 0, 0\right)$. Equilibrium point E_1 always exists if $\frac{g+v}{\gamma} < 1$.

ii. Macroalgae-free equilibrium, $E_2 = \left(0, \frac{d+e+\omega}{\lambda}, \frac{(d+e+\omega)[r(\lambda-d-e-\omega)-d\lambda]}{\lambda[r(\lambda+e+\omega)+\lambda(d+e)]}\right)$. E_2 exists if $\lambda > \frac{r(d+e+\omega)}{r-d}$ and $r > d$.

iii. Macroalgae and infected coral-free equilibrium $E_3 = (0, \frac{r-d}{r}, 0)$. Equilibrium point E_3 exists if $r > d$.

iv. $E^* = (M^*, C_S^*, C_I^*)$ is the interior equilibrium point of the system (2.3). Where $M^* = \frac{\lambda C_S^* - (d+e+\omega)}{a} = f_1^*(C_S^*)$ (say),
and C_S^* is a positive solution of the equation
$a(C_S + f_2(C_S^*)) - \frac{g}{1-C_S-f_2(C_S^*)} + \gamma(1 - f_1(C_S^*) - C_S - f_2(C_S^*)) - v = 0$,
with $C_I^* = \frac{(C_S^*)^2(r\lambda+ar+a\lambda) - C_S^*[ra+r(d+e+\omega)+a(d+e+\omega)-ad]}{a\omega - arC_S^* - a\lambda C_S^*} = f_2(C_S^*)$.

2.3.2.2 Local Stability Analysis

We summarize the stability analysis of the system (2.3) in the following theorem.

Theorem 2.2 *The stability behaviour of the system (2.3) around the equilibrium points are described below.*

i. Coral free equilibrium $E_1 = \left(1 - \frac{g+v}{\gamma},\ 0,\ 0\right)$ *is locally asymptotically stable (LAS) if* $\frac{g+v}{\gamma} < 1$ *and* $r + \frac{a(g+v)}{\gamma} < a + d$.

ii. Macroalgae-free equilibrium $E_2 = \left(0,\ \frac{d+e+\omega}{\lambda},\ \frac{(d+e+\omega)[r(\lambda-d-e-\omega)-d\lambda]}{\lambda[r(\lambda+e+\omega)+\lambda(d+e)]}\right)$ *is LAS if* $(a-\gamma)(C_{S_2} + C_{I_2}) - \frac{g}{(1-C_{S_2}-C_{I_2})^2} + \gamma - v < 0$, $b_{22} + b_{33} < 0$ *and* $b_{22}b_{33} > b_{23}b_{32}$.
Where $C_{S_2} = \frac{d+e+\omega}{\lambda}$, $C_{I_2} = \frac{(d+e+\omega)[r(\lambda-d-e-\omega)-d\lambda]}{\lambda[r(\lambda+e+\omega)+\lambda(d+e)]}$ *and* b_{ij} *is the element of the Jacobian matrix* J_2 *at* E_2.

iii. Macroalgae and infected coral-free equilibrium $E_3 = (0, \frac{r-d}{r}, 0)$ *is LAS if* $(a-\gamma)C_{S_3} - \frac{g}{(1-C_{S_3})^2} + \gamma - v < 0$, $(\lambda C_{S_3} - d - e - \omega) < 0$ *and* $d < r$ *with* $C_{S3} = \frac{r-d}{r}$.

iv. Interior equilibrium $E^* = (M^*, C_S^*, C_I^*)$ *is LAS if* $R_1 > 0, \quad R_3 > 0$ *and* $R_1 R_2 > R_3$.

Proof:

(i) Now the Jacobian matrix of the system (2.3) at E_1 is given by

$$J_1 = \begin{pmatrix} (-g+\gamma-2\gamma M_1 - v) & (a-g-\gamma)M_1 & (a-g-\gamma)M_1 \\ 0 & r - rM_1 - aM_1 - d & \omega \\ 0 & 0 & -(aM_1 + d + e + \omega) \end{pmatrix},$$

with $M_1 = (1 - \frac{g+v}{\gamma})$.

The eigenvalues of the Jacobian matrix $J_1(E_1)$ are given by

$-g+\gamma-2\gamma M_1 - v$, $r - rM_1 - aM_1 - d$, $-(aM_1 + d + e + \omega)$.

All, the eigen values are negative if $\frac{g+v}{\gamma} < 1$ and $\frac{g+v}{\gamma}(r+a) < a+d$.

Therefore, the system is locally asymptotically stable at E_1 if $\frac{g+v}{\gamma} < 1$ and $\frac{g+v}{\gamma}(r+a) < a+d$.

(ii) The Jacobian matrix of the system (2.3) at E_2 is given by

$$J_2 = \begin{pmatrix} b_{11} & 0 & 0 \\ b_{21} & b_{22} & b_{23} \\ b_{31} & b_{32} & b_{33} \end{pmatrix},$$

where,

$$\begin{aligned} b_{11} &= aC_{S2} + aC_{I2} - \frac{g}{(1 - C_{S2} - C_{I2})} + \gamma - \gamma C_{S2} - \gamma C_{I2} - v, \\ b_{21} &= -(r+a)C_{S2}, \\ b_{22} &= r - 2rC_{S2} - rC_{I2} - d - \lambda C_{I2}, \\ b_{23} &= -rC_{S2} - \lambda C_{S2} + \omega, \\ b_{31} &= -aC_{I2}, \\ b_{32} &= \lambda C_{I2}, \\ b_{33} &= \lambda C_{S2} - d - e - \omega, \end{aligned}$$

with $C_{S2} = \frac{d+e+\omega}{\lambda}$ and $C_{I2} = \frac{(d+e+\omega)[r(\lambda-d-e-\omega)-d\lambda]}{\lambda[r(\lambda+e+\omega)+\lambda(d+e)]}$.

Now the characteristic equation of J_2 is given by

$$| J_2 - xI_3 | = 0.$$

The one root of the characteristic equation of J_2 is: $aC_{S2}+aC_{I2}-\frac{g}{(1-C_{S2}-C_{I2})^2}+\gamma-\gamma C_{S2}-\gamma C_{I2}-v$,
and the remaining two roots are given by the equation:

$$x^2-(b_{22}+b_{33})x+(b_{22}b_{33}-b_{23}b_{32})=0.$$

Therefore, all the eigenvalues of the Jacobian matrix J_2 are negative if $aC_{S2}+aC_{I2}-\frac{g}{(1-C_{S2}-C_{I2})^2}+\gamma-\gamma C_{S2}-\gamma C_{I2}-v<0$, $b_{22}+b_{33}<0$, $b_{22}b_{33}>b_{23}b_{32}$. Thus, the system (2.3) is locally asymptotically stable at E_2.
(iii) The Jacobian matrix of the system (2.3) at E_3 is

$$J_3=\begin{pmatrix} d_{11} & 0 & 0 \\ d_{21} & d_{22} & d_{23} \\ 0 & 0 & d_{33} \end{pmatrix},$$

where,

$$\begin{aligned} d_{11} &= aC_{S3}-\frac{g}{(1-C_{S3})}+\gamma-\gamma C_{S3}-v, \\ d_{21} &= -(r+a)C_{S3}, \\ d_{22} &= r-2rC_{S3}-d, \\ d_{23} &= -rC_{S3}-\lambda C_{S3}+\omega, \\ d_{33} &= \lambda C_{S3}-d-e-\omega, \end{aligned}$$

with $C_{S3}=\frac{r-d}{r}$.
Now the characteristic equation of J_3 is given by

$$|\,J_3-qI_3\,|=0.$$

The roots of the characteristic equation of J_3 are:
$aC_{S3}-\frac{g}{(1-C_{S3})^2}+\gamma-\gamma C_{S3}-v$, $r-2rC_{S3}-d$, $\lambda C_{S3}-d-e-\omega$.
Therefore, all the eigenvalues of the Jacobian matrix J_3 are negative if $aC_{S3}-\frac{g}{(1-C_{S3})^2}+\gamma-\gamma C_{S3}-v<0$, $r-2rC_{S3}-d<0$, $\lambda C_{S3}-d-e-\omega<0$. Thus, the system (2.3) is locally asymptotically stable at E_3.
(iv) The Jacobian matrix of the system (2.3) at E^* is

$$J^*=\begin{pmatrix} c_{11} & c_{12} & c_{13} \\ c_{21} & c_{22} & c_{23} \\ c_{31} & c_{32} & c_{33} \end{pmatrix},$$

with

$$
\begin{aligned}
c_{11} &= aC_S^* + aC_I^* - \frac{g}{(1-C_S^*-C_I^*)} + \gamma - 2\gamma M^* - \gamma C_S^* - \gamma C_I^* - v,\\
c_{12} &= aM^* - \frac{gM^*}{(1-C_S^*-C_I^*)^2} - \gamma M^*,\\
c_{13} &= aM^* - \frac{gM^*}{(1-C_S^*-C_I^*)^2} - \gamma M^*,\\
c_{21} &= -(r+a)C_S^*,\\
c_{22} &= r - rM^* - 2rC_S^* - rC_I^* - aM^* - d - \lambda C_I^*,\\
c_{23} &= -rC_S^* - \lambda C_S^* + \omega,\\
c_{31} &= -aC_I^*,\\
c_{32} &= \lambda C_I^*,\\
c_{33} &= \lambda C_S^* - aM^* - d - e - \omega.
\end{aligned}
$$

Now, the characteristic equation of J^* is given by

$$| J^* - lI_3 | = 0.$$

i.e,

$$l^3 + R_1 l^2 + R_2 l + R_3 = 0. \tag{2.4}$$

Where,

$$
\begin{aligned}
R_1 &= -c_{11} - c_{22} - c_{33},\\
R_2 &= c_{11}c_{22} + c_{11}c_{33} + c_{22}c_{33} - c_{23}c_{32} - c_{12}c_{21} - c_{13}c_{31},\\
R_3 &= c_{11}c_{23}c_{32} - c_{11}c_{22}c_{33} + c_{12}c_{21}c_{33} - c_{12}c_{31}c_{23} - c_{13}c_{21}c_{32} + c_{13}c_{31}c_{22}.
\end{aligned}
$$

Using *Routh-Hurwitz* criteria, E^* will be locally asymptotically stable, if
(i) $R_1 > 0$ and $R_3 > 0$
(ii) $R_1 R_2 > R_3$.

2.3.2.3 Bifurcation Analysis

The bifurcation nature of the system (2.3) with respect to the parameter **g** and λ can be described in the following theorem.

Theorem 2.3 *When the grazing parameter g exceeds a critical value g^*, the system (2.3) demonstrates a Hopf-bifurcation around the interior equilibrium E^* if the following conditions are satisfied: renewcommandiviv*

i. $R_1(g^*) > 0$, $R_3(g^*) > 0$,

ii. $R_1(g^*)R_2(g^*) - R_3(g^*) = 0$,

iii. $R_3'(g^*) > R_1'(g^*)R_2(g^*) + R_1(g^*)R_2'(g^*)$,

iv. $\left[\frac{d(Rel(g))}{dg}\right]_{g=g^*} \neq 0$.

Proof: We have already shown that the interior equilibrium point E^*=(M^*, C_S^*, C_I^*) is locally asymptotically stable provided the characteristic equation (2.4) when Routh-Hurwitz criteria satisfied. We would like to know if E^* will lose its stability when one of the parameters changes. We choose g, the force of grazing as the bifurcation parameter.
For the Hopf-bifurcation to occur at $g = g^*$, the characteristic equation must be of the following form:

$$\begin{aligned} & l^3 + R_1 l^2 + R_2 l + R_3 = 0 \\ \Rightarrow & (l^2 + R_2)(l + R_1) = 0 \quad [\text{since}, R_1 R_2 = R_3]. \end{aligned} \tag{2.5}$$

Then the equation has three roots: $\pm i\sqrt{R_2}$ and $-R_1$. Now, for $g \in (g^* - \delta, g^* + \delta)$, where $\delta > 0$ then we have,

$$\begin{aligned} l_1(g) &= \mu(g) + i\nu(g) \\ l_2(g) &= \mu(g) - i\nu(g) \\ l_3(g) &= -R_1. \end{aligned}$$

Now, put the value of $l(g) = \mu(g) + i\nu(g)$ into the characteristic equation (2.5), i.e. $(l^2 + R_2)(l + R_1) = 0$, we have,

$$\{(\mu + i\nu)^2 + R_2\}(\mu + i\nu + R_1) = 0. \tag{2.6}$$

Taking partial derivative of (2.6) w.r.t. μ, we have:

$$(\mu^2 - \nu^2 + 2i\mu\nu + R_2)(\mu + i\nu + R_1) = 0,$$

$$\Longrightarrow (2\mu\mu' - 2\nu\nu' + 2i\mu'\nu + 2i\mu\nu' + R_2')(\mu + i\nu + R_1) + (\mu' + i\nu' + R_1')(\mu^2 - \nu^2 + 2i\mu\nu + R_2) = 0,$$

$$\Longrightarrow [2\mu^2\mu' i\nu + 2\mu\mu' R_1 - 2\nu\nu'\mu - 2\nu^2 i\nu' - 2\nu\nu' R_1 + 2i\mu'\mu\nu$$
$$+ 2i^2\mu'\nu^2 + 2i\mu'\nu R_1 + 2i\mu^2\nu' + 2i^2\mu\nu\nu' + 2i\mu\mu' R_1 + R_2'\mu + R_2' i\nu + R_2' R_1] + [\mu'\mu^2 - \mu'\nu^2 + 2i\mu'\mu\nu$$
$$+ \mu' R_2 + i\nu'\mu^2 - i\nu'\nu^2 + 2i^2\mu\nu\nu' + i\nu' R_2 + R_1'\mu^2 - R_1'\nu^2 + 2iR_1'\mu\nu + R_1' R_2] = 0,$$

$$\Longrightarrow [2\mu^2\mu' + 2\mu\mu' R_1 - 2\nu\nu'\mu - 2\nu\nu' R_1 - 2\mu'\nu^2 - 2\mu\nu\nu' + R_2'\mu + R_2' R_1 + \mu'\mu^2$$
$$- \mu'\nu^2 + \mu' R_2 - 2\mu\nu\nu' + R_1'\mu^2 - R_1'\nu^2 + R_1' R_2]$$

$$+i[2\mu\mu'\nu - 2\nu^2\nu' + 2\mu'\mu\nu$$
$$+2\mu'\nu R_1 + 2\mu^2\nu' + 2\mu\nu' R_1 + R_2'\nu + 2\mu'\mu\nu + \nu'\mu^2 - \nu'\nu^2 + \nu' R_2 + 2R_1'\mu\nu] = 0,$$
$$\implies \mu'[2\mu^2 + 2\mu R_1 - 2\nu^2 + \mu^2 - \nu^2 + R_2] + \nu'[-2\mu\nu - 2\nu R_1 - 2\mu\nu + 2\mu\nu]$$
$$+[R_2'\mu + R_2' R_1 + R_1'\mu^2 - R_1'\nu^2 + R_1' R_2]$$
$$+i[\mu'(2\mu\nu + 2\mu\nu + 2\nu R_1 + 2\mu\nu) + \nu'(-2\nu^2 + 2\mu^2 + 2\mu R_1 + \mu^2 - \nu^2 + R_2) + (R_2'\nu + 2\mu R_1'\nu)] = 0,$$
$$\implies [\mu'(3\mu^2 - 3\nu^2 + 2\mu R_1 + R_2) - \nu'(2\nu R_1 + 2\nu\mu) + (R_2'\mu + R_1'\mu^2 - R_1'\nu^2 + R_3')]$$
$$i[(6\mu\nu + 2\nu R_1)\mu' + \nu'(3\mu^2 - 3\nu^2 + 2\mu R_1 + R_2) + (R_2'\nu + 2\mu R_1'\nu)] = 0,$$
$$\implies [K\mu' - L\nu' + M] + i[L\mu' + K\nu' + N] = 0.$$

Now, for bifurcation parameter g, we have

$$[K(g)\mu'(g) - L(g)\nu'(g) + M(g)] + i[L(g)\mu'(g) + K(g)\nu'(g) + N(g])) = 0. \tag{2.7}$$

By taking

$$K(g)\mu'(g) - L(g)\nu'(g) + M(g)) = 0,$$
$$L(g)\mu'(g) + K(g)\nu'(g) + N(g) = 0.$$

We have,

$$\Rightarrow \mu'(g) = -\left(\frac{K(g)M(g) + N(g)L(g)}{K^2(g) + L^2(g)}\right), \tag{2.8}$$

where

$$K(g) = 3\mu^2(g) - 3\nu^2(g) + 2\mu(g)R_1(g) + R_2(g),$$
$$L(g) = 6\mu(g)\nu(g) + 2\nu(g)R_1(g),$$
$$M(g) = \mu^2(g)R_1'(g) + \mu(g)R_2'(g) + R_3'(g) - \nu^2(g)R_1'(g),$$
$$N(g) = 2\mu(g)\nu(g)R_1'(g) + \nu(g)R_2'(g).$$

For the bifurcation parameter $g = g^*$ we have $\mu(g^*) = 0$ and $\nu(g^*) = \sqrt{R_2(g^*)}$.
Then,

$$K(g^*) = -2R_2(g^*),$$
$$L(g^*) = 2R_1(g^*)\sqrt{R_2(g^*)},$$
$$M(g^*) = R_3'(g^*) - R_1'(g^*)R_2'(g^*),$$
$$N(g^*) = -R_2'(g^*)\sqrt{R_2(g^*)}.$$

Now from the equation (2.8) we have

$$\left[\frac{dRel(g^*)}{dg^*}\right]_{g=g^*} = \mu'(g^*) = -\left[\frac{K(g^*)M(g^*)+N(g^*)L(g^*)}{K^2(g^*)+L^2(g^*)}\right],$$
$$= \left[\frac{R_3'(g^*)-R_1'(g^*)R_2(g^*)-R_1(g^*)R_2'(g^*)}{2R_2(g^*)+2R_1^2(g^*)}\right].$$

Now, if $R_3'(g^*) > R_1'(g^*)R_2(g^*)+R_1(g^*)R_2'(g^*)$ then we have $\left[\frac{d(Rel(g))}{dg}\right]_{g=g^*} > 0$. Hence, $\left[\frac{d(Rel(g))}{dg}\right]_{g=g^*} \neq 0$. Which completes the proof.

Theorem 2.4 *If $r \neq d$ and $r\omega \neq (r+\lambda_*)(r-d)$ the proposed system (2.3) exhibits a transcritical bifurcation at E_3 when λ crosses λ_*, where λ_*=$r(\frac{d+e+\omega}{r-d})$, with $r > d$. At this threshold, the conditions of the emergence of such pivotal bifurcation are given by:*

i. $W^T f_\lambda(E_3;\lambda_*)$=0,

ii. $W^T[Df_\lambda(E_3,\lambda_*)V] \neq 0$,

iii. $W^T[D^2 f_\lambda(E_3,\lambda_*)(V,V)] \neq 0$.

Proof: At $\lambda = \lambda_*$ the Jacobian matrix of the system (2.3) at E_3 is

$$J_3 = \begin{pmatrix} aC_{S3} - \frac{g}{(1-C_{S3})} + \gamma - \gamma C_{S3} - v & 0 & 0 \\ -(r+a)C_{S3} & r-2rC_{S3}-d & -(r+\lambda_*)C_{S3}+\omega \\ 0 & 0 & \lambda_* C_{S3} - d - e - \omega \end{pmatrix}.$$

Therefore, the Jacobian matrix has a simple zero eigenvalue if

$$\lambda_* C_{S3} - d - e - \omega = 0,$$

i.e., if

$$\lambda_* = r\left(\frac{d+e+\omega}{r-d}\right).$$

Let V and W be the eigenvectors corresponding to the zero eigenvalue for J_3 and J_3^T, respectively.
Then we get V=$(0,\ v_2,\ 1)^T$ and $W = (0,\ 0,\ 1)^T$, where
$v_2 = \frac{r\omega-(r+\lambda)(r-d)}{r(r-d)}$.
We obtain $W^T f_\lambda(E_3;\lambda_*) = 0$, where $\lambda_* = r(\frac{d+e+\omega}{r-d})$. and so no saddle-node bifurcation occurs at E_3 when λ crosses λ_*.
Also, $Df_\lambda(E_3,\lambda_*)V = (0,\ -C_{S3},\ C_{S3})^T$ gives $W^T[Df_\lambda(E_3,\lambda_*)V] = \frac{r-d}{r} \neq 0$, if $r \neq d$.

Now, we have

$$D^2 f(E_3, \lambda_*)(V,V) = \begin{pmatrix} 0 \\ -2rv_2^2 - 2(r+\lambda_*)v_2 \\ 2\lambda_* v_2 \end{pmatrix},$$

this gives $W^T[D^2 f(E_3, \lambda_*)(V,V)] = 2\lambda_* \frac{r\omega - (r+\lambda_*)(r-d)}{r(r-d)} \neq 0$, if $r \neq d$ and $r\omega \neq (r+\lambda_*)(r-d)$.

2.4 Description of the Parameters

Table 2.1: Parameters used in the system (2.3)

Parameters	Description	Value	Refference
a	rate of macroalgal direct overgrowth over coral	0.24	[124, 159, 160]
g	The maximum grazing rate of harbivorous fish	0.2	[159]
γ	Rate of macroalgae vegetative spread over algal turfs	0.8	[161]
r	Recruitment rate of corals on turf algae	1	[161]
v	Natural mortality rate of macroalge	0.01	[161]
λ	Disease transmission rate through contagious way	3	
d	Natural mortality rate of corals	0.024	[144, 162]
ω	Rate of infected coral colonies revert to the susceptible class due to regeneration of tissue	0.1	–
e	Disease induced death rate of infected corals	0.1	[143]

2.5 Numerical Analysis

In this section, we examine the effects of key parameters on the aquatic ecosystem using the proposed model (2.3). These parameters play a crucial role in coral disease dynamics,

influencing both disease spread and potential recovery, either individually or through combined effects.

Numerical results are essential in mathematical modeling as they provide a visual representation of the system's behavior, enhance the analytical findings, and offer a clearer biological interpretation. For the following simulations, all numerical results are generated by using MATCONT (dhooge2003matcont, dhooge2008new) within the MATLAB environment (version 2021a). Except for the parameters used in the bifurcation analysis, all other parameter values are taken from Table 2.1.

2.5.1 Towards Reefs Abundances Concerning Transmission Rate (λ)

In the first case, we consider the grazing rate of herbivorous fish is fixed at g =0.15 and the recovery rate of an infected coral community set at $\omega = 0.2$. In Figure (2.1a), we plotted the entire dynamical scenario with respect to the transmission rate λ. In the low disease transmission rate ($0 < \lambda < 0.3319$), only the stable equilibrium state is E_3, In this low transmission rate, corals thrive in a healthy state, free from disease. Now, at $\lambda = 0.3319$, system (2.3) exhibits a transcritical bifurcation (TB1) where the existing stable state E_3 becomes unstable and exchanges its stability with the coexisting state E^*. Until λ =1.8187, only the coexisting equilibrium is stable in the ecosystem. Therefore, the infection cannot influence the coexistence disbalance under our existing condition for a certain parameter range ($0.3319 < \lambda < 1.8187$). This indicates that in the underwater ecosystem, there is always a certain disease at a particular level, but if no external force (sometimes caused by internal issues of the coral reefs) does not arise, the entire community can survive. Now, with further increase of the parameter λ, at λ= 1.8187, the coexisting state, E^* becomes unstable and changes its stability with the state E_2 via another transcritical bifurcation (TB2) and there is no macro algae present in the state E_2 with higher density of the infected coral reef. Interestingly, after TB2 there is no stable state exist after this bifurcation at $\lambda = 1.8187$, but when we extend the unstable branch of the existing unstable coexisting equilibrium point E^*, there is a saddle-node bifurcation occurs at $\lambda = 1.393$ where two coexisting equilibrium points created (vanish) through this bifurcation point. Notable things, from $\lambda = 1.393$, our considered system has a bistable region of two coexisting equilibrium points with one corresponding a coexistence via lower disease state and another one is higher disease state, which is a very interesting phenomenon in the coral-reef ecosystem. Therefore, for certain increments of the disease transmission, the disease may exist in higher density or exist with lower density depending on the initial value of the state. After the bistable region if we further increase the higher state coexisting equilibrium points, a Hopf bifurcation arises at $\lambda = 1.8771$, and the higher state becomes unstable.

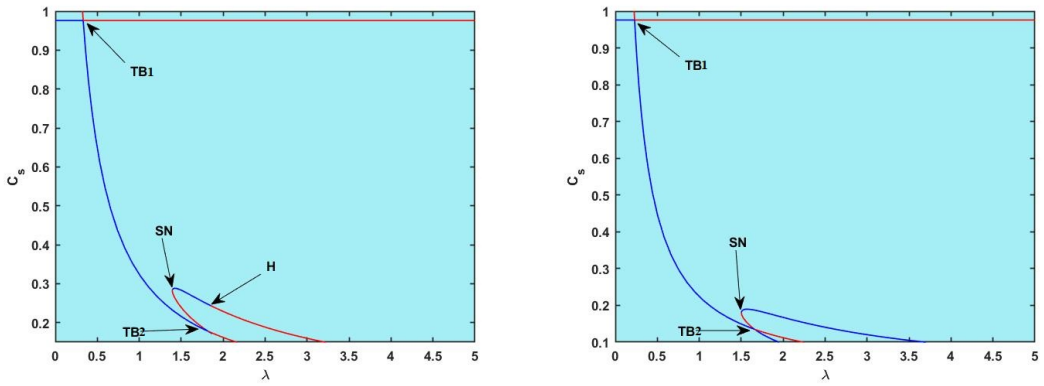

(a) (b)

Figure 2.1: Bifurcation behavior of the model system (2.3) with respect to λ for $g = 0.15$, $\omega = 0.2$, (Fig. a) and for $g = 0.2$, $\omega = 0.1$, (Fig. b), while rest of the parameter values are keep remain same as Table 2.1.

In the above bifurcation, we can observed that in the low transmission rate (λ), the coral can be more healthily in the absence of macro algae, the disease transmission rate increases to a certain level, and then coexisting state becomes more suitable position (may exist a single coexisting state or a bistable satiation or a stable oscillation arise) which play a role like double edge sward phenomenon.

Now we extend our exploration by changing the respective grazing rate (g), and disease recovery rate (ω), slightly differentl from the previous one. Set $g = 0.2$ (observing the high grazing effect from the previous bifurcation) and $\omega = 0.1$ (taken low recovery rate). From Fig. 2.1b, the bifurcation phenomenon are look like same the Fig. 2.1a, but the major change is there is no hopf bifurcation present in the diagram as well as there is two bistable region one is same as previous one and another with higher disease state with E_2. Therefore, for different combinations of the parameters, g and ω, the transmission of disease shows different characteristics in the underwater coral reef ecosystem, and we explore this whole change in our bi-parameter dependency section via two parameters bifurcation.

2.5.2 Effect of Other Parameters

The disease burden in the under water ecosystem (like coral-algae adjustment). We have already seen in the previous subsection that the role of fish predation or the coral disease's recovery rate is crucial in the underwater ecosystem's sustainability. Therefore, to observe the critical aspects of these important parameters, we also observe the dependency of these parameters through single parameter bifurcation. Initially, we set the disease transmission rate at $\lambda = 1.65$ to stay in the bistable region and vary the respective parameters g, ω.

2.5.2.1 Fish Predations

In Figure 2.2, we plot the entire bifurcation diagram of the system (2.3) with respect to the fish predation rate, g. It is observed that when the density of the macro algae is higher, then the coral-free state E_1 is stable; in other words, when the grazing rate, g is in the domain $0 < g < 0.1603$, then there is no coral in the space. After that, when we increase the grazing rate, at g= 0.1603, there is a transcritical bifurcation (TB3), and E_1 becomes unstable. Now we extend the unstable disease-free equilibrium point for the backward direction. Interestingly, when the density of macro algae is diminishing as well as increases susceptible coral reefs, there is another transcritical bifurcation (TB1) that occurs at g= 0.1328 and the disease-free state remain unstable also the unstable coexisting state appear in this parameter changes.

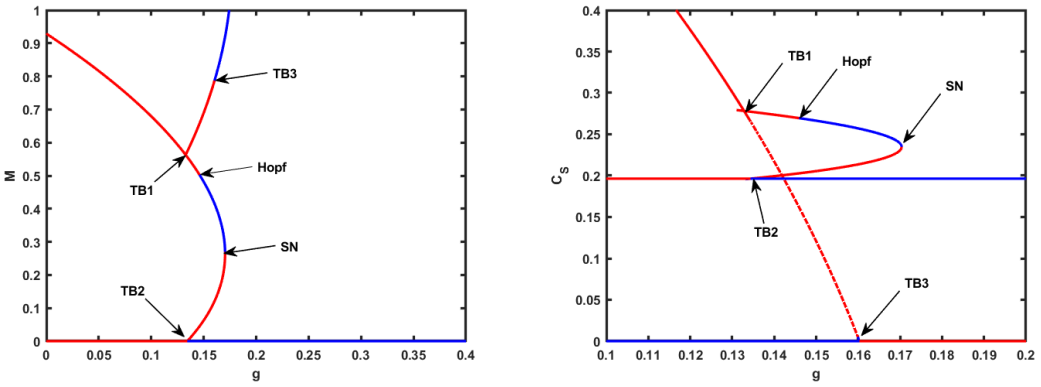

(a) (b)

Figure 2.2: Bifurcation behavior of the model system (2.3) with respect to g for $\lambda = 1.65$, $\omega = 0.2$, (Fig. a) and for $\lambda = 1.65$, $\omega = 0.2$, (Fig. b), while rest of the parameter values are keep remain same as Table 2.1.

Again, we extend the unstable branch around equilibrium E^* and for increasing the value of g, at g = 0.1459, a Hopf bifurcation (supercritical) arise at the equilibrium point E^* and the coexisting state is now stable after this bifurcation. If we further increase the parameter g, the state E^* annihilates via saddle-node bifurcation (SN) at g = 0.1703. Surprisingly, we again extend the unstable branch from the SN bifurcation point in the backward direction of the parameter value g, there is another transcritical bifurcation (TB2) happens at g = 0.1328 and the new state arise which is macro algae free coral state, E_2 and in the forward direction it stay in stable state and in the reverse direction it remains unstable state.

2.5.2.2 Recovery rate, ω

To examine the ultimate recovery mechanism for observing the parameter variation of the recovery rate (ω), in our system (2.3) is of utmost priority in the coral reef ecosystem.

Therefore, we also represent the bifurcation diagram with respect to (ω) in Figure (2.3). The analysis observed that when the recovery rate is low (in between $0 < \omega < 0.0091$), there is only a stable oscillation around the unstable coexisting equilibrium points, E^*, with a low level of disease present in this coexisting state. If we increase the rate of ω, the stable oscillation vanishes via a supercritical Hopf bifurcation, and E^* becomes a stable state. Further, we increase the recovery rate (ω), and system (2.3) has a saddle-node bifurcation at $\omega = 0.1268$. The unstable coexisting equilibrium points vanish in the higher density of infected coral reefs through a transcritical bifurcation (TB) at $\omega = 0.09881$. Moreover, through this TB bifurcation, the new equilibrium state, E_2 arises, which is stable in the forward direction and unstable in the other direction.

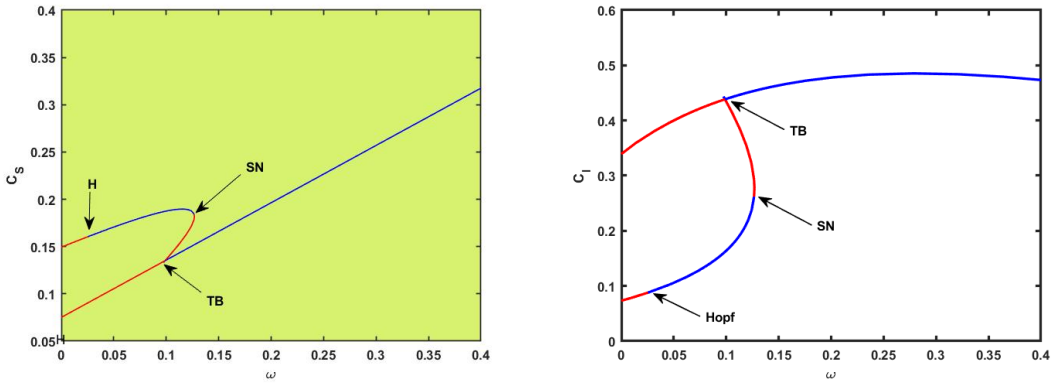

(a) (b)

Figure 2.3: Bifurcation behavior of the model system (2.3) with respect to ω for $g = 0.2$, $\lambda = 1.65$, (Fig. a) and for $g = 0.2$, $\lambda = 1.65$, (Fig. b), while rest of the parameter values are keep remain same as Table 2.1.

2.5.3 Joint Effect

In the preceding section, we conducted an in-depth analysis of single-parameter bifurcations with respect to all key parameters of the proposed system (2.3). While previous analysis provided valuable insights into the individual roles of parameters, it does not fully capture the interactive effects of the disease transmission rate and the coral recovery rate. Understanding how these two parameters jointly reflect change system dynamics is essential, particularly given their central role in determining the persistence or suppression of disease within coral reef ecosystems. Therefore, this section adopts a two-parameter bifurcation approach to examine their combined influence.

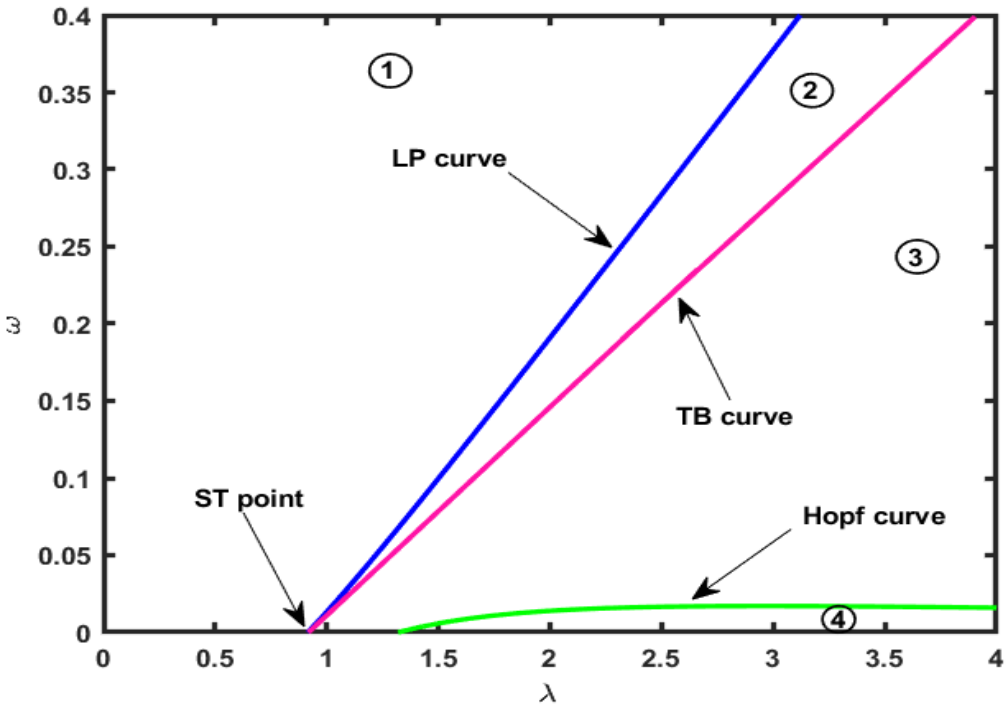

Figure 2.4: Two-parameter bifurcation diagram with respect to the contagious pathway transmission rate (λ) and the recovery rate (ω). **Region** ①: Macroalgae free coral state E_2; **Region** ②: bistability between macroalgae free coral state E_2 and endemic state E^*; **Region** ③: Endemic state E^*; **Region** ④: No stable equilibrium exists. Instead, the system exhibits sustained oscillations around the unstable coexisting state E^*. **TB**: Transcritical bifurcation, **LP**: Saddle-node bifurcation, **ST** point: Saddla-node transcritical curve intersection point. The other parameters values taken from Table Table 2.1.

The two-parameter bifurcation diagram in the (λ, ω) plane offers critical insight into how the interaction between disease transmission rate (λ) and coral recovery rate (ω) governs the overall dynamics of the coral reef ecosystem. This parameter space is partitioned by three key bifurcation curves saddle-node bifurcation (LP) curve, the Transcritical Bifurcation (TB) curve, and the Hopf bifurcation curve into four biologically meaningful regions. In Region ①, found in the upper-left portion of the diagram, the macroalgae-free coral equilibrium point E_2 is stable, indicating that high recovery and low transmission favor coral dominance. As we move across the diagram, Region ② appears between the LP and TB curves, exhibiting bistability between E_2 and the coexisting state E^*, where outcomes depend on initial conditions. Beyond the TB curve lies Region ③, where only the coexisting state E^* is stable, reflecting dominance by mixed coral-macroalgae-disease interactions. Lastly, Region ④, located below the Hopf curve, is marked by persistent oscillations with no stable equilibrium, driven by high transmission and insufficient recovery.

2.6 Discussion and Conclusion

2.6.1 Discussion

This study presents a mathematical framework that captures the complex interplay between coral disease transmission, macroalgal competition, fish grazing, and recovery mechanisms. Through both analytical and numerical bifurcation analyses, the model uncovers rich dynamical behavior, including transcritical, saddle-node, and Hopf bifurcations, which govern transitions between ecological states in coral reef systems.

One of the central findings is the presence of *bistability*, meaning that coral reefs can settle into either a low-disease or a high-disease state, depending on initial conditions and parameter values. This emphasizes the ecological concept of *alternative stable states*, where even small environmental changes can tip the system from a healthy to a degraded state.

Fish grazing is identified as a critical ecological force. While insufficient grazing allows macroalgae to dominate and suppress coral, moderate grazing supports a stable coexistence. On the other hand, excessive grazing can destabilize the system and even induce oscillatory behavior. The role of coral recovery is equally important. The analysis shows that even under high disease pressure, increasing the recovery rate can prevent coral extinction and shift the system from unstable oscillations to a stable equilibrium. This highlights the importance of natural healing processes and assisted recovery strategies in coral reef conservation. Importantly, at high disease transmission rates, the system can undergo a Hopf bifurcation, leading to sustained oscillations in coral and disease levels rather than settling into a stable equilibrium. This reflects real-world observations of recurrent disease outbreaks and underscores the need for adaptive, ongoing management.

2.6.2 Conclusion

The study concludes that coral reef ecosystems exist in a fragile balance that can be disrupted or stabilized by several interacting factors. The model confirms that:

- Bistability and tipping points are inherent features of coral-disease dynamics.
- Fish grazing acts as a regulator: too little or too much can be destabilizing.
- Coral recovery is a powerful factor that can prevent collapse, even under stress.
- Oscillatory disease dynamics may emerge under high transmission, requiring constant ecological monitoring.

From a conservation standpoint, the model highlights the importance of managing disease transmission and promoting coral resilience. Practical strategies such as regulating fishing pressure, reducing pollution, and implementing active restoration (e.g., coral transplants or probiotics) are vital.

3

Effect of Delay on Coral Reef Ecosystem with Disease Presence in Coral Species

3.1 Introduction

Coral reefs are vital marine ecosystems, providing habitat and food for diverse species while supporting coastal economies and protecting shorelines [164, 165]. These reefs, built by coral colonies in mutualistic association with algae, are increasingly threatened by biotic (e.g., pathogens) and abiotic (e.g., temperature shifts) stressors [166, 167]. Coral diseases, such as White Band Disease (WBD), spread through direct contact, waterborne transmission, and vectors like corallivorous reef fish [112, 168]. Human activities, climate change, and pollution exacerbate disease outbreaks, leading to significant coral decline [97, 169]. Understanding disease transmission is crucial, yet gaps remain in identifying key pathogens and their vectors. Recent research highlights the role of corallivores and plastic marine debris in disease spread [170, 171]. Additionally, time delays in biological interactions, such as incubation periods, influence disease dynamics and ecosystem stability [120, 122]. This study extends existing coral disease models by incorporating an incubation time lag, allowing for a more realistic representation of disease progression. By analyzing different transmission pathways and their long-term impact on coral populations, we aim to provide insights into reef ecosystem stability and potential recovery mechanisms.

3.2 Basic Assumptions and Mathematical Model

We proposed a mathematical model studied by Briggs *et al.* [156] that captures the temporal nature of coral reef ecosystem, where the space on a reef is inhabited by vital benthic organisms namely coral, macroalgae, and turf algae. This model has revealed that the dynamics of fraction of the space inhabited by these key groups changes over time. In the natural environment, these groups can exhibit a significant species diversity. However, for modelling the coral reef ecosystem, Briggs *et al.* [156] treated macroalgae as a singular, unstructured state variable (commonly used hypothesis), where all life stages were considered equally susceptible to herbivory. They also assumed that any vacant space on the reef was promptly filled by turf, refering to low-growing filamentous algae with a height of less than 10 mm. They classified crustose coralline algae as a part of the turf category for the reason that both turf and crustose coralline algae substrates could be overgrown by either coral or macroalgae. Herbivorous fish have the potential to control macroalgae, which are competitors of corals for space [123]. In their model, they did not explicitly account for the population dynamics of fish but incorporated the loss of algae caused by herbivory into the macroalgae mortality rate.

The model [156] delineates the changes over time in the proportions of seabed within the reef ecosystem and is governed by a system of coupled nonlinear ordinary differential equations:

$$\begin{aligned} \frac{dC}{dt} &= rT + gTC - \gamma g_1 MC - dC \\ \frac{dM}{dt} &= \mu T + g_1 TM + \gamma g_1 MC - vM. \end{aligned} \tag{3.1}$$

Where the reef space is occupied by coral (C), macroalgae (M), and turf (T). At any given time t, the total reef area is divided among these three states ($C(t)$, $M(t)$, $T(t)$), with the condition that $C(t)+M(t)+T(t)=1$. Following [156], we propose that both coral and macroalgae can be recruited either from local sources or through external/open recruitment. Open recruitment of propagules exclusively arises due to the free space available for corals as well as macroalgae. Coral can only expand laterally into available free space, whereas macroalgae have the ability to grow over both unoccupied areas and existing coral. The term $r(\mu)$ indicates the recruitment rate of coral (macroalgae) and g signifies the rate at which free space is colonized by coral, resulting from both the local recruitment of coral and its horizontal expansion. The term g_1TM represents the overall rate of macroalgae recruitment and its lateral expansion into available free space. It is assumed that macroalgae grow more slowly on coral compared to their growth rate in free space. Consequently, the macroalgae growth rate over coral is γg_1 with a scaling parameter $\gamma\,(\leq 1)$. The parameters d and v denote the mortality rates for coral and susceptibl macroalgae, respectively. In this model, all macroalgae are assumed to be vulnerable, and herbivorous fish are not included as dynamic variables. Consequently, the grazing pressure exerted by fish on macroalgae

is incorporated into the macroalgae death rate (v). If the population of herbivorous fish is reduced due to fishing, the value of the parameter v will decrease accordingly.
It is well established from experimental studies [115, 117, 168, 172–174] that disease spreads from infected to susceptible corals via vectors and may influence reef structure and dynamics. Black band disease (BBD) is spread from infected to susceptible corals via direct contact [122]. Williams et al. [134] and Vollmer et al. [175] point out that white band disease (WBD) spreads through coral-coral contact. Hence, coral disease is a major factor contributing to coral degradation. Considering these factors, we modify the model proposed by Briggs *et al.* [156] by incorporating disease in coral reef. Given the occurrence of disease in corals [97, 176], our model for coral populations is based on traditional disease models (SIR models), which forecast the behavior of healthy and infected individuals [177, 178]. To simplify our model, we assume that the disease spreads into the coral species via contact, i.e., susceptible corals (S) can be infected through adequate direct contact with infected corals (I). The disease transmission process obeys the mass-action principle as λSI, where the parameter λ represents the disease transmission rate and it roughly indicates the fraction of encounters leading to instantaneous infection. Infected coral colonies experience an additional mortality rate of e. Coral colonies have an ability to recover from lesions through tissue regeneration or by shedding diseased tissue, giving rise to no longer visible signs of infection [145]. Moreover, we assume that colonies that have recovered from the disease continue to be susceptible and that infected colonies transition back to the susceptible group at an instantaneous rate of ω. Based on the aforementioned assumptions, the model (3.1) takes the form:

$$\begin{aligned} \frac{dS}{dt} &= rT + gT(S+I) - \gamma g_1 M(S+I) - dS - \lambda SI + \omega I \\ \frac{dI}{dt} &= \lambda SI - (d+e)I - \omega I \\ \frac{dM}{dt} &= \mu T + g_1 TM + \gamma g_1 M(S+I) - vM. \end{aligned} \tag{3.2}$$

It is widely recognised that time lags are a prevalent and complex occurrence in the field of population biology. So, in reality, there's a temporal gap between the first contact of a healthy individual with an infected individual and the onset of the latter's infectious period. We accounted for the delay (τ), which represents the time it takes for infectious agents to establish themselves in the healthy coral, after which the coral becomes infectious. Therefore, this time lag is incorporated into the model (3.2) in the following manner:

$$\begin{aligned} \frac{dS}{dt} &= rT + gT(S+I) - \gamma g_1 M(S+I) - dS - \lambda \int_{-\infty}^{t} S(\tilde{\kappa})I(\tilde{\kappa})\Pi(t-\tilde{\kappa})d\tilde{\kappa} + \omega I \\ \frac{dI}{dt} &= \lambda \int_{-\infty}^{t} S(\tilde{\kappa})I(\tilde{\kappa})\Pi(t-\tilde{\kappa})d\tilde{\kappa} - (d+e)I - \omega I \\ \frac{dM}{dt} &= \mu T + g_1 TM + \gamma g_1 M(S+I) - vM. \end{aligned} \tag{3.3}$$

The number of infected coral at time t is determined by the number of healthy coral that became infected at a previous time, $t - \tilde{\kappa}$. The probability distribution of this delay, $\tilde{\kappa}$, is

represented by the memory function Π. This function is defined as follows:

$$\Pi = \frac{\sigma^{j+1}\tilde{\kappa}^j}{j!} exp(-\sigma\tilde{\kappa}),$$

where σ is a positive constant and $j \in \mathbb{Z}$ is representing the order of the time lag. According to [179], the average time lag is determined as

$$\tilde{T} = \int_0^\infty \tilde{\kappa}\Pi(\tilde{\kappa})d\tilde{\kappa} = \frac{j+1}{\sigma}.$$

Now we consider the memory function in terms of the delta function as

$$\Pi = \delta(\tilde{\kappa} - \tau),$$

where τ is a non-negative constant. Thus, the model (3.3) becomes

$$\begin{array}{rcl} \frac{dS}{dt} & = & rT + gT(S+I) - \gamma g_1 M(S+I) - dS - \lambda S(t-\tau)I(t-\tau) + \omega I \\ \frac{dI}{dt} & = & \lambda S(t-\tau)I(t-\tau) - (d+e)I - \omega I \\ \frac{dM}{dt} & = & \mu T + g_1 TM + \gamma g_1 M(S+I) - vM. \end{array} \tag{3.4}$$

In this model, it is assumed that a particular region of the seabed is covered entirely by healthy coral (S), infected coral (I), macroalgae (M), and algal turfs (T), so that $S+I+M+T=1$. Thus, the model takes the form:

$$\begin{array}{rcl} \frac{dS}{dt} & = & \Big[r+g(S+I)\Big]\Big[1-(S+I+M)\Big] - \gamma g_1 M(S+I) - dS \\ & & -\lambda S(t-\tau)I(t-\tau) + \omega I \equiv F_1(S,I,M), \\ \frac{dI}{dt} & = & \lambda S(t-\tau)I(t-\tau) - (d+e)I - \omega I \equiv F_2(S,I,M), \\ \frac{dM}{dt} & = & \Big[\mu + g_1 M\Big]\Big[1-(S+I+M)\Big] + \gamma g_1 M(S+I) - vM \equiv F_3(S,I,M). \end{array} \tag{3.5}$$

The initial conditions for the system (3.5) are taken to be of the form:

$$S(\phi) = \psi_1(\phi), I(\phi) = \psi_2(\phi), M(\phi) = \psi_3(\phi), -\tau \le \phi \le 0, \tag{3.6}$$

where $\psi = (\psi_1, \psi_2, \psi_3)^T \in \mathscr{C}_+$ such that $\psi_i(\phi) \ge 0$ $(i = 1,2,3)$, $\forall\ \phi \in [-\tau, 0]$ and $\mathscr{C}_+$ denotes the Banach space $\mathscr{C}_+([-\tau,0], \mathbf{R}^3_{+0})$ of continuous functions mapping the interval $[-\tau,0]$ into $\mathbf{R}^3_{+0}$ with the norm of an element ψ in $\mathscr{C}_+$ defined by $\|\psi\| = \sup_{-\tau\le\phi\le 0}\{|\ \psi_1(\phi)\ |, |\ \psi_2(\phi)\ |, |\ \psi_3(\phi)\ |\}$. For biological feasibility, we further assume that $\psi_i(0) > 0$, for $i = 1,2,3$.

3.3 Preliminary Result

Lemma 3.1 *(Existence and positive invariance) There exists a unique solution* $(S(t),I(t),M(t))$ *for the system (3.5) with initial conditions (3.6) in the interval* $[0,\infty)$ *and remains positive* $\forall\, t > 0$.

Proof: The model (3.5) can be expressed as $\dot{Z} = F(Z)$, where $Z \equiv (S,I,M)^T$ and $F : \mathscr{C}_+ \longrightarrow \mathbf{R}^3_{+\mathbf{0}}$ with $F = (F_1,F_2,F_3)^T$, $F_i \in \mathscr{C}^\infty(\mathbf{R}_{+\mathbf{0}})$ for $i = 1,2,3$. Then, we have

$$
\begin{aligned}
F_1 &= \Big[r+g(S+I)\Big]\Big[1-(S+I+M)\Big] - \gamma g_1 M(S+I) - dS - \lambda S(t-\tau)I(t-\tau) + \omega I,\\
F_2 &= \lambda S(t-\tau)I(t-\tau) - (d+e)I - \omega I,\\
F_3 &= \Big[\mu + g_1 M\Big]\Big[1-(S+I+M)\Big] + \gamma g_1 M(S+I) - vM.
\end{aligned}
$$

Let $Z(\phi) = (\psi_1(\phi),\psi_2(\phi),\psi_3(\phi)) \in \mathscr{C}_+$ and $\psi_i(\phi) \geq 0$ for $i = 1,2,3$ with $\phi \in [-\tau,0]$, $\tau > 0$. As the vector function F is a locally Lipschitzian and completely continuous function of variables S,I,M in $\Omega = \{(S(t),I(t),M(t)); S > 0, I > 0, M > 0\}$. According to the lemma [180], any solution (S,I,M) of (3.5) with initial conditions (3.6) exists and is unique in the interval $[0,a_0]$, $\forall\, t \geq 0$, where a_0 is a finite positive real number.

3.4 Qualitative Analysis of the Model Without Time Lag

In the absence of time lag $(\tau = 0)$, the system (3.5) has two non-negative equilibria. The disease free equilibrium point is $L_1(S_1,0,M_1)$, where $S_1 = \frac{\mu+(g_1-v-\mu)M_1-gM_1^2}{\mu+(1-\gamma)g_1M_1}$ and M_1 is the positive zero of the polynomial equation

$$a_0M_1^4 + a_1M_1^3 + a_2M_1^2 + a_3M_1 + a_4 = 0, \tag{3.7}$$

with

$$
\begin{aligned}
a_0 &= g^3+g_1^3(1-\gamma)^2-gg_1^2(1-\gamma),\\
a_1 &= 2\mu g_1^2(1-\gamma)-g^2g_1(1-\gamma)-\mu gg_1+g_1^2(1-\gamma)(g_1-v-\mu)-\frac{dgg_1(1-\gamma)}{r+\mu+1}+\frac{vg_1^2(1-\gamma)^2}{r+\mu+1},\\
a_2 &= g(g_1-v-\mu)^2-2g^2(g_1-v-\mu)-2\mu g^2+g_1\mu^2-g^2\mu+g_1(1-\gamma)(g_1-v-\mu)\\
&+ \mu g_1(g_1-v-\mu)+\mu g_1^2(1-\gamma)-\frac{gd\mu}{r+\mu+1}+\frac{dg_1(1-\gamma)(g_1-v-\mu)}{r+\mu+1}+\frac{2v\mu g_1(1-\gamma)}{r+\mu+1}\\
&- \frac{(r+\mu)g_1^2(1-\gamma)^2}{r+\mu+1},\\
a_3 &= \mu g(g_1-v-\mu)+\mu gg_1(1-\gamma)+g_1\mu^2+\frac{d\{(g_1-v-\mu)\mu+\mu g_1(1-\gamma)\}}{r+\mu+1}+\frac{v\mu^2}{r+\mu+1}\\
&- \frac{(r+\mu)2\mu g_1(1-\gamma)}{r+\mu+1},\\
a_4 &= 2g\mu^2+2\mu g(g_1-v-\mu)+\frac{d\mu^2}{r+\mu+1}-\frac{(r+\mu)\mu^2}{r+\mu+1}.
\end{aligned}
$$

The coexisting positive interior equilibrium point is $L_*(S_*,I_*,M_*)$, where $S_*=\frac{d+e+\omega}{\lambda}$ and $I_*=\frac{(\mu+g_1M_*)(1-S_*-M_*)+(\gamma g_1S_*-v)M_*}{\mu+(1-\gamma)g_1M_*}$ with M_* being the positive root of the following equation

$$b_0M^5+b_1M^4+b_2M^3+b_3M^2+b_4M+b_5=0, \tag{3.8}$$

with

$$
\begin{aligned}
b_0 &= rg_1^2,\\
b_1 &= -2g_1(-\mu+g_1-g_1S_*+\gamma g_1S_*-v)r,\\
b_2 &= r(-\mu+g_1-g_1S_*+\gamma g_1S_*-v)^2-2\mu g_1(1-S_*)-g_1\{2rS_*+(1+\gamma)g\}+(g-r-\lambda S_*\\
&+ \omega)g_1^2(1-\gamma),\\
b_3 &= 2r\mu(1-S_*)(-\mu+g_1-g_1S_*+\gamma g_1S_*-v)+\{2rS_*+(1+\gamma)g\}(-\mu+g_1-g_1S_*+\gamma g_1S_*-v)\\
&+ \{rS_*^2+(1+\gamma)gS_*\}g_1(1-\gamma)-(g-r-\lambda S_*+\omega)\{g_1(1-\gamma)(-\mu+g_1-g_1S_*+\gamma g_1S_*-v\\
&- g_1\mu)\}-\{r+(g-r-d)S_*\}g_1^2(1-\gamma)^2,\\
b_4 &= r\mu^2(1-S_*)^2+\{2rS_*+(1+\gamma)g\}\mu(1-S_*)+\{rS_*^2+(1+\gamma)gS_*\}\mu-(g-r-\lambda S_*+\omega)\\
&\{\mu(-\mu+g_1-g_1S_*+\gamma g_1S_*-v)+g_1(1-\gamma)\mu(1-S_*)\}-\{r+(g-r-d)S_*\}2\mu g_1(1-\gamma),\\
b_5 &= -[(g-r-\lambda S_*+\omega)\mu^2(1-S_*)+\{r+(g-r-d)S_*\}\mu^2].
\end{aligned}
$$

So the disease free equilibrium point $L_1(S_1,0,M_1)$ is admissible for $g_1 > g_1^0$ with $g_1^0 = gM_1+v+\mu(1-\frac{1}{M_1})$ and the sufficient condition for existence of positive interior equilibrium point $L_*(S_*,I_*,M_*)$ is $S_* > \frac{v}{\gamma g_1}$.

3.4.1 Stability Analysis

In this section, we deal with local stability of the system (3.5) around the disease free and interior equilibrium points. At the disease free equilibrium point $L_1(S_1,0,M_1)$, the Jacobian matrix is

$$
J_1 = \begin{bmatrix}
\frac{\partial F_1}{\partial S}|_{(S_1,0,M_1)} & \frac{\partial F_1}{\partial I}|_{(S_1,0,M_1)} & \frac{\partial F_1}{\partial M}|_{(S_1,0,M_1)}\\
0 & \frac{\partial F_2}{\partial I}|_{(S_1,0,M_1)} & 0\\
\frac{\partial F_3}{\partial S}|_{(S_1,0,M_1)} & \frac{\partial F_3}{\partial I}|_{(S_1,0,M_1)} & \frac{\partial F_3}{\partial M}|_{(S_1,0,M_1)}
\end{bmatrix}.
$$

The characteristic values of the Jacobian matrix J_1 are $\lambda_1 = \frac{\partial F_2}{\partial I}|_{(S_1,0,M_1)} = \lambda S_1-(d+e+\omega)$ and other two values are the zeros of the equation

$$
\lambda^2-\lambda\left(\frac{\partial F_1}{\partial S}|_{(S_1,0,M_1)}+\frac{\partial F_3}{\partial M}|_{(S_1,0,M_1)}\right)+\frac{\partial(F_1,F_3)}{\partial(S,M)}|_{(S_1,0,M_1)}=0.
$$

The zeros of the equation are negative or having negative real parts if $\frac{\partial F_1}{\partial S}|_{(S_1,0,M_1)} + \frac{\partial F_3}{\partial M}|_{(S_1,0,M_1)} < 0$ and $\frac{\partial (F_1,F_3)}{\partial (S,M)}|_{(S_1,0,M_1)} > 0$. Now the characteristic value $\lambda_1 = \frac{\partial F_2}{\partial I}|_{(S_1,0,M_1)} < 0$ when $R_0 < 1$, where the threshold parameter R_0 is defined by

$$R_0 = \left\{ \frac{\lambda S_1}{d+e+\omega} \right\} = \left\{ \frac{\text{Infection rate of a new infective coral}}{\text{Removal rate of infected coral}} \right\},$$

that is, the ratio between the infection rate of a new infective coral appearing in fully susceptible/healthy coral species and the removal rate of infected coral species around $L_1(S_1,0,M_1)$. After some algebraic manipulation, we have $\frac{\partial F_1}{\partial S}|_{(S_1,0,M_1)} + \frac{\partial F_3}{\partial M}|_{(S_1,0,M_1)} < 0$ when $r > r_{[0]}$, where $r_{[0]} = \frac{(g+g_1)\{1-(S_1+M_1)\}+g_1(\gamma S_1 - M_1)-(gS_1+d+v+\mu)}{1+g_1 M_1}$.

For the stability analysis of steady state interior equilibrium point is $L_*(S_*,I_*,M_*)$, we linearize the system (3.5) around L_* and obtain the corresponding Jacobian matrix

$$J_* = \begin{bmatrix} a_{11} & a_{12} & a_{13} \\ a_{21} & 0 & 0 \\ a_{31} & a_{32} & a_{33} \end{bmatrix},$$

where

$$\begin{aligned}
a_{11} = \frac{\partial F_1}{\partial S}|_{(S_*,I_*,M_*)} &= -\{r+g(S_*+I_*)\} + \{1-(S_*+I_*+M_*)\}g - \gamma g_1 M_* - d - \lambda I_*, \\
a_{12} = \frac{\partial F_1}{\partial I}|_{(S_*,I_*,M_*)} &= -\{r+g(S_*+I_*)\} + \{1-(S_*+I_*+M_*)\}g - \gamma g_1 M_* - \lambda S_* + \omega, \\
a_{13} = \frac{\partial F_1}{\partial M}|_{(S_*,I_*,M_*)} &= -\{r+g(S_*+I_*)\} - \gamma g_1 (S_*+I_*), \\
a_{21} = \frac{\partial F_2}{\partial S}|_{(S_*,I_*,M_*)} &= \lambda I_*, \\
a_{31} = \frac{\partial F_3}{\partial S}|_{(S_*,I_*,M_*)} &= -(\mu + g_1 M_*) + \gamma g_1 M_*, \\
a_{32} = \frac{\partial F_3}{\partial S}|_{(S_*,I_*,M_*)} &= -(\mu + g_1 M_*) + \gamma g_1 M_*, \\
a_{33} = \frac{\partial F_3}{\partial I}|_{(S_*,I_*,M_*)} &= \{1-(S_*+I_*+M_*)\}g_1 - (\mu + g_1 M_*) + \gamma g_1 (S_*+I_*) - v.
\end{aligned}$$

The characteristic equation for J_* is

$$\mu^3 - Trace(J_*)\mu^2 + \Delta\mu - \frac{\partial (F_1,F_2,F_3)}{\partial (S,I,M)}|_{(S_*,I_*,M_*)} = 0, \tag{3.9}$$

where

$$\begin{aligned} Trace(J^*) &= a_{11}+a_{33}, \\ \Delta &= a_{11}a_{33}-a_{12}a_{21}-a_{13}a_{31}, \\ \frac{\partial(F_1,F_2,F_3)}{\partial(S,I,M)}|_{(S_*,I_*,M_*)} &= a_{12}a_{21}a_{33}-a_{13}a_{32}a_{21}. \end{aligned}$$

According to the Routh-Hurwitz criteria, the interior equilibrium point L_* is stable if $Trace(J_*)<0$, $\frac{\partial(F_1,F_2,F_3)}{\partial(S,I,M)}|_{(S_*,I_*,M_*)}<0$ and $Trace(J_*)\Delta<\frac{\partial(F_1,F_2,F_3)}{\partial(S,I,M)}|_{(S_*,I_*,M_*)}$.
We summarize the dynamics of system (3.5) in form of the following theorem.

Theorem 3.2 *In the absence of time lag ($\tau=0$), the stability of the system (3.5) around two equilibrium points can be described as follows:*
(i) The disease-free equilibrium point $L_1(S_1,0,M_1)$ of the system (3.5) is locally asymptotically stable for $R_0<1$, $r>r_{[0]}$ and $\frac{\partial(F_1,F_3)}{\partial(S,M)}|_{(S_1,0,M_1)}>0$, otherwise it is unstable;
(ii) The interior equilibrium point $L_*(S_*,I_*,M_*)$ of the system (3.5) is locally asymptotically stable for $Trace(J_*)<0$, $\frac{\partial(F_1,F_2,F_3)}{\partial(S,I,M)}|_{(S_*,I_*,M_*)}<0$ and $Trace(J_*)\Delta<\frac{\partial(F_1,F_2,F_3)}{\partial(S,I,M)}|_{(S_*,I_*,M_*)}$.

3.5 Qualitative Analysis of the Model With Time Lag

3.5.1 Local Stability Analysis

The linearized system of (3.5) at any equilibrium point $\widehat{L}=(\widehat{S},\widehat{I},\widehat{M})$ can be expressed as

$$\begin{aligned} \dot{x}(t) &= \Big[-\{r+g(\widehat{S}+\widehat{I})\}+\{1-(\widehat{S}+\widehat{I}+\widehat{M})\}g-\gamma g_1\widehat{M}-d-\lambda\widehat{I}\Big]x(t) \\ &+ \Big[-\{r+g(\widehat{S}+\widehat{I})\}+\{1-(\widehat{S}+\widehat{I}+\widehat{M})\}g-\gamma g_1\widehat{M}+\omega\Big]y(t) \\ &+ \Big[-\{r+g(\widehat{S}+\widehat{I})\}-\gamma g_1(\widehat{S}+\widehat{I})\Big]z(t)-\lambda\widehat{I}x(t-\tau)-\lambda\widehat{S}y(t-\tau), \\ \dot{y}(t) &= -(d+e+\omega)y(t)+\lambda\widehat{I}x(t-\tau)+\lambda\widehat{S}y(t-\tau), \\ \dot{z}(t) &= \Big[-(\mu+g_1\widehat{M})+\gamma g_1\widehat{M}\Big]x(t)+\Big[-(\mu+g_1\widehat{M})+\gamma g_1\widehat{M}\Big]y(t)+\Big[\{1-(\widehat{S}+\widehat{I}+\widehat{M})\}g_1 \\ &- (\mu+g_1\widehat{M})+\gamma g_1(\widehat{S}+\widehat{I})-v\Big]z(t). \end{aligned} \tag{3.10}$$

Then, the characteristic equation of the delayed system (3.5) around any equilibrium point $\widehat{L}=(\widehat{S},\widehat{I},\widehat{M})$ is given by

$$det\begin{bmatrix} -\{r+g(\widehat{S}+\widehat{I})\}+\{1-(\widehat{S}+\widehat{I}+\widehat{M})\}g & -\{r+g(\widehat{S}+\widehat{I})\}+\{1-(\widehat{S}+\widehat{I}+\widehat{M})\}g & -\{r+g(\widehat{S}+\widehat{I})\} \\ -\gamma g_1\widehat{M}-d-\lambda\widehat{I}-\lambda\widehat{I}e^{-\rho\tau}-\rho & -\gamma g_1\widehat{M}+\omega-\lambda\widehat{S}e^{-\rho\tau} & -\gamma g_1(\widehat{S}+\widehat{I}) \\ \lambda\widehat{I}e^{-\rho\tau} & -(d+e+\omega)+\lambda\widehat{S}e^{-\rho\tau}-\rho & 0 \\ -(\mu+g_1\widehat{M})+\gamma g_1\widehat{M} & -(\mu+g_1\widehat{M})+\gamma g_1\widehat{M} & \{1-(\widehat{S}+\widehat{I}+\widehat{M})\}g_1 \\ & & -(\mu+g_1\widehat{M})+\gamma g_1(\widehat{S}+\widehat{I})-v \end{bmatrix}=0. \tag{3.11}$$

The characteristic equation at $L_*(S_*, I_*, M_*)$ reduces to the following transcendental equation

$$\rho^3 + A_1\rho^2 + A_2\rho + A_3 + (B_1\rho^2 + B_2\rho + B_3)\mathrm{e}^{-\rho\tau} = 0, \tag{3.12}$$

where

$$\begin{aligned} A_1 &= -(l_{11}+l_{22}+l_{33}), \quad A_2 = l_{11}(l_{22}+l_{33}) + l_{22}l_{33} + l_{13}l_{31}, \quad A_3 = l_{13}l_{31}l_{22} - l_{11}l_{22}l_{33}, \\ B_1 &= l_{11}^{'} - l_{12}^{'}, \quad B_2 = l_{11}l_{12}^{'} - l_{11}^{'}(l_{12}+l_{22}) + l_{33}l_{12}^{'} - l_{33}l_{11}^{'}, \quad B_3 = l_{22}l_{33}l_{11}^{'} - l_{11}l_{33}l_{12}^{'} \\ &+ l_{12}l_{33}l_{11}^{'} - l_{13}l_{32}l_{11}^{'} + l_{13}l_{31}l_{12}^{'}, \end{aligned}$$

with

$$\begin{aligned} l_{11} &= -\{r + g(S_* + I_*)\} + \{1 - (S_* + I_* + M_*)\}g - \gamma g_1 M_* - d, \\ l_{12} &= -\{r + g(S_* + I_*)\} + \{1 - (S_* + I_* + M_*)\}g - \gamma g_1 M_* + \omega, \\ l_{13} &= -\{r + g(S_* + I_*)\} - \gamma g_1 (S_* + I_*), \\ l_{22} &= -(d + e + \omega), \quad l_{31} = -(\mu + g_1 M_*) + \gamma g_1 M_*, \quad l_{32} = -(\mu + g_1 M_*) + \gamma g_1 M_*, \\ l_{33} &= \{1 - (S_* + I_* + M_*)\}g_1 - (\mu + g_1 M_*) + \gamma g_1 (S_* + I_*) - v, \\ l_{11}^{'} &= \lambda I_*, \quad l_{12}^{'} = \lambda S_*. \end{aligned}$$

It is widely understood that the delay-induced system (Equation 3.5) will exhibit asymptotic stability at the equilibrium point $\widehat{L}$ if all the characteristic roots of equation (3.11) possess negative real parts. The equation (3.11) has infinitely many eigenvalues due to a transcendental form. Consequently, the conventional Routh-Hurwitz criterion is inapplicable for determining the stability of the system. To analyse the stability characteristics, we must determine the signs of the real parts of the roots of equation (3.11). We assume that the equilibrium point $\widehat{L}$ of the system (3.5) is asymptotically stable without any time delay ($\tau = 0$). Next, we identify the condition(s) for which $\widehat{L}$ becomes unstable. According to Rouche's theorem [181] and the continuity with respect to τ, the transcendental equation (3.11) will have roots with positive real parts if and only if it has purely imaginary zeros. Therefore, we investigate intricate solutions to the equation (3.11) in order to identify the conditions that lead to a change in stability. Let $\mu(\tau) = u(\tau) + iw(\tau)$ denote the eigenvalue of equation (3.11), where $u(\tau)$ and $w(\tau)$ are real numbers. If the equilibrium point $\widetilde{L}$ of the system without delay is stable, it follows that $u(0) < 0$. By continuity, for a small enough positive value of τ such that $u(\tau) < 0$, $\widehat{L}$ remains stable. Stability switching occurs at a specific positive value of τ, denoted by $\widehat{\tau}$, where $u(\widehat{\tau}) = 0$ and $w(\widehat{\tau}) \neq 0$. This means that $\mu = iw(\widehat{\tau})$ is a purely imaginary root of equation(3.11). Therefore, $\widehat{L}$ becomes unstable

when $u(\widehat{\tau}) > 0$. Conversely, the equilibrium point $\widehat{L}$ remains stable as long as $w(\widehat{\tau})$ is absent. In this situation, equation (3.11) has no purely imaginary roots for any value of τ.
When there is no time delay ($\tau = 0$), the steady state solution $L_*(S_*, I_*, M_*)$ of the system (3.5) is stable if $Trace(J_*) < 0$, $\frac{\partial(F_1,F_2,F_3)}{\partial(S,I,M)}|_{(S_*,I_*,M_*)} < 0$ and $Trace(J_*)\Delta < \frac{\partial(F_1,F_2,F_3)}{\partial(S,I,M)}|_{(S_*,I_*,M_*)}$, as stated in Theorem 3.2 (ii).
Next, let $\rho = \xi + i\delta$ be the eigenvalue of the characteristic equation (3.12). By substituting this value into (3.12) and separating it into real and imaginary components, we get the following results:

$$\begin{aligned}&\xi^3 - 3\xi\delta^2 + A_1(\xi^2 - \delta^2) + A_2\xi + A_3 + [\{B_1(\xi^2 - \delta^2) + B_2\xi + B_3\}\cos\delta\tau \\ &+ (2B_1\xi\delta + \delta B_2)\sin\delta\tau]e^{-\xi\tau} = 0,\end{aligned} \tag{3.13}$$

and

$$\begin{aligned}&3\xi^2\delta - \delta^3 + 2A_1\xi\delta + A_2\delta + [(2B_1\xi\delta + B_2\delta)\cos\delta\tau - \{(\xi^2 - \delta^2)B_1 \\ &+ \xi B_2 + B_3\}\sin\delta\tau]e^{-\xi\tau} = 0.\end{aligned} \tag{3.14}$$

For a stability change to occur at the equilibrium point L_* , it is essential that the characteristic equation (3.12) must have purely imaginary roots. By setting $\xi = 0$ in equations (3.13) and (3.14), we get

$$A_3 - A_1\delta^2 = (B_1\delta^2 - B_3)\cos\delta\tau - \delta B_2\sin\delta\tau, \tag{3.15}$$

$$A_2\delta - \delta^3 = -B_2\delta\cos\delta\tau - (B_1\delta^2 - B_3)\sin\delta\tau. \tag{3.16}$$

Eliminating τ by squaring and adding (3.15) and (3.16), we get the equation in terms of δ as

$$\delta^6 + (A_1^2 - 2A_2 - B_1^2)\delta^4 + (A_2^2 - 2A_1A_3 - B_2^2 + 2B_1B_3)\delta^2 + (A_3^2 - B_3^2) = 0. \tag{3.17}$$

Substituting $\delta^2 = \vartheta$ in Eq. (3.17) leads to a cubic equation of the form

$$k(\vartheta) = \vartheta^3 + \kappa_1\vartheta^2 + \kappa_2\vartheta + \kappa_3 = 0, \tag{3.18}$$

where $\kappa_1 = (A_1^2 - 2A_2 - B_1^2)$, $\kappa_2 = (A_2^2 - 2A_1A_3 - B_2^2 + 2B_1B_3)$, $\kappa_3 = (A_3^2 - B_3^2)$. From (3.18), we have

$$\frac{dk(\vartheta)}{d\vartheta} = 3\vartheta^2 + 2\kappa_1\vartheta + \kappa_2. \tag{3.19}$$

Solving

$$\frac{dk(\vartheta)}{d\vartheta} = 3\vartheta^2 + 2\kappa_1\vartheta + \kappa_2 = 0, \tag{3.20}$$

we obtain

$$\vartheta_{1,2} = \tfrac{1}{3}[-\kappa_1 \pm \sqrt{\kappa_1^2 - 3\kappa_2}]. \tag{3.21}$$

The zeros $\vartheta_{1,2}$ are negative or have negative real part when $\kappa_1 > 0$ and $\kappa_2 > 0$. Thus, the Eq. (3.20) has no positive zeros. If $\kappa_3 \geq 0$, then $k(0) = \kappa_3 \geq 0$ and $\lim\limits_{\vartheta\to\infty} k(\vartheta) \to \infty$, which implies that (3.18) has only negative root(s). Moreover, if $\kappa_1 > 0$, $\kappa_2 > 0$ and $\kappa_3 \geq 0$, then there does not exist any δ for which $i\delta$ is a characteristic value of (3.12). Hence, the real parts of all characteristic values of (3.12) are negative $\forall\ \tau \geq 0$. In addition, if (a) $\kappa_1 > 0$ and $\kappa_2 < 0$, or (b) $\kappa_1 < 0$ and $\kappa_2 > 0$, or (c) $\kappa_3 < 0$, or (d) $\kappa_3 \geq 0$ and $\kappa_2 < 0$ holds, then (3.18) has at least one positive root ϑ_0. Consequently, Eq. (3.17) has at least one positive root, denoted by δ_0.

Thus, the characteristic Eq. (3.12) has a pair of purely complex zeros $\pm i\delta_0$. From (3.15) and (3.16), it follows that τ_p^* is a function of δ_0 for $p = 0, 1, 2, ...$, given by

$$\tau_p^* = \frac{1}{\delta_0}\arccos\left[\frac{(-A_1B_1+B_2)\delta_0^4+(-A_2B_2+A_1B_3+A_3B_1)\delta_0^2-A_3B_3}{(B_2\delta_0)^2+(-B_3+B_1\delta_0^2)^2}\right] + \frac{2\pi p}{\delta_0}. \tag{3.22}$$

Now, the system becomes locally asymptotically stable around the interior equilibrium point L_* for $\tau = 0$, if the condition (ii) of Theorem 3.2 is satisfied. According to Butler's lemma [182], L_* remain stable for $\tau < \tau^*$ with $\tau^* = \min\limits_{p\geq 0} \tau_p^*$.

Next, we verify the transversality condition

$$\frac{d}{d\tau}\left[Re\{\rho(\tau)\}\right]_{\tau=\tau^*} \neq 0.$$

Differentiating (3.13) and (3.14) with respect to τ and putting $\xi = 0$ in the resulting expressions, we obtain

$$\begin{aligned} S(\delta)\frac{d\zeta}{d\tau} + B(\delta)\frac{d\delta}{d\tau} &= A(\delta), \\ -B(\delta)\frac{d\zeta}{d\tau} + S(\delta)\frac{d\delta}{d\tau} &= M(\delta), \end{aligned} \tag{3.23}$$

where

$$\begin{aligned} S(\delta) &= -3\delta^2 + A_2 + B_2\cos\delta\tau + 2B_1\delta\sin\delta\tau + \tau\left\{(\delta^2B_1 - B_3)\cos\delta\tau - \delta B_2\sin\delta\tau\right\}, \\ B(\delta) &= -2\delta A_1 - 2B_1\delta\cos\delta\tau + B_2\sin\delta\tau + \tau\left\{(\delta^2B_1 - B_3)\sin\delta\tau + \delta B_2\cos\delta\tau\right\}, \\ A(\delta) &= -\delta^2B_2\cos\delta\tau - (\delta^2B_1 - B_3)\delta\sin\delta\tau, \\ M(\delta) &= \delta^2B_2\sin\delta\tau - (\delta^2B_1 - B_3)\delta\cos\delta\tau. \end{aligned} \tag{3.24}$$

Solving the above system of equations, we obtain
$\frac{d}{d\tau}\Big[Re\{\mu(\tau)\}\Big]_{\tau=\tau^*,\delta=\delta_0} = \Big[\frac{S(\delta)A(\delta)-B(\delta)M(\delta)}{S^2(\delta)+B^2(\delta)}\Big]_{\tau=\tau^*,\delta=\delta_0}$,
which indicates that $\frac{d}{d\tau}\Big[Re\{\mu(\tau)\}\Big]_{\tau=\tau^*,\delta=\delta_0} \neq 0$ when $S(\delta_0)A(\delta_0)-B(\delta_0)M(\delta_0) \neq 0$. Therefore, the transversality condition is satisfied and hence, the Hopf-bifurcation occurs when τ crosses through the critical value $\tau = \tau^*$.
Based on the foregoing discussion, we summarize the dynamics of the delay system (3.5) in form of the following theorem.

Theorem 3.3 *(i) In the absence of time lag* $(\tau = 0)$*, the interior equilibrium point* $L_*(M_*, I_*, M_*)$ *of the system (3.5) is locally asymptotically stable. Further, if* $\kappa_1 > 0$*,* $\kappa_2 > 0$*,* $\kappa_3 \geq 0$*, then the interior equilibrium point* L_* *of the delay system (3.5) is asymptotically stable for all* $\tau \in [0\ \infty)$.
(ii) In the absence of time lag $(\tau = 0)$*, the interior equilibrium point* $L_*(M_*, I_*, M_*)$ *of the system (3.5) is locally asymptotically stable. In addition, if* $\kappa_1 > 0$ *and* $\kappa_2 < 0$*, or* $\kappa_1 < 0$ *and* $\kappa_2 > 0$*, or* $\kappa_3 < 0$*, or* $\kappa_3 \geq 0$ *and* $\kappa_2 < 0$ *and* $\vartheta_0 = \delta_0^2$ *is a positive root of (3.18), then there exists* $\tau = \tau^*$ *for which the interior equilibrium point* L_* *of the delay system (3.5) is asymptotically stable in* $(0,\ \tau^*]$ *and unstable in* $(\tau^*,\ +\infty)$*, provided that* $S(\delta_0)A(\delta_0) - B(\delta_0)M(\delta_0) \neq 0$*. Thus the system undergoes a Hopf-bifurcation at* L_* *when* τ *cross the threshold value* τ^**, where*

$$\tau^* = \frac{1}{\delta_0}\arccos\left[\frac{(-A_1B_1+B_2)\delta_0^4+(-A_2B_2+A_1B_3+A_3B_1)\delta_0^2-A_3B_3}{(B_2\delta_0)^2+(B_3-B_1\delta_0^2)^2}\right].$$

3.5.2 Evaluation of the Length of Delay to Maintain Stability

Here, we discuss the local asymptotic stability of the interior equilibrium point L_* of non-delayed system. Due to continuity of τ and for sufficiently small positive real number τ $(i.e.\ \tau << 1)$, all characteristic roots of (3.12) have negative real parts and accordingly there is no characteristic root with positive real part bifurcating from infinity. Next, we assume that the space of real valued continuous functions defined on $[-\tau, \infty)$ satisfies the initial conditions (3.6). We linearized system (3.5) around its interior equilibrium $L_*(S_*, I_*, M_*)$. Let $x(t)$, $y(t)$ and $z(t)$ be the respective linearized variables of system (3.5). In consequence, (3.5) leads to

$$\begin{aligned}
\tfrac{dx}{dt} &= \bar{A}_1x(t)+\bar{A}_2y(t)+\bar{A}_3z(t)+\bar{A}_4x(t-\tau)+\bar{A}_5y(t-\tau),\\
\tfrac{dy}{dt} &= \bar{B}_1y(t)+\bar{B}_2x(t-\tau)+\bar{B}_3y(t-\tau),\\
\tfrac{dz}{dt} &= \bar{C}_1x(t)+\bar{C}_2y(t)+\bar{C}_3z(t),
\end{aligned} \tag{3.25}$$

where $\bar{A_1} = -\{r+g(S_*+I_*)\}+\{1-(S_*+I_*+M_*)\}g-\gamma g_1 M_*-d$,
$\bar{A_2} = -\{r+g(S_*+I_*)\}+\{1-(S_*+I_*+M_*)\}g-\gamma g_1 M_*+\omega$,
$\bar{A_3} = -\{r+g(S_*+I_*)\}-\gamma g_1(S_*+I_*)$, $\bar{A_4} = -\lambda I_*$, $\bar{A_5} = -\lambda S_*$, $\bar{B_1} = -(d+e+\omega)$,
$\bar{B_2} = \lambda I_*$, $\bar{B_3} = \lambda S_*$, $\bar{C_1} = -(\mu+g_1 M_*)+\gamma g_1 M_*$,
$\bar{C_2} = -(\mu+g_1 M_*)+\gamma g_1 M_*$, $\bar{C_3} = \{1-(S_*+I_*+M_*)\}g_1-(\mu+g_1 M_*)+\gamma g_1(S_*+I_*)-v$.
Taking the Laplace transformation of the system (3.25), we obtain

$$\begin{aligned}
(p-\bar{A_1})L_x(p) &= \bar{A_2}L_y(p)+\bar{A_3}L_z(p)+\bar{A_4}K_x(p)e^{-p\tau}+\bar{A_4}L_x(p)e^{-p\tau} \\
&\quad +\bar{A_5}K_y(p)e^{-p\tau}+\bar{A_5}L_y(p)e^{-p\tau}+x(0), \\
(p-\bar{B_1})L_y(p) &= \bar{B_2}K_x(p)e^{-p\tau}+\bar{B_2}L_x(p)e^{-p\tau}+\bar{B_3}K_y(p)e^{-p\tau}+\bar{B_3}L_y(p)e^{-p\tau}+y(0), \\
(p-\bar{C_3})L_z(p) &= \bar{C_1}L_x(p)+\bar{C_2}L_y(p)+z(0),
\end{aligned}$$

where

$$K_x = \int_{-\tau}^{0} e^{-pt}x(t)dt,\ K_y = \int_{-\tau}^{0} e^{-pt}y(t)dt, L_x(p) = \mathscr{L}\{x(t)\},\ L_y(p) = \mathscr{L}\{y(t)\},\ L_z(p) = \mathscr{L}\{z(t)\}.$$

Due to Nyquist criteria [183] and utilizing the results due to Freedman et al. [182], the conditions for the local asymptotic stability around L_* are found to be

$$Re[G(i\chi_0)] = 0,\ Im[G(i\chi_0)] > 0, \tag{3.26}$$

where χ_0 is the smallest positive zero of first equation of (3.26) and

$$G(p) = p^3+A_1p^2+A_2p+A_3+[B_1p^2+B_2p+B_3]\mathrm{e}^{-p\tau}.$$

From (3.26), we get

$$A_3-A_1\chi_0^2 = (B_1\chi_0^2-B_3)\cos\chi_0\tau-\chi_0 B_2\sin\chi_0\tau, \tag{3.27}$$

$$A_2\chi_0-\chi_0^3 > -B_2\chi_0\cos\chi_0\tau-(B_1\chi_0^2-B_3)\sin\chi_0\tau. \tag{3.28}$$

Utilizing the above sufficient conditions for the stability of L_*, we estimate the magnitude of time delay (τ) for stability. Next, we calculate an upper bound χ_+ of χ_0 that is independent of τ, and determine the magnitude of τ such that (3.28) holds for all values of χ, $0 \le \chi \le \chi_+$ at $\chi = \chi_0$. We maximize

$$(B_1\chi_0^2-B_3)\cos\chi_0\tau-\chi_0 B_2\sin\chi_0\tau,$$

subject to $|\sin\chi_0\tau|\leq 1$ and $|\cos\chi_0\tau|\leq 1$. Thus, we obtain

$$|A_3|-|A_1|\chi_0^2\leq|B_1|\chi_0^2+|B_3|+|B_2|\chi_0. \tag{3.29}$$

From the inequality (3.29), we get

$$\chi_+\leq\frac{-|B_2|+\sqrt{|B_2|^2+4(|A_1|+|B_1|)(|A_3|-|B_3|)}}{|A_1|+|B_1|}, \tag{3.30}$$

which implies that $\chi_0\leq\chi_+$. In the absence of time lag, L_* is locally asymptotically stable when the inequality (3.28) is satisfied for sufficiently small positive real number τ. Rearranging (3.28) by utilizing the inequality (3.29), we obtain

$$\begin{aligned}&sin\chi_0\tau[(B_2\chi_0-A_1B_1\chi_0)+\tfrac{A_1B_3}{\chi_0}]+(cos\chi_0\tau-1)(B_3-B_1\chi_0^2-A_1B_2)\\&<A_1A_2+A_1B_2-A_3-B_3+B_1\chi_0^2.\end{aligned} \tag{3.31}$$

Now, using the relations $|\sin\chi_0\tau|\leq\chi_0\tau$, $|1-\cos\chi_0\tau|\leq\frac{\chi_0^2\tau^2}{2}$, and upper bound of χ_0, we have

$$sin\chi_0\tau[(B_2\chi_0-A_1B_1\chi_0)+\frac{A_1B_3}{\chi_0}]\leq\tau[|(B_2-A_1B_1)|\chi_+^2+|A_1B_3|],$$

and

$$(cos\chi_0\tau-1)(B_3-B_1\chi_0^2-A_1B_2)\leq\frac{\chi_+^2\tau^2}{2}|B_1\chi_+^2+A_1B_2-B_3|.$$

After simplifying the inequality (3.31), we obtain

$$A_\phi\tau^2+B_\phi\tau-C_\phi\leq 0, \tag{3.32}$$

where

$$\begin{aligned}&A_\phi=\frac{\chi_+^2}{2}|B_1\chi_+^2+A_1B_2-B_3|,\ B_\phi=|(B_2-A_1B_1)|\chi_+^2+|A_1B_3|,\\&C_\phi=A_1A_2+A_1B_2-A_3-B_3+B_1\chi_+^2.\end{aligned}$$

So, the Nyquist criteria is satisfied for $0\leq\tau\leq\tau_+$ with

$$\tau_+=\frac{-B_\phi+\sqrt{B_\phi^2+4A_\phi C_\phi}}{2A_\phi}.$$

Thus, τ_+ gives an estimate magnitude of the delay that maintains the stability of the limit cycle. Now, we summarize the foregoing outcome in form of the following result.

Theorem 3.4 *If there exists $\tau\in(0,\ \tau_+]$ satisfying the inequality $A_\phi\tau^2+B_\phi\tau-C_\phi\leq 0$, then τ_+ represents the maximum magnitude of the time lag τ for which the interior equilibrium point L_* is locally asymptotically stable.*

3.5.3 The Direction and Stability of Hopf-Bifurcating Periodic Solutions

In the last section, we obtained the sufficient conditions for the system (3.5) to experience Hopf-bifurcation at the interior equilibrium L_* when τ passes through the critical value τ^*. Here, we investigate the direction, stability and period of Hopf bifurcating periodic solutions at $\tau = \tau^*$ of the system (3.5) by applying the method of 'normal form theory' and 'center manifold theorem' due to Hassard et. al. [184]. We consider the following coordinate transformations:

$$z_1(t) = S(\tau t) - S_*, z_2(t) = I(\tau t) - I_*, z_3(t) = M(\tau t) - M_*,$$

where $\tau = \tau_0^* + \mu$ and μ is a real number. Then, the system (3.5) becomes a functional differential equation in $C = \mathbf{C}([-1,0], \mathbf{R_+^3})$ given by

$$\dot{z}(t) = L_\mu(z_t) + F(\mu, z_t), \tag{3.33}$$

where $z(t) = (z_1(t), z_2(t), z_3(t))^T \in \mathbf{R^3}$. For any $\psi = (\psi_1, \psi_2, \psi_3)^T$ in $\mathbf{C}([-1,0], \mathbf{R_+^3})$; the functions $L_\mu : \mathbf{C} \to \mathbf{R}$ and $F : \mathbf{R} \times \mathbf{C} \to \mathbf{R}$ are given by

$$L_\mu(\psi) = (\tau_0^* + \mu)A(\psi_1(0)\ \psi_2(0)\ \psi_3(0))^T + (\tau_0^* + \mu)B(\psi_1(-1)\ \psi_2(-1)\ \psi_3(-1))^T \tag{3.34}$$

and

$$F(\mu, \psi) = (\tau_0^* + \mu)C, \tag{3.35}$$

where $A = \begin{pmatrix} l_{11} & l_{12} & l_{13} \\ 0 & l_{22} & 0 \\ l_{31} & l_{32} & l_{33} \end{pmatrix}$, $B = \begin{pmatrix} -l_{11}' & -l_{12}' & 0 \\ l_{11}' & l_{12}' & 0 \\ 0 & 0 & 0 \end{pmatrix}$,

$$C = \begin{pmatrix} m_{11}\psi_1^2(0) + m_{12}\psi_2^2(0) + m_{13}\psi_1(0)\psi_2(0) + m_{14}\psi_1(0)\psi_3(0) + m_{15}\psi_2(0)\psi_3(0) \\ +m_{16}\psi_1(-1)\psi_2(-1) \\ \\ m_{21}\psi_1(-1)\psi_2(-1) \\ \\ m_{31}\psi_3^2(0) + m_{32}\psi_1(0)\psi_3(0) + m_{33}\psi_2(0)\psi_3(0) \end{pmatrix},$$

$$m_{11} = m_{12} = -g, \quad m_{13} = -2g, \quad m_{14} = m_{15} = -(g + \gamma g_1), \quad m_{16} = -\lambda, \quad m_{21} = \lambda,$$
$$m_{31} = -g_1, \quad m_{32} = m_{33} = (-g + \gamma g_1).$$

Here, the system (3.5) experiences Hopf-bifurcation near L_* for $\mu = 0$. Applying the normal form theory and central manifold theorem as proposed by Hassard et al. [184], we have the following theorem.

Theorem 3.5 *Suppose that the condition (ii) of Theorem 3.3 is satisfied for the system (3.5). If $\mu_2 < 0$ $(\mu_2 > 0)$, then the Hopf bifurcating periodic solution is subcritical (supercritical) for $\tau < \tau_0^*$ $(\tau > \tau_0^*)$. If $\beta_2 > 0$ $(\beta_2 < 0)$, then the bifurcating periodic solution is orbitally unstable (stable). Moreover, τ_2 represents the period of the bifurcating periodic solution and the period decreases (increases) for $\tau_2 < 0$ $(\tau_2 > 0)$.*

Proof: According to the Riesz representation theorem, there exists a function $\eta(\theta,\mu)$ of bounded variation for $\theta \in [-1,0]$ such that

$$L_\mu \psi = \int_{-1}^{0} d\eta(\theta,\mu)\psi(\theta), \quad for \ \ \psi \in \mathbf{C}. \tag{3.36}$$

In particular, we set

$$\eta(\theta,\mu) = (\tau_0^* + \mu)A\delta(\theta) - (\tau_0^* + \mu)B\delta(\theta+1), \tag{3.37}$$

with

$$\delta(\theta) = \begin{cases} 1, & \theta=0, \\ 0, & \theta\neq 0. \end{cases}$$

Now, for ψ in $\mathbf{C}^1([-1,0],\mathbf{R}^3_+)$, we define

$$A(\mu)\psi = \begin{cases} \frac{d\psi(\theta)}{d\theta} & \theta \in [-1,0), \\ \int_{-1}^{0} d\eta(\mu,s)\psi(s) & \theta = 0, \end{cases}$$

and

$$R(\mu)\psi = \begin{cases} 0, & \theta \in [-1,0), \\ F(\mu,\psi), & \theta = 0. \end{cases}$$

Then, the system (3.33) takes the form

$$\dot{z}_t = A(\mu)z_t + R(\mu)z_t, \tag{3.38}$$

where $z_t(\theta) = z_t(t+\theta)$ for $\theta \in [-1,0]$.
For any ϕ in $\mathbf{C}^1([0,1],(\mathbf{R}^3_+)^*)$, we define

$$A^*\phi(s) = \begin{cases} -\frac{d\phi(s)}{ds}, & s \in (0,1], \\ \int_{-1}^{0} d\eta^T(t,0)\phi(-t), & s = 0, \end{cases}$$

and a bilinear inner product of the form

$$\langle \phi(s), \psi(\theta) \rangle = \overline{\phi}(0)\psi(0) - \int_{-1}^{0} \int_{\alpha=0}^{\theta} \overline{\phi}(\alpha-\theta) d\eta(\theta) \psi(\alpha) d\alpha, \tag{3.39}$$

where $\eta(\theta) = \eta(\theta, 0)$, $A(0)$ and A^* denote the adjoint operators. From the section (3.5.1), we know that $\pm i\delta_0\tau_0^*$ are characteristic values of $A(0)$, which are also characteristic values of A^*. Now, we find the characteristic function of $A(0)$ and A^* associated with $i\delta_0\tau_0^*$ and $-i\delta_0\tau_0^*$ respectively. We assume that $q(\theta) = (1, u, w)^T e^{i\delta_0\tau_0^*\theta}$ and $q^*(s)$ are the characteristic functions of $A(0)$ and A^* associated with $i\delta_0\tau_0^*$ and $-i\delta_0\tau_0^*$, respectively. Thus we have $A(0)q(\theta) = i\delta_0\tau_0^* q(\theta)$. From the definition of $A(0)$, (3.36) and (3.37), it follows that

$$\tau_0^* \begin{pmatrix} l_{11} - l_{11}^{'} e^{-i\delta_0\tau_0^*} - i\delta_0 & l_{12} - l_{12}^{'} e^{-i\delta_0\tau_0^*} & l_{13} \\ l_{11}^{'} e^{-i\delta_0\tau_0^*} & l_{22} + l_{12}^{'} e^{-i\delta_0\tau_0^*} - i\delta_0 & 0 \\ l_{31} & l_{32} & l_{33} - i\delta_0 \end{pmatrix} q(\theta) = \begin{pmatrix} 0 \\ 0 \\ 0 \end{pmatrix}.$$

So, we obtain

$$\begin{aligned} q(\theta) &= (1, u, w)^T e^{i\delta_0\tau_0^*\theta} \\ &= \left(1, -\frac{l_{11}^{'} e^{-i\delta_0\tau_0^*}}{l_{22} + l_{12}^{'} e^{-i\delta_0\tau_0^*} - i\delta_0}, -\frac{l_{31}(l_{22} + l_{12}^{'} e^{-i\delta_0\tau_0^*} - i\delta_0) - l_{32} l_{11}^{'} e^{-i\delta_0\tau_0^*}}{(l_{33} - i\delta_0)(l_{22} + l_{12}^{'} e^{-i\delta_0\tau_0^*} - i\delta_0)}\right)^T e^{i\delta_0\tau_0^*\theta}. \end{aligned}$$

In a similar manner, one can obtain

$$\begin{aligned} q^*(s) &= D(1, u^*, w^*)^T e^{i\delta_0\tau_0^* s} \\ &= \left(1, -\frac{(l_{33} + i\delta_0)(l_{11} - l_{11}^{'} e^{i\delta_0\tau_0^*} + i\delta_0) - l_{13} l_{31}}{(l_{33} + i\delta_0) l_{11}^{'} e^{i\delta_0\tau_0^*}}, -\frac{l_{13}}{(l_{33} + i\delta_0)}\right)^T e^{i\delta_0\tau_0^* s}. \end{aligned}$$

We choose D with the property of $\langle q^*(s), q(\theta) \rangle = 1$, $\langle q^*(s), \overline{q}(\theta) \rangle = 0$. Then, we have

$$\begin{aligned} \langle q^*(s), q(\theta) \rangle &= \overline{D}(1, \overline{u^*}, \overline{w^*})(1, u, w)^T \\ &\quad - \int_{-1}^{0} \int_{\alpha=0}^{\theta} \overline{D}(1, \overline{u^*}, \overline{w^*}) e^{-i\delta_0\tau_0^*(\alpha-\theta)} d\eta(\theta)(1, u, w)^T e^{i\delta_0\tau_0^*\alpha} d\alpha \\ &= \overline{D}\left[1 + \overline{u^*}u + \overline{w^*}w - \int_{-1}^{0} (1, \overline{u^*}, \overline{w^*}) \theta e^{i\delta_0\tau_0^*\theta} d\eta(\theta)(1, u, w)^T\right] \\ &= \overline{D}\left[1 + \overline{u^*}u + \overline{w^*}w - \tau_0^*\{l_{11}^{'}(u^* - 1) + l_{12}^{'}(w^* - 1)u\} e^{-i\delta_0\tau_0^*}\right]. \end{aligned}$$

Thus, we get D as given by

$$D = \frac{1}{1 + u^*\overline{u} + w^*\overline{w} - \tau_0^*\{l_{11}^{'}(\overline{u^*} - 1) + l_{12}^{'}(\overline{w^*} - 1)\overline{u}\} e^{i\delta_0\tau_0^*}}.$$

To describe the center manifold $\mathbf{C}_0$ near $\mu = 0$, we determine the components by using the same notation and procedure as developed by [184].
Letting z_t to be the solution of (3.33) for $\mu = 0$, we define

$$\mathrm{z}(t) = \langle q^*, z_t \rangle, \quad W(t,\theta) = z_t(\theta) - 2Re\{\mathrm{z}(t)q(\theta)\}. \tag{3.40}$$

On the center manifold $\mathbf{C}_0$, we have

$$W(t,\theta) = W\Big(\mathrm{z}(t), \bar{\mathrm{z}}(t), \theta\Big),$$

where

$$W(\mathrm{z},\bar{\mathrm{z}},\theta) = W_{20}(\theta)\frac{\mathrm{z}^2}{2} + W_{11}(\theta)\mathrm{z}\bar{\mathrm{z}} + W_{02}(\theta)\frac{\bar{\mathrm{z}}^2}{2} + W_{30}(\theta)\frac{\mathrm{z}^3}{6} + \cdots,$$

z and $\bar{\mathrm{z}}$ are local coordinates for center manifold $\mathbf{C}_0$ in the direction of q^* and $\bar{q}^*$, respectively. Here, W is real for real values of z_t. For the value z_t in $\mathbf{C}_0$ of (3.33) with $\mu = 0$, we obtain

$$\begin{aligned}
\dot{\mathrm{z}}(t) &= i\ \ \delta_0\tau_0^*\mathrm{z} + \Big\langle \bar{q}^*(\theta), F\Big(0, W(\mathrm{z},\bar{\mathrm{z}},\theta) + 2Re\{\mathrm{z}q(\theta)\}\Big)\Big\rangle \\
&= \ \ i\delta_0\tau_0^*\mathrm{z} + \bar{q}^*(0)F\Big(0, W(\mathrm{z},\bar{\mathrm{z}},0) + 2Re\{\mathrm{z}q(0)\}\Big) \stackrel{\text{def}}{=} i\delta_0\tau_0^*\mathrm{z} + \bar{q}^*(0)F_0(\mathrm{z},\bar{\mathrm{z}}),
\end{aligned}$$

which can be rewritten as

$$\dot{\mathrm{z}} = i\delta_0\tau_0^*\mathrm{z} + g(\mathrm{z},\bar{\mathrm{z}}),$$

with

$$g(\mathrm{z},\bar{\mathrm{z}}) = \bar{q}^*(0)F_0(\mathrm{z},\bar{\mathrm{z}}) = g_{20}\frac{\mathrm{z}^2}{2} + g_{11}\mathrm{z}\bar{\mathrm{z}} + g_{02}\frac{\bar{\mathrm{z}}^2}{2} + g_{21}\frac{\mathrm{z}^2\bar{\mathrm{z}}}{2} + \cdots. \tag{3.41}$$

Then, from (3.40), we have

$$\begin{aligned}
z_t(\theta) &= (z_{1t}(\theta), z_{2t}(\theta), z_{3t}(\theta))^T = W(t,\theta) + 2Re\{\mathrm{z}(t)q(\theta)\} \\
&= W_{20}(\theta)\frac{\mathrm{z}^2}{2} + W_{11}(\theta)\mathrm{z}\bar{\mathrm{z}} + W_{02}(\theta)\frac{\bar{\mathrm{z}}^2}{2} + (1,u,w)^T e^{i\delta_0\tau_0^*\theta}\mathrm{z} + (1,\bar{u},\bar{w})^T e^{-i\delta_0\tau_0^*\theta}\bar{\mathrm{z}} \\
&\quad + O(|\ (\mathrm{z},\bar{\mathrm{z}})\ |^3).
\end{aligned} \tag{3.42}$$

In consequence, from Eq. (3.41), we can get

$$
\begin{aligned}
g(z,\bar{z}) &= \overline{q}^*(0)F_0(z,\bar{z}) \\
&= \overline{D}(1,\overline{u^*},\overline{w^*})\tau_0^* \begin{pmatrix} m_{11}z_{1t}^2(0)+m_{12}z_{2t}^2(0)+m_{13}z_{1t}(0)z_{2t}(0)+m_{14}z_{1t}(0)z_{3t}(0)+m_{15}z_{2t}(0)z_{3t}(0) \\ +m_{16}z_{1t}(-1)z_{2t}(-1) \\ m_{21}z_{1t}(-1)z_{2t}(-1) \\ m_{31}z_{3t}^2(0)+m_{32}z_{1t}(0)z_{3t}(0)+m_{33}z_{2t}(0)z_{3t}(0) \end{pmatrix}.
\end{aligned}
$$

By direct calculation and comparing the coefficients with (3.41), we obtain

$$
\begin{aligned}
g_{20} &= 2\overline{D}\tau_0^*\Big[m_{11}+m_{12}u^2+m_{13}u+m_{14}w+m_{15}uw+m_{16}ue^{-2i\delta_0\tau_0^*} \\
&\quad +\overline{u^*}m_{21}ue^{-2i\delta_0\tau_0^*}+\overline{w^*}\Big\{m_{31}+m_{32}w+m_{33}uw\Big\}\Big], \\
g_{11} &= 2\overline{D}\tau_0^*\Big[m_{11}+m_{12}|u|^2+m_{13}Re\{u\}+m_{14}Re\{w\}+m_{15}Re\{u\overline{w}\} \\
&\quad +m_{16}Re\{u\}+\overline{u^*}m_{21}Re\{u\}+\overline{w^*}\Big\{m_{31}+m_{32}Re\{w\}+m_{33}Re\{u\overline{w}\}\Big\}\Big], \\
g_{02} &= 2\overline{D}\tau_0^*\Big[m_{11}+m_{12}\overline{u}^2+m_{13}\overline{u}+m_{14}\overline{w}+m_{15}\overline{uw}+m_{16}\overline{u}e^{2i\delta_0\tau_0^*} \\
&\quad +\overline{u}^*m_{21}\overline{u}e^{2i\delta_0\tau_0^*}+\overline{w}^*\Big\{m_{31}+m_{32}\overline{w}+m_{33}\overline{uw}\Big\}\Big], \\
g_{21} &= \overline{D}\tau_0^*\Big[m_{11}\Big(2W_{20}^1(0)+4W_{11}^1(0)\Big)+m_{12}\Big(2\overline{u}W_{20}^2(0)+4uW_{11}^2(0)\Big) \\
&\quad +m_{13}\Big(W_{20}^2(0)+2W_{11}^2(0)+\overline{u}W_{20}^1(0)+2uW_{11}^1(0)\Big) \\
&\quad +m_{14}\Big(W_{20}^3(0)+2W_{11}^3(0)+\overline{w}W_{20}^1(0)+2wW_{11}^1(0)\Big) \\
&\quad +m_{15}\Big(\overline{u}W_{20}^3(0)+2uW_{11}^3(0)+\overline{w}W_{20}^2(0)+2wW_{11}^2(0)\Big) \\
&\quad +m_{16}\Big(2W_{20}^2(-1)e^{i\delta_0\tau_0^*}+2W_{11}^2(-1)e^{-i\delta_0\tau_0^*}+\overline{u}W_{20}^1(-1)e^{i\delta_0\tau_0^*}+2uW_{11}^1(-1)e^{-i\delta_0\tau_0^*}\Big) \\
&\quad +\overline{u}^*m_{21}\Big(2W_{20}^2(-1)e^{i\delta_0\tau_0^*}+2W_{11}^2(-1)e^{-i\delta_0\tau_0^*}+\overline{u}W_{20}^1(-1)e^{i\delta_0\tau_0^*}+2uW_{11}^1(-1)e^{-i\delta_0\tau_0^*}\Big) \\
&\quad +\overline{w}^*\Big\{m_{31}\Big(2W_{20}^1(0)+4W_{11}^1(0)\Big)+m_{32}\Big(\overline{w}W_{20}^2(0)+2W_{11}^3(0)+2wW_{11}^1(0)+2W_{20}^3(0)\Big) \\
&\quad +m_{33}\Big(\overline{u}W_{20}^3(0)+2uW_{11}^3(0)+\overline{w}W_{20}^2(0)+2wW_{11}^2(0))\Big)\Big\}\Big].
\end{aligned}
$$

To compute the value of g_{21}, we need to calculate the magnitude for the terms $W_{20}^i(\theta)$ and $W_{11}^i(\theta)$ $(i=1,2,3)$. From (3.38) and (3.40), we have

$$
\begin{aligned}
\dot{W} &= \dot{z}_t-\dot{z}q-\dot{\bar{z}}\,\bar{q} = \begin{cases} AW-2Re\{\overline{q}^*(0)F_0q(\theta)\}, & \theta\in[-1,0), \\ AW-2Re\{\overline{q}^*(0)F_0q(\theta)\}+F_0, & \theta=0, \end{cases} \\
&\overset{\text{def}}{=} AW+H(z,\bar{z},\theta),
\end{aligned} \tag{3.43}
$$

where

$$H(\mathrm{z},\bar{\mathrm{z}},\theta) = H_{20}(\theta)\frac{\mathrm{z}^2}{2} + H_{11}(\theta)\mathrm{z}\bar{\mathrm{z}} + H_{02}(\theta)\frac{\bar{\mathrm{z}}^2}{2} + \cdots . \tag{3.44}$$

Expanding the above series explicitly and comparing the corresponding coefficients, we get

$$(A - i2\delta_0\tau_0^* I)W_{20}(\theta) = -H_{20}(\theta), \quad AW_{11}(\theta) = -H_{11}(\theta). \tag{3.45}$$

From (3.43), we have

$$H(\mathrm{z},\bar{\mathrm{z}},\theta) = -\overline{q}^*(0)F_0 q(\theta) - q^*(0)\overline{F}_0\overline{q}(\theta) = -gq(\theta) - \overline{g}\,\overline{q}(\theta)\ for \theta\ \in [-1,0). \tag{3.46}$$

Comparing the associated coefficients with (3.44) yields

$$H_{20}(\theta) = -g_{20}q(\theta) - \overline{g}_{02}\overline{q}(\theta), \tag{3.47}$$

$$H_{11}(\theta) = -g_{11}q(\theta) - \overline{g}_{11}\overline{q}(\theta). \tag{3.48}$$

From (3.45), (3.47), (3.48) and utilizing the definition of A we obtain

$$\dot{W}_{20}(\theta) = i2\delta_0\tau_0^* W_{20}(\theta) + g_{20}q(\theta) + \overline{g}_{02}\overline{q}(\theta), \tag{3.49}$$

$$\dot{W}_{11}(\theta) = g_{11}q(\theta) + \overline{g}_{11}\overline{q}(\theta). \tag{3.50}$$

Since $q(\theta) = (1,u,w)^T e^{i\delta_0\tau_0^*\theta}$, therefore we have

$$W_{20}(\theta) = \frac{ig_{20}}{\delta_0\tau_0^*}q(0)e^{i\delta_0\tau_0^*\theta} + \frac{i\overline{g}_{20}}{3\delta_0\tau_0^*}\overline{q}(0)e^{-i\delta_0\tau_0^*\theta} + E_1 e^{i2\delta_0\tau_0^*\theta}, \tag{3.51}$$

and

$$W_{11}(\theta) = -\frac{ig_{11}}{\delta_0\tau_0^*}q(0)e^{i\delta_0\tau_0^*\theta} + \frac{i\overline{g}_{11}}{\delta_0\tau_0^*}\overline{q}(0)e^{-i\delta_0\tau_0^*\theta} + E_2, \tag{3.52}$$

where $E_1 = (E_1^{(1)}, E_1^{(2)}, E_1^{(3)})$, $E_2 = (E_2^{(1)}, E_2^{(2)}, E_2^{(3)}) \in \mathbf{R}^3$ are constant vectors.
From the definition of A and utilizing (3.45) with $\eta(\theta) = \eta(0,\theta)$, we get

$$\int_{-1}^{0} d\eta(\theta)W_{20}(\theta) = i2\delta_0\tau_0^* W_{20}(0) - H_{20}(0), \tag{3.53}$$

and

$$\int_{-1}^{0} d\eta(\theta)W_{11}(\theta) = -H_{11}(0). \tag{3.54}$$

From (3.45), we have

$$H_{20}(0) = -g_{02}q(0) - \overline{g}_{02}\overline{q}(0) + 2\tau_0^* \begin{pmatrix} m_{11} + m_{12}u^2 + m_{13}u + m_{14}w + m_{15}uw + m_{16}ue^{-2i\delta_0\tau_0^*} \\ m_{21}ue^{-2i\delta_0\tau_0^*} \\ m_{31} + m_{32}w + m_{33}uw \end{pmatrix} \quad (3.55)$$

and

$$H_{11}(0) = -g_{11}q(0) - \overline{g}_{11}\overline{q}(0) + 2\tau_0^* \begin{pmatrix} m_{11} + m_{12}|u|^2 + m_{13}Re\{u\} + m_{14}Re\{w\} + m_{15}Re\{u\overline{w}\} + m_{16}Re\{u\} \\ m_{21}Re\{u\} \\ m_{31} + m_{32}Re\{w\} + m_{33}Re\{u\overline{w}\} \end{pmatrix} \quad (3.56)$$

Notice that

$$\left(i\delta_0\tau_0^* I - \int_{-1}^{0} e^{i\delta_0\tau_0^*\theta} d\eta(\theta)\right) q(0) = 0, \quad \left(-i\delta_0\tau_0^* I - \int_{-1}^{0} e^{-i\delta_0\tau_0^*\theta} d\eta(\theta)\right) \overline{q}(0) = 0.$$

Substituting (3.51) and (3.55) into (3.53), we get

$$\left(i2\delta_0\tau_0^* I - \int_{-1}^{0} e^{i2\delta_0\tau_0^*\theta} d\eta(\theta)\right) E_1 = 2\tau_0^* \begin{pmatrix} m_{11} + m_{12}u^2 + m_{13}u + m_{14}w + m_{15}uw + m_{16}ue^{-2i\delta_0\tau_0^*} \\ m_{21}ue^{-2i\delta_0\tau_0^*} \\ m_{31} + m_{32}w + m_{33}uw \end{pmatrix},$$

which implies that

$$\begin{pmatrix} i2\delta_0 - l_{11} + l_{11}'e^{-i2\delta_0\tau_0^*} & -l_{12} + l_{12}'e^{-i2\delta_0\tau_0^*} & -l_{13} \\ -l_{11}'e^{-i2\delta_0\tau_0^*} & i2\delta_0 - l_{22} - l_{12}'e^{-i2\delta_0\tau_0^*} & 0 \\ -l_{31} & -l_{32} & i2\delta_0 - l_{33} \end{pmatrix} E_1$$

$$= 2 \begin{pmatrix} m_{11} + m_{12}u^2 + m_{13}u + m_{14}w + \\ m_{15}uw + m_{16}ue^{-2i\delta_0\tau_0^*} \\ \\ m_{21}ue^{-2i\delta_0\tau_0^*} \\ \\ m_{31} + m_{32}w + m_{33}uw \end{pmatrix}$$

It then follows that

$$E_1 = (E_1^{(1)}, E_1^{(2)}, E_1^{(3)}) = \left(\frac{|\Delta_{11}|}{|\Delta_1|}, \frac{|\Delta_{12}|}{|\Delta_1|}, \frac{|\Delta_{13}|}{|\Delta_1|}\right), \quad (3.57)$$

where

$$\Delta_1 = \begin{pmatrix} i2\delta_0 - l_{11} + l_{11}'e^{-i2\delta_0\tau_0^*} & -l_{12} + l_{12}'e^{-i2\delta_0\tau_0^*} & -l_{13} \\ -l_{11}'e^{-i2\delta_0\tau_0^*} & i2\delta_0 - l_{22} - l_{12}'e^{-i2\delta_0\tau_0^*} & 0 \\ -l_{31} & -l_{32} & i2\delta_0 - l_{33} \end{pmatrix}$$

and Δ_{1j} is obtained from Δ_1 by replacing jth column in to $2(m_{11}+m_{12}u^2+m_{13}u+m_{14}w+m_{15}uw+m_{16}ue^{-2i\delta_0\tau_0^*}, m_{21}ue^{-2i\delta_0\tau_0^*}, m_{31}+m_{32}w+m_{33}uw)^T$.
Similarly, substituting (3.52) and (3.56) into (3.54), we have

$$\left(\int_{-1}^{0} d\eta(\theta)\right)E_2 = 2\tau_0^* \begin{pmatrix} m_{11}+m_{12}|u|^2+m_{13}Re\{u\}+m_{14}Re\{w\}+m_{15}Re\{u\overline{w}\}+m_{16}Re\{u\} \\ m_{21}Re\{u\} \\ m_{31}+m_{32}Re\{w\}+m_{33}Re\{u\overline{w}\} \end{pmatrix},$$

which implies that

$$\begin{pmatrix} l_{11}-l_{11}^{'} & l_{12}-l_{12}^{'} & l_{13} \\ -l_{11}^{'} & l_{22}-l_{12}^{'} & 0 \\ l_{31} & l_{32} & l_{33} \end{pmatrix} E_2$$

$$= 2\begin{pmatrix} m_{11}+m_{12}|u|^2+m_{13}Re\{u\}+m_{14}Re\{w\}+m_{15}Re\{u\overline{w}\}+m_{16}Re\{u\} \\ m_{21}Re\{u\} \\ m_{31}+m_{32}Re\{w\}+m_{33}Re\{u\overline{w}\} \end{pmatrix}$$

and hence

$$E_2 = (E_2^{(1)}, E_2^{(2)}, E_2^{(3)}) = \left(\frac{|\Delta_{21}|}{|\Delta_2|}, \frac{|\Delta_{22}|}{|\Delta_2|}, \frac{|\Delta_{23}|}{|\Delta_2|}\right), \tag{3.58}$$

where

$$\Delta_2 = \begin{pmatrix} l_{11}-l_{11}^{'} & l_{12}-l_{12}^{'} & l_{13} \\ -l_{11}^{'} & l_{22}-l_{12}^{'} & 0 \\ l_{31} & l_{32} & l_{33} \end{pmatrix}$$

and Δ_{2j} is obtained from Δ_2 by replacing jth column in to $2(m_{11}+m_{12}|u|^2+m_{13}Re\{u\}+m_{14}Re\{w\}+m_{15}Re\{u\overline{w}\}+m_{16}Re\{u\}, m_{21}Re\{u\}, m_{31}+m_{32}Re\{w\}+m_{33}Re\{u\overline{w}\})^T$.
Based on the foregoing arguments, we find that

$$C_1(0) = \frac{i}{2\delta_0\tau_0^*}\left(g_{20}g_{11}-2|g_{11}|^2-\frac{1}{3}|g_{02}|^2\right)+\frac{1}{2}g_{21},$$

$$\mu_2 = -\frac{Re\{C_1(0)\}}{Re\{\acute{\mu}(\tau_0^*)\}}, \beta_2 = 2Re\{C_1(0)\}, \tau_2 = -\frac{Im\{C_1(0)\}+\mu_2 Im\{\acute{\mu}(\tau_0^*)\}}{\delta_0\tau_0^*}.$$

It is well known that μ_2 and β_2 determine the direction of Hopf-bifurcation and stability of bifurcating periodic solutions of the system (3.5) at $\tau=\tau_0^*$ on center manifold. From the above analysis, the proof of Theorem 3.5 is complete.

3.6 Numerical Investigations

In this section, we perform some numerical experiments on the system (3.5) to check the feasibility of our analytical findings concerning the stability criteria. We focus on the role

Table 3.1: The set of values of parameters for numerical simulation

Parameter	Ecological meaning	Parameter values	Sources
r	recruitment rate of coral	0.07	Briggs *et al.* (2018) [156]
g	combined rate of local recruitment including the lateral growth of coral over free space	0.1	Briggs *et al.* (2018) [156]
g_1	combined rate of local recruitment and lateral growth of macroalgae over free space	0.4	Briggs *et al.* (2018) [156]
d	death rate of coral	0.05	Briggs *et al.* (2018) [156]
μ	recruitment rate of macroalgae	0.1	–
v	death rate of macroalgae	0.5	Briggs *et al.* (2018) [156]
λ	disease transmission rate	0.1	–
ω	rate of infected coral colonies revert to the susceptible class due to regeneration of tissue	0.01	–
e	additional mortality rate of infected coral due to infection	0.01	–
γ	dimensionless parameter $(0 < \gamma \leq 1]$	0.6	Briggs *et al.* (2018) [156]

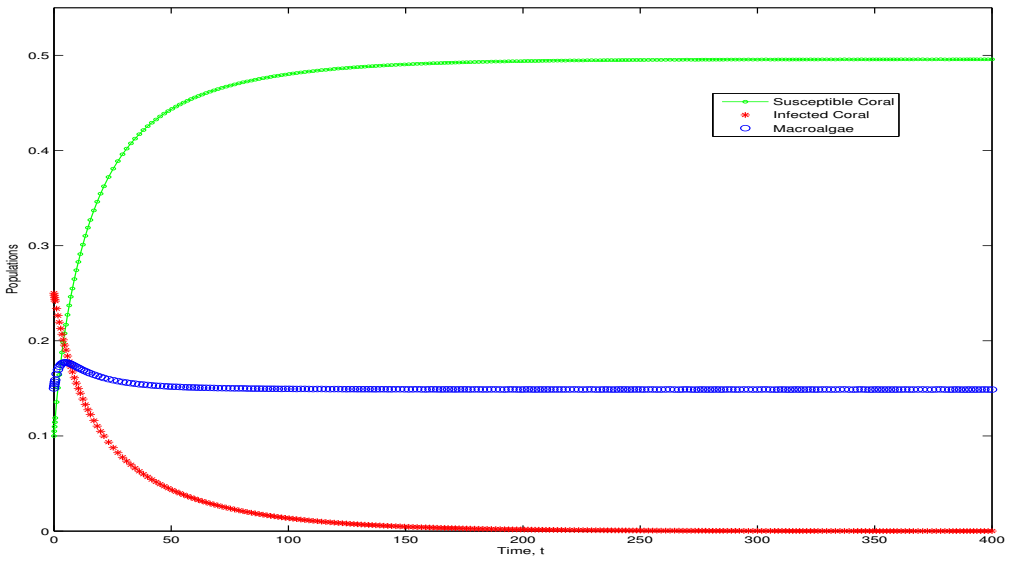

Figure 3.1: Numerical simulation in the absence of delay for system (3.5). The parameter values are $r = 0.07$; $g = 0.1$; $g_1 = 0.4$; $d = 0.05$; $\mu = 0.1$; $v = 0.5$; $\lambda = 0.1$; $\omega = 0.01$; $e = 0.01$; $\gamma = 0.6$; $\tau = 0$; [.10 .250 .15] (see Table 3.1).

of vital parameters: disease transmission rate λ, conversion rate ω of infected colonies to healthy class and time lag τ due to incubation in the coral-reef system. In our numerical computation, we utilize MATLAB and MATHEMATICA and choose the biologically feasible parameter values from the previous published works as indicated in the Table 3.1, that

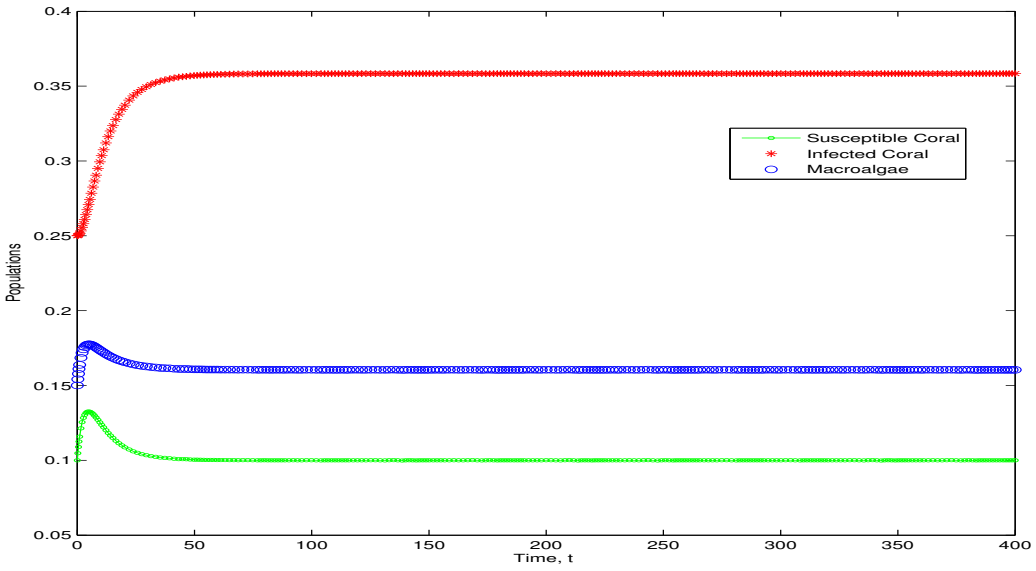

Figure 3.2: Numerical simulation for $\lambda = 0.7$ in the absence of delay for system (3.5). The rest parameter values are taken as in the Figure 3.1

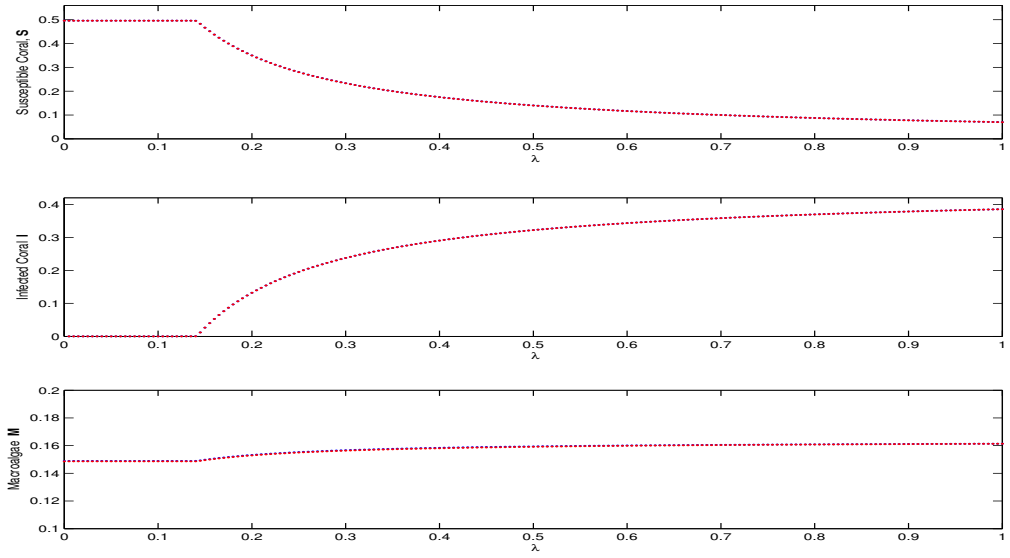

Figure 3.3: Bifurcation diagram of system (3.5) for λ. The parameter values are taken as in the Figure 3.1.

is, $r = 0.07$; $g = 0.1$; $g_1 = 0.4$; $d = 0.05$; $\mu = 0.1$; $v = 0.5$; $\lambda = 0.1$; $\omega = 0.01$; $e = 0.01$; $\gamma = 0.6$; and the initial species sizes are $[S(0), I(0), M(0)] = [0.10,\ 0.25,\ 0.15]$. In the absence of time lag, we have verified that the criteria for the existence and stability of disease free equilibrium L_1 of system (3.5) is satisfied. For $\lambda = 0.1$ and the values of rest of the parameters from Table 3.1, we have disease free equilibrium point $L_1(0.495832, 0, 0.148789)$ and $g_1^0 = gM_1 + v + \mu(1 - \frac{1}{M_1}) = -0.0572138$. Thus, the admissible criterion: $g_1(0.4) >$

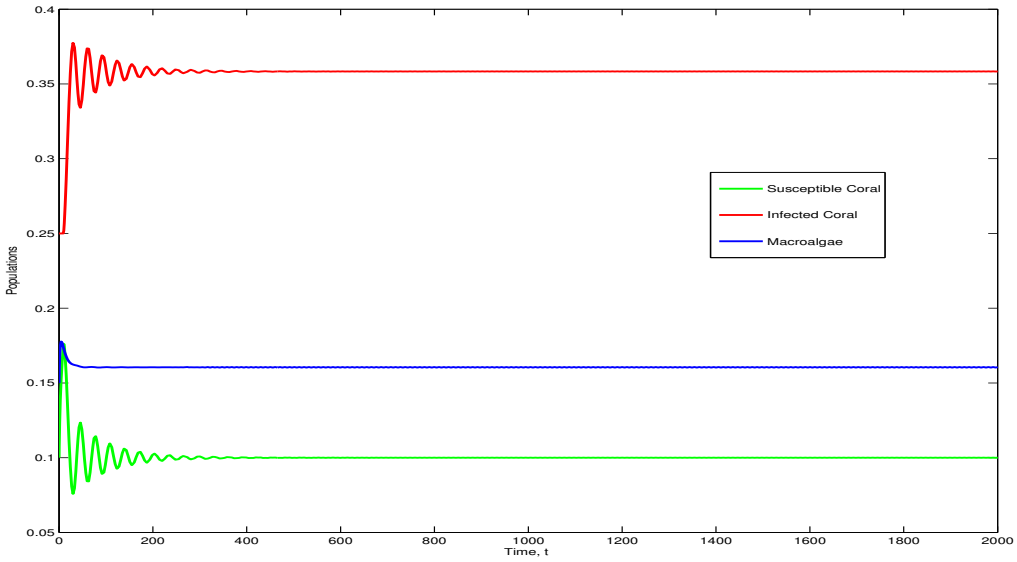

Figure 3.4: Numerical simulation in the presence of delay $\tau = 9.0$ for system (3.5). The parameter values are taken as in the Figure 3.2.

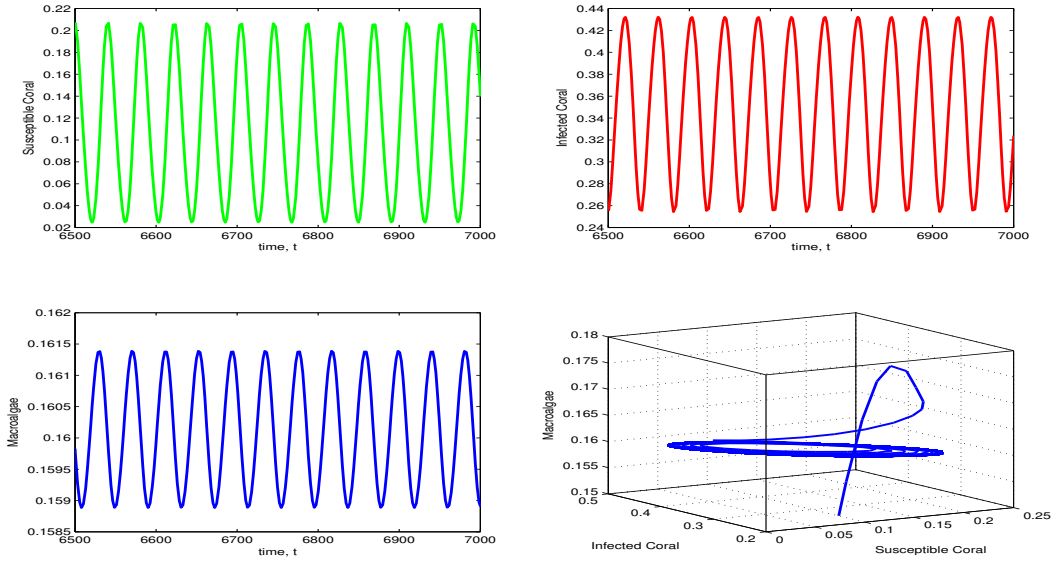

Figure 3.5: Numerical simulation for $\tau = 12.548$ in the presence of delay for system (3.5). The other parameter values as in Figure 3.2.

$g_1^0(-0.0572138)$ for disease free equilibrium point L_1 is satisfied. Using the same set of the values of parameters, we have computed the disease threshold parameter $R_0 = 0.708331 < 1$ ($R_0 = \frac{\lambda S_1}{d+e+\omega}$), $r > r_{[0]} = -0.436435$ and $\frac{\partial(F_1,F_3)}{\partial(S,M)}|_{(S_1,0,M_1)} = 0.038086 > 0$. Moreover, eigenvalues associated with $L_1(0.495832, 0, 0.148789)$ are -0.490466, -0.077653, -0.0204168. Due to Theorem 3.2, Without a time delay (τ), the system is stable around the equilibrium point L_1. In this scenario, the disease does not spread through the coral reef ecosystem

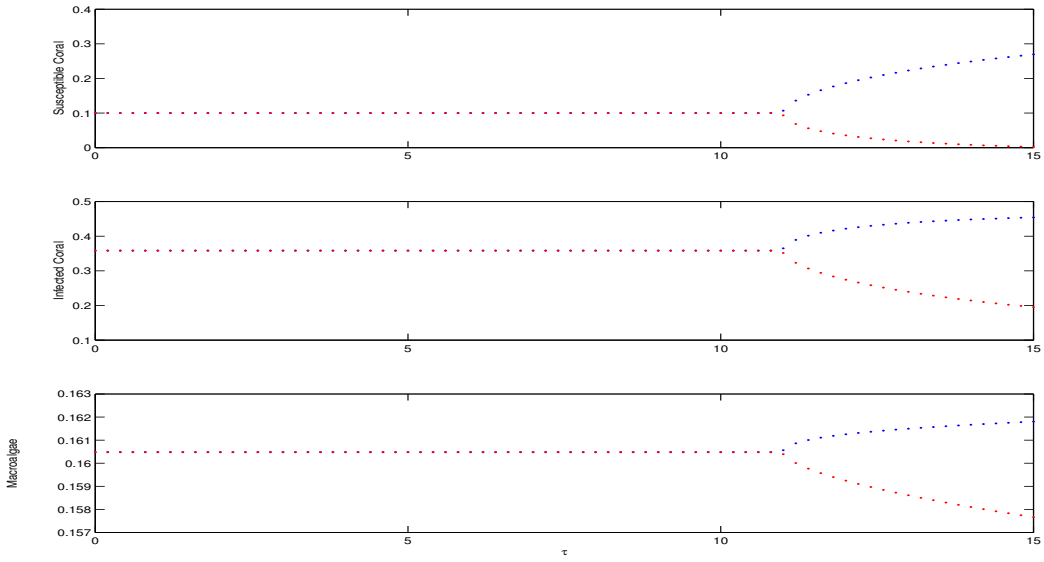

Figure 3.6: Bifurcation diagram of system (3.5) for time delay τ. The parameter values are taken as in the Figure 3.2.

because healthy coral and macroalgae species co-exist stably around the disease-free state (as shown in Figure 3.1). Further, the disease continues to exist within the coral reef populations when the disease transmission rate, λ, exceeds a certain threshold. Figure 3.2 illustrates that for $\lambda = 0.7$, all species coexist stably around the interior equilibrium point, L_*. In this scenario, the disease threshold parameter $R_0 = 4.95832 > 1$ indicates that the disease is likely to propagate within the coral reef populations. Without any time lag, our numerical simulation indicates that a minimum infection force ($\lambda_{min} \approx 0.1412$) is necessary for the disease to spread among the coral reef species in the system (3.5). To illustrate the system's dynamics more clearly, we present the diagram (Figure 3.3) for various values of λ. It is also imperative to mention that a transcritical bifurcation happens for gradually enhancing the magnitude of λ through λ_{min}, that is, the disease-free equilibrium loses stability, and the interior equilibrium point becomes stable in nature at λ_{min}. Similar observations have been reported by the authors in [185–188]. Next, we examine the effect of time lag on the dynamics of the disease. In order to reach our goal, we set $\lambda = 0.7$, while the remaining parameter values are provided in Table 3.1. The endemic steady state takes the form $L_*(S_*, I_*, M_*)$ with species densities $S_* = 0.1, I_* = 0.358343, M_* = 0.160479$. It is noted that the interior equilibrium point L_* exhibits stability when there is no time lag ($\tau = 0$). By introducing a time lag into the system, we observe that for $\tau = 9.0$, all species coexist in a locally asymptotically stable state near the interior equilibrium point (see Fig.3.4), since $Trac(J_*) = -0.81879 < 0$, $\frac{\partial(F_1,F_2,F_3)}{\partial(S,I,M)}|_{(S_*,I_*,M_*)} = -0.0106389 < 0$ and $Trace(J_*)\Delta[-0.150141] < \frac{\partial(F_1,F_2,F_3)}{\partial(S,I,M)}|_{(S_*,I_*,M_*)}[-0.0106389]$. With the same set of parameters values, we get $\kappa_1 = 0.104442$, $\kappa_2 = 0.00657864$, $\kappa_3 = -0.0000559973$, which reveals

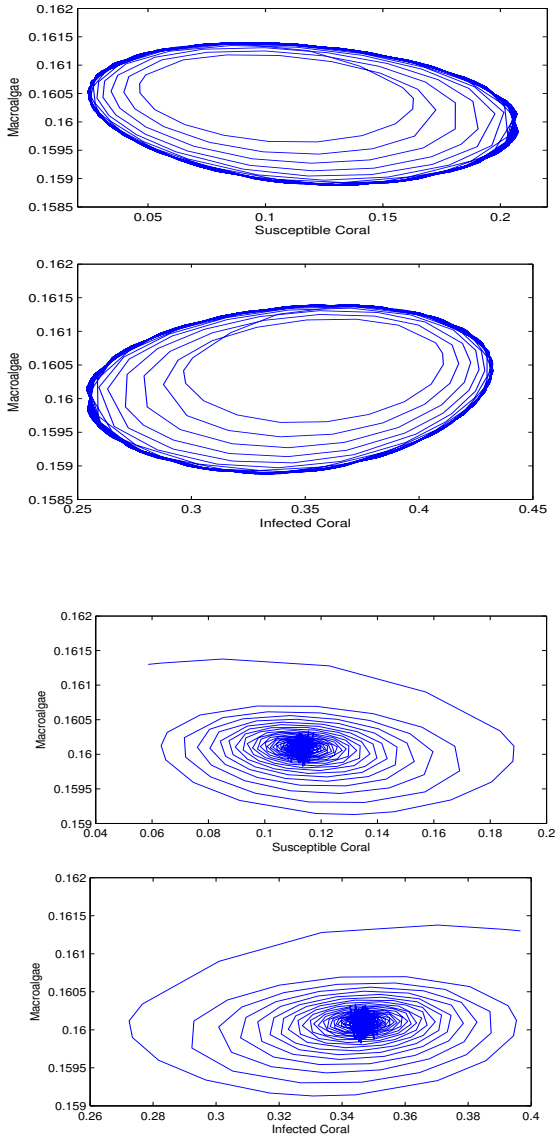

Figure 3.7: Numerical simulation of system (3.5) for $\omega = 0.01$ in of delay of the system (3.5). (b) Numerical simulation of system (3.5) for $\omega = 0.019$. The other parameters values are same as in Figure 3.5.

the existence of a positive zero, $\vartheta_0 \approx 0.00754336$ of the Eq. (3.18). As a result, (3.17) has at least one positive zero, namely, $\delta_0 \approx 0.0868525$. Due to Theorem 3.3, we notice that the stability switching may arise as τ increases. The value of τ for which stability switching occurs is $\tau^* \approx 10.919$ and it can easily be calculated from (3.15) and (3.16). Furthermore, we have verified through numerical calculations that $S(\delta_0)A(\delta_0) - B(\delta_0)M(\delta_0) = 0.000156696 \neq 0$, confirming that the transversality condition holds:

$$\frac{d}{d\tau}\left[Re\rho(\tau)\right]_{\tau=\tau^*} = 0.00562687 \neq 0.$$

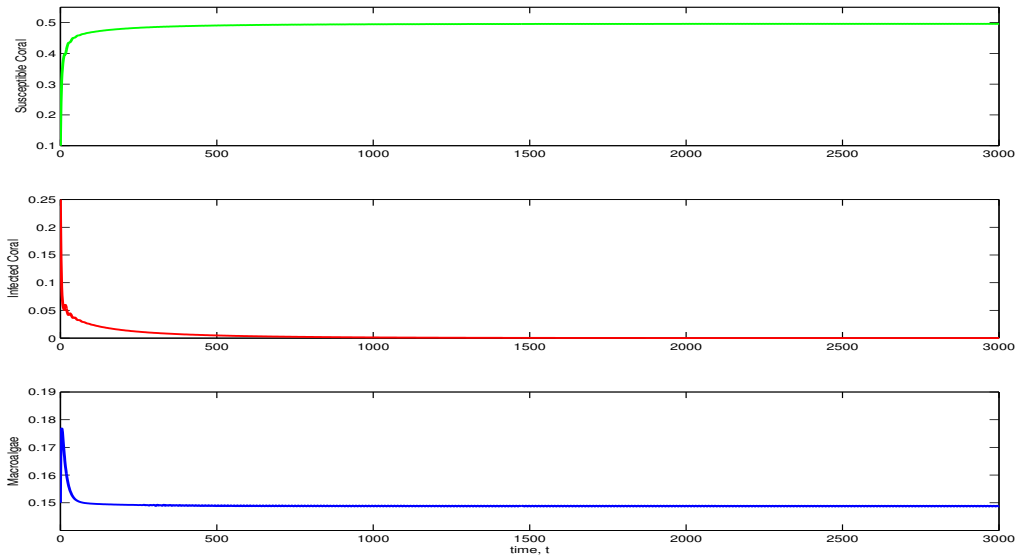

Figure 3.8: Population abundances for $\omega = 0.30$ in of delay of the system (3.5) and other parameter values are same as in Figure 3.5.

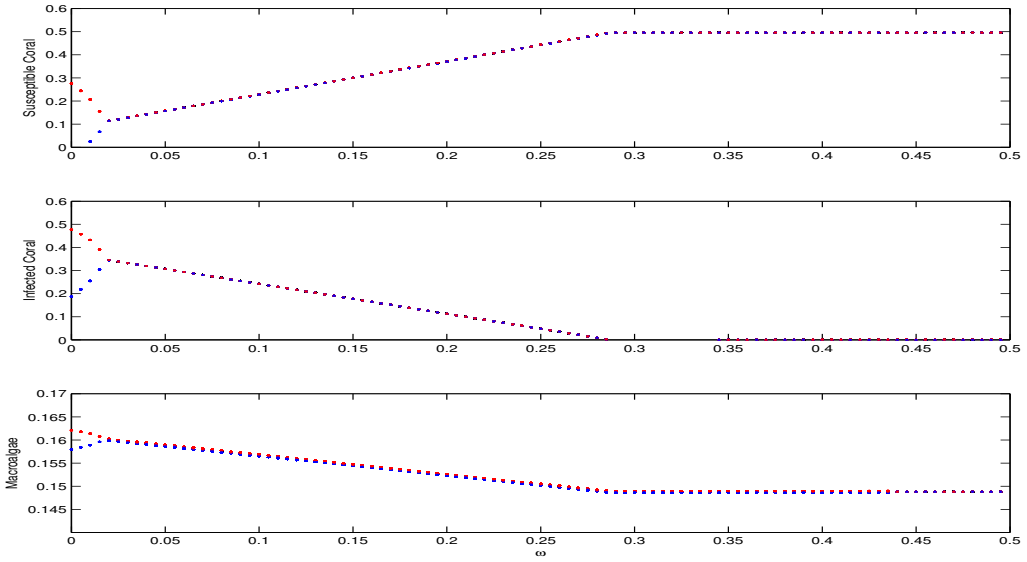

Figure 3.9: Bifurcation diagram of system (3.5) for time delay ω. The parameter values are taken as in the Figure 3.5.

Butler's lemma predicts that L_* remains stable when $\tau < \tau^*$, as shown in Figure 3.4. This corresponds to a solution of system 3.5 for $\tau = 9.0$. As the value of τ increases beyond $\tau^*(\approx 10.919)$, a periodic solution emerges, indicating the occurrence of a Hopf bifurcation (Figure 3.5). It is also observed that the system's oscillation amplitude grows as τ increases when τ exceeds τ^*. This observation is in agreement with the result of Bhattacharyya et . al. [122]. To better understand the dynamics of the coral reef system, we create a

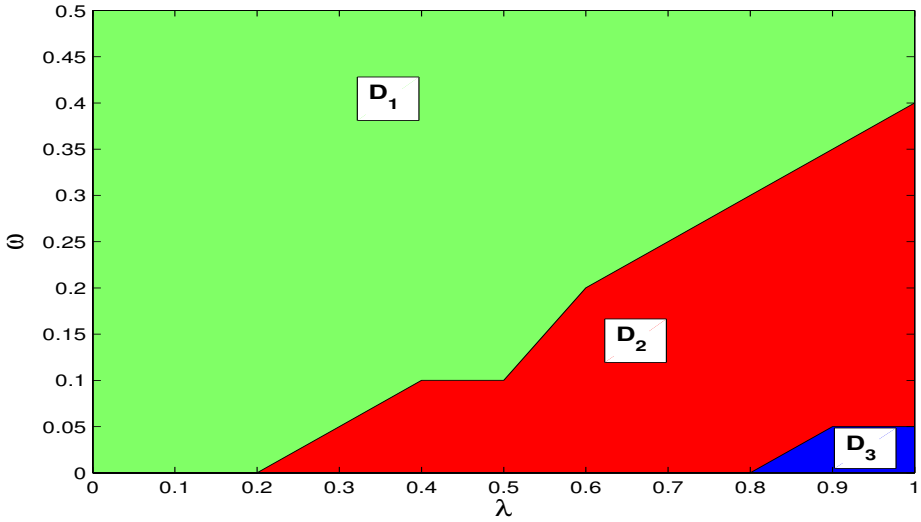

Figure 3.10: Domains of stability and instability of the model (3.5) in two dimensional $\lambda - \omega$ parameter space where other parameter values are fixed as in Table 3.1. The horizontal axis represents the rate of disease transmission λ and the vertical axis represent recovery rate ω. The D_1 (green) domain depicts that the disease-free equilibrium point $L_1(S_1,0,M_1)$ is stable; the D_2 (red) domain indicates the stability region of the interior equilibrium point $L_*(S_*,I_*,M_*)$ and the D_3 (blue) domain depicts oscillatory nature around interior equilibrium L_*.(Color figure online)

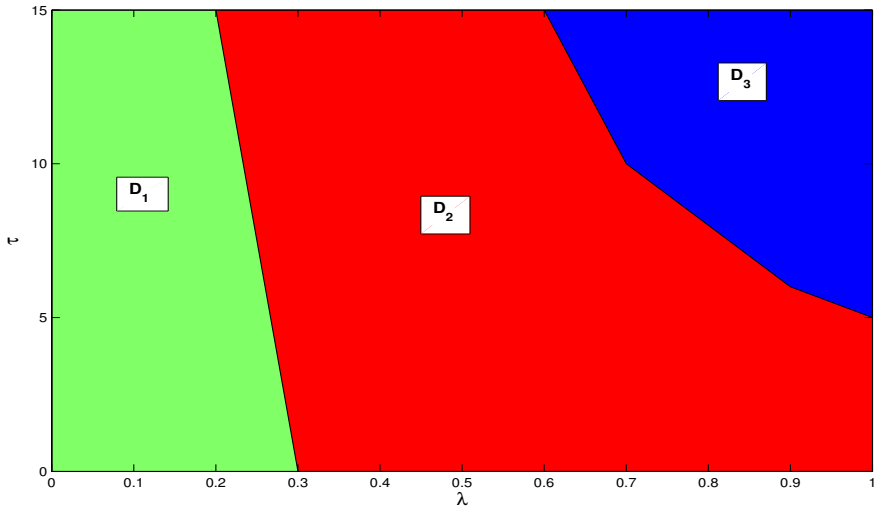

Figure 3.11: Domains of stability and instability of the model (3.5) in two dimensional $\lambda - \tau$ parameter space where other parameter values are fixed as in Table 3.1. The horizontal axis represents the rate of disease transmission λ and the vertical axis represent recovery rate ω. The D_1 (green) domain depicts that the disease-free equilibrium point $L_1(S_1,0,M_1)$ is stable; the D_2 (red) domain indicates the stability region of the interior equilibrium point $L_*(S_*,I_*,M_*)$ and the D_3 (blue) domain depicts oscillatory nature around interior equilibrium L_*.(Color figure online)

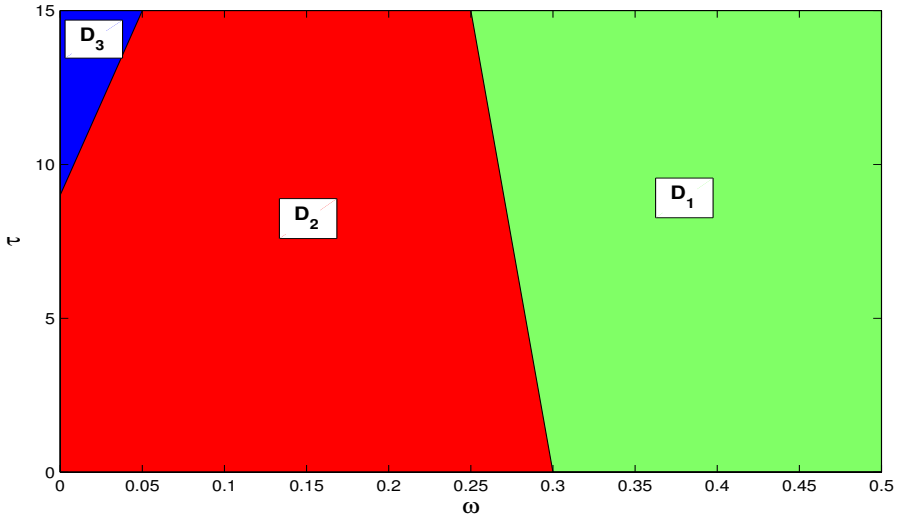

Figure 3.12: Domains of stability and instability of the model (3.5) in two dimensional $\omega-\tau$ parameter space where other parameter values are fixed as in Table 3.1. The horizontal axis represents the rate of disease transmission λ and the vertical axis represent recovery rate ω. The D_1 (green) domain depicts that the disease-free equilibrium point $L_1(S_1,0,M_1)$ is stable; the D_2 (red) domain indicates the stability region of the interior equilibrium point $L_*(S_*,I_*,M_*)$ and the D_3 (blue) domain depicts oscillatory nature around interior equilibrium L_*.(Color figure online)

bifurcation diagram (Figure 3.6) by varying the values of the time delay τ. Moreover, using the algorithms detailed in Section 3.5.3, we find $C_1(0) = -0.006698 - 0.08857i$ for $\tau = \tau^*$, which gives $\mu_2 = 1.190359$, $\beta_2 = -0.013396$, and $\tau_2 = 0.086$. Thus, the Hopf bifurcation of system (3.5) near the interior equilibrium point $L_*(0.1, 0.358343, 0.160479)$ is supercritical. The bifurcating periodic solution emerges for $\tau > \tau^*$, is orbitally stable, and its period decreases as τ increases. A critical aspect of Hopf-bifurcation in this scenario is the emergence of a limit cycle around the equilibrium point, L_*, at the bifurcation point. In this case, two distinct solutions arising from different initial values converge to the limit cycle, leading to a stable periodic solution. We also describe the effect of conversion rate ω of infected colonies to healthy class on the disease dynamics of the system (3.5). To demonstrate the impact of ω in the system, we slowly increase the magnitude of ω and settle the value of τ at 12.648, and the remaining parameter values are identical to those in Figure 3.2. For $\omega = 0.019$, the endemic steady state is stable focus. For sufficiently higher value of $\omega > \omega_0[\approx 0.0181]$, can control the oscillation among the species due to presence of time lag. If we continue to gradually increase the value of ω, it becomes apparent that ω regulates the disease transmission within the coral reef ecosystem when it reaches a sufficiently high level, specifically $\omega > \omega_c[\approx 0.288]$. Therefore, a transcritical bifurcation takes place between the interior equilibrium point and the disease-free equilibrium point at ω_c. So, effect of conversion rate ω of infected colonies to healthy class can control the oscillation among the system, and control disease transmission among coral species.

To gain a comprehensive understanding of the model's stability behavior as described by Equation (3.5), we present two parameters bifurcation diagrams (Fig. [3.10-3.12]) that illustrate the regions of stability and instability around the equilibrium points L_1 and L_*. In Fig. [3.10-3.12], the green region (D_1) outlines the stability zone of the disease-free equilibrium point L_1, the red region (D_2) shows the stability area of the interior equilibrium point L_*, and the blue region (D_3) represents the system's periodic oscillation behavior around the equilibrium point L_*. Initially, we trace two parameter bifurcation in $\lambda - \omega$ space (see the Fig 3.10). It is noted that for any given value of ω, the system remains stable around the disease-free equilibrium point L_1 when the disease transmission rate (λ) is below a critical threshold (≈ 0.2). For sufficiently moderate to higher value of ω and for the disease transmission rate (λ) crossing a critical value (≈ 0.2), the system shows stable nature around L_*. Consequently, the disease persists among the species of coral reef system. On the other hand, all species of the system indicate oscillation nature around L_* for a sufficiently higher value of λ and a sufficiently smaller value of ω. Subsequently, we produce the stability and oscillation domain of the model (3.5) in $\lambda - \tau$ parameter space (see the Fig. 3.11). From Fig. 3.11, we observe that for any moderate value λ up to (≈ 0.3) and arbitrary value of time lag τ, the model (3.5) exhibits stable nature around the equilibrium L_* and the coral species become disease-free. It is also observe that the disease persists among the coral species with stable nature for sufficiently moderate to higher value of λ and arbitrary value of time lag τ. On the other hand, the species show the periodic nature around the interior equilibrium point L_* when disease transmission rate λ is quite high and the magnitude of time lag τ between sufficiently moderate to high values. Further, we draw domain of the species dynamics for the system (3.5) in $\omega - \tau$ parameter space. From Fig. 3.12, one can observe the model indicates the oscillation nature among the all species when the recovery rate ω and the magnitude of time lag τ are sufficiently low and high respectively. For any value of time lag τ and for sufficiently moderate value of ω, the periodic oscillation around the interior equilibrium L_* disappears and the system becomes unstable from its stable nature around L_*. Next, if the magnitude of ω is high enough, then the system switches form oscillation around interior equilibrium point L_* to stable nature around the disease free equilibrium point L_1 for an arbitrary magnitude of time lag τ. The above observations indicate that the time lag τ can produce the oscillation among the species whereas the conversion efficiency or recovery rate ω can control the oscillation among the system as well as disease transmission among coral species.

3.7 Conclusion

It is widely recognized that time delay plays a crucial role in studying biological processes, as the system's behavior does not manifest immediately.Consequently, it is crucial to investigate how time delays influence the stability of the coral reef ecosystem. Coral diseases are

a significant factor in coral reef decline, so it is necessary to incorporate them in the study of the coral reef system. In this study, we developed and analysed a mathematical model of coral reef epidemiology using a system of 3D coupled ordinary differential equations representing the dynamics of susceptible, infected coral and macroalgaeIn the face of disease, the coral population can be segregated into two distinct groups: healthy and infected. The healthy coral turns into infected through a contagious pathway (e.g, black band and white band diseases). The healthy coral does not become infected instantaneously but it is induced by time delay due to the incubation. The spread of disease among coral follows a mass-action principle. Hence, it is imperative to consider the effects of disease transmission rate (λ), incubation time lag (τ), and conversion/recovery rate (ω) in the coral reef dynamical system.

We have investigated the biologically feasible distinct equilibrium points of the system. The preliminary result, presented in Section 3.3, is concerned with the existence and positivity of solutions of (3.5). We computed the disease basic reproduction number R_0 and threshold parameter $r_{[0]}$ for recruitment rate of coral. Analytical results indicate that the disease-free equilibrium is locally asymptotically stable when $R_0 < 1$ and $r > r_{[0]}$ provided that $\frac{\partial(F_1,F_3)}{\partial(S,M)}|_{(S_1,0,M_1)}$ is positive definite. This result demonstrates that the disease will propagate among the corals if the rate of disease transmission (λ) exceeds a certain critical threshold, as R_0 increases monotonically with λ. On the contrary, a sufficiently higher recovery rate (ω) of coral reef is necessary to wipe out the disease from system as R_0 is monotone decreasing function with increasing value of recovery rate ω. Therefore, while the disease transmission rate facilitates the spread of the disease within the system, the recovery rate is crucial in managing and controlling the disease's spread in the coral reef ecosystem. When a time delay (τ) is present, the system exhibits stable behaviour if the delay is below a certain threshold value (τ^*) and unstable behaviour if the delay exceeds this threshold. Thus, the system experiences a Hopf-bifurcation around L_*. We have presented the condition required for the occurrence of Hopf-bifurcation around L_*. The delay duration necessary to maintain the system's stability has also been calculated. Moreover, it is observed that the oscillation among the corals can be controlled when the conversion efficiency rate (ω) crosses a threshold value. Also, one can notice that the magnitude of ω increases when the system becomes disease free. Using the notation introduced by Hassard et al., we have investigated the direction of the Hopf bifurcation, the stability of the bifurcating periodic solution, and its period.

The results obtained in this study suggest that the conversion efficiency or recovery rate and incubation delay time play a crucial role in controlling the disease transmission and oscillations among the species of coral-reef ecosystem. The introduction of incubation delay in a coral reef ecosystem demonstrates that the all species coexist in oscillatory nature. In fact, the conversion or recovery rate of infected colonies to healthy coral can prevent the oscillation among the species of the system and control the disease transmission among

coral species.

4

Dynamics of Zooplankton-Mediated Disease Outbreak in Coral-Reef [1]

4.1 Introduction

Coral reefs are vital ecosystems supporting marine biodiversity and coastal economies. However, coral diseases, driven by biological (bacteria, fungi, viruses) and environmental stressors (rising sea temperatures, pollution), are accelerating reef degradation worldwide [189, 190]. Among these, white band disease (WBD) is a major contributor to coral decline, particularly affecting key reef-building species *Acropora palmata* and *Acropora cervicornis* [101, 191]. WBD spreads through direct contact, waterborne transmission, and corallivores such as fireworms and reef fish [115, 117]. Although the exact pathogens remain uncertain, bacteria from *Vibrionaceae* and *Flavobacteriaceae* have been implicated [116, 192].

The increasing prevalence of coral diseases has been linked to declining water quality and climate change [193, 194]. Disease outbreaks significantly reduce coral cover, disrupt reef structures, and promote macroalgal dominance, further threatening ecosystem stability [195, 196]. While past studies modeled disease transmission via direct contact or free-living pathogens [122, 143], recent research suggests that zooplankton may also act as

[1]The bulk of this chapter has been published in *Journal of Theoretical Biology* by Ranjit, B., Biswas, S., Bhattacharyya, J., & Chattopadhyay, J. Springer 1-29., (2023). DOI- `https://doi.org/10.1007/s12591-023-00643-0`

vectors for coral infections [136].

In this study, we develop a phytoplankton-zooplankton-coral model to examine both contagious and non-contagious transmission of WBD. By incorporating pathogen dynamics, we aim to determine the most detrimental transmission mode and explore the role of coral-phytoplankton mutualism in reef recovery. Our findings will provide insights into disease-driven coral declines and potential mitigation strategies.

4.2 The Basic Model

To study the coral disease dynamics due to both contagious and non-contagious pathway, we constructed a mathematical model incorporating phytoplankton-zooplankton population in coral ecosystems with the presence of free-living pathogens (see the schematic diagram). Phytoplankton (P) grows logistically and is preyed by the zooplankton (Z). Zooplankton again consumed by the corals and die at a constant rate. The fraction of phytoplankton that lives in a mutualism relationship with the coral, commonly referred as zooxanthellae lives in coral's gastrodermis [29, 197]. Thus, it's a process of endosymbiosis and the phytoplankton is within the host's cell and protected from any attack from zooplankton in the system [53]. The relationship is intimate with a symbiont in the vacuole of the host cell, a gastrodermal cell of the symbiosome, through which the partners usually exchange food and other molecules [53]. Furthermore, corals in which larvae develops with in polyp, releases zooxanthellae planulae. In these corals, the zooxanthellae that occurs in parental gastoderm cells are transferred from mother colonies to the oocytes or planula (termed vertical transmission), while in other corals species the offspring acquire symbionts from the environment (termed horizontal transmission) [198]. Both the phyto- and zoo-plankton population is regulated by some constant inflow due to immigration. Coral population is subdivided into two classes, namely susceptible (C_S) and infected (C_I). Disease mainly transmit in two ways. Firstly, the direct interaction of susceptible and infected corals is responsible for the disease spreading among corals, known as contagious pathway of transmission. Here the transmission term is taken to be the product of susceptible and infected corals. The second way of coral disease transmission is known as the non-contagious pathway; due to the predation of the zooplankton by the coral and also due to the free-living pathogens (W). The first component of the non-contagious pathway is taken to be proportional to the predation term of the zooplankton by the corals. Zooplanktone plays an importent role as a vector for coral disease [136], exactly white band disease (WBD). The latter is taken as the product of the susceptible corals with the pathogens. In addition, susceptible coral makes symbiosis with phytoplankton. Both susceptible and infected coral dies at a constant rate and there is an additional mortality due to the disease of infected corals. Zooplankton helps to grow pathogens by the shedding effect and infected coral release pathogen at a constant rate in the environment. Additionally, pathogen growth

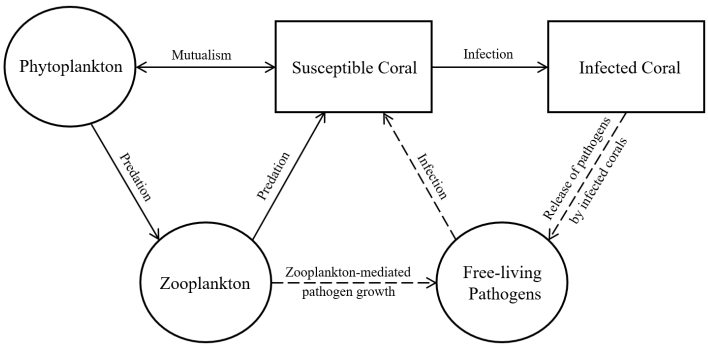

Figure 4.1: A schematic representation of the model.

is mediated by some self-limiting term and natural mortality. A schematic diagram of the system is given in Fig. 4.1. Incorporating all the terms, our model takes the following form:

$$\begin{aligned}
\frac{dP}{dt} &= rP\left(1-\tfrac{P}{K}\right)-\alpha_1(1-\sigma)PZ+\tfrac{m_1\sigma PC_S}{a_1+\sigma P}+\eta_P,\\
\frac{dZ}{dt} &= e_1\alpha_1(1-\sigma)PZ-\alpha_2C_SZ-d_1Z+\eta_Z,\\
\frac{dC_S}{dt} &= \tfrac{m_2\sigma PC_S}{a_2+C_S}+(e_2\alpha_2-\lambda_1)C_SZ-\lambda_2C_SC_I-\lambda_3C_SW-d_2C_S,\\
\frac{dC_I}{dt} &= \lambda_1C_SZ+\lambda_2C_SC_I+\lambda_3C_SW-(d_2+\gamma)C_I,\\
\frac{dW}{dt} &= W(\beta_1Z+\beta_2C_I-d_3-\delta W),
\end{aligned} \tag{4.1}$$

where $P(0)\geq 0$, $Z(0)\geq 0$, $C_S(0)\geq 0$, $C_I(0)\geq 0$ and $W(0)\geq 0$.

- $P\equiv$ Phytoplankton.
- $Z\equiv$ Zooplankton.
- $C_S\equiv$ Susceptible Corals.
- $C_I\equiv$ Infected Corals.
- $W\equiv$ Free-living Pathogens.
- The intrinsic growth rate of phytoplankton is r.
- The carrying capacity of phytoplankton is K.
- Phytoplankton-predation rate of zooplankton is α_1.
- Predation rate of zooplankton by susceptible corals is α_2.
- σ is the fraction of phytoplankton population having mutualism with corals.
- η_P and η_Z are the (constant) immigration rates of phytoplankton and zooplankton re-

spectively.

• m_1 and m_2 are the maximum benefits of mutualistic interaction.

• a_1 and a_2 are the half saturation coefficients of the functional responce representing mutualism.

• e_1 and e_2 are conversion efficiency of zooplankton and corals respectively.

• d_1 and d_2 are the mortality rates of zooplankton and corals respectively.

• γ is the disease-induced death rate of infectious corals.

• λ_1, λ_2 and λ_3 are the disease transmission rates due to the consumption of zooplankton by susceptible corals, through contagious pathway (from infectious to susceptible corals) and through non-contagious pathway (from the environment to susceptible corals) respectively.

• β_1 and β_2 are the shedding rates of pathogens into the environment by zooplankton and infectious corals respectively.

• $\frac{1}{d_3}$ is the average time of existence of the pathogens in the environment.

• δ is the crowding parameter.

Let us change the variables of the system (4.1) to non-dimensional ones so that the scaled system contains a minimal number of parameters by substituting

$$P = K\bar{P},\ Z = \frac{r\bar{Z}}{\alpha_1},\ C_S = \frac{Kr\bar{C}_S}{m_1},\ C_I = \frac{Kr\bar{C}_I}{m_1},\ W = \frac{Kr\bar{W}}{m_1},\ t = \frac{\bar{t}}{r}$$

and defining non-dimensional parameters

$$\bar{\alpha}_1 = \frac{\alpha_1 K}{r},\ \bar{\alpha}_2 = \frac{\alpha_2 K}{r},\ \bar{d}_1 = \frac{d_1}{r},\ \bar{d}_2 = \frac{d_2}{r},\ \bar{d}_3 = \frac{d_3}{r},\ \bar{a}_1 = \frac{a_1}{K},\ \bar{a}_2 = \frac{a_2 m_1}{Kr},$$

$$\bar{m} = \frac{m_1 m_2}{r^2},\ \bar{\lambda}_1 = \frac{\lambda_1}{\alpha_1},\ \bar{\eta}_P = \frac{\eta_P}{rK},\ \bar{\eta}_Z = \frac{\alpha_1 \eta_Z}{r^2},\ \bar{\lambda}_2 = \frac{\lambda_2 K}{m_1},\ \bar{\lambda}_3 = \frac{\lambda_3 K}{m_1},$$

$$\bar{\gamma} = \frac{\gamma}{r},\ \bar{\delta} = \frac{\delta K}{m_1},\ \bar{\beta}_1 = \frac{\beta_1}{\alpha_1},\ \bar{\beta}_2 = \frac{\beta_2 K}{m_1}.$$

Under these substitutions, by dropping the 'bars', the system (4.1) reduces to

$$\begin{aligned}
\frac{dP}{dt} &= P(1-P)-(1-\sigma)PZ+\tfrac{\sigma PC_S}{a_1+\sigma P}+\eta_P \equiv F_1,\\
\frac{dZ}{dt} &= e_1\alpha_1(1-\sigma)PZ-\alpha_2C_SZ-d_1Z+\eta_Z \equiv F_2,\\
\frac{dC_S}{dt} &= \tfrac{m\sigma PC_S}{a_2+C_S}+(e_2\alpha_2-\lambda_1)C_SZ-\lambda_2C_SC_I-\lambda_3C_SW-d_2C_S \equiv F_3,\\
\frac{dC_I}{dt} &= \lambda_1C_SZ+\lambda_2C_SC_I+\lambda_3C_SW-(d_2+\gamma)C_I \equiv F_4,\\
\frac{dW}{dt} &= W(\beta_1Z+\beta_2C_I-d_3-\delta W) \equiv F_5,
\end{aligned} \tag{4.2}$$

where $P(0)\geq 0$, $Z(0)\geq 0$, $C_S(0)\geq 0$, $C_I(0)\geq 0$ and $W(0)\geq 0$.

4.3 Results

4.3.1 Positive Invariance

Theorem 4.1 *With positive beginning values, every solution to our system is both unique and existing in* $[0,\infty)$ *and* $P(t)>0$, $Z(t)>0$, $C_S(t)>0$, $C_I(t)>0$, $W(t)>0$, $\forall\, t\geq 0$.

Proof: Let $G=(P,\ Z,\ C_S,\ C_I,W)^T$ and $F(G)=[F_1,\ F_2,\ F_3,\ F_4,\ F_5]^T$. Then the system (4.2) can be put in the form

$$\dot{G}=F(G),$$

where $F: R_+\rightarrow R_+^5$ with $G(0)=G_0\in R_+^5, F_i\in R^\infty(R_+)$, for $i=1,2,3,4,5$. As a result, vector function F is an entirely continuous, locally lipschitzian variable function $(P,\ Z,\ C_S,\ C_I,\ W)$ in $E=[P(t),\ Z(t),\ C_S(t),\ C_I(t),\ W(t)]$; $P>0$, $Z>0$, $C_S>0$, $C_I>0$, $W>0$. Applying the lemma in [199], we can say that any solution $(P,\ Z,\ C_S,\ C_I,\ W)$ of the system (4.2) with positive initial values exits and is unique in the interval $[0,M]$, $\forall\, t\geq 0$. Where M is a finite positive real number.

4.3.2 Equilibrium and Local Stability Analysis

4.3.2.1 Existence of Equilibrium Points

The system (4.2) has four equilibrium points.

(i) $E_1=(P_1,\ Z_1,\ 0,\ 0,\ W_1)$, where $Z_1=\frac{P_1(1-P_1)+\eta_P}{(1-\sigma)P_1}$, $W_1=\frac{\beta_1Z_1-d_3}{\delta}$ and P_1 is positive

real root of $\psi(P)=0$, where

$$\psi = e_1\alpha_1(1-\sigma)P^3 - \{e_1\alpha_1(1-\sigma)+d_1\}P^2 + \{d_1-(1-\sigma)(\eta_Z+e_1\alpha_1\eta_P)\}P + d_1\eta_P.$$

We note that $\psi(P)=0$ has either no positive solution or a pair of positive solutions. The equilibrium point E_1 exists if $Z_1 > d_3/\beta_1$.
From Fig. 4.2 it follows that out of the two possible positive solutions of $\psi(P)=0$, only one gives the value of Z_1 so that $Z_1 > d_3/\beta_1$ is satisfied. Therefore, E_1 exists uniquely.

(ii) $E_2 = (P_2,\ Z_2,\ 0,\ 0,\ 0)$, where $Z_2 = \frac{P_2(1-P_2)+\eta_P}{(1-\sigma)P_2}$ and P_2 is the positive solution of the equation $\psi(P)=0$. Fig. 4.2 depicts a unique E_2 for the system (4.2).

(iii) $E_3 = (P_3,\ Z_3,\ C_{S3},\ C_{I3},\ 0)$, where P_3 is a positive solution of the equation $\frac{m\sigma P}{a_2+f_1(P)} + (e_2\alpha_2-\lambda_1)f_2(P) - \lambda_2 f_3(P) = d_2$, $C_{S3} = f_1(P_3) = \frac{-B_0(P_3)\pm\sqrt{B_0^2(P_3)-4A_0(P_3)C_0(P_3)}}{2A_0(P_3)}$, $Z_3 = f_2(P_3) = \frac{\eta_z}{\alpha_2 f_1(P_3)+d_1-e_1\alpha_1(1-\sigma)P_3}$, $C_{I3} = f_3(P_3) = \frac{\lambda_1 f_1(P_3) f_2(P_3)}{d_2+\gamma-\lambda_2 f_1(P_3)}$, $A_0(P_3) = \sigma P_3\alpha_2$, $B_0(P_3) = \sigma P_3(d_1-e_1\alpha_1(1-\sigma)P_3)+\alpha_2(a_1+\sigma P_3)\{P_3(1-P_3)+\eta_p\}$, and $C_0(P_3) = (a_1+\sigma P_3)[\{P_3(1-P_3)+\eta_p\}\{d_1-e_1\alpha_1(1-\sigma)P_3\}-(1-\sigma)P_3\eta_z]$.

(iv) $E^* = (P^*,\ Z^*,\ C_S^*,\ C_I^*,\ W^*)$ is the interior equilibrium point of the system (4.2), where P^* is a positive solution of the system of equation $\frac{m\sigma P}{a_2+f_1(P)} + (e_2\alpha_2-\lambda_1)f_2(P) - \lambda_2 g_3(P) - \lambda_3 g_4(P) = d_2$, $C_S^* = f_1(P^*)$, $Z^* = f_2(P^*)$, $C_I^* = g_3(P^*) = \frac{\{d_3\lambda_3-(\lambda_1\delta+\beta_1\lambda_3)f_2(P^*)\}f_1(P^*)}{(\lambda_2\delta+\beta_2\lambda_3)f_1(P^*)-\delta(d_2+\gamma)}$, and $W^* = g_4(P^*) = \frac{1}{\delta}\{\beta_1 f_2(P^*)+\beta_2 g_3(P^*)-d_3\}$.

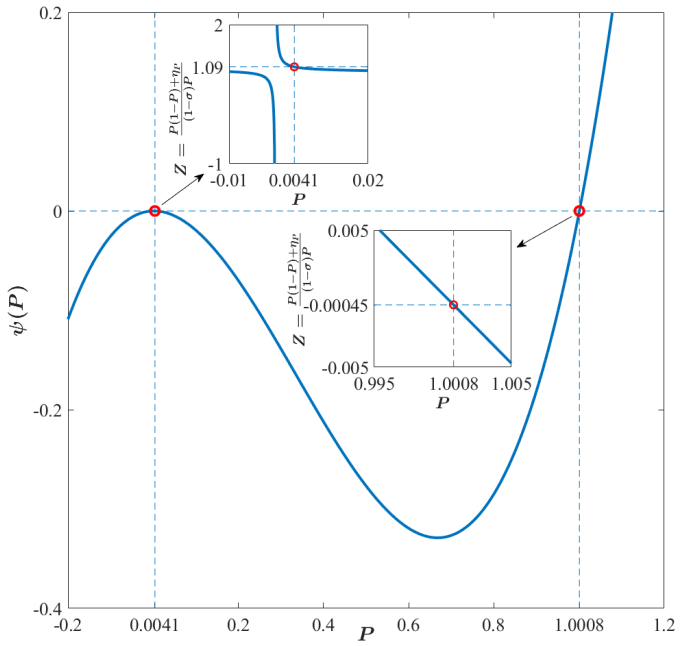

Figure 4.2: The graph of $\psi(P)$ showing the existence of two positive roots of $\psi(P)=0$. The inset figures verify the existence of E_1 and E_2 uniquely. The parameter values are taken from Table 4.1.

4.3.2.2 Local Stability Analysis

Now the Jacobian matrix of the system (4.2) at E_1 is

$$J_1 = \begin{pmatrix} a_1 & a_2 & a_3 & 0 & 0 \\ a_4 & a_5 & a_6 & 0 & 0 \\ 0 & 0 & a_7 & 0 & 0 \\ 0 & 0 & a_8 & a_9 & 0 \\ 0 & a_{10} & 0 & a_{11} & a_{12} \end{pmatrix},$$

with $a_1 = (1-2P_1) - (1-\sigma)Z_1$,
$a_2 = -(1-\sigma)P_1$,
$a_3 = \frac{\sigma P_1}{a_1+\sigma P_1}$,
$a_4 = e_1\alpha_1(1-\sigma)Z_1$,
$a_5 = e_1\alpha_1(1-\sigma)P_1 - d_1$,
$a_6 = -\alpha_2 Z_1$,
$a_7 = \frac{m\sigma P_1}{a_2} + (e_2\alpha_2 - \lambda_1)Z_1 - \lambda_3 W_1 - d_2$,
$a_8 = \lambda_1 Z_1 + \lambda_3 W_1$,
$a_9 = -(d_2+\gamma)$,
$a_{10} = \beta_1 W_1$,
$a_{11} = \beta_2 W_1$,
$a_{12} = \beta_1 Z_1 - d_3 - 2\delta W_1$.
Now, the characteristic equation of J_1 is given by

$$| J_1 - pI_5 | = 0.$$

The three roots of the characteristic equation of J_1 are:
$\frac{m\sigma P_1}{a_2} + (e_2\alpha_2 - \lambda_1)Z_1 - \lambda_3 W_1 - d_2$, $-(d_2+\gamma)$, $\beta_1 Z_1 - d_3 - 2\delta W_1$,
and the remaining two roots are given by the equation:

$$p^2 - (a_1+a_5)p + (a_1a_5 - a_2a_4) = 0.$$

Therefore, all the eigenvalues of the Jacobian matrix J_1 are negative if $\frac{m\sigma P_1}{a_2} + (e_2\alpha_2 - \lambda_1)Z_1 - \lambda_3 W_1 - d_2 < 0$, $\beta_1 Z_1 - d_3 - 2\delta W_1 < 0$, $a_1 + a_5 < 0$, $a_1a_5 > a_2a_4$. Thus, the system (4.2) is locally asymptotically stable at E_1.

The Jacobian matrix of the system (4.2) at E_2 is

$$J_2 = \begin{pmatrix} b_1 & b_2 & 0 & b_3 & 0 \\ b_4 & b_5 & b_6 & 0 & 0 \\ 0 & 0 & b_7 & 0 & 0 \\ 0 & 0 & b_8 & b_9 & 0 \\ 0 & 0 & 0 & 0 & b_{10} \end{pmatrix},$$

with $b_1 = (1-2P_2) - (1-\sigma)Z_2$,
$b_2 = -(1-\sigma)P_2$,
$b_3 = \frac{\sigma P_2}{a_1+\sigma P_2}$,
$b_4 = e_1\alpha_1(1-\sigma)Z_2$,
$b_5 = e_1\alpha_1(1-\sigma)P_2 - d_1$,
$b_6 = -\alpha_2 Z_2$,
$b_7 = \frac{m\sigma P_2}{a_2} + (e_2\alpha_2 - \lambda_1)Z_2 - d_2$,
$b_8 = \lambda_1 Z_2$,
$b_9 = -(d_2+\gamma)$,
$b_{10} = \beta_1 Z_2 - d_3$.
Now, the characteristic equation of J_2 is given by

$$| J_2 - qI_5 | = 0.$$

The three roots of the characteristic equation of J_2 are:
$\frac{m\sigma P_2}{a_2} + (e_2\alpha_2 - \lambda_1)Z_2 - \lambda_3 W_2 - d_2,\ -(d_2+\gamma),\ \beta_1 Z_2 - d_3$,
and the remaining two roots are given by the equation:

$$q^2 - (b_1+b_5)q + (b_1b_5 - b_2b_4) = 0.$$

Therefore, all the eigenvalues of the Jacobian matrix J_2 are negative if $\frac{m\sigma P_2}{a_2} + (e_2\alpha_2 - \lambda_1)Z_2 - \lambda_3 W_2 - d_2 < 0,\ \beta_1 Z_2 - d_3 < 0,\ b_1+b_5 < 0,\ b_1b_5 > b_2b_4$. Thus, the system (4.2) is locally asymptotically stable at E_2.
The Jacobian matrix of the system (4.2) at E_3 is

$$J_3 = \begin{pmatrix} c_1 & c_2 & c_3 & 0 & 0 \\ c_4 & c_5 & c_6 & 0 & 0 \\ c_7 & c_8 & c_9 & c_{10} & c_{11} \\ 0 & c_{12} & c_{13} & c_{14} & c_{15} \\ 0 & 0 & 0 & 0 & c_{16} \end{pmatrix},$$

with
$c_1 = (1-2P_3) - (1-\sigma)Z_3 + \frac{a_1\sigma C_{S_3}}{(a_1+\sigma P_3)^2}$,

$c_2 = -(1-\sigma)P_3,$
$c_3 = \frac{\sigma P_3}{a_1+\sigma P_3},$
$c_4 = e_1\alpha_1(1-\sigma)Z_3,$
$c_5 = e_1\alpha_1(1-\sigma)P_3 - \alpha_2 C_{S_3} - d_1,$
$c_6 = -\alpha_2 Z_3,$
$c_7 = \frac{m\sigma C_{S_3}}{a_2+C_{S_3}},$
$c_8 = (e_2\alpha_2 - \lambda_1)C_{S_3},$
$c_9 = \frac{a_2 m\sigma P_3}{(a_2+C_{S_3})^2} + (e_2\alpha_2 - \lambda_1)Z_3 - \lambda_2 C_{I_3} - d_2,$
$c_{10} = -\lambda_2 C_{S_3},$
$c_{11} = -\lambda_3 C_{S_3},$
$c_{12} = \lambda_1 C_{S_3},$
$c_{13} = \lambda_1 Z_3 + \lambda_2 C_{I_3},$
$c_{14} = \lambda_2 C_{S_3} - (d_2+\gamma),$
$c_{15} = \lambda_3 C_{S_3},$
$c_{16} = \beta_1 Z_3 + \beta_2 C_{I_3} - d_3.$
Now, the characteristic equation of J_3 is given by

$$| J_3 - sI_5 | = 0.$$

A root of the characteristic equation of J_3 is:
$\beta_1 Z_3 + \beta_2 C_{I_3} - d_3,$
and the remaining four roots are given by the equation:

$$s^4 + A_1 s^3 + A_2 s^2 + A_3 s + A_4 = 0.$$

Where,
$A_1 = -c_1 - c_5 - c_9 - c_{14},$
$A_2 = c_1c_5 + c_1c_9 + c_1c_{14} + c_5c_9 + c_5c_{14} + c_9c_{14} - c_{10}c_{13} - c_6c_8 - c_2c_4 - c_3c_7,$
$A_3 = c_1c_{10}c_{13} + c_5c_{10}c_{13} + c_1c_6c_8 + c_6c_8c_{14} + c_2c_4c_9 + c_2c_4c_{14} + c_3c_5c_7 + c_3c_7c_{14} - c_6c_{10}c_{12} - c_1c_5c_9 - c_1c_5c_{14} - c_1c_9c_{14} - c_5c_9c_{14} - c_2c_6c_7 - c_3c_4c_8,$
$A_4 = c_1c_6c_{10}c_{12} + c_2c_4c_{10}c_{13} + c_1c_5c_9c_{14} + c_2c_6c_7c_{14} + c_3c_4c_8c_{14} - c_1c_5c_{10}c_{13} - c_3c_4c_{10}c_{12} - c_1c_6c_8c_{14} - c_2c_4c_9c_{14} - c_3c_5c_7c_{14}.$
Using *Routh-Hurwitz* criteria, E_3 will be locally asymptotically stable, if
$A_i > 0\ (i = 1,2,3,4),$
$A_1A_2A_3 > A_3^2 + A_1^2A_4$
and also satisfied the condition
$\beta_1 Z_3 + \beta_2 C_{I_3} - d_3 < 0.$

The Jacobian matrix of the system (4.2) at E^* is

$$J^* = \begin{pmatrix} g_1 & g_2 & g_3 & 0 & 0 \\ g_4 & g_5 & g_6 & 0 & 0 \\ g_7 & g_8 & g_9 & g_{10} & g_{11} \\ 0 & g_{12} & g_{13} & g_{14} & g_{15} \\ 0 & g_{16} & 0 & g_{17} & g_{18} \end{pmatrix},$$

with

$g_1 = (1-2P^*) - (1-\sigma)Z^* + \frac{a_1\sigma C_S^*}{(a_1+\sigma P^*)^2}$,
$g_2 = -(1-\sigma)P^*$,
$g_3 = \frac{\sigma P^*}{a_1+\sigma P^*}$,
$g_4 = e_1\alpha_1(1-\sigma)Z^*$,
$g_5 = e_1\alpha_1(1-\sigma)P^* - \alpha_2 C_S^* - d_1$,
$g_6 = -\alpha_2 Z^*$,
$g_7 = \frac{m\sigma C_S^*}{a_2+C_S^*}$,
$g_8 = (e_2\alpha_2 - \lambda_1)C_S^*$,
$g_9 = \frac{a_2 m\sigma P^*}{(a_2+C_S^*)^2} + (e_2\alpha_2 - \lambda_1)Z^* - \lambda_2 C_I^* - \lambda_3 W^* - d_2$,
$g_{10} = -\lambda_2 C_S^*$,
$g_{11} = -\lambda_3 C_S^*$,
$g_{12} = \lambda_1 C_S^*$,
$g_{13} = \lambda_1 Z^* + \lambda_2 C_I^* + \lambda_3 W^*$,
$g_{14} = \lambda_2 C_S^* - (d_2+\gamma)$,
$g_{15} = \lambda_3 C_S^*$,
$g_{16} = \beta_1 W^*$,
$g_{17} = \beta_2 W^*$,
$g_{18} = \beta_1 Z^* + \beta_2 C_I^* - d_3 - 2\delta W^*$.

Now, the characteristic equation of J^* is given by

$$| J^* - xI_5 | = 0.$$

i.e.

$$x^5 + Q_1 x^4 + Q_2 x^3 + Q_3 x^2 + Q_4 x + Q_5 = 0.$$

Where,

$Q_1 = -g_1 - g_5 - g_9 - g_{14} - g_{18}$,
$Q_2 = g_1g_5 + g_1g_9 + g_1g_{14} + g_1g_{18} + g_5g_9 + g_5g_{14} + g_5g_{18} + g_9g_{14} + g_9g_{18} + g_{14}g_{18} - g_{15}g_{17} - g_{10}g_{13} - g_6g_8 - g_2g_4 - g_3g_7$,
$Q_3 = g_1g_{15}g_{17} + g_5g_{15}g_{17} + g_9g_{15}g_{17} + g_1g_{10}g_{13} + g_5g_{10}g_{13} + g_{10}g_{13}g_{18} + g_1g_6g_8 + g_6g_8g_{14} + g_6g_8g_{18} + g_2g_4g_9 + g_2g_4g_{14} + g_2g_4g_{18} + g_3g_5g_7 + g_3g_7g_{14} + g_3b_7g_{18} - g_1g_5g_9 - g_1g_5g_{14} -$

$g_1g_5g_{18} - g_1g_9g_{14} - g_1g_9g_{18} - g_1g_{14}g_{18} - g_5g_9g_{14} - g_5g_9g_{18} - g_5g_{14}g_{18} - g_9g_{14}g_{18} - g_{11}g_{13}g_{17} - g_6g_{10}g_{12} - g_6g_{11}g_{12} - g_3g_4g_8 - g_2g_6g_7$,

$Q_4 = g_1g_5g_9g_{14} + g_1g_5g_9g_{18} + g_1g_5g_{14}g_{18} + g_1g_9g_{14}g_{18} + g_5g_9g_{14}g_{18} + g_1g_{11}g_{13}g_{17} + g_5g_{11}g_{13}g_{17} + g_6g_8g_{15}g_{17} + g_1g_6g_{10}g_{12} + g_6g_{10}g_{12}g_{18} + g_1g_6g_{11}g_{16} + g_6g_{11}g_{14}g_{16} + g_2g_4g_{15}g_{17} + g_2g_4g_{10}g_{13} + g_3g_4g_8g_{14} + g_3g_4g_8g_{18} + g_2b_6g_7g_{14} + g_2g_6g_7g_{18} + g_3g_7g_{15}g_{17} - g_1g_5g_{15}g_{17} - g_1g_9g_{15}g_{17} - g_5g_9g_{15}g_{17} - g_1g_5g_{10}g_{13} - g_1g_{10}g_{13}g_{18} - g_5g_{10}g_{13}g_{18} - g_1g_6g_8g_{14} - g_1g_6g_8g_{18} - g_6g_8g_{14}g_{18} - g_6g_{11}g_{12}g_{17} - g_6g_{10}g_{15}g_{16} - g_2g_4g_9g_{14} - g_2g_4g_9g_{18} - g_2g_4g_{14}g_{18} - g_3g_4g_{10}g_{12} - g_3g_5g_7g_{14} - g_3g_5g_7g_{18} - g_3g_7g_{14}g_{18}$,

$Q_5 = -|J^*|$.

Using *Routh-Hurwitz* criteria, E^* will be locally asymptotically stable, if

(i) $Q_i > 0$ $(i = 1,2,3,4,5)$,

(ii) $Q_1Q_2Q_3 > Q_3^2 + Q_1^2Q_4$,

(iii) $(Q_1Q_4 - Q_5)(Q_1Q_2Q_3 - Q_3^2 - Q_1^2Q_4) > Q_5(Q_1Q_2 - Q_3)^2 + Q_1Q_5^2$. We can encapsulate the outcomes in the following theorem.

Theorem 4.2 *The stability behavior of the system (4.2) around the equilibrium points are described below.*

(i) Equilibrium point $E_1 = (P_1,\ Z_1,\ 0,\ 0,\ W_1)$ *is locally asymptotically stable (LAS) if* $\frac{m\sigma P_1}{a_2} + (e_2\alpha_2 - \lambda_1)Z_1 - \lambda_3 W_1 - d_2 < 0,\ \beta_1 Z_1 - d_3 - 2\delta W_1 < 0,\ a_1 + a_5 < 0,\ a_1a_5 > a_2a_4$.

(ii) Equilibrium point $E_2 = (P_2,\ Z_2,\ 0,\ 0,\ 0)$ *is locally asymptotically stable (LAS) if* $\frac{m\sigma P_2}{a_2} + (e_2\alpha_2 - \lambda_1)Z_2 - \lambda_3 W_2 - d_2 < 0,\ \beta_1 Z_2 - d_3 < 0,\ b_1 + b_5 < 0,\ b_1b_5 > b_2b_4$.

(iii) Equilibrium point $E_3 = (P_3,\ Z_3,\ C_{S3},\ C_{I3},\ 0)$ *is LAS if* $A_i > 0$, $(i = 1,2,3,4)$, $A_1A_2A_3 > A_3^2 + A_1^2A_4,\ \beta_1 Z_3 + \beta_2 C_{I_3} - d_3 < 0$.

(iv) Equilibrium point $E^* = (P^*,\ Z^*,\ C_S^*,\ C_I^*,\ W^*)$ *is LAS if* $Q_i > 0$ $i = 1,2,3,4,5$, $Q_1Q_2Q_3 > Q_3^2 + Q_1^2Q_4,\ (Q_1Q_4 - Q_5)(Q_1Q_2Q_3 - Q_3^2 - Q_1^2Q_4) > Q_5(Q_1Q_2 - Q_3)^2 + Q_1Q_5^2$.

4.3.3 Bifurcation Analysis

In this section, we study two types of bifurcation analysis namely Hopf-bifurcation and Transcritical Bifurcation for the model system (4.2) with respect to the vital parameters λ_i $(i = 1,2,3\ )$ and σ.

4.3.3.1 Hopf Bifurcation Analysis

Here we investigate Hopf bifurcation analysis for the model system (4.2), with respect to the disease transmission rate λ_1. That's why we rewrite our system of equations (4.2) in

vector forms [200] to perform the analytical conditions for the Hopf bifurcation as follows:

$$\dot{y} = f(y, \lambda_1),\ y \in R^5,\ f \in C^\infty$$

with $\lambda_1 \in R$ a bifurcation parameter.
Now, the Jacobian matrix of the above system around y^* is

$$J(\lambda_1) = Df(y^*(\lambda_1), \lambda_1) = (f_{ij})$$

where $f_{ij} = \frac{\partial f_i}{\partial y_j}, i, j = 1, 2, ...5.$
and corresponding characteristics equation is

$$P(x) = x^5 + Q_1 x^4 + Q_2 x^3 + Q_3 x^2 + Q_4 x + Q_5 = 0.$$

Where x is the eigenvalue of the above characteristic equation and the coefficient $Q_i \in R(i = 1, 2, ..., 5)$ which are described above depend on the parameter λ_1.

Now, we discuss the roots of the above polynomial by the following theorems [201]

Theorem 4.3 *If and only if one of the following sets of requirements with coefficient criterion is met, the polynomial P(x) has exactly one pair of imaginary roots* $x_{1,2} = \pm i\sqrt{\theta}$, $\theta > 0$.
(C_1): $\psi = (Q_3 - Q_1Q_2)(Q_5Q_2 - Q_3Q_4) - (Q_5 - Q_1Q_4)^2 = 0$, *with* $\theta = (Q_5 - Q_1Q_4)/(Q_3 - Q_1Q_2) > 0$,
(C_2): $Q_5 = Q_1Q_4,\ Q_3 = Q_1Q_2,$ *and* $Q_4 < 0$, *with* $\theta = \frac{Q_2 + \sqrt{Q_2^2 - 4Q_4}}{2} > 0$,
(C_3): $Q_5 = Q_1Q_4,\ Q_3 = Q_1Q_2$, *and* $Q_4 = 0,\ Q_2 > 0$, *with* $\theta = Q_2 > 0$.

Theorem 4.4 *If and only if one of the following coefficient requirements is met, the polynomial P(x) has one pair of imaginary roots* $x_{1,2} = \pm i\sqrt{\theta},\ \theta > 0$ *and all other roots have non-zero real portions.*
(D_1): $(C_1),\ Q_3 - Q_1\theta_1 \neq 0$, *where* $\theta = \theta_1 = (Q_5 - Q_1Q_4)/(Q_3 - Q_1Q_2) > 0$,
(D_2): $(C_2),\ Q_3Q_1 \neq 0$.

Theorem 4.5 *If and only if the following coefficient criteria are met, the polynomial P(x) has one pair of imaginary roots* $x_{1,2} = \pm i\sqrt{\theta},\ \theta > 0$ *and all other roots have negative real portions.*
(E): $(C_1), Q_1 > 0, Q_1 - Q_1Q_2 < 0, Q_3 - Q_1\theta > 0$.

The dynamical system (4.2) undergoes a Hopf-bifurcation around the interior equilibrium E^* when the disease transmission parameter λ_1 crosses a critical value say $\lambda_1 = \lambda_c$. The Hopf-bifurcation occurs at $\lambda_1 = \lambda_c$ if the following conditions are satisfied.

(i) The characteristic equation at the critical value of λ_1 say λ_c, the Jacobian matrix of the given system has a pair of purely imaginary roots i.e, $(x(\lambda_c), \bar{x}(\lambda_c)) = (i\sqrt{\theta}, -i\sqrt{\theta})$, $\theta > 0$ and no other roots with zero real parts.
(ii) The real part $Re(x(\lambda_c))$ of $x(\lambda_1)$ satisfies

$$\frac{dRe(x(\lambda_1))}{d\lambda_1}|_{\lambda_1=\lambda_c} \neq 0.$$

This is true only when either the condition (D_1) or (E) holds.
We can also prove the Hopf-bifurcation theorem in the same way with the others bifurcation parameter λ_2, λ_3 and σ.

4.3.3.2 Transcritical Bifurcation Analysis

Our model (4.2) experiences a transcritical bifurcation at the equilibrium point E_1 as a control parameter λ_1 passes through the bifurcation value $\lambda_1 = \lambda_1^*$ and satisfied the following conditions:

$$W^T f_{\lambda_1}(E_1, \lambda_1^*) = 0,$$

$$W^T [D f_{\lambda_1}(E_1, \lambda_1^*)V] \neq 0,$$

$$W^T [D^2 f_{\lambda_1}(E_1, \lambda_1^*)(V, V)] \neq 0.$$

Here, V and W are eigenvectors related to simple zero (its means only one zero eigenvalue) eigenvalue corresponding to the Jacobian matrix J and J^T of our system (4.2) at the equilibrium point E_1, respectively. In addition, λ_1^* is the bifurcation point in the parameter space of the system (4.2). Also in above relation $f_{\lambda_1}(E_1, \lambda_1^*)$ is a derivative of the vector field f with respect to the parameter λ_1. Since our model is higher dimensional, the analytical expression corresponding to the conditions of the Sotomayor's theorem becomes very difficult to deal with. We verify the conditions of the Sotomayor's theorem numerically in section 4.4 and illustrate the result in Fig. 4.6. Also we performed numerically, transcritical bifurcation for the disease transmission parameter λ_3 in (Fig. 4.10).

4.3.4 Permanence:

In this part, we talk about the system (4.2) persistence under favourable initial conditions. No matter what the beginning population is, for a system to be considered permanent in biology, all of its populations must survive over the long run. Permanence in mathematics

refers to the absence of omega limit points on the non-negative cone's border for strictly positive solutions.

Definition 4.6 *If u_1, u_2, u_3, u_4, u_5 and v_1, v_2, v_3, v_4, v_5 are positive constants does not dependent on the initial conditions of the system (4.2). If the subsequent inequalities hold:*
$u_1 \leq \liminf_{t\to\infty} P(t) \leq \limsup_{t\to\infty} P(t) \leq v_1$,
$u_2 \leq \liminf_{t\to\infty} Z(t) \leq \limsup_{t\to\infty} Z(t) \leq v_2$,
$u_3 \leq \liminf_{t\to\infty} C_S(t) \leq \limsup_{t\to\infty} C_S(t) \leq v_3$,
$u_4 \leq \liminf_{t\to\infty} C_I(t) \leq \limsup_{t\to\infty} C_I(t) \leq v_4$,
$u_5 \leq \liminf_{t\to\infty} W(t) \leq \limsup_{t\to\infty} W(t) \leq v_5$.
With initial conditions $P(0) > 0$, $Z(0) > 0$, $C_s(0) > 0$, $C_I(0) > 0$, $W(0) > 0$, then the system (4.2) is permanent.

Theorem 4.7 *The system (4.2) is permanent if*
$(1-\sigma)P^1Z^1 > (P^1 + \eta_P)$,
$d_3 > \beta_1 Z^1$,
$d_2 > Max\left[\frac{m\sigma d_1}{e_1\alpha_1}, \frac{(\lambda_1 Z^1 + \lambda_2 C_I^1)C_S^1}{C_I^1} - \gamma\right]$,
$d_1^2 m\sigma \geq Max\left[\frac{(1-\sigma)(d_2+\gamma)\eta_Z(\lambda_1\eta_Z + d_1 d_2)}{(d_2+\gamma)\eta_P}, \frac{(1-\sigma)\eta_Z(\lambda_1\eta_Z + d_1 d_2)}{\eta_P}, \frac{(1-\sigma)\eta_Z(\lambda_1\beta_2\eta_Z + d_1 d_2\beta_2 + d_1 d_2\lambda_1)}{\beta_2\eta_Z}\right]$.

Proof: From the system of equation (4.2) we obtain,

$$\frac{dP}{dt} \leq P + \sigma P C_S + \eta_P,$$

$$\frac{dZ}{dt} \leq e_1\alpha_1 PZ - d_1 Z + \eta_Z,$$

$$\frac{dC_S}{dt} \leq C_S(m\sigma P + e_2\alpha_2 Z - d_2),$$

$$\frac{dC_I}{dt} \leq C_S(\lambda_1 Z + \lambda_2 C_I + \lambda_3 W),$$

$$\frac{dW}{dt} \leq W(\beta_1 Z + \beta_2 C_I - d_3).$$

Now, by using the standard comparison theorem [199]

$$\lim_{t\to\infty} supP(t) \leq v_1,\ \lim_{t\to\infty} supZ(t) \leq v_2,\ \lim_{t\to\infty} supC_S(t) \leq v_3,$$
$$\lim_{t\to\infty} supC_I(t) \leq v_4,\ \lim_{t\to\infty} supW(t) \leq v_5, \tag{4.3}$$

where
$v_1 = \frac{d_2 - e_2\alpha_2 Z^1}{m\sigma}$,
$v_2 = \frac{(e_1\alpha_1 d_2 - m\sigma d_1) + \sqrt{(m\sigma d_1 - e_1\alpha_1 d_2)^2 + 4e_1 e_2\alpha_1\alpha_2 m\sigma\eta_Z}}{2e_1 e_2\alpha_1\alpha_2}$,

$v_3 = \frac{(1-\sigma)P^1Z^1-(P^1+\eta_P)}{\sigma P^1}$,
$v_4 = \frac{d_3-\beta_1 Z^1}{\beta_2}$,
$v_5 = \frac{(d_2+\gamma)C_I^1-C_S^1(\lambda_1 Z^1+\lambda_2 C_I^1)}{\lambda_3 C_S^1}$.
Here,
v_1 is positive if $d_2 > e_1\alpha_1 Z^1$,
v_2 is positive if $e_1\alpha_1 d_2 > m\sigma d_1$,
v_3 is positive if $(1-\sigma)P^1Z^1 > (P^1+\eta_P)$,
v_4 is positive if $d_3 > \beta_1 Z^1$,
v_5 is positive if $(d_2+\gamma)C_I^1 > (\lambda_1 Z^1+\lambda_2 C_I^1)C_S^1$.
Similarly, we get from equation (4.2)

$$\begin{aligned}
\frac{dP}{dt} &\geq \eta_P - (1-\sigma)PZ,\\
\frac{dZ}{dt} &\geq \eta_Z - d_1 Z,\\
\frac{dC_S}{dt} &\geq (m\sigma P - \lambda_1 Z - d_2 C_I)C_S,\\
\frac{dC_I}{dt} &\geq \lambda_1 C_S Z - (d_2+\gamma)C_I,\\
\frac{dW}{dt} &\geq W(\beta_2 C_I - d_3 - \delta W).
\end{aligned}$$

Again applying the standard comparison theorem [199]

$$\begin{aligned}
\lim_{t\to\infty} infP(t) \geq u_1,\ \lim_{t\to\infty} infZ(t) \geq u_2,\ \lim_{t\to\infty} infC_S(t) \geq u_3,\\
\lim_{t\to\infty} infC_I(t) \geq u_4,\ \lim_{t\to\infty} infW(t) \geq u_5,
\end{aligned} \tag{4.4}$$

where
$u_1 = \frac{d_1\eta_P}{(1-\sigma)\eta_Z}$,
$u_2 = \frac{\eta_Z}{d_1}$,
$u_3 = \frac{(d_2+\gamma)d_1^2 m\sigma\eta_P-(1-\sigma)\eta_Z(d_2+\gamma)(\lambda_1\eta_Z+d_1 d_2)}{\lambda_1\lambda_2\eta_Z^2(1-\sigma)}$,
$u_4 = \frac{d_1^2 m\sigma\eta_P-(1-\sigma)\eta_Z(\lambda_1\eta_Z+d_1 d_2)}{d_1\lambda_1\eta_Z(1-\sigma)}$,
$u_5 = \frac{d_1^2 m\sigma\beta_2\eta_P-\eta_Z(1-\sigma)(\lambda_1\beta_2\eta_Z+d_1 d_2\beta_2+d_1 d_3\lambda_1)}{d_1\lambda_2\eta_Z\delta(1-\sigma)}$.
Here, u_1 and u_2 are always positive because $(1-\sigma)$ is always positive.
Also, u_3 is positive if $(d_2+\gamma)d_1^2 m\sigma\eta_P \geq (1-\sigma)(d_2+\gamma)\eta_Z(\lambda_1\eta_Z+d_1 d_2)$,
u_4 is positive if $d_1^2 m\sigma\eta_P \geq (1-\sigma)\eta_Z(\lambda_1\eta_Z+d_1 d_2)$,
u_5 is positive if $d_1^2 m\sigma\beta_2\eta_Z \geq (1-\sigma)\eta_Z(\lambda_1\beta_2\eta_Z+d_1 d_2\beta_2+d_1 d_2\lambda_1)$.
From above two inequalities (4.3) and (4.4), we conclude that the system (4.2) is permanent.

Table 4.1: Parameters used in the system (4.1)

Parameter	Description	Value	Reference
r	The intrinsic growth rate of P	1 time^{-1}	–
K	The carrying capacity of P	3 individual	–
α_1	Predation rate of Z	1 individual^{-1}time^{-1}	–
α_2	Predation rate of C_S	0.2 individual^{-1}time^{-1}	–
σ	Fraction of P involves in mutualism	0.01	–
η_P	Immigration rate of P	0.001 individual time^{-1}	–
η_Z	Immigration rate of Z	0.001 individual time^{-1}	–
m_i	Maximum benefits in mutualism	5 time^{-1}	–
a_i	Half saturation coefficients of the function representing mutualism	0.1 individual	[124, 159, 160]
e_i	Conversion efficiency of Z and corals	0.75	[159, 202]
d_i	Mortality rates of Z and corals	0.01 time^{-1}	–
γ	Disease-induced death rate of C_I	0.5 time^{-1}	[144]
λ_i	Disease transmission rates	0.02 individual^{-1}time^{-1}	–
β_i	Shedding rates of W into the environment	0.1 individual^{-1}time^{-1}	–
$\frac{1}{d_3}$	Average time of existence of the W	100 time	[122]
δ	Crowding parameter	0.1 individual^{-1}time^{-1}	—

4.4 Numerical Simulation

To substantiate our analytical findings, we perform numerical simulations utilizing MATLAB and MATHEMATICA with a set of non-dimensionalized parameters as given in Table 4.2. We perform a sensitivity analysis to understand the most sensitive parameters of the model. Firstly, we discuss sensitivity analysis of the system (4.2) to identify how

Table 4.2: Parameters used in the system (4.2)

$\alpha_1 = 3.0$, $\alpha_2 = 0.12$, $d_1 = 0.01$, $d_2 = 0.01$, $d_3 = 0.01$, $a_1 = 0.0333$, $a_2 = 0.1667$, $m = 25$, $\lambda_1 = 0.02$, $\lambda_2 = 0.012$, $\lambda_3 = 0.012$, $\gamma_1 = 0.5$, $\delta = 0.06$, $\sigma = 0.01$, $\beta_1 = 0.1$, $\beta_2 = 0.06$, $e_1 = 0.75$, $e_2 = 0.75$, $\eta_P = 0.003$, $\eta_Z = 0.001$.

the changes in the original parameters underlying the model affect the densities of phytoplankton (P), zooplankton (Z), susceptible corals (C_S), infected corals (C_I) and free-leving pathogens (W) considered in our model. The sensitivity of the model parameters of the original system (4.1) is determined by either increasing or decreasing each of the parameters which are either 20% of its original value or 120% of its original value. From Fig. 4.3

it is observed that the population densities of susceptible corals and infected corals are sensitive to the changes in the disease transmission rates λ_1, λ_2, λ_3 due to the consumption of zooplankton by susceptible corals, through the contagious pathway (from infectious to susceptible corals) and non-contagious pathway (from the environment to susceptible corals). It is also observed that coral population density is highly sensitive to mutualism (σ).
In order to identify which of the non-dimensional parameters are important for the system (4.2), we re-write the system (4.2) in the form

$$\dot{\mathbf{X}} = \mathbf{F}(\mathbf{t},\, \mathbf{X},\, \mathbf{P}) \tag{4.5}$$

$$where, \mathbf{X} = (P,\, Z,\, C_S,\, C_I,\, W)^T \in R^5,$$

$$\mathbf{P} = (\alpha_1,\, \alpha_2,\, m_1,\, \lambda_1,\, \lambda_2,\, \lambda_3,\, \beta_1,\, \beta_2,\, \sigma)^T,$$

$$\mathbf{F} = (F_1,\, F_2,\, F_3,\, F_4,\, F_5)^T \in R^5, and\ \ \mathbf{X}(0) \geq 0.$$

The local sensitivity of the solution to (4.5) at the interior equilibrium $E^* = (P^*,\, Z^*,\, C_S^*,\, C_I^*,\, W^*)$ under small changes in $\mathbf{P}$ can be determined by differentiating $\mathbf{X}(\mathbf{t},\, \mathbf{P})$ partially with respect to each of the non-dimensional parameters $p \in \mathbf{P}$. We denote the sensitivity indices of the population density $\mathbf{X}(\mathbf{t},\, \mathbf{P})$ with respect to a selected parameter $p \in \mathbf{P}$ by $\mathbf{S}_{\mathbf{X},\,p}(\mathbf{t}) = \frac{\partial \mathbf{X}(\mathbf{t},\,\mathbf{P})}{\partial p}$. The sensitivity indices $\mathbf{S}_{\mathbf{X},\,p}(\mathbf{t})$ allow us to measure the relative change in the state variables $\mathbf{X}$ when a parameter $p \in \mathbf{P}$ changes. The sensitivity indices can be estimated by using direct differential method [203]. The sensitivity equation of the system (4.5) with respect to the parameter $p \in \mathbf{P}$, satisfying the initial conditions $\mathbf{S}_{\mathbf{X},\,p}(\mathbf{0}) = 0$, is given by

$$\dot{\mathbf{S}}_{\mathbf{X},p} = \mathbf{F}_p^* + \mathbf{J}^* \mathbf{S}_{\mathbf{X},p},$$

where,

$$\mathbf{S}_{\mathbf{X},p} = \left(\frac{\partial P}{\partial p}, \frac{\partial Z}{\partial p}, \frac{\partial C_S}{\partial p}, \frac{\partial C_I}{\partial p}, \frac{\partial W}{\partial p}\right)^T$$

is the vector of sensitivities with respect to the parameter $p \in \mathbf{P}$,

$$\mathbf{F}_p^* = \left(\frac{\partial F_1}{\partial p}, \frac{\partial F_2}{\partial p}, \frac{\partial F_3}{\partial p}, \frac{\partial F_4}{\partial p}, \frac{\partial_5}{\partial p}\right)_{E^*}^T$$

and J^* is the Jacobian of the system (4.5) evaluated at the non-trivial equilibrium E^*.
The steady state $\mathbf{S}_{\mathbf{X},p}^*$ of the sensitivity coefficients exists when $\mathrm{Det}(J^*) \neq 0$ and is given by

$$\mathbf{S}_{\mathbf{X},p}^* = \left(\mathbf{S}_{\mathbf{P},p}^*, \mathbf{S}_{\mathbf{Z},p}^*, \mathbf{S}_{\mathbf{C_S},p}^*, \mathbf{S}_{\mathbf{C_I},p}^*, \mathbf{S}_{\mathbf{W},p}^*\right)^T = -(J^*)^{-1}\mathbf{F}_p^*.$$

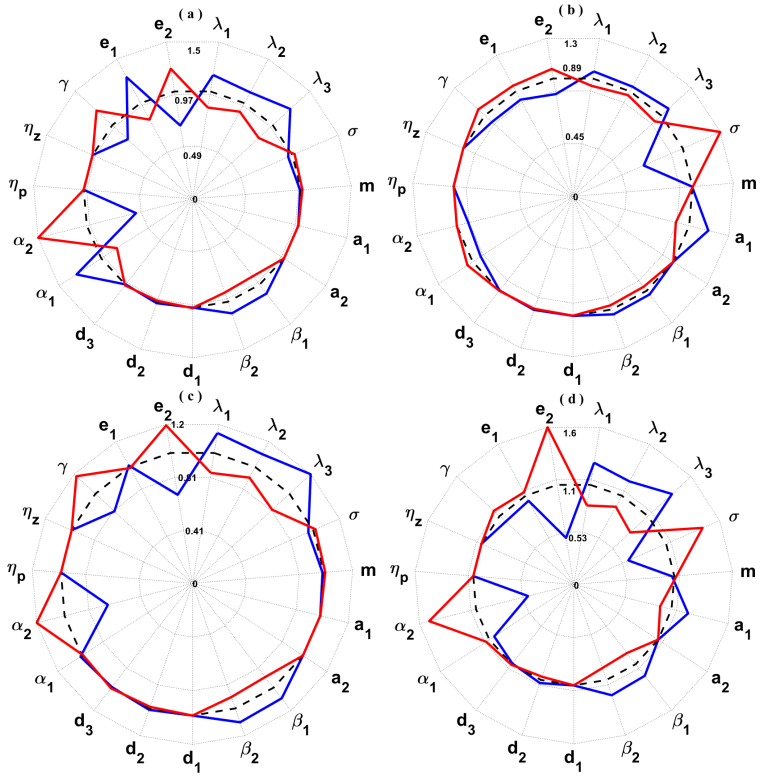

Figure 4.3: Local sensitivity of (a) phytoplankton, (b) zooplankton, (c) susceptible corals, (d) infected coral populations where particular parameter values were increased (decreased) by 20% as shown in red (blue) lines.

According to sensitivity analysis, disease transmission rates λ_1, λ_2, λ_3 due to the consumption of zooplankton by susceptible corals, through contagious pathway (from infectious to susceptible corals), through non-contagious pathway (from the environment to susceptible corals) and fraction of phytoplankton population σ due to mutualism with corals respectively are important parameters under investigation. The main purpose of this section is to study the dynamical behavior of the model for a wide range of above parameter values. It is observed from Fig. 4.4 that the four benthic groups species coexist with oscillatory nature for the set of parameter values as given in Table 4.2 with a certain disease transmission rate $\lambda_1 = 0.008$. But Fig. 4.5 (A) demonstrates, the stable around the coexistence equilibrium point (0.65326,3.4094,12.0453,7.3268,12.8425) for the parameters remain same as in Table 4.2. For $\lambda_1 = 0.008$, the system (4.2) has only one positive interior equilibrium point $(0.653176,\ 3.43232,\ 12.0437,\ 7.37456,\ 12.9284)$. The eigenvalues of the system at E^* are -1.18699, $-0.848778 \pm 0.0i$ and $-0.0280388 \pm 0.0i$ the system is always oscillation nature around E^*. Moreover, the system (4.2) has positive interior equilibrium point with equilibrium densities $(P^*,\ Z^*,\ C_S^*,\ C_I^*,\ W^*) = (0.65326,\ 3.4094,\ 12.0453,\ 7.3268,\ 12.8425)$ for $\lambda_1 = 0.02$. The eigenvalues of the system at $E^*(0.65326,\ 3.4094,\ 12.0453,\ 7.3268,\ 12.8425)$ are -0.96871, $-0.655657 \pm 2.2257i$ and $-0.0116283 \pm 0.256216i$. Since all the eigenvalues are negative with negative real

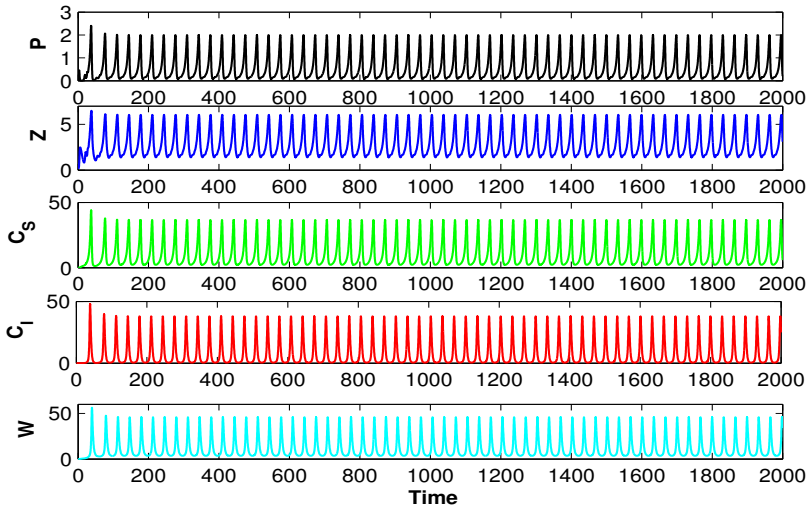

Figure 4.4: Time series evolution of system (4.2) for $\lambda_1 = 0.008$ of all species around interior equilibrium point $E^*(0.803057,\ 3.82601,\ 14.8256,\ 10.1085,\ 16.9284)$ with initial values $[0.1,\ 0.1,\ 0.1,\ 0.1,\ 0.1]$ and rest of system parameters are given in Table 4.2. The time series solutions of (4.2) represents the periodic oscillations around $(0.803057,\ 3.82601,\ 14.8256,\ 10.1085,\ 16.9284)$.

parts then the co-existing equilibrium point E^* is asymptotically stable. Thus the system is always locally asymptotically stable around E^*. According to the Theorem 4.2 (iv), we obtained that $Q_1(2.31581) > 0,\ Q_2(6.82305) > 0,\ Q_3(5.57971) > 0,\ Q_4(0.56377) > 0,$ $Q_5(0.349882) > 0,\ Q_1Q_2Q_3(88.1643695) > Q_3^2 + Q_1^2Q_4(34.1566487), (Q_1Q_4 - Q_5)(Q_1Q_2Q_3 - Q_3^2 - Q_1^2Q_4)[51.6152976] > Q_5(Q_1Q_2 - Q_3)^2 + Q_1Q_5^2[36.8365312]$, which ensure that the stability of the interior equilibrium point E^* of the system (4.2). For $\lambda_1 = 0.072$, we obtain the coral-free equilibrium point $E_1(0.0042287,\ 1.72243,\ 0,\ 0,\ 2.70406)$ and $\frac{m\sigma P_1}{a_2} + (e_2\alpha_2 - \lambda_1)Z_1 - \lambda_3 W_1 - d_2 = -0.0051031984 < 0,\ \beta_1 Z_1 - d_3 - 2\delta W_1 = -0.1622442 < 0,$ $a_1 + a_5 = -0.71424367 < 0, a_1a_5 (= 0.000414331921) > a_2a_4 (= -0.0160620644)$, which follows the stability criteria of coral-free equilibrium point $E_1(0.0042287,\ 1.72243,\ 0,\ 0,\ 2.70406)$. Thus, the system (4.2) is locally asymptotically stable around E_1. Figure 4.5 (B) shows that the species coexist in a stable position around the coral-free equilibrium point E_1 for $\lambda_1 = 0.072$.

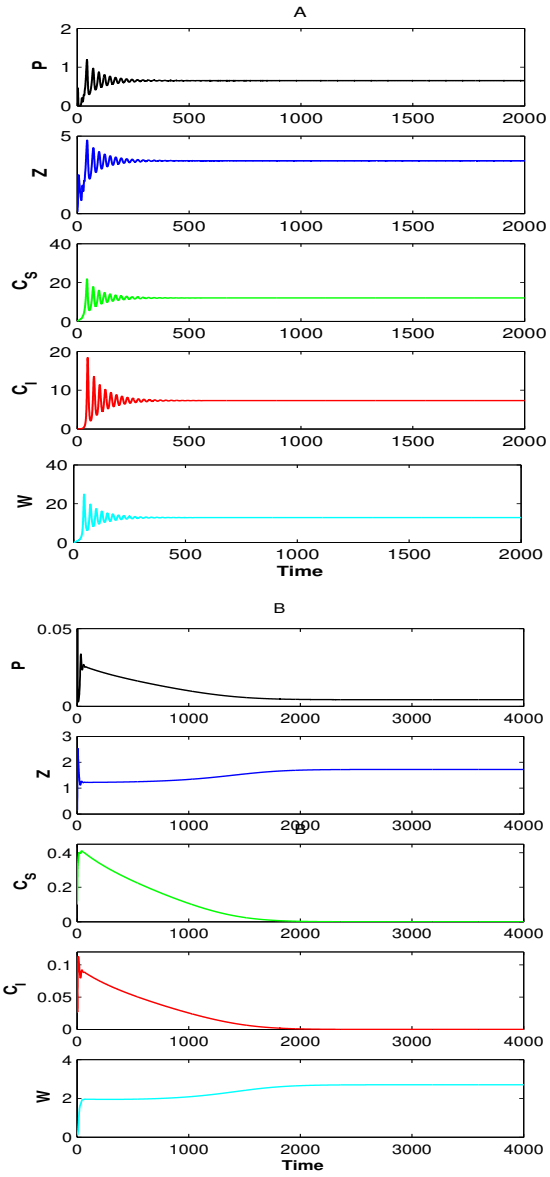

Figure 4.5: The column (A) and the column (B) shows that the time series solutions of system (4.2) for $\lambda_1 = 0.02$ and $\lambda_1 = 0.072$, respectively of all species P, Z, C_S, C_I and W with the set of parameter values as given in Table 4.2. The time series solutions of system (4.2) represents the local asymptotic stability for $\lambda_1 = 0.02$ at the interior equilibrium $(0.653176,\ 3.43232,\ 12.0437,\ 7.37456,\ 12.9284)$ and local asymptotic stability for $\lambda_1 = 0.072$ at the coral free equilibrium $(0.0042287,\ 1.72243,\ 0,\ 0,\ 2.70406)$.

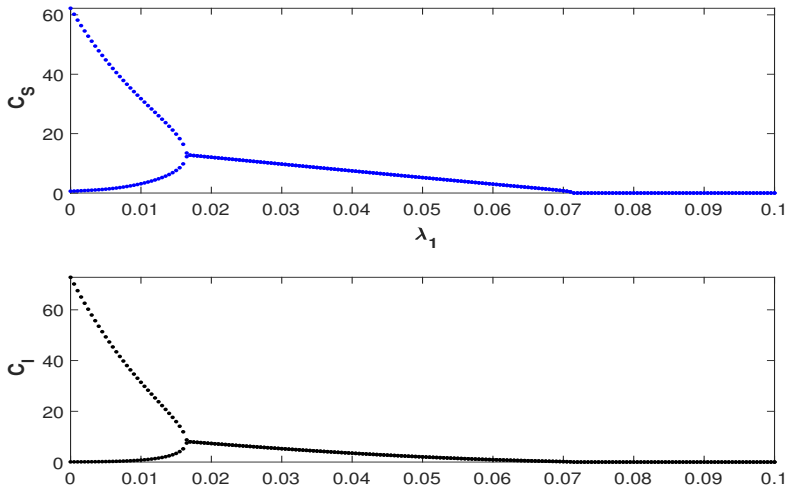

Figure 4.6: Bifurcation diagram with λ_1 as a bifurcation parameter.

Numerical simulation of the system (4.2) shows that all benthic groups coexist in limit cycle oscillation nature for $0 \leq \lambda_1 \leq 0.01647$. Interior equilibrium point exhibits stable nature for $0.01647 < \lambda_1 \leq 0.0712$. Finally, system (4.2) goes into coral-free (E_1) stable situation from the stable position around the interior equilibrium point E^* for $0.0712 < \lambda_1 \leq 0.1$. The bifurcation diagram (Fig. 4.6) of the system (4.2) for variation of λ_1 also reflects the above fact. It follows that there are two critical values of disease transmission rate λ_1 so that (i) the oscillation nature around interior equilibrium switches to interior equilibrium in stable situation (ii) further increasing of λ_1, stable equilibrium E^* switches to coral-free equilibrium E_1 in stable nature. Thus, there exist two threshold values of λ_1 which are denoted by $\lambda_1^c(\approx 0.01647)$ and $\lambda_1^*(\approx 0.0712)$. Furthermore, we also use numerical simulations for determine the nature of bifurcation at $\lambda_1 = \lambda_1^*(\approx 0.0712)$ as well as verify the analytical result. At $\lambda_1 = \lambda_1^*(\approx 0.0712)$, we have $E_1 = (0.0042287,\ 1.72243,\ 0,\ 0,\ 2.70406)$ and

$$J_1 = \begin{pmatrix} -0.71365617 & -0.004186413 & 0.0012797843 & 0 & 0 \\ 3.83671282 & -0.0005805705 & -0.2066916 & 0 & 0 \\ 0 & 0 & -0.0037252544 & 0 & 0 \\ 0 & 0 & 0.155085736 & -0.51 & 0 \\ 0 & 0.270406 & 0 & 0.1622436 & -0.1622442 \end{pmatrix}$$

has a single zero eigenvalue. Also, we obtain $V = (0.00316746,\ -0.521535,\ 0.060261,\ 0.0183247,\ -0.850896)^T$, $W = (0,\ 0,\ 1,\ 0,\ 0)^T$,
$W^T f_{\lambda_1}(E_1, \lambda_1^*) = 0,\ W^T[Df_{\lambda_1}(E_1, \lambda_1^*)V] = -0.1039 < 0,\ W^T[D^2 f_{\lambda_1}(E_1,\ \lambda_1^*)(V,\ V)] = 0.06285413$. Therefore, according to Sotomayor theorem [151] it follows that the system undergoes a transcritical bifurcation at $E_1 = (0.0042287,\ 1.72243,\ 0,\ 0,\ 2.70406)$ when λ_1 passes through $\lambda_1^*(\approx 0.0712)$.

The above numerical observations indicate that sufficiently small magnitude of λ_1, all species coexist through an oscillatory manner. But it is interesting to note that all the species settle down to a stable position from the oscillatory behavior due to sufficiently large value of λ_1. Finally, all species in coral reef ecosystem settle down to a coral free system for sufficiently higher value of λ_1. Therefore, disease transmission rate λ_1 due to the consumption of zooplankton by susceptible corals can prevent the population oscillations and finally lead to coral free system.

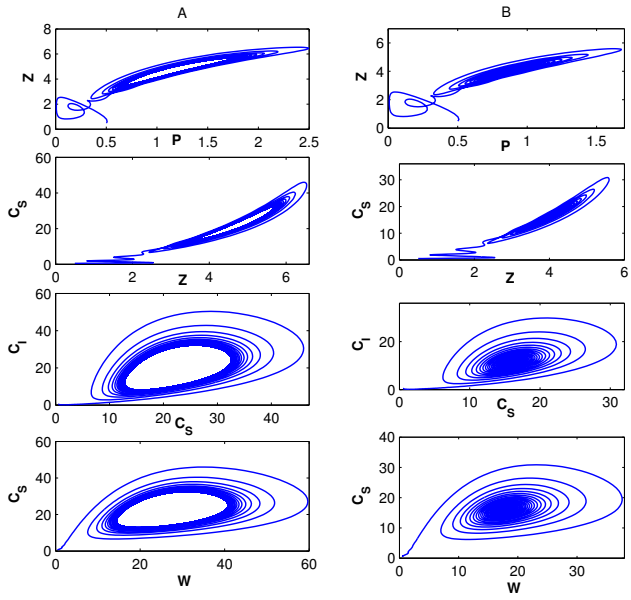

Figure 4.7: Numerical illustration shows the phase portraits of system (4.2) at the interior equilibrium $(1.1779,\ 4.70391,\ 21.7832,\ 18.2281,\ 25.9013)$. The left column (A) represents phase diagram with oscillation nature for $\lambda_2 = 0.0012$ and the right column (B) represents phase diagram with stable nature for $\lambda_2 = 0.006$ and other values of parameters are same as Table 4.2.

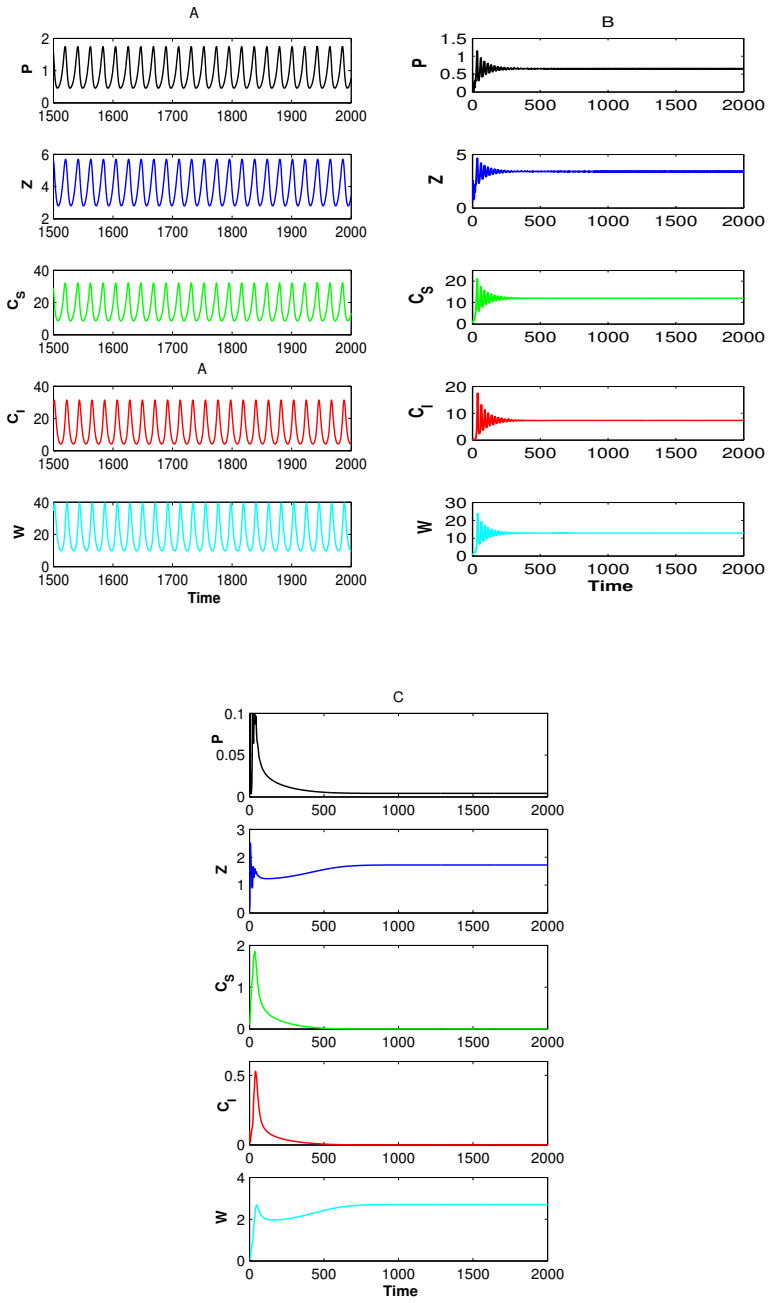

Figure 4.8: The left column (A), the middle column (B) and the right column (C) shows that the time series solutions of system (4.2) for $\lambda_3 = 0.006$, $\lambda_3 = 0.012$ and $\lambda_3 = 0.048$, respectively of all benthic groups P, Z, C_S, C_I and W and rest of system parameters are same as Table 4.2.

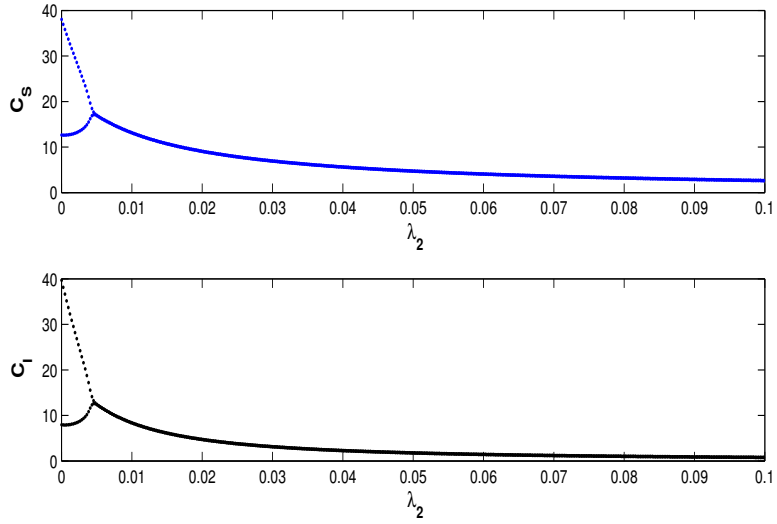

Figure 4.9: Bifurcation diagram with λ_2 as a bifurcation parameter.

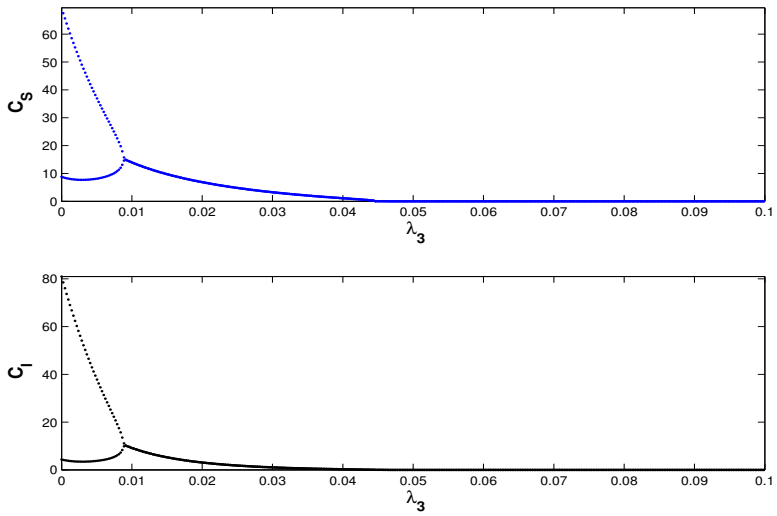

Figure 4.10: Bifurcation diagram with λ_3 as a bifurcation parameter.

We like to observe the dynamics of the system (4.2) for changing the values of λ_2. The phase portraits of Figure 4.7 (A) show oscillatory dynamics for $\lambda_2 = 0.0012$ at the coexistence equilibrium. On the other hand, phase portraits (cf. Figure 4.7 (B)) represents stable coexistence of all the species around the interior equilibrium point $(0.867134,\ 3.99193,\ 16.0149,\ 11.3885,\ 17.8751)$ for $\lambda_2 = 0.006$. The above results indicate that for a sufficiently small magnitude of λ_2, all the species coexist through an oscillatory manner, whereas stable coexistence behaviour can be observed due to a sufficiently higher magnitude of λ_2. Moreover, from Fig. 4.8 (A) we observe that the system exhibits limit cycle oscillations at $\lambda_3 = 0.006$ (below than the bifurcating threshold value $\lambda_3 \approx 0.0088$). For $\lambda_3 = 0.012$, the system becomes stable [Fig. 4.8 (B)]. This result shows

that sufficiently low values of λ_3 give rise to limit cycle oscillations about the coexistence steady state. Moreover, if we keep increasing the value of λ_3, the coral will get extinct from the system (for $\lambda_3 = 0.048$) [Fig. 4.8 (C)]. It is well established that nonlinear interactions among the species make endogenous oscillations. We have shown that the disease transmission through the non-contagious pathway from the environment to susceptible corals can act as a stabilizing factor in the coral-reef system.

To make the dynamics clearer, we plot the Hopf-bifurcation diagrams of the system (4.2) taking λ_2 (disease transmission rate through contagious pathway) and λ_3 (disease transmission rate through non-contagious pathway) as the bifurcation parameters in the Fig. 4.9 and Fig. 4.10, accordingly. From Fig. 4.9 we noticed that when $\lambda_2 < 0.0047$ $(approx.)$, the equilibrium values for four benthic groups divided into minimum/maximum of the periodic solutions and interior equilibrium point becomes unstable. The amplitude of periodic oscillation nature decreases with increasing of λ_2 and when crosses the critical level λ_2 (≈ 0.0047), the system becomes stable around an interior equilibrium point. From Fig. 4.10 it is clear that when λ_3 passes through the critical value λ_3 (≈ 0.0088) then the minimum/maximum of the periodic solutions for four benthic groups are merged into the steady state value indicating the stability of interior equilibrium point, that is, E^* is asymptotically stable. Further when λ_3 cross the critical value λ_3 (≈ 0.0445), the interior equilibrium point E^* switches to coral fee equilibrium point E_1. In this case, it is to be noted that if we increase λ_3 gradually, a transcritical bifurcation occurs at λ_3 (≈ 0.0445).

On coral-reef biological system, fraction of phytoplankton population σ due to mutualism play also an important role in species dynamics. So, we observe the dynamics of the four benthic group population dynamics of the model for a wide range of parameter values of the mutualism coefficient σ. It is observed from phase diagram [Fig. 4.11 (A)] that the all species coexist with stable nature for $\sigma = 0.01$ and the other set of parameter values as given in Table 4.2. Where as phase diagram Fig. 4.11 (B) demonstrates, the oscillatory nature around the coexistence equilibrium point $(0.680007, 7.41004, 12.2854, 16.8108, 28.9942)$ for $\sigma = 0.03$. We have drawn the bifurcation diagram (Fig. 4.12) of the system (4.2) for susceptible coral and infected coral with respect to σ. We have seen that when σ crosses threshold level $\sigma(\approx 0.013)$ then the equilibrium values of every species are divided into minimum/maximum of the periodic solutions and the interior interior equilibrium point becomes unstable.

To identify the effect of λ_1 in the presence of varying densities of phytoplankton involved in mutualism with susceptible corals, we plot a two-parameter bifurcation diagram with σ and λ_1 as active parameters while keeping all other parameters fixed as in Table 4.2. From Figure $4.13(a)$ it is observed that the system (4.2) becomes oscillatory when the rate of zooplankton-mediated disease transmission is sufficiently low even with a decrease in the rate of mutualism. The system (4.2) becomes stable at the coexistence state for a moderate increase in λ_1 even with a higher rate of mutualism (cf. Fig. $4.13(a)$). However, corals

cannot survive a sufficiently high rate of zooplankton-mediated disease transmission. In this case, a higher rate of mutualism helps in recovering the coral population.

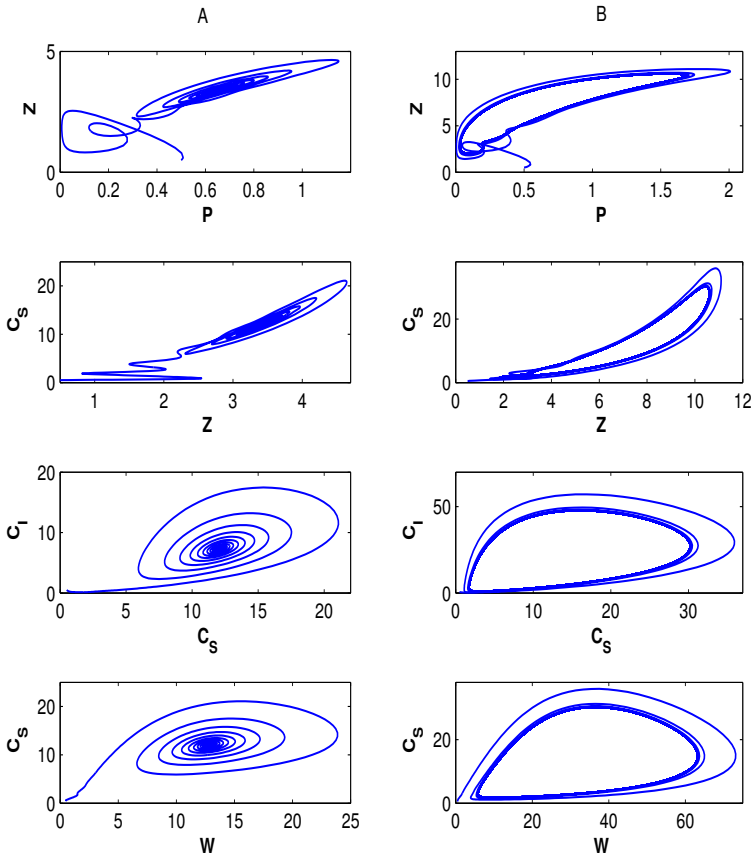

Figure 4.11: Numerical illustration shows the phase portraits of system (4.2) at the interior equilibrium $(0.68007, 7.41004, 12.2854, 16.8108, 28.9942)$. The left column (A) represents stable phase diagram for $\sigma = 0.01$ and the right column (B) represents unstable phase diagram for $\sigma = 0.03$ and other values of parameters are same as Table 4.2.

The combined effect of λ_2 and σ is represented in Figure 4.13(b). It is observed that a low rate of mutualism helps in stabilizing the system at E^* even with a higher rate of contagious infection. Figure 4.13(c) represents a two-parameter bifurcation plot with λ_3 and σ as active parameters. It is also observed that a higher rate of vector-mediated infection (λ_3) eliminates the coral population from the system. However, greater mutualism helps in recovering the coral population. To compare the effect of disease transmission on corals, we plot two-parameter bifurcation plots in the $\lambda_1 - \lambda_2$, $\lambda_1 - \lambda_3$, and $\lambda_2 - \lambda_3$ planes (cf. Fig. 4.14). It is observed that zooplankton-mediated infection induces the most detrimental effect on corals followed by pathogen-mediated transmission of coral disease, while the infected coral-mediated contagious mode of disease transmission has the least detrimental effect on corals (cf. Fig. 4.14).

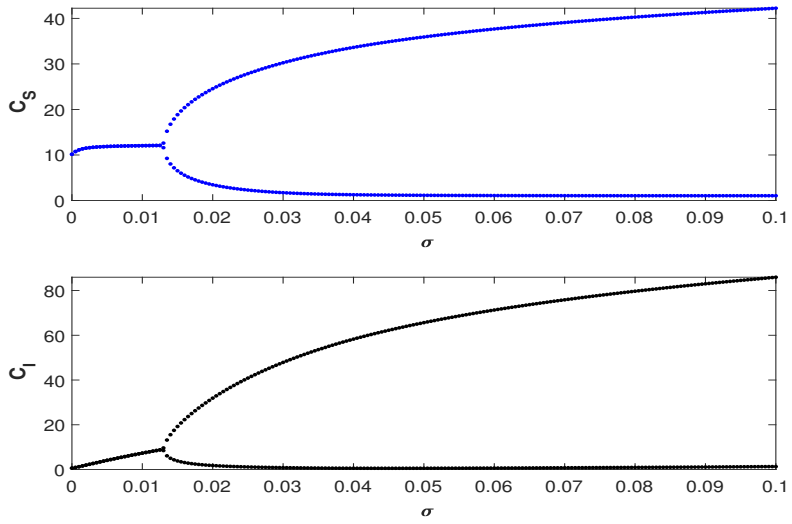

Figure 4.12: Bifurcation diagram with σ as a bifurcation parameter.

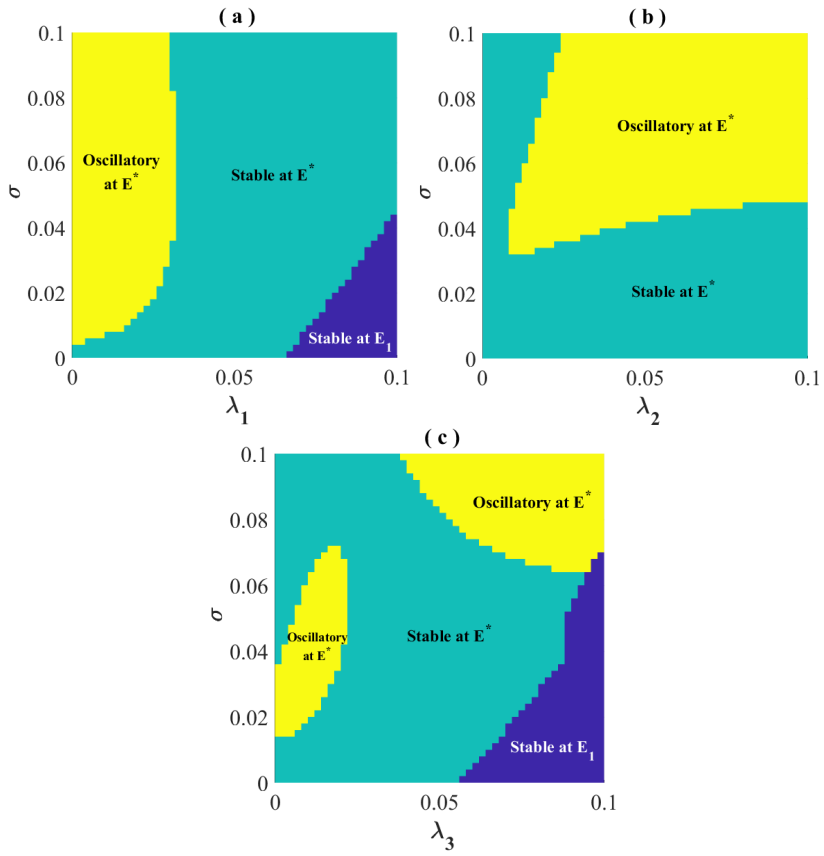

Figure 4.13: Two-parameter bifurcation plots with (a) σ and λ_1 as active parameters, (b) σ and λ_2 as active parameters, and (c) σ and λ_3 as active parameters.

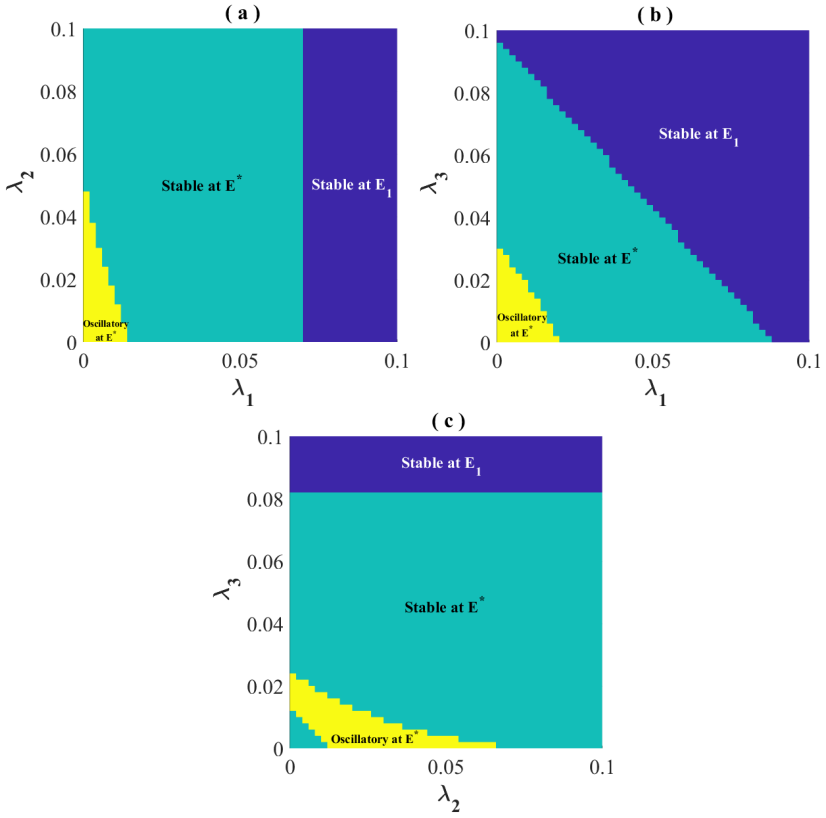

Figure 4.14: Two-parameter bifurcation plots with (a) λ_1 and λ_2 as active parameters, (b) λ_1 and λ_3 as active parameters, and (c) λ_2 and λ_3 as active parameters.

4.5 Conclusion

In this study, we proposed and analyzed a five-dimensional non-linear eco-epidemiological model under the assumption that the transmission of WBD occurs through contagious and non-contagious pathways. The WBD is assumed to be transmitted through not only the exposure of corals to zooplankton but also the direct contact with infected corals and the presence of free-living pathogens in the environment. It is also assumed that a fraction of the microscopic phytoplankton population has a mutualistic relationship with the corals. We have considered that the contact rates among the coral, zooplankton and free-living pathogen obey the law of mass action principle. The main objective of this work is to study the effects of disease transmission rates λ_i $(i = 1,2,3)$ and the fraction of phytoplankton population σ having mutualism with corals in the system dynamics. We found that the system admits two boundary equilibrium points and one interior equilibrium point under suitable parametric conditions. We determine the conditions for the local stability of the system around each equilibrium point. We have also analyzed the system and have determined the critical threshold values of the transmission rates for the changes in the dynamics of the system. Our model system experiences Hopf bifurcation when each of

the three modes of the WBD transmission rates exceeds some critical threshold value. To visualize the role of key parameters λ_i $(i = 1,2,3)$ and σ, we provide the Hopf-bifurcation diagrams with respect to the key parameters. The stability switching of coral species is observed from bifurcation diagrams.

Our numerical observations reveal that the system exhibits a Hopf bifurcation when the infection rate of different modes of transmission of WBD is sufficiently low. With a sufficient increase in the transmission rates, the system stabilizes at an interior steady state. So, in a Hopf bifurcation oscillatory state around the positive equilibrium stabilized at the positive equilibrium. Further, by increasing the value of the parameters, the coral density is zero and eventually, it stabilizes at the coral-free equilibrium. On the other hand, with a sufficiently small value of the mutualism coefficient, the four benthic group species coexist. Next, the equilibrium densities of every species are divided into the minimum or maximum of the periodic solutions and the interior equilibrium point becomes unstable when the mutualism coefficient is sufficiently higher.

Comparing the effects of different transmission modes, it is seen that the contagious mode of transmission is the least lethal to corals compared to the two non-contagious transmission modes, while zooplankton-mediated transmission of coral disease is the most detrimental to corals. However, a higher rate of mutualism between susceptible corals and phytoplankton helps in recovering the coral population even with a high rate of transmission of coral disease.

5

Beyond Predation: Fish-Coral Interactions Can Tip the Scales of Coral Disease [1]

5.1 Introduction

Coral reefs are crucial for biodiversity and human livelihoods, supporting fisheries, coastal protection, and tourism [1, 17, 18]. However, they face significant threats, including infectious diseases that alter reef structure and reduce coral cover [34, 35]. White Plague Disease (WPD), White Band Disease (WBD), and Black Band Disease (BBD) are among the most prevalent, driven by microbial communities that disrupt coral-zooxanthellae symbiosis, causing bleaching and mortality [98, 99, 109].

Coral diseases spread through direct contact and more effectively via indirect pathways, including water-borne and vector-borne transmission. Reef fish, particularly corallivores, play a critical role in disease dynamics by consuming infected coral and transporting pathogens across reefs [115–117]. While some fish exacerbate disease transmission, others may aid coral recovery by removing diseased tissue without introducing additional pathogens [134, 204].

The balance between fish predation and coral health is complex. While corallivory can accelerate disease spread, fish grazing on macroalgae helps mitigate competition for space,

[1] The bulk of this chapter has been published in *Journal of Theoretical Biology* by Ranjit, B., Chattopadhyay, A., Mandal, A., Biswas, S., & Chattopadhyay, J. (2025). *Journal of Theoretical Biology*, 599, 112031. DOI: `https://doi.org/10.1016/j.jtbi.2024.112031`

benefiting coral reefs [205]. To explore this dynamic, we develop a mathematical model to examine:

- The role of fish predation in coral disease dynamics.
- The impact of reef fish grazing on coral vulnerability and extinction risks.
- The effects of fish harvesting on coral recovery, macroalgae suppression, and reef sustainability.

This study provides insights into the intricate interactions between fish behavior, disease progression, and coral reef conservation.

5.2 Methods

We investigate the temporal dynamics of the spatial distribution of key benthic space holders, focusing on the fractions occupied by coral ($C(t)$), macroalgae ($M(t)$), and turf algae ($T(t)$). Corals are susceptible to being overgrown by macroalgae at a rate of α, whereas turfs are overgrown by macroalgae at a rate of a. Additionally, newly immigrated macroalgae can colonize the turfs at a rate of b. Opportunistic turf algae can rapidly proliferate in the space left by the mortality of macroalgae and corals. Corals settle and grow on existing turf algae at a rate of r. Macroalgae and corals experience natural mortality rates of d_1 and d_2, respectively. Turf algae subsequently colonize the vacated space left behind by fish consumption. Here, g is the maximal grazing rate of herbivorous fish. Based on these assumptions, coral reef dynamics can be modelled using a system of coupled nonlinear differential equations, a common approach in previous studies (see [123, 124, 126, 129, 156–158]):

$$\begin{aligned}
\frac{dM}{dt} &= \alpha MC - g\frac{M}{M+T} - d_1 M + (aM+b)T, \\
\frac{dC}{dt} &= rCT - \alpha MC - d_2 C, \\
\frac{dT}{dt} &= g\frac{M}{M+T} + d_1 M + d_2 C - (aM+b+rC)T,
\end{aligned} \tag{5.1}$$

where $M+C+T=1$.

Coral disease is a severe issue that threatens reef ecosystems, leading to widespread coral degradation and loss of biodiversity. Corals, like all living organisms, are susceptible to infections from a range of pathogens. The emergence of pathogens, often linked to environmental stressors such as increased sea-surface temperature, pollution, and ocean acidification, can trigger outbreaks of coral disease. These pathogens can be found in the water column, sediment, or other surfaces and can infect corals through multiple routes [112]. Once established, these pathogens can spread rapidly through coral colonies, altering the coral microbiome and creating conditions that facilitate infection. There have been only a

few mathematical models developed to study coral disease [110, 122, 143]. There are two primary pathways for infection: direct (or contagious) and indirect (or non-contagious). Let C_S and C_I be the susceptible and infected corals at time t (i.e., $C_S + C_I = C$). Susceptible corals can become infected through direct contact with infected corals at a rate of λ_c, a process known as the contagious pathway.

The other route, the indirect or non-contagious pathway, is particularly severe in cases of coral disease since corals are sessile organisms. In this scenario, susceptible corals become infected through contact with pathogens at a rate of λ_{nc}. Let $W(t)$ be the concentration of free-living pathogens in the environment at time t. Macroalgae (M) and infected corals ($C_I(t)$) both can contribute to pathogen proliferation through several mechanisms. Macroalgae provide a shedding effect on pathogens. Macroalgae, such as *Halimeda opuntia*, can serve as reservoirs for the bacterium *Aurantimonas coralicida*, the causative agent of white plague disease of corals in the Caribbean [206]. Benthic algae can harbour pathogens like *Vibrio sp.* and *Philaster ciliates*, which are linked to coral diseases such as White Syndrome and Yellow Band Disease [196]. Furthermore, the intricate relationship between infected corals and pathogens is a complex interplay. Pathogens, upon invading coral tissues, can cause direct damage and weaken the coral's immune response, causing coral bleaching and thus creating a favourable environment for secondary infections [207–210]. On the other hand, infected corals release nutrients that can nourish pathogens [209], while the resulting tissue damage provides a hospitable environment for their proliferation [211]. This cyclical interaction between infected corals and pathogens forms a positive feedback loop as the weakened coral becomes more susceptible to further infections, perpetuating the cycle of pathogen growth and coral decline.

Let v_1 and v_2 represent the macroalgae and infected coral-mediated growth rates of the pathogen, which will influence the relative growth rate (RGR) of the pathogen growth (i.e., $\frac{1}{W}\frac{dW}{dt}$). Limited nutrient availability is a key factor in microbial competition. Microorganisms compete for essential nutrients, and the specific nutrient ratios in an environment determine its persistence. Increased competition for limited nutrients can lead to heightened stress on microbial populations, influencing growth rates and survival. To account for this, we consider the parameter δ, which represents the competition effect of pathogens [212–215], a widespread phenomenon for aquatic pathogens. Let d_3 account for the decay rate, which is likely attributed to natural mortality. Furthermore, infected corals incur additional mortality at a rate of γ due to the disease, known as virulence. Therefore, in the

presence of infection, the governing equations take the form:

$$\begin{aligned}
\frac{dM}{dt} &= \alpha M(C_S + C_I) - g\frac{M}{M+T} - d_1 M + (aM+b)T, \\
\frac{dC_S}{dt} &= rC_S T - \alpha M C_S - \lambda_c C_S C_I - \lambda_{nc} W C_S - d_2 C_S, \\
\frac{dC_I}{dt} &= \lambda_c C_S C_I + \lambda_{nc} W C_S - \alpha M C_I - d_2 C_I - \gamma C_I, \\
\frac{dT}{dt} &= g\frac{M}{M+T} + d_1 M + d_2(C_S + C_I) + \gamma C_I - (aM + b + rC_S)T, \\
\frac{dW}{dt} &= W(v_1 M + v_2 C_I - d_3 - \delta W).
\end{aligned} \tag{5.2}$$

Fish are integral components of coral reef ecosystems, playing crucial roles in maintaining ecological balance through processes like grazing, predation, and nutrient cycling. Different fish species have distinct predation behaviours. Some fish are primarily herbivores, focusing on consuming macroalgae [216, 217]. Others are primarily carnivores, targeting corals and other invertebrates [218, 219]. However, many fish exhibit omnivorous feeding patterns, consuming both macroalgae and corals, often depending on their availability and nutritional needs [220]. For simplicity, we assume that fish consume both macroalgae and corals at an equal rate. Thus, the predation of macroalgae and coral by fish is represented by $a(P,M)$ and $a(P,C)$, respectively, where $a(P,X) = \frac{g_{1,2}PX}{M+T+C} = g_{1,2}PX$, since $M+T+C=1$ (X represents either M or C, and P represents the fish population). Here the predation rates for macroalgae and coral, g_1 and g_2, are given by $g_1 = gh$ and $g_2 = g(1-h)$, respectively, and the parameter h ($0 \leq h \leq 1$) represents the food preference of fishes, where $h = 0$ (1) represents the case where the coral (macroalgae) is the only food for fishes.

Fish predation significantly influences the rate of coral infections. Pathogens are often harboured in the mouths and guts of fish when they graze infected corals [149]. In the vicinity of coral reefs, fish frequently interact with corals as a part of their habitat utilization and feeding behaviour [221]. When fish feed on healthy corals, they can create wounds or stress the coral tissue, making it more susceptible to infection. Pathogens may get into the coral's surface during this feeding process [174], to a lesser extent, by uptake from the surrounding water [169]. This non-contagious disease transmission pathway involving fish as a carrier of pathogens is an important aspect of coral health and ecosystem dynamics [117, 222]. Consequently, this transmission rate (λ_{nc}) increases as a function of the rate at which coral diminishes due to fish predation. Without fish predation, the transmission rate through the non-contagious λ_{nc} pathway remains constant. To model this relationship, we employ a Holling type II functional response, a common approach to model the transmission rate of a disease, when it is influenced by external factors [223, 224], i.e.,

$$\lambda_{nc} = \lambda\left[1 + \frac{a(P,C)}{m + a(P,C)}\right]. \tag{5.3}$$

While increased fish predation can initially lead to a rise in viral load within coral, further predation may result in a saturating effect. The Holling type II functional form encapsulates that while an increase in fish predation can lead to a rise in disease transmission, the marginal impact of additional predation pressure on transmission rates decreases as the population grows.

A schematic diagram of the system is given in Fig. 5.1. The reef dynamics are thus described as a system of nonlinear differential equations:

$$\begin{aligned}
\frac{dM}{dt} &= \alpha M(C_S + C_I) - gPM - d_1 M + (aM + b)T \equiv F_1, \\
\frac{dC_S}{dt} &= rC_S T - \alpha M C_S - \lambda_c C_S C_I - \lambda_{nc} W C_S - d_2 C_S - gPC_S \equiv F_2, \\
\frac{dC_I}{dt} &= \lambda_c C_S C_I + \lambda_{nc} W C_S - \alpha M C_I - d_2 C_I - \gamma C_I - gPC_I \equiv F_3, \\
\frac{dW}{dt} &= W(v_1 M + v_2 C_I - d_3 - \delta W) \equiv F_4,
\end{aligned} \tag{5.4}$$

where $T = 1 - M - C_S - C_I$, and the transmission rate λ_{nc} is given in (5.3).

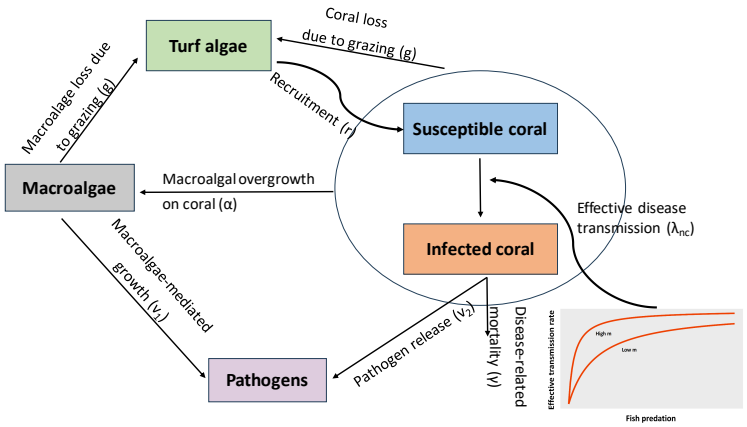

Figure 5.1: A schematic diagram of the coral reef dynamics. Coral and turfs are overrun by macroalgae, and turfs rapidly spread in the space left by the mortality of macroalgae and corals. Fish grazes on macroalgae and coral and hence affects the rate of non-contagious disease transmission, as illustrated in the panel.

To analyze model (5.4), we consider non-negative initial conditions: $M(0) \geq 0$, $C_S(0) \geq 0$, $C_I(0) \geq 0$ and $W(0) \geq 0$. The parameters used in the simulations and bifurcation analysis are described in Table 5.1. In the subsequent part, we present comprehensive numerical simulations to uncover the intricate dynamical behaviours of the diseased reef system (5.4) in addition to the local stability analysis. We utilize MATLAB's ode45 solver to generate time series solutions for the system. To track changes in the steady-state behaviours of interacting populations.

5.3 Description of the Parameters

Table 5.1: Parameters used in the system (5.4)

Parameters	Description	Value	Refference
α	Rate of macroalgal direct overgrowth over coral	0.1	[124], [159], [160]
g	Maximum grazing rate of herbivorous fish	-	[159]
P	Fish population	2	–
d_1	Natural mortality rate of macroalgae	0.13	[143]
a	Rate of macroalgae vegetative spread over algal turfs	0.8	[143]
b	Immigration rate of macroalgae on algal turf	0.005	[159], [143]
r	Recruitment rate of corals on turf algae	4.5	[143]
λ_c	Disease transmission rate through contact	0.02	[143]
λ	Disease transmission rate through noncontagious way	-	
d_2	Natural mortality rate of corals	0.24	[144], [162]
γ	Disease induced death rate of infected corals	-	–
v_1	Pathogen shedding rate by macroalgae	0.1	[143]
v_2	coral(infected)-mediated growth rates of the pathogen	0.1	[143]
d_3	Average time pathogen exists into the environment	0.01	[226]
m	Saturation coefficient	0.1	
δ	Crowding parameter	0.01	[143]

5.4 Results

5.4.1 Positivity

Since the state variables of the system (5.4) represent population densities, positivity implies that the population is never zero and always survives.

Theorem 5.1 *With positive beginning values, every solution to our system (5.4) exists and is unique in* $[0,\infty)$ *and* $M(t)>0$, $C_S(t)>0$, $C_I(t)>0$, $W(t)>0$, $\forall\, t>0$.

Proof: Let $G=(M,C_S,C_I,W)^T$ and $F(G)=[F_1,\ F_2,\ F_3,\ F_4]^T$. Then the system (5.4) can be put in the form:

$$\dot{G}=F(G),$$

where $F:R^4\to R^4_+$ with $G(0)=G_0\in R^4_+$, $F_i\in R^\infty(R_+)$, for $i=1,2,3,4$. As a result, the vector function F is an entirely continuous, local Lipschitzian variable function (M,C_S,C_I,W) in $E=\{M(t),\ C_S(t),\ C_I(t),\ W(t)\}$; $M>0$, $C_S>0$, $C_I>0$, $W>0$. Applying the lemma in [199], we can conclude that any solution $(M,\ C_S,\ C_I,\ W)$ of the system (5.4) with positive initial values exits and is unique in the interval $[0,\ L]$, $\forall\, t\geq 0$. Where L is a finite positive real number.

5.4.2 Boundedness

Theorem 5.2 *For all* $\phi>0$, *there exists* $t_\phi>0$ *such that all the solutions of (5.4) enter into the set* $\{\ (M,\ C_S,\ C_I,\ W)\in R^4 : M(t)+C_S(t)+C_I(t)+W(t)<\frac{v_1+v_2+\delta-d_3}{\delta}+\phi\}$ *whenever* $t>t_\phi$.

Proof: Since $M(t),C_I(t)\leq 1$ for all t, then we obtained $\frac{dW}{dt}\leq\delta W(\frac{v_1+v_2-d_3}{\delta}-W)$. Let Z(t) be the solution of $\frac{dW}{dt}\leq\delta W(\frac{v_1+v_2-d_3}{\delta}-W)$ with $Z(0)=W(0)$ so it must satisfied the equation i.e $\frac{dZ}{dt}\leq\delta Z(\frac{v_1+v_2-d_3}{\delta}-Z)$.
Then we have $Z(t)=\frac{R(v_1+v_2-d_3)e^{(v_1+v_2-d_3)t}}{\delta(1+Re^{(v_1+v_2-d_3)t})}$, where $R=\frac{\delta W(0)}{v_1+v_2-d_3-\delta W(0)}$.
If $v_1+v_2<d_3$, then $Z(t)\to 0$ as $t\to\infty$.
If $v_1+v_2>d_3$, then $Z(t)\to(\frac{v_1+v_2-d_3}{\delta})$ as $t\to\infty$.
Applying the standard theorem of differential inequality, we obtain $\limsup_{t\to\infty} W(t)\leq\frac{v_1+v_2-d_3}{\delta}$.
Therefore, $\limsup_{t\to\infty}[M(t)+C_S(t)+C_I(t)+W(t)]\leq\frac{v_1+v_2-d_3}{\delta}+1$, as
$M(t)+C_S(t)+C_I(t)+W(t)\leq 1$
i.e $\limsup_{t\to\infty}[M(t)+C_S(t)+C_I(t)+W(t)]\leq\frac{v_1+v_2+\delta-d_3}{\delta}$.

5.4.3 Stability and Bifurcation Analysis

5.4.3.1 Existence of Equilibrium Points

The system (5.4) has four different equilibrium points, which are described as follows:

i. Coral and pathogen-free equilibrium E_1=$(M_1,\ 0,\ 0,\ 0)$,
where $M_1 = \frac{(a-b-d_1-gP)+\sqrt{(a-b-d_1-gP)^2+4ab}}{2a}$.The equilibrium point E_1 always exists.

ii. Coral-free equilibrium $E_2 = (M_1,\ 0,\ 0,\ W_2)$, where $W_2 = \frac{v_1M_1-d_3}{\delta}$. The equilibrium E_2 exists if $v_1 > \frac{d_3}{M_1}$.

iii. Infected coral and pathogen-free equilibrium E_3=$(M_2,\ C_{S3},\ 0,\ 0)$, where M_2 is a positive solution of the equation $L_0M^2 + L_1M + L_2$=0,
where L_0=$(\alpha - a)s_2 - a$,
L_1=$-\left((a-\alpha)s_1 + bs_2 + b - a + d_1 + gP\right)$,
L_2=$b(1-s_1)$,
C_{S3}=$s_1 + s_2M_2$. The quantities s_1 and s_2 are given by s_1=$1 - \frac{d_2}{r} - \frac{gP}{r}$ and s_2=$-\frac{(r+\alpha)}{r}$.

iv. The interior equilibrium E^*=$(M^*,\ C_S^*,\ C_I^*,\ W^*)$, where M^*,C_S^*,C_I^*, and W^* are positive solutions of the system of equation: $F_1 = F_2 = F_3 = F_4 = 0$.

5.4.3.2 Local Stability Analysis

We summarize the stability analysis of the system (5.4) in the following theorem.

Theorem 5.3 *The stability behaviour of the system (5.4) around the equilibrium points is described below.*

i. *Coral and pathogen-free equilibrium* E_1=$(M_1,\ 0,\ 0,\ 0)$ *is locally asymptotically stable (LAS) if* $\frac{(r-d_2-gP)}{r+\alpha} < M_1 < \frac{d_3}{v_1}$.

ii. *Coral-free equilibrium* $E_2 = (M_1,\ 0,\ 0,\ W_2)$ *is LAS if*
$\frac{(r-\lambda W_2-d_2-gP)}{r+\alpha} < M_1 < \frac{d_3+2\delta W_2}{v_1}$.

iii. *Infected coral and pathogen-free equilibrium* $E_3 = (M_2,\ C_{S3},\ 0,\ 0)$ *is LAS if*
$(\lambda_c C_{S_3} - \alpha M_2 - d_2 - \gamma - gP) < 0,\ v_1M_2 - d_3 < 0,\ a_{11} + a_{22} < 0,\ a_{11} + a_{22} > a_{12} + a_{21}$.

iv. *Endemic equilibrium* E^*=$(M^*,\ C_S^*,\ C_I^*,\ W^*)$ *is LAS if*
$Q_i > 0\ (i = 1,2,3,4)$ *and* $Q_1Q_2Q_3 > Q_3^2 + Q_1^2Q_4$.

Proof: (i) The Jacobian matrix of the system (5.4) at E_1 is

$$J_1 = \begin{pmatrix} (a-b-d_1-gP-2aM_1) & (\alpha-a)M_1-b & (\alpha-a)M_1-b & 0 \\ 0 & r-(r+\alpha)M_1-d_2-gP & 0 & 0 \\ 0 & 0 & -\alpha M_1-d_2-\gamma-gP & 0 \\ 0 & 0 & 0 & v_1M_1-d_3 \end{pmatrix},$$

with $M_1=\frac{(a-b-d_1-gP)+\sqrt{(a-b-d_1-gP)^2+4ab}}{2a}$.
The eigenvalues of the Jacobian matrix $J_1(E_1)$ are given by
$-\sqrt{(a-b-d_1-gP)^2+4ab},\ r-(r+\alpha)M_1-d_2-gP,\ -(\alpha M_1+d_2+\gamma+gP),\ v_1M_1-d_3.$
All the eigenvalues are negative if $\frac{(r-d_2-gP)}{r+\alpha} < M_1 < \frac{d_3}{v_1}$.
Therefore, the system is locally asymptotically stable at E_1 if $\frac{(r-d_2-gP)}{r+\alpha} < M_1 < \frac{d_3}{v_1}$.
(ii) The Jacobian matrix of the system (5.4) at E_2 is

$$J_2 = \begin{pmatrix} a-b-d_1-gP-2aM_1 & (\alpha-a)M_1-b & (\alpha-a)M_1-b & 0 \\ 0 & r-(r+\alpha)M_1-\lambda W_2-d_2-gP & 0 & 0 \\ 0 & \lambda W_2 & -\alpha M_1-d_2-gP & 0 \\ v_1W_2 & 0 & v_2W_2 & v_1M_1-d_3-2\delta W_2 \end{pmatrix},$$

with $M_1=\frac{(a-b-d_1-gP)+\sqrt{(a-b-d_1-gP)^2+4ab}}{2a}$.

The eigenvalues of the Jacobian matrix $J_2(E_2)$ are given by
$-\sqrt{(a-b-d_1-gP)^2+4ab},\ r-(r+\alpha)M_1-\lambda W_1-d_2-gP,\ -(\alpha M_1+d_2+\gamma+gP),$
$v_1M_1-d_3-2\delta W_2.$
All the eigenvalues are negative if $\frac{(r-\lambda W_2-d_2-gP)}{r+\alpha} < M_1 < \frac{d_3+2\delta W_2}{v_1}$.
Therefore, the system is locally assymptotically stable at E_2 if $\frac{(r-\lambda W_2-d_2-gP)}{r+\alpha} < M_1 < \frac{d_3+2\delta W_2}{v_1}$.
(iii) The Jacobian matrix of the system (5.4) at E_3 is

$$J_3 = \begin{pmatrix} a_{11} & a_{12} & a_{13} & 0 \\ a_{21} & a_{22} & a_{23} & a_{24} \\ 0 & 0 & a_{33} & a_{34} \\ 0 & 0 & 0 & a_{44} \end{pmatrix},$$

with
$a_{11} = (a+\alpha C_{S_3}-aC_{S_3}-b-d_1-gP)+\frac{a_1\sigma C_{S_3}}{(a_1+\sigma P_3)^2},$
$a_{12} = M_2(\alpha-a)-b,$
$a_{13} = M_2(\alpha-a)-b,$
$a_{21} = -C_{S_3}(\alpha+r),$
$a_{22} = (r-rM_2-\alpha M_2-2rC_{S_3}-d_2-gP),$

$a_{23} = -C_{S_3}(r+\lambda_c)$,
$a_{24} = -(\lambda C_{S_3} + \frac{\lambda g P C_{S_3}^2}{m+gPC_{S_3}})$,
$a_{33} = (\lambda_c C_{S_3} - \alpha M_2 - d_2 - \gamma - gP)$,
$a_{34} = \lambda C_{S_3} + \frac{\lambda g P C_{S_3}^2}{m+gPC_{S_3}}$,
$a_{44} = v_1 M_2 - d_3$.
Now, the characteristic equation of J_3 is given by

$$| J_3 - qI_4 | = 0.$$

The two roots of the characteristic equation of J_3 are:
$(\lambda_c C_{S_3} - \alpha M_2 - d_2 - \gamma - gP)$, $v_1 M_2 - d_3$,
and the remaining two roots are given by the equation:

$$q^2 - (a_{11} + a_{22})q + (a_{11}a_{22} - a_{12}a_{21}) = 0.$$

Therefore, all the eigenvalues of the Jacobian matrix J_3 are negative if $(\lambda_c C_{S_3} - \alpha M_2 - d_2 - \gamma - gP) < 0$, $v_1 M_2 - d_3 < 0$, $a_{11} + a_{22} < 0$, $a_{11} + a_{22} > a_{12} + a_{21}$.
Thus, under the above conditions, the system (5.4) is locally asymptotically stable at E_3.
(iv) The Jacobian matrix of the system (5.4) at E^* is

$$J^* = \begin{pmatrix} g_{11} & g_{12} & g_{13} & 0 \\ g_{21} & g_{22} & g_{23} & g_{24} \\ g_{31} & g_{32} & g_{33} & g_{34} \\ g_{41} & 0 & g_{43} & g_{44} \end{pmatrix},$$

with
$g_{11} = (a + \alpha C_S^* + \alpha C_I^* - b - d_1 - gP - 2aM^* - aC_S^* - aC_I^*)$,
$g_{12} = M^*(\alpha - a) - b$,
$g_{13} = M^*(\alpha - a) - b$,
$g_{21} = -C_S^*(r+\alpha)$,
$g_{22} = r - (r+\alpha)M^* - 2rC_S^* - (r+\lambda_c)C_I^* - \lambda W^* - d_2 - gP - \frac{gP\lambda C_I^* W^*(m+gPC_I^*)}{(m+gP(C_S^*+C_I^*))^2} - \frac{gP\lambda C_S^* W^*(2m+gP(C_S^*+2C_I^*))}{(m+gP(C_S^*+C_I^*))^2}$,
$g_{23} = -C_S^*(r+\alpha) - \frac{gP\lambda C_S^* W^*(m+gPC_S^*)}{(m+gP(C_S^*+C_I^*))^2} + \frac{\lambda g^2 P^2 C_S^2 W^*}{(m+gP(C_S^*+C_I^*))^2}$,
$g_{24} = -\lambda C_S - \frac{gP\lambda C_S^2}{m+gP(C_S^*+C_I^*)} - \frac{\lambda gPC_S^* C_I^*}{m+gP(C_S^*+C_I^*)}$,
$g_{31} = -\alpha C_I^*$,
$g_{32} = \lambda_c C_I^* + \lambda W^* + \frac{gP\lambda C_S^* W^*(2m+gP(C_S^*+C_I^*))}{(m+gP(C_S^*+C_I^*))^2} + \frac{gP\lambda C_I^* W^*(m+gPC_I^*)}{(m+gP(C_S^*+C_I^*))^2}$,
$g_{33} = \lambda_c C_S^* - \alpha M^* - d_2 - \gamma - gP - \frac{\lambda g^2 p^2 C_S^2 W^*}{(m+gP(C_S^*+C_I^*))^2} + \frac{gP\lambda C_I^* W^*(m+gPC_I^*)}{(m+gP(C_S^*+C_I^*))^2}$,
$g_{34} = \lambda C_S^* + \frac{gP\lambda C_S^2}{m+gP(C_S^*+C_I^*)} + \frac{\lambda gPC_S^* C_I^*}{m+gP(C_S^*+C_I^*)}$,
$g_{41} = v_1 W^*$,

$g_{43} = v_2 W^*$,
$g_{44} = v_1 M + v_2 C_I^* - d_3 - 2\delta W^*$.
Now, the characteristic equation of J^* is given by

$$| J^* - xI_4 | = 0,$$

i.e.,

$$x^4 + Q_1 x^3 + Q_2 x^2 + Q_3 x + Q_4 = 0,$$

where,
$Q_1 = -g_{11} - g_{22} - g_{33} - g_{44}$,
$Q_2 = g_{11}g_{22} + g_{11}g_{33} + g_{11}g_{44} + g_{22}g_{33} + g_{22}g_{44} + g_{33}g_{44} - g_{34}g_{43} - g_{23}g_{32} - g_{12}g_{21} - g_{13}g_{31}$,
$Q_3 = g_{11}g_{34}g_{43} + g_{11}g_{23}g_{32} + g_{22}g_{34}g_{43} + g_{32}g_{44}g_{23} + g_{12}g_{21}g_{33} + g_{12}g_{21}g_{44} + g_{13}g_{44}g_{31} + g_{13}g_{31}g_{22} - g_{11}g_{22}g_{33} - g_{11}g_{22}g_{44} - g_{11}g_{33}g_{44} - g_{22}g_{33}g_{44} - g_{24}g_{32}g_{43} - g_{12}g_{23}g_{31} - g_{12}g_{24}g_{41} - g_{13}g_{41}g_{34} - g_{13}g_{21}g_{32}$,
$Q_4 = g_{11}g_{22}g_{33}g_{44} + g_{11}g_{24}g_{32}g_{43} + g_{12}g_{21}g_{34}g_{43} + g_{12}g_{23}g_{31}g_{44} + g_{12}g_{24}g_{41}g_{33} + g_{13}g_{41}g_{34}g_{22} + g_{13}g_{44}g_{21}g_{32} - g_{11}g_{22}g_{34}g_{43} - g_{11}g_{32}g_{44}g_{23} - g_{12}g_{21}g_{33}g_{44} - g_{12}g_{23}g_{41}g_{34} - g_{12}g_{24}g_{31}g_{43} - g_{13}g_{41}g_{24}g_{32} - g_{13}g_{44}g_{31}g_{22}$.
Using *Routh-Hurwitz* criteria, E^* will be locally asymptotically stable if
(i) $Q_i > 0$ $(i = 1,2,3,4)$, and
(ii) $Q_1 Q_2 Q_3 > Q_3^2 + Q_1^2 Q_4$.

5.4.3.3 Bifurcation Analysis

The bifurcation nature of the system (5.4) with respect to the parameter λ can be described in the following theorem.

Theorem 5.4 *The proposed system (5.4) exhibits a* **transcritical bifurcation** *at E_2 when λ crosses λ_*, where $\lambda_* = \frac{r-d_2}{W_2} - \frac{gP}{W_2} - \frac{(r+\alpha)M_1}{W_2}$. At this threshold, the conditions of the emergence of such pivotal bifurcation are given by:*

$$(i)\ V^T f_\lambda(E_2;\lambda_*) = 0,$$
$$(ii)\ V^T [D f_\lambda(E_2;\lambda_*)U] \neq 0,$$
$$(ii)\ V^T [D^2 f_\lambda(E_2;\lambda_*)(U,U)] \neq 0.$$

Proof: At $\lambda = \lambda_*$ the Jacobian matrix of the system (5.4) at E_2 is

$$J_2 = \begin{pmatrix} a-b-d_1-gP-2aM_1 & (\alpha-a)M_1-b & (\alpha-a)M_1-b & 0 \\ 0 & r-(r+\alpha)M_1-\lambda_* W_2-d_2-gP & 0 & 0 \\ 0 & \lambda_* W_2 & -\alpha M_1-d_2-\gamma-gP & 0 \\ v_1 W_2 & 0 & v_2 W_2 & v_1 M_1 - d_3 - 2\delta W_2 \end{pmatrix},$$

Therefore, the Jacobian matrix has a simple zero eigenvalue if

$$r-(r+\alpha)M_1-\lambda_* W_2-d_2-gP=0,$$

i.e., if

$$\lambda_*=\frac{r-d_2}{W_2}-\frac{gP}{W_2}-\frac{(r+\alpha)M_1}{W_2}.$$

Let U and V be the eigenvectors corresponding to the zero eigenvalue for J_2 and J_2^T, respectively.

Then we get U=$(u_1,\ u_2,\ 1,\ u_3)^T$ and $V=(0,\ 1,\ 0,\ 0)^T$.

Where,

$u_1=\frac{1}{(a-b-d_1-2aM_1)-gP}(\frac{(\alpha+M_1+d_2+\gamma)+gP}{\lambda_* W_2}-1)$,

$u_2=\frac{(\alpha M_1+d_2+\gamma)+gP}{\lambda_* W_2}$,

$u_3=\frac{1}{v_1M_1-d_3-2\delta W_2}(-v_2W_2+\frac{v_1W_2}{(a-b-d_1-2aM_1)-gP}(\frac{(\alpha M_1+d_2+\gamma)+gP}{\lambda_* W_2}-1))$.

We obtain $V^T f_\lambda(E_2;\ \lambda_*)=0$, where $\lambda_*=\frac{r-d_2}{W_2}-\frac{gP}{W_2}-\frac{(r+\alpha)M_1}{W_2}$, and so no saddle-node bifurcation occurs at E_2 when λ crosses λ_*.

Also, $Df_\lambda(E_2,\ \lambda_*)U=(0,\ -u_2W_2,\ \ u_2W_2,\ \ 0)^T$ gives $V^T[Df_\lambda(E_2,\lambda_*)U]=-u_2W_2<0$

Now, we have $D^2f(E_2,\ \lambda_*)(U,\ U)$=

$$\begin{pmatrix} -2au_1^2+2(\alpha-a)u_1u_2+2(\alpha-a)u_1 \\ -2(\alpha+r)u_1u_2-2(\lambda_c+r)u_2-2\lambda_*u_2u_3-\frac{2\lambda_* gPW_2}{m}u_2-\frac{2\lambda gPW_2}{m}u_2^2-2ru_2^2 \\ -2\alpha u_1+2\lambda_*u_2u_3+\frac{2\lambda_* gPW_2}{m}u_2^2+\frac{\lambda_* gPW_2}{m}u_2+\frac{2\lambda_* g^2P^2W_2}{m^2}u_2+\frac{\lambda_* gPW_2}{m}u_3+\lambda_*u_2u_3+\lambda_cu_2+\lambda_cu_3 \\ v_1u_1u_3+v_2u_3+v_1u_1u_3+v_2u_3-2\delta u_3^2 \end{pmatrix},$$

This gives $V^T[D^2f(E_2,\lambda_*)(U,U)]=\eta$,

where

$\eta=-2\alpha u_1+2\lambda_*u_2u_3+\frac{2\lambda_* gPW_2}{m}u_2^2+\frac{\lambda_* gPW_2}{m}u_2+\frac{2\lambda_* g^2P^2W_2}{m^2}u_2+\frac{\lambda_* gPW_2}{m}u_3+\lambda_*u_2u_3+\lambda_cu_2+\lambda_cu_3$.

5.4.4 Role of Fish Predation on the Disease Dynamics

5.4.4.1 Corals Face Risk Due to Low Fish Predation Despite Appearing Disease-Free

We first consider low fish predation rate ($g=0.2$) to investigate the effect of the disease transmission rate for the non-contagious pathway (λ) on the coral disease dynamics (see Fig. 5.2(A, B)). For lower values of λ (i.e., $\lambda<0.2$), E_3 is the only stable state of the system. So, the coral population is disease-free and coexists with macroalgae. With increasing λ, we see a small parameter window ($0.2<\lambda<0.3$, approx), where the system possesses bistability between E_3 and E_L^* (low prevalence endemic equilibrium). At the transcritical bifurcation (at $\lambda=0.3$), the coral population dies out in the stable state, and

now the system has bistability between E_3 and E_2 for $\lambda > 0.3$. So, in this case, if coral exists, it remains disease-free. Otherwise, it will become extinct, depending on the initial population levels.

At low fish predation rates, there is minimal pressure on macroalgae. When disease transmission rates are low, the disease cannot persist within the coral population, allowing corals to thrive. However, as disease transmission rates increase, coral populations experience suppression due to disease-related mortality. Eventually, macroalgae begin to dominate the system, and if the initial coral population is low, corals are ultimately wiped out.

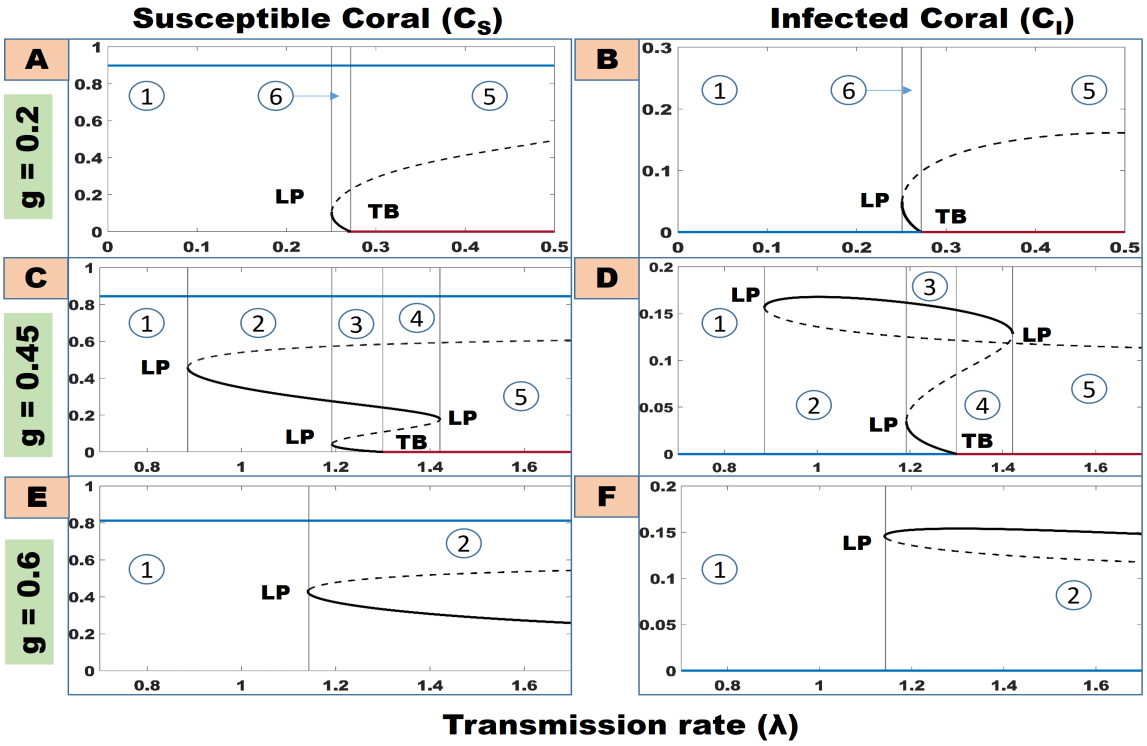

Figure 5.2: Bifurcation diagram of the system (5.4) with respect to λ, the non-contagious pathway transmission rate, for $g = 0.2$ (A, B), $g = 0.45$ (C, D) and $g = 0.6$ (E, F). Here, black solid and dashed curves represent stable and unstable endemic steady states; blue and red curves indicate disease-free coral states and coral extinction states, respectively. The number mentioned in the circles represents the regions mentioned in Fig. 5.3. The other parameter values are mentioned in Table 5.1 unless otherwise stated.

5.4.4.2 Medium Fish Predation Level Triggers Sudden Emergence of Disease and Coral Extinction

A moderate fish predation rate (g) introduces intricate complexities into coral disease dynamics (Fig. 5.2(C, D)). At low levels of disease transmission rates, the coexistence of macroalgae and healthy corals is observed, resembling the scenario described earlier. However, a minimum level of λ is required for the disease establishment. For $\lambda < 0.88$, the system experiences monostability at E_3. At $\lambda = 0.88$, the system exhibits the onset of

a pair of coexistence steady states of opposite stability nature through the emergence of a saddle-node bifurcation, and the sudden emergence of the disease is observed at this threshold. In the region $0.88 < \lambda < 1.19$, the phenomenon of bistability is captured between the infection-free equilibrium E_3 and the endemic equilibrium E_H^* with a higher prevalence. Therefore, depending upon the level of λ, the initial species densities determine the persistence of the disease in the coral population. As λ increases, the density of the coral decreases. Disease-related mortality suppresses the coral population, as we assumed there is no recovery from the disease. At $\lambda = 1.19$, an additional coexistence attractor with the least infected coral density emerges through another saddle-node bifurcation. The region of tristability $\lambda \in (1.19, 1.29)$ determines the boundary attractor E_3 and a pair of coexistence attractors E_L^* and E_H^* for all non-negative initial species densities. In the low abundance endemic equilibrium, corals become extinct due to the disease through a transcritical bifurcation at $\lambda = 1.29$, where the stable branch E_L^* of the coexistence equilibria merges with the unstable coral-free equilibrium E_2, and the equilibrium E_2 regains stability. The system possesses another tristability between disease-free equilibrium, endemic equilibrium with high disease prevalence, and the coral-free state (i.e., E_2, E_3 and E_H^*) in the parameter window $1.3 < \lambda < 1.42$. This phenomenon is of special interest as the initial conditions determine the existence of the coral and the establishment of the disease. Under elevated fish predation rates, the coexistence of macroalgae and infected coral becomes feasible due to increased grazing pressure on the macroalgae. Consequently, in this scenario, corals can coexist with macroalgae even when partially infected, a phenomenon not observed under low fish predation rates. At the threshold $\lambda \approx 1.42$, two coexistence steady states collide and disappear, yielding a saddle-node bifurcation. Thus, a sudden collapse of the endemic steady-state is observed at this threshold. Beyond this threshold rate, the system possesses bistability between the disease-free state and the coral-free equilibria. So, for higher values of λ, initial population levels will determine the initiation of the disease in the system. Healthy coral may persist in the system. However, if the disease initiates, the entire coral population may become extinct.

5.4.4.3 High Fish Predation Rates Curb Disease Outbreaks and Coral Extinction Risk

Now, to capture the effect of λ on the system configuration for a high level of fish predation, we fix $g = 0.6$ (see Fig. 5.2(E, F)). We document that the equilibrium E_3 is always an attractor. Biologically, this scenario prognosticates that the coral reef system always tends to settle for an infection-free environment in which macroalgae and healthy coral can maintain harmonic coexistence. As in the previous case, for $\lambda < 1.14$, the non-contagious pathway of transmission does not become effective. At $\lambda = 1.14$, the ecological system experiences a sudden appearance of a pair of endemic steady states, out of which the state

E_H^* with higher infected coral equilibrium density is locally asymptotically stable. Therefore, for elevated fish predation, the minimum strength of infection required for disease establishment through a non-contagious way increases significantly. In the bistability region $\lambda > 1.14$, the system settles either to an infection-free environment or endemic state depending upon initial population sizes. Even under severe disease conditions, the substantial grazing pressure on macroalgae prevents it from surpassing coral in competition. It is noteworthy that the total coral equilibrium density at the stable endemic steady state has a decreasing trend with increasing λ, but coral does not go extinct for any initial conditions, unlike in the case of low or intermediate fish predation rate and high disease transmission rates (i.e., in Fig. 5.2(A - D)).

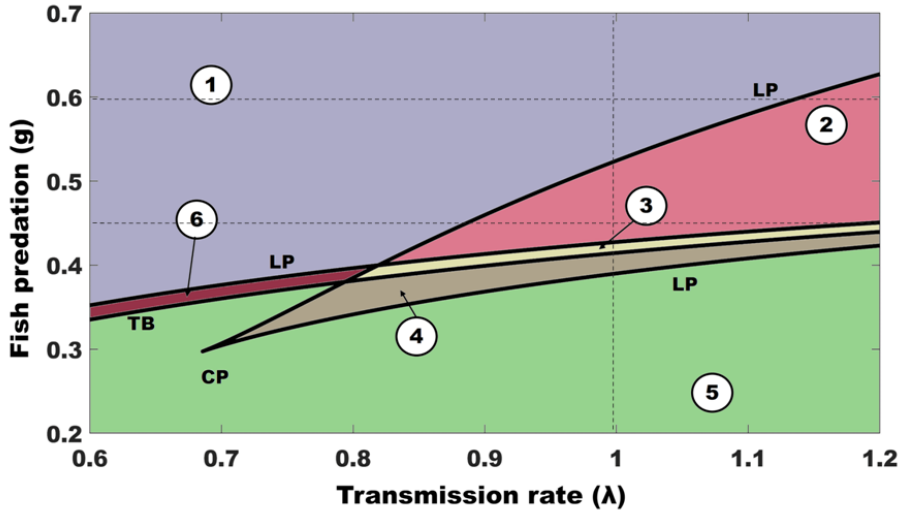

Figure 5.3: Two-parameter bifurcation diagram with respect to λ and g, the non-contagious pathway transmission rate, and the fish predation rate. **Region 1**: Disease-free coral state $(M, C_S, 0, 0)$; **Region 2**: Bistability between disease-free coral state $(M, C_S, 0, 0)$ and endemic state with high prevalence (M, C_S, C_{IH}, W); **Region 3**: Tristability between disease-free coral state $(M, C_S, 0, 0)$, endemic state with high prevalence (M, C_S, C_{IH}, W), and endemic state with low prevalence (M, C_S, C_{IL}, W); **Region 4**: Tristability between disease-free coral state $(M, C_S, 0, 0)$, endemic state with high prevalence (M, C_S, C_{IH}, W), and coral extinction state $(M, 0, 0, W)$; **Region 5**: Bistability between disease-free coral state $(M, C_S, 0, 0)$ and coral extinction state $(M, 0, 0, W)$; **Region 6**: Bistability between disease-free coral state $(M, C_S, 0, 0)$ and endemic state with low prevalence (M, C_S, C_{IL}, W). **TB**: Transcritical bifurcation curve, **LP**: Saddle-node bifurcation curve, **CP**: Cusp point.

5.4.4.4 The Interplay Between Transmission Rate and Fish Predation: High Fish Predation Facilitates Coral Survival Even in Extreme Disease Conditions

In order to gain a clearer understanding of the impact of fish predation on disease dynamics within coral populations, we conducted a two-parameter bifurcation analysis with disease

transmission rate (λ) and fish predation rate (g) as the key parameters (Fig. 5.3). When the fish predation rate is low, even with a high disease transmission rate (λ), the disease cannot be established in the system. This scenario corresponds to region 5, where the coral population either thrives or faces extinction, depending on the initial conditions. For the disease with a low transmission rate, the disease will be established in the system with low prevalence (see Region 6). After the disease establishment, a further increase in g will catastrophically eliminate the infected coral. Then, the coral population will exist in the system, irrespective of initial conditions (region 1). In the case of diseases with high transmission rates, an increase in fish predation can rapidly infect a significant proportion of coral (Region 4) through a saddle-node bifurcation. Within this range, the persistence of the coral population depends on the initial conditions. If the coral population survives, it may either remain healthy or harbour the disease. For slight elevation in g, the coral will always exist in the system; disease prevalence may be high, low, or null, depending on the initial condition (region 3). For further increase in g, disease prevalence will be high if it persists (see Region 2). For a high fish predation rate, the coral will always exist in a healthy manner unless the disease transmission rate is significantly high (region 1). Overall, for low and high fish predation rates, disease does not persist in the system. For an intermediate range of g, the disease will persist in the system; the initial condition will determine the degree of prevalence of the infected coral.

As a whole, we see that, for low or high levels of predation rate, the disease cannot persist in the system. For the low level of g, coral exists disease-free or extinct, whereas, for the higher level of g, coral always exists disease-free. Intermediate-range predation leads to the establishment of the disease. In this range, coral exists with high, low, or zero prevalence, depending on the initial population. Both events, disease invasion or elimination, occur abruptly with varying g. We found that our overall results remained unchanged when we considered a type-1 functional response for non-contagious disease transmission (See Fig. 5.4)

Here, we investigate the dynamics of the coral reef system when the increase in disease transmission rate through fish predation follows Holling type I functional response (Fig. 5.4), where the disease transmission in the non-contagious pathway increases linearly with fish predation of corals (i.e., $\lambda_{nc} = \lambda(1 + m_2 a(P,C))$, where $a(P,C) = gPC$). At low values of λ, the coral population remains disease-free and coexists with macroalgae. However, under low levels of fish predation, increasing λ does not lead to disease establishment, unlike the emergence of disease in a narrow range of λ observed in the type II response. In this case, if coral persists, it remains disease-free; otherwise, it becomes extinct, depending on the initial population levels. With moderate fish predation, we see a sudden emergence of disease and coral extinction similar to the Holling type II scenario. However, there is no abrupt emergence of a low-prevalence infection scenario, indicating that the infection level does not depend on initial species densities. At high levels of fish predation, as with the Holling type II response, disease establishes abruptly. As λ increases, the initial conditions determine whether the coral population will be disease-free or infected. Therefore, both Holling Type I and Type II functional responses lead to almost identical dynamical behaviours, with some exceptions in the complexity of disease emergence and prevalence patterns.

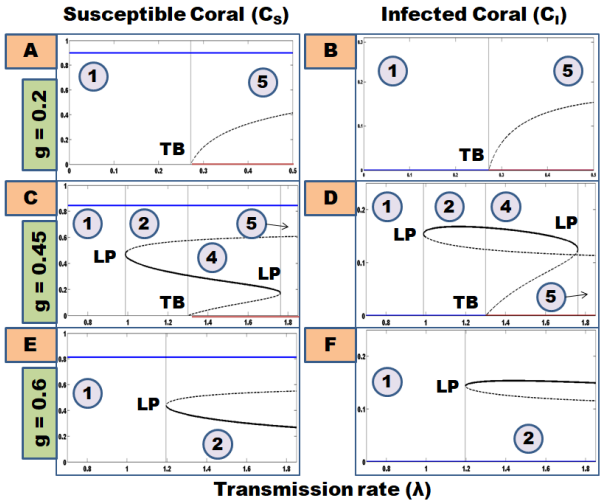

Figure 5.4: Bifurcation diagram of the system (5.4) with respect to λ, the non-contagious pathway transmission rate, with type-I functional response, for $g = 0.2$ (A, B), $g = 0.45$ (C, D) and $g = 0.6$ (E, F). Here, $m_2 = 2$ and the other parameter values are mentioned in Table 5.1 in Appendix 5.3. The number mentioned in the circles represents the regions mentioned in Fig. 5.3. The colour of the equilibrium curves and the name of the bifurcations are mentioned in Fig. 5.3. The overall dynamical behaviour of this system is similar to the case with the type-II response, depicted in Fig. 5.2.

5.4.5 Virulence and its Interplay with Fish Predation Rates

Understanding virulence and the severity of disease-induced mortality is critical for studying coral reef disease dynamics. While high virulence causes steeper population decline and hinders coral recovery from outbreaks, it can also limit the disease itself [227–230]. A high death rate among infected hosts reduces the pool of infected individuals, potentially preventing the chances of further outbreaks. Therefore, unravelling the influence of virulence on coral reef epidemics remains crucial. To achieve this, we employed one and two-parameter bifurcation analysis to explore the role of virulence and its interaction with fish predation rates.

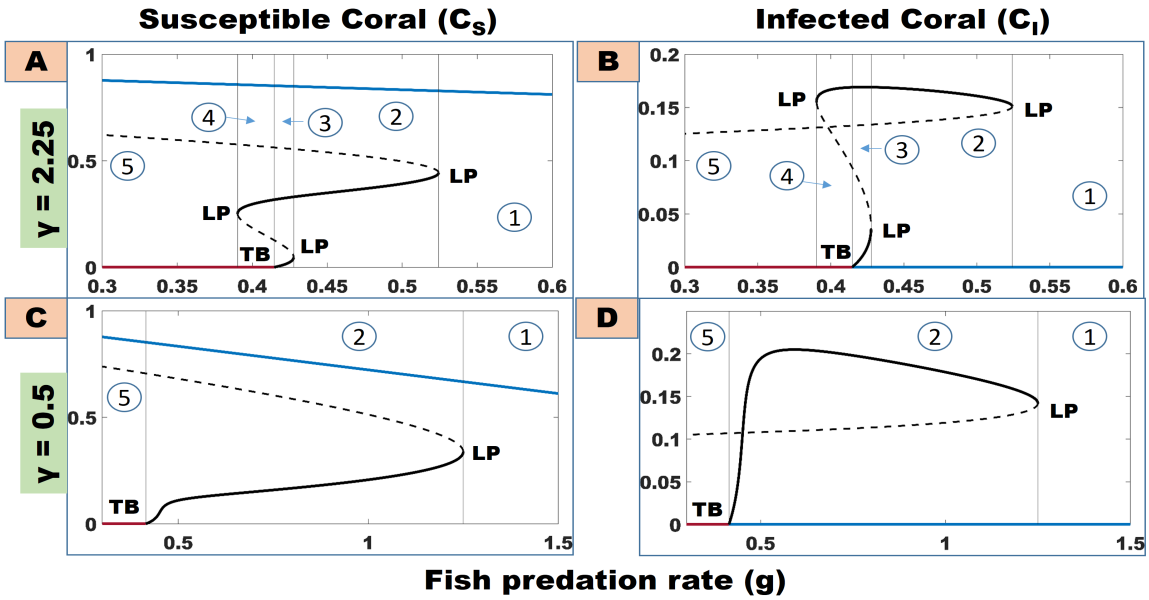

Figure 5.5: Bifurcation diagram of the system (5.4) with respect to the fish predation rate g, for $\gamma = 2.25$ (A, B) and $\gamma = 0.5$ (C, D). Here, the transmission rate (λ) = 1. The number mentioned in the circles represents the regions mentioned in Fig. 5.8.

5.4.5.1 The Delayed Onset and Abrupt Submergence of Coral Disease Under Escalating Fish Predation

To observe the role of fish predation on the coral disease dynamics, we consider g as the bifurcation parameter (Fig. 5.5). We observe that E_3 is always an attractor of the system where coral lives disease-free. However, the abundance of coral decreases with g in this stable state due to the increased predation pressure on corals. The system has an alternative stable state, E_2, for a low predation rate. So, in this range of g, the coral will either coexist in a healthy form with macroalgae or will go extinct, depending on the initial population densities (Fig. 5.6, panel 5). When increasing g, another stable state of endemic coexistence appears abruptly through a saddle-node bifurcation at $g = 0.39$. Therefore, for the range $0.39 < g < 0.41$, the system possesses tristability between E_2, E_3, and E_H^*; the

initial population size will determine whether the coral will live with or without the disease, or will go to extinction (Fig. 5.6, panel 4). However, the equilibrium E_2 loses its stability through the origination of a stable endemic equilibrium E_L^* with the lowest prevalence via a transcritical bifurcation (at $g = 0.41$). The stable equilibrium E_L^* collides with its unstable branch and vanishes through a saddle-node bifurcation at $g = 0.43$. For the range $0.41 < g < 0.43$, the system has tristability between E_3, E_H^* and E_L^* (Fig. 5.6, panel 3). Beyond the saddle-node bifurcation point at $g = 0.43$, bistability between E_3 and E_H^* is observed (Fig. 5.6, panel 2). Interestingly, further elevated g eliminates the disease from the system through another saddle-node bifurcation, where the endemic equilibrium (E_H^*) vanishes, and E_3 becomes the only stable attractor of the system (Fig. 5.6, panel 1). Additionally, when we considered different food preferences for macroalgae and coral, we found that the overall dynamics of the system remained unchanged when the preferences were equal or biased towards macroalgae. However, when the preference was biased towards coral, coral eventually became extinct abruptly, first from the endemic state and then from the healthy state (See Fig. 5.7)

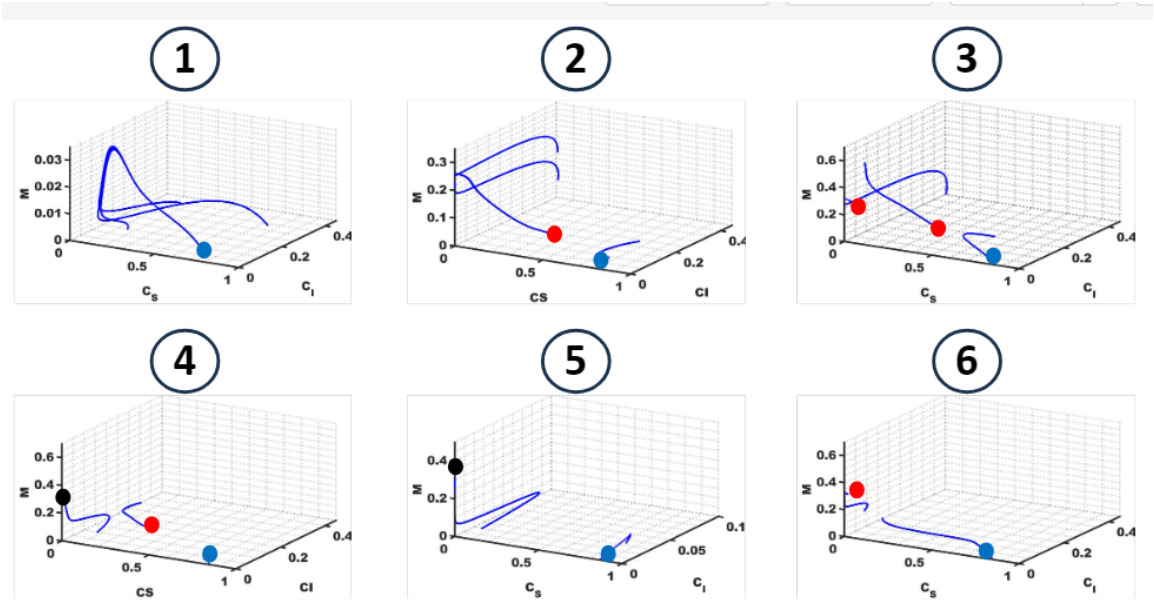

Figure 5.6: Phase portrait diagrams of the system (5.4) in (M, C_S, C_I) space. Here, the presence of endemic, disease-free, and coral-free stable steady states are indicated by the red, blue, and black dots, respectively. Dynamical regimes with regional analogues are highlighted with circles.

We discus the impact of varying fish preferences for macroalgae and coral on coral disease dynamics. The predation terms are $a(P,M) = g_1 PM$ and $a(P,C) = g_2 PC$, where g_1 and g_2 are given by $g_1 = gh$ and $g_2 = g(1-h)$. The parameter h $(0 \leq h \leq 1)$ represents the food preference of fishes, where $h = 0$ (1) represents the case where the coral (macroalgae) is the only food for fishes. Fish feeding preferences significantly impact coral health. When fish primarily consume coral, coral populations can decline or even vanish. Conversely, a strong preference for macroalgae can lead to disease outbreaks in coral, but the severity of these outbreaks depends on initial coral and macroalgae densities. If fish exhibit a balanced preference for both, disease prevalence is likely high. As fish increasingly favour macroalgae, disease prevalence tends to rise, indicating a positive correlation between macroalgae preference and disease risk. This indicates that coral disease dynamics can be understood by simplifying to the assumption of equal preference for both coral and macroalgae.

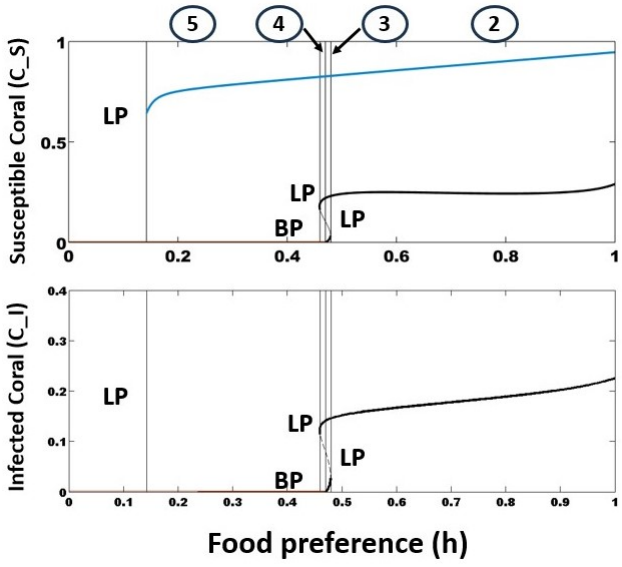

Figure 5.7: Bifurcation diagram of the system (5.4) with respect to the food preference (h) for fishes. $h = 0$ (1) represents the extreme case where the coral (macroalgae) is the only food for fish. In the region where h is low, meaning the fish primarily consume coral, the system reaches a macroalgae-dominated state $(M,0,0,W)$. The system exhibits similar dynamical behaviour when fish have an equal preference for both coral and macroalgae (the assumption made in the main text analysis), as well as when fish are predominantly herbivores, which is ecologically more realistic. Here, $g = 0.5$, $\lambda = 1.5$ and the other parameter values are mentioned in Table 5.1. The number mentioned in the circles represents the regions mentioned in Fig. 5.3. The colour of the equilibrium curves and the name of the bifurcations are mentioned in Fig. 5.3.

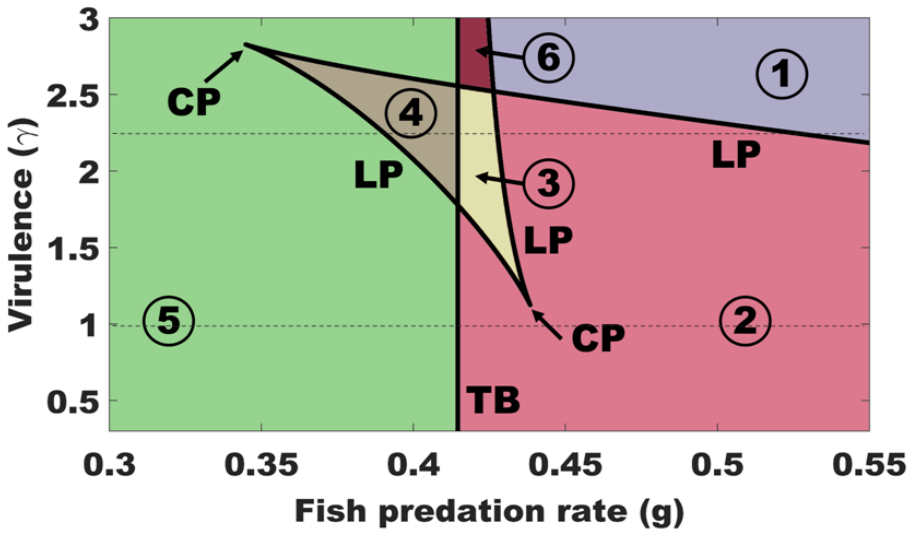

Figure 5.8: Two-parameter bifurcation diagram with respect to fish predation rate g and virulence of infection γ. The descriptions of the regions and bifurcation curves are the same as in Fig. 5.3.

Fig. 5.8 illustrates the combined influence of fish grazing and virulence on coral reef sustainability. When there's minimal fish predation, while the disease can establish itself briefly within a small window (region 4, Fig. 5.8; panel 4, Fig. 5.6), it is swiftly eradicated with even a slight increase in virulence. As high virulence wipes out the coral hosts and reduces the chance of disease spreading. For high grazing rates, while disease emergence is likely, a sufficiently high virulence level can abruptly eliminate the disease. Overall, high virulence tends to eliminate the disease regardless of fish grazing levels. However, the risk of coral extinction due to competition with macroalgae still depends on the grazing intensity.

To examine the combined effects of transmission, virulence, and grazing on the system's tipping behaviour, we plotted the transmission-virulence ratio against the grazing rate. The transmission rate to virulence ratio can serve as a proxy for the basic reproduction number (R_0) of a disease, which represents the average number of secondary infections caused by a single infected individual, the potential for a disease to spread within a community [231, 232]. We focused on parameter values that triggered a sharp transition from a healthy coral-dominated state (**Region 1**) to a disease-endemic state (**Region 2**) (see Fig. 5.9). Our analysis reveal a strong, nearly linear relationship between the transmission-virulence ratio and predation rate (with a high r^2 value). As fish predation increases, the system's tipping point shifts towards higher transmission-to-virulence ratios, favouring a healthier coral-dominated state. This highlights the critical role of fish predation in regulating the balance between transmission and virulence within coral populations. Excessive overfishing can disrupt this balance, potentially leading to harmful consequences for coral ecosystems.

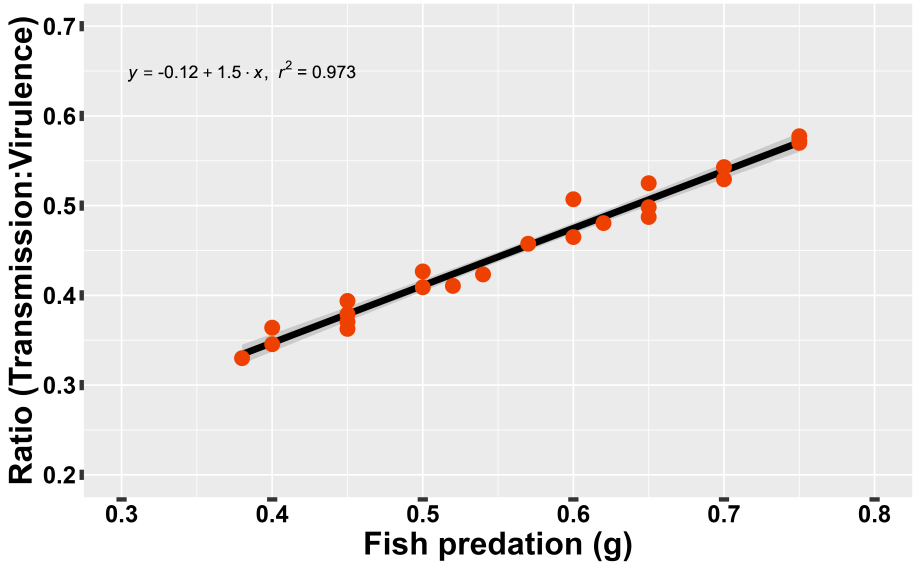

Figure 5.9: Orange points represent the pair of transmission-virulence ratio and fish predation rate, where the system undergoes a tipping point and becomes disease-dominated from a healthier state (i.e., **Region 2** from **Region 1**) through a saddle-node bifurcation. The parameter combination above (below) the line corresponds to **Region 2** (**Region 1**). The black line represents the linear regression line, the equation of which is mentioned in the upper-left corner.

5.4.6 Effect of the Disease Intensity

The transmission rate and virulence are crucial factors that determine the severity of a disease. In order to investigate how these epidemiological characteristics affect coral population dynamics under different levels of fish predation, we examined the two-parameter bifurcation of the system in the $\lambda - \gamma$ space. We varied the level of fish predation and analyzed the results (Fig. 5.10).

5.4.6.1 Predation Intensity Modulates the Impact of Virulence on Coral Epidemics

First, we study the case where the fish predation is low (e.g., $g = 0.2$, Fig. 5.10A). We observe that disease establishes in the system for some intermediate range of λ (region 2-4, 6). As there is no recovery from the disease, elevated λ will increase the disease prevalence, which eventually wipes out the coral from the system (region 5). On account of that, there is no effect of the virulence (γ) for low and high levels of λ. But γ eliminates the disease abruptly from the system for the intermediate level of λ (see regime shifts from region 2-1). However, we observe a narrow window of λ for which disease is not completely eradicated from the system, though a shift from the high prevalence to the low prevalence is seen for γ (region 3 to 6). Overall, disease-free states dominate the system for the low level of fish predation.

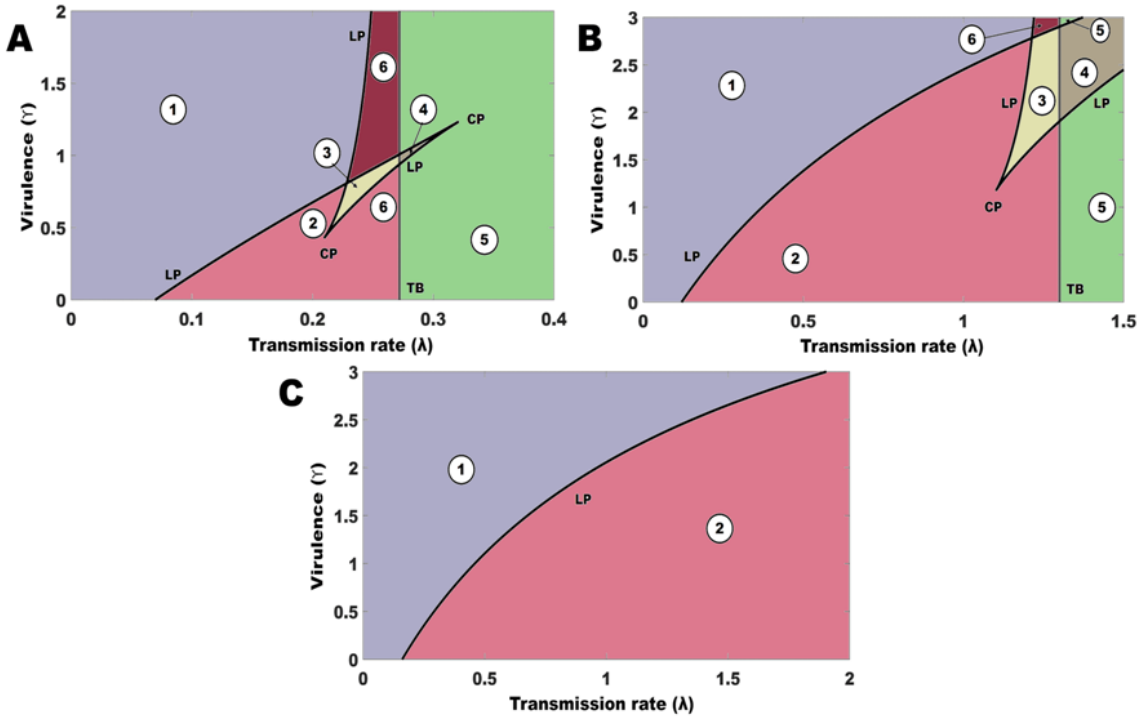

Figure 5.10: Two-parameter bifurcation diagram with respect to λ and γ, the non-contagious pathway transmission rate and the disease-induced death rate. The fish predation rate is taken as g=0.2 (A), 0.45 (B), and 0.6 (C). The descriptions of the regions are the same as in Fig. 5.3.

But, we observe that disease-induced states dominate the system for elevated fish predation (Fig. 5.10B). Similar to the previous scenario, we observe a sudden eradication of the disease with increasing γ. The range of λ values, within which the disease persists regardless of the level of γ, expands as g increases. For a high level of fish predation (g), the degree of γ determines the persistence of the disease (Fig. 5.10C). For low γ, the disease persists with a higher prevalence (region 2), which is eradicated suddenly with increasing γ (region 1). The non-existence of a range of λ, in which disease persists irrespective of γ, is observed in this case; γ will eventually eliminate the disease if it persists.

5.5 Discussion and Conclusion

Infectious diseases are pivotal in shaping coral community dynamics, notably by significantly reducing live coral coverage and density [38, 105, 106, 142, 169, 233]. Transmission in coral reefs occurs through two primary pathways: direct and indirect [111, 112]. While the former is less common due to corals' limited mobility, the latter, particularly via pathogens, is more prevalent and effective. The indirect transmission, facilitated especially by various reef fish, amplifies disease spread [116, 117]. However, a critical knowledge gap remains regarding the intricate interplay between biotic interactions and disease dy-

namics. This study addresses this gap by employing a mathematical modelling approach to provide a deeper understanding of these complex processes.

Our study encapsulates that the coral reef ecosystem exhibits dynamic responses to infections triggered by fish predation. Coral faces minimal risk at both low and high levels of grazing. At low grazing levels, the absence of disease is clear, promoting coral health. However, the reduced predation pressure on macroalgae allows it to outcompete coral. Previous studies [123, 124, 126, 129, 156] have consistently demonstrated that low grazing levels facilitate macroalgal dominance on coral reefs. These studies emphasize the concept of hysteresis, where the transition from coral- to algae-dominated states is irreversible beyond a critical grazing threshold, resulting in a significant loss of coral reef resilience. Our study demonstrates that, under these conditions, even minor disease outbreaks can trigger a catastrophic shift from a healthy coral ecosystem to a coral-extinction state, resulting in a clear bistability between a disease-free and a coral-extinction.

For a sufficiently high level of fish predation, it becomes evident (from subsection 5.4.4.3) that infection takes hold and continues to persist, and the bistability between the endemic state and the disease-free state is observed. It is also evident in literature, that the Great Barrier Reef is the epicentre of coral disease [234] and is also known for its high fish assemblages [235], which aligns with our findings. However, the minimum strength of infection required for disease establishment increases significantly, as well as the risk of tipping to the coral extinction state decreases. These findings align with previous research [123, 124, 126] indicating enhanced coral persistence under higher grazing pressure. The resilience of the endemic state under high grazing rates can be ascribed to the substantial predation pressure exerted on macroalgae, curtailing their competitive edge over coral. Additionally, reducing macroalgae can lower pathogen levels by minimizing shedding, indirectly benefiting coral health by decreasing disease prevalence. A high abundance of corallivorous fishes, particularly chaetodontids, is associated with increased coral disease prevalence in the central Philippines and the Great Barrier Reef (GBR) due to their feeding on damaged corals, which can facilitate disease spread [236]. The farming behaviour of Stegastes reef fishes increases coral disease prevalence by promoting environments rich in coral pathogens [237]. Interestingly, the medium level of the grazing rate leads to various non-trivial dynamical outcomes (see subsection 5.4.4.2, Fig. 5.2, 5.3), especially the tristability between healthy, endemic and coral extinction states, a phenomenon previously unexplored in the context of coral reef dynamics. In this case, the sudden emergence of disease and the abrupt extinction of coral are both evident. Consequently, the fate of the coral reef becomes highly sensitive to the initial coral population size.

We observed that the initiation and eradication of disease occur abruptly with changing grazing rates and disease conditions. Even a slight change in the associated demographic and epidemic parameters or the initial values of interacting populations can induce regime shifts—from a disease-free, healthy coral state to an endemic state with high prevalence

or vice versa. Disease virulence profoundly impacts coral reef fate. For highly virulent diseases, corals face extinction risk from disease-related mortality when grazing rates are low, and macroalgae dominates. Highly virulent diseases can indirectly benefit coral populations by rapidly removing infected corals, thereby slowing disease transmission. This occurs through reduced contact between healthy and infected corals, and decreased pathogen load due to the less availability of nutrients from decaying infected individuals. This phenomenon, where high virulence drives disease eradication, has been previously documented in several eco-epidemic models [228, 238, 239]. As a result, corals can survive, with or without disease burden, when grazing rates are high. While low-virulence diseases gradually increased with rising fish predation, high-virulence diseases led to sudden outbreaks followed by sharp declines, creating a non-linear relationship between predation and infection prevalence. In both cases, a decrease in the grazing rate in the infected population can indicate abrupt disease eradication, offering a glimmer of hope for coral reef resilience.

More specifically, the transmission-virulence ratio, above which high prevalence occurs abruptly, grows linearly with grazing rate (see Fig. 5.9). This suggests that overharvesting-induced fish population decline can be harmful in such scenarios. Despite accelerating disease outbreaks, a plentiful fish population is crucial for coral reef ecosystem health. These findings emphasize the need for effective fishery management strategies to ensure healthy fish populations, fostering a critical buffer against disease outbreaks and promoting the health of coral reef ecosystems.

Our study does come with a set of limitations. We assumed a time-independent fish stock level, neglecting their system variability. This simplification overlooks potential complexities. Future research efforts should incorporate fish populations as a state variable within the model. This would allow us to examine how interactions between fish populations and other biotic and abiotic factors influence the dynamics of coral epidemics. Additionally, investigating the impact of environmental noise, such as fluctuations in temperature or nutrient levels, on the transitions between healthy and diseased coral states would be valuable. Understanding the role of such stochasticity could provide further insights into coral reef resilience in the face of changing environmental conditions.

6

Conclusions and Future Directions

6.1 Conclusions and Future Directions

6.1.1 Conclusions

Mathematical models play a crucial role in predicting disease spread within coral ecosystems by simulating pathogen transmission. These models consider both biotic factors, such as host-pathogen dynamics and fish behavior, and abiotic factors, including temperature and pollution. By analyzing these complex interactions, they help identify key drivers of disease and their role in triggering outbreaks. Additionally, these models provide estimates of the long-term impacts of climate conditions and human interventions on coral health. They also serve as tools for testing management strategies to control disease outbreaks, allowing for effective conservation efforts without directly impacting real coral reefs.

Our thesis focuses on developing a mathematical model to examine the dynamics of the coral reef ecosystem, with a particular emphasis on disease progression and its management. The modeling approach adopted in this research offers valuable insights into the interaction between biotic and abiotic factors and their influence on coral health. Specifically, the model evaluates the relationship between infected and susceptible corals, incorporating disease recovery mechanisms. These mechanisms highlight the ability of corals to regenerate tissue and engage in microbial competition to recover from infections. The recovery rate is identified as a crucial determinant in sustaining coral populations, with higher recovery rates shifting reef ecosystems toward a healthier state.

Stability and bifurcation analyses reveal that the system exhibits multiple equilibrium states, including coral-free and macroalgae-dominated conditions. High grazing rates by herbivorous fish help prevent macroalgae overgrowth, thereby supporting coral health. The model demonstrates bi-stability and tri-stability, indicating that reefs can exist in multiple stable states under varying environmental conditions. A Hopf bifurcation occurs when the grazing rate exceeds a critical threshold, resulting in oscillatory fluctuations in coral populations.

This study further investigates the effects of incubation time delay on coral reefs impacted by disease. A short delay maintains system stability, whereas exceeding a critical delay threshold disrupts equilibrium, leading to periodic oscillations in coral populations. Stability analysis identifies two key equilibrium states: disease-free and endemic. The model confirms that higher grazing rates reduce macroalgal dominance and contribute to coral recovery. However, disease transmission significantly affects coral stability, with elevated transmission rates pushing the system toward coral decline. Numerical simulations indicate that increasing disease transmission reduces the population of healthy corals, while a higher conversion rate of infected corals to healthy ones helps mitigate disease spread. Prolonged incubation delays exacerbate the destabilizing effects on coral health.

Additionally, this study explores the role of zooplankton in mediating disease transmission within coral reefs, with a specific focus on White Band Disease (WBD). The disease spreads both through direct contact between corals and indirectly via zooplankton consumption and free-living pathogens. The findings indicate that zooplankton-mediated transmission is particularly harmful to coral populations. The model identifies multiple equilibrium states, including coral-free and coexisting stable conditions. A Hopf bifurcation occurs when WBD transmission rates surpass a critical threshold, leading to oscillatory disease outbreaks. Mutualistic interactions between phytoplankton and corals play a crucial role in coral recovery, with zooxanthellae contributing to coral resilience and survival. Simulation results suggest that controlling zooplankton populations can help mitigate disease outbreaks, and enhancing phytoplankton mutualism may serve as an effective conservation strategy.

Lastly, this study examines the intricate relationship between fish predation and coral disease dynamics. While fish feeding behavior can facilitate the spread of infectious pathogens, it also helps control macroalgal overgrowth, which benefits coral health. The findings suggest that both very low and very high fish predation rates provide protection for corals, whereas moderate predation levels increase the risk of disease outbreaks. Coral ecosystems experience tipping points, where transitions from disease-dominated to healthier states occur as fish predation increases. The model highlights bistability and tristability in reef states, demonstrating that coral populations persist under specific conditions. The transmission-to-virulence ratio scales linearly with fish predation rates, indicating that higher virulence can limit disease spread by reducing pathogen reservoirs. Conservation

efforts should focus on maintaining balanced fish populations, as excessive overfishing of herbivorous fish can increase coral disease prevalence by allowing macroalgae to dominate. Proper fishery management can help prevent abrupt coral declines and promote long-term reef sustainability.

Overall, this research provides valuable insights into coral reef resilience, emphasizing the importance of adaptive conservation strategies to mitigate disease outbreaks and enhance coral recovery. Effective management of disease transmission, incubation delays, fish predation, and zooplankton populations is essential for preserving reef ecosystems. The findings underscore the need to incorporate biotic interactions into coral disease ecology, offering critical guidance for reef conservation and management strategies.

6.1.2 Future Research Directions

The scope of future research on coral disease modeling extends to several promising directions:

i. **Stochastic Modeling**: Introducing stochasticity into disease transmission models can provide a more comprehensive understanding of how random environmental fluctuations impact reef health.

ii. **Fractional-Order Models**: Exploring fractional differential equations can offer deeper insights into long-memory effects in disease progression and coral-algae competition.

iii. **Impulsive Control Strategies**: Investigating the impact of periodic interventions, such as controlled coral transplantation or antibiotic treatments, on disease mitigation.

iv. **Coupling Hydrodynamic Models**: Integrating disease models with oceanographic circulation patterns to assess pathogen dispersal across reef systems.

v. **Multi-Species Interactions**: Expanding the model to incorporate competition between coral species, pathogen evolution, and potential microbial interventions.

vi. **Optimal Control Approaches**: Evaluating cost-effective disease control strategies through mathematical optimization techniques.

By addressing these areas, future research can further refine our understanding of coral disease dynamics and inform effective conservation strategies. This interdisciplinary approach—combining mathematical modeling, ecological insights, and field data—will be crucial for safeguarding coral reef ecosystems in the face of global environmental challenges.

References

[1] Marjorie L Reaka-Kudla et al. The global biodiversity of coral reefs: a comparison with rain forests. *Biodiversity II: Understanding and protecting our biological resources*, 2:551, 1997.

[2] Marjorie L Reaka-Kudla. Known and unknown biodiversity, risk of extinction and conservation strategy in the sea. In *Waters in peril*, pages 19–33. Springer, 2001.

[3] Johanna Johnson and Paul Marshall. Climate change and the great barrier reef. 2007.

[4] Yann Laurans, Nicolas Pascal, Thomas Binet, Luke Brander, Eric Clua, Gilbert David, Dominique Rojat, and Andrew Seidl. Economic valuation of ecosystem services from coral reefs in the south pacific: Taking stock of recent experience. *Journal of environmental management*, 116:135–144, 2013.

[5] James PG Spurgeon. The economic valuation of coral reefs. *Marine pollution bulletin*, 24(11):529–536, 1992.

[6] Luke Brander and Pieter van Beukering. The total economic value of us coral reefs: a review of the literature. 2013.

[7] Nancy Knowlton, Russell E Brainard, Rebecca Fisher, Megan Moews, Laetitia Plaisance, M Julian Caley, et al. Coral reef biodiversity. *Life in the world's oceans: diversity distribution and abundance*, pages 65–74, 2010.

[8] Sergio Rossi, Lorenzo Bramanti, Andrea Gori, and Covadonga Orejas. An overview of the animal forests of the world. *Marine animal forests*, pages 1–26, 2017.

[9] Eva Ramirez-Llodra, Angelika Brandt, Roberto Danovaro, Ben De Mol, Elva Escobar, Christopher R German, Lisa A Levin, Pedro Martinez Arbizu, Lenaick Menot, Pal Buhl-Mortensen, et al. Deep, diverse and definitely different: unique attributes of the world's largest ecosystem. *Biogeosciences*, 7(9):2851–2899, 2010.

[10] Paul VR Snelgrove. Getting to the bottom of marine biodiversity: sedimentary habitats: ocean bottoms are the most widespread habitat on earth and support high biodiversity and key ecosystem services. *BioScience*, 49(2):129–138, 1999.

[11] Robert Mccredie May. Biological diversity: differences between land and sea. *Philosophical Transactions of the Royal Society of London. Series B: Biological Sciences*, 343(1303):105–111, 1994.

[12] Peter W Glynn and Ian C Enochs. Invertebrates and their roles in coral reef ecosystems. *Coral reefs: an ecosystem in transition*, pages 273–325, 2010.

[13] R Gibson, R Atkinson, J Gordon, I Smith, and D Hughes. Coral-associated invertebrates: diversity, ecological importance and vulnerability to disturbance. *Oceanography and Marine Biology; Taylor & Francis: Oxford, UK*, 49:43–104, 2011.

[14] Mark Spalding, Corinna Ravilious, and Edmund Peter Green. *World atlas of coral reefs*. Univ of California Press, 2001.

[15] ISJM Nagelkerken, SJM Blaber, Steven Bouillon, P Green, M Haywood, LG Kirton, J-O Meynecke, J Pawlik, HM Penrose, A Sasekumar, et al. The habitat function of mangroves for terrestrial and marine fauna: a review. *Aquatic botany*, 89(2):155–185, 2008.

[16] Oliver E Williamson. Outsourcing: Transaction cost economics and supply chain management. *Journal of supply chain management*, 44(2):5–16, 2008.

[17] Fredrik Moberg and Carl Folke. Ecological goods and services of coral reef ecosystems. *Ecological economics*, 29(2):215–233, 1999.

[18] OVE HOEGH-GULDBERG. Coral reefs in a century of rapid environmental change. *Symbiosis*, 2004.

[19] Dirk Bryant, Lauretta Burke, John McMnus, and Mark Spalding. *Reefs at risk: a map-based indicator of threats to the world's coral reefs*. Washington, DC: World Resources Institute (WRI), International Center for . . . , 1998.

[20] Bernard Salvat. Coral reefs—a challenging ecosystem for human societies. *Global environmental change*, 2(1):12–18, 1992.

[21] Edwin A Hernández-Delgado. The emerging threats of climate change on tropical coastal ecosystem services, public health, local economies and livelihood sustainability of small islands: Cumulative impacts and synergies. *Marine Pollution Bulletin*, 101(1):5–28, 2015.

[22] C Reid Nichols, Julie Zinnert, and Donald R Young. Degradation of coastal ecosystems: causes, impacts and mitigation efforts. *Tomorrow's Coasts: Complex and Impermanent*, pages 119–136, 2019.

[23] Edison D Macusi, Robert E Katikiro, KA Deepananda, Leah A Jimenez, Alen R Conte, and Nur Fadli. Human induced degradation of coastal resources in asia pacific and implications on management and food security. *Journal of Nature Studies*, 9(10):13–28, 2011.

[24] Nicholas AJ Graham, Tracy D Ainsworth, Andrew H Baird, Natalie C Ban, Line K Bay, Joshua E Cinner, Debora M De Freitas, Guillermo Diaz-Pulido, Maria Dornelas, Simon R Dunn, et al. From microbes to people: tractable benefits of no-take areas for coral reefs. *Oceanography and Marine Biology-an Annual Review*, 49:105, 2011.

[25] Andreas J Andersson, Alexander A Venn, Linwood Pendleton, Angelique Brathwaite, Emma F Camp, Sarah Cooley, Dwight Gledhill, Marguerite Koch, Samir Maliki, and Carrie Manfrino. Ecological and socioeconomic strategies to sustain caribbean coral reefs in a high-co2 world. *Regional Studies in Marine Science*, 29:100677, 2019.

[26] Bhavesh Choudhary, Venerability Dhar, and Anil S Pawase. Blue carbon and the role of mangroves in carbon sequestration: Its mechanisms, estimation, human impacts and conservation strategies for economic incentives. *Journal of Sea Research*, 199:102504, 2024.

[27] EA Titlyanov and TV Titlyanova. Symbiotic relationships between microalgal zooxanthellae and reef-building coral polyps in the process of autotrophic and heterotrophic nutrition. *Russian Journal of Marine Biology*, 46:307–318, 2020.

[28] Noga Stambler. Zooxanthellae: the yellow symbionts inside animals. *Coral Reefs: an ecosystem in transition*, pages 87–106, 2011.

[29] Walter M Goldberg. Coral food, feeding, nutrition, and secretion: a review. *Marine organisms as model systems in biology and medicine*, pages 377–421, 2018.

[30] Gisèle Muller-Parker, Christopher F D'elia, and Clayton B Cook. Interactions between corals and their symbiotic algae. *Coral reefs in the Anthropocene*, pages 99–116, 2015.

[31] Mahdokht Jouiaei, Angel A Yanagihara, Bruno Madio, Timo J Nevalainen, Paul F Alewood, and Bryan G Fry. Ancient venom systems: a review on cnidaria toxins. *Toxins*, 7(6):2251–2271, 2015.

[32] Ramasamy Santhanam. *Biology and ecology of venomous marine Cnidarians*. Springer, 2020.

[33] Stephen D Cairns, Lisa A Gerhswin, Fred Brook, Philip R Pugh, Elliott W Dawson, Oscar Ocaña V, Will Vervoort, Gary Williams, Jeanette Watson, Dennis M Opresko, et al. Phylum cnidaria; corals, medusae, hydroids, myxozoa. *New Zealand Inventory of Biodiversity. Volume 1. Kingdom Animalia: Radiata, Lophotrochozoa, Deuterostomia*, 2009.

[34] Nancy Knowlton. The future of coral reefs. *Proceedings of the National Academy of Sciences*, 98(10):5419–5425, 2001.

[35] John EN Veron, Ove Hoegh-Guldberg, Timothy Michael Lenton, JANICE M Lough, David O Obura, PAUL Pearce-Kelly, Charles RC Sheppard, Marianne Spalding, Mary Gillian Stafford-Smith, and Alex David Rogers. The coral reef crisis: The critical importance of< 350 ppm co2. *Marine pollution bulletin*, 58(10):1428–1436, 2009.

[36] Makoto Omori. Coral reefs are dying, we can only prevent it if we act now. *Journal of Black Sea/Mediterranean Environment*, 18(1):1–10, 2012.

[37] Ross J Jones, Jocelyn Bowyer, Ove Hoegh-Guldberg, and Linda L Blackall. Dynamics of a temperature-related coral disease outbreak. *Marine Ecology Progress Series*, 281:63–77, 2004.

[38] Raymond L Hayes and Nora I Goreau. The significance of emerging diseases in the tropical coral reef ecosystem. *Rev. Biol. Trop*, 46(Supl 5):173–185, 1998.

[39] Deborah L Santavy and Esther C Peters. Microbial pests: coral disease in the western atlantic. In *Proc 8th Int Coral Reef Symp*, volume 1, pages 607–612, 1997.

[40] William F Precht, Brooke E Gintert, Martha L Robbart, Ryan Fura, and Robert Van Woesik. Unprecedented disease-related coral mortality in southeastern florida. *Scientific reports*, 6(1):31374, 2016.

[41] Mebrahtu Ateweberhan, David A Feary, Shashank Keshavmurthy, Allen Chen, Michael H Schleyer, and Charles RC Sheppard. Climate change impacts on coral reefs: synergies with local effects, possibilities for acclimation, and management implications. *Marine pollution bulletin*, 74(2):526–539, 2013.

[42] Brian D Keller, Daniel F Gleason, Elizabeth McLeod, Christa M Woodley, Satie Airamé, Billy D Causey, Alan M Friedlander, Rikki Grober-Dunsmore, Johanna E Johnson, Steven L Miller, et al. Climate change, coral reef ecosystems, and management options for marine protected areas. *Environmental management*, 44:1069–1088, 2009.

[43] Tasneem Abbasi and SA Abbasi. Ocean acidification: The newest threat to the global environment. *Critical Reviews in Environmental Science and Technology*, 41(18):1601–1663, 2011.

[44] Christopher E Cornwall, Steeve Comeau, Niklas A Kornder, Chris T Perry, Ruben van Hooidonk, Thomas M DeCarlo, Morgan S Pratchett, Kristen D Anderson, Nicola Browne, Robert Carpenter, et al. Global declines in coral reef calcium carbonate production under ocean acidification and warming. *Proceedings of the National Academy of Sciences*, 118(21):e2015265118, 2021.

[45] Paramita Roy, Subodh Chandra Pal, Rabin Chakrabortty, Indrajit Chowdhuri, Asish Saha, and Manisa Shit. Effects of climate change and sea-level rise on coastal habitat: Vulnerability assessment, adaptation strategies and policy recommendations. *Journal of Environmental Management*, 330:117187, 2023.

[46] Ove Hoegh-Guldberg. Climate change, coral bleaching and the future of the world's coral reefs. *Marine and freshwater research*, 50(8):839–866, 1999.

[47] Peter W Glynn. Coral reef bleaching: facts, hypotheses and implications. *Global change biology*, 2(6):495–509, 1996.

[48] Jamie K Oliver, Ray Berkelmans, and C Mark Eakin. Coral bleaching in space and time. *Coral bleaching: patterns, processes, causes and consequences*, pages 27–49, 2018.

[49] BE Brown. Coral bleaching: causes and consequences. *Coral reefs*, 16:S129–S138, 1997.

[50] Haradhan Mohajan. Greenhouse gas emissions increase global warming. 2011.

[51] H Kumar Mohajan. Greenhouse gas emissions, global warming and climate change. In *Proceedings of the 15th Chittagong Conference on Mathematical Physics, Jamal Nazrul Islam Research Centre for Mathematical and Physical Sciences (JNIRCMPS), Chittagong, Bangladesh*, volume 16, 2017.

[52] Alexey Mikhaylov, Nikita Moiseev, Kirill Aleshin, and Thomas Burkhardt. Global climate change and greenhouse effect. *Entrepreneurship and Sustainability Issues*, 7(4):2897, 2020.

[53] Melissa S Roth. The engine of the reef: photobiology of the coral–algal symbiosis. *Frontiers in microbiology*, 5:422, 2014.

[54] Merinda C Nash. *Assessing ocean acidification impacts on the reef building properties of crustose coralline algae*. PhD thesis, The Australian National University (Australia), 2015.

[55] Kenneth RN Anthony. Coral reefs under climate change and ocean acidification: challenges and opportunities for management and policy. *Annual Review of Environment and Resources*, 41(1):59–81, 2016.

[56] Bradley D Eyre, Andreas J Andersson, and Tyler Cyronak. Benthic coral reef calcium carbonate dissolution in an acidifying ocean. *Nature climate change*, 4(11):969–976, 2014.

[57] Bernhard Riegl, Andy Bruckner, Steve L Coles, Philip Renaud, and Richard E Dodge. Coral reefs: threats and conservation in an era of global change. *Annals of the New York Academy of Sciences*, 1162(1):136–186, 2009.

[58] Hongwei Zhao, Meile Yuan, Maryna Strokal, Henry C Wu, Xianhua Liu, AlberTinka Murk, Carolien Kroeze, and Ronald Osinga. Impacts of nitrogen pollution on corals in the context of global climate change and potential strategies to conserve coral reefs. *Science of the Total Environment*, 774:145017, 2021.

[59] ZVY Dubinsky and Noga Stambler. Marine pollution and coral reefs. *Global change biology*, 2(6):511–526, 1996.

[60] Jiaxin Lan, Pengfei Liu, Xi Hu, and Shanshan Zhu. Harmful algal blooms in eutrophic marine environments: causes, monitoring, and treatment. *Water*, 16(17):2525, 2024.

[61] Michelle Devlin and Jon Brodie. Nutrients and eutrophication. In *Marine pollution–monitoring, management and mitigation*, pages 75–100. Springer, 2023.

[62] Katharina E Fabricius. Factors determining the resilience of coral reefs to eutrophication: a review and conceptual model. *Coral reefs: an ecosystem in transition*, pages 493–505, 2011.

[63] PRF Bell. Eutrophication and coral reefs—some examples in the great barrier reef lagoon. *Water Research*, 26(5):553–568, 1992.

[64] Donald M Anderson, Joann M Burkholder, William P Cochlan, Patricia M Glibert, Christopher J Gobler, Cynthia A Heil, Raphael M Kudela, Michael L Parsons, JE Jack Rensel, David W Townsend, et al. Harmful algal blooms and eutrophication: examining linkages from selected coastal regions of the united states. *Harmful algae*, 8(1):39–53, 2008.

[65] Michael King. *Fisheries biology, assessment and management*. John Wiley & Sons, 2013.

[66] Miguel Fortes. The effects of siltation on tropical coastal ecosystems. In *Oceanographic processes of coral reefs*, pages 113–132. CRC Press, 2000.

[67] Chris Perry. Tropical coastal environments: coral reefs and mangroves. *Environmental sedimentology*, pages 302–350, 2007.

[68] Stelios Katsanevakis. Marine debris, a growing problem: Sources, distribution, composition, and impacts. *Marine Pollution: New Research. Nova Science Publishers, New York*, pages 53–100, 2008.

[69] Suman Nama, Ashna Shanmughan, Binaya Bhusan Nayak, Shashi Bhushan, and Karankumar Ramteke. Impacts of marine debris on coral reef ecosystem: A review for conservation and ecological monitoring of the coral reef ecosystem. *Marine Pollution Bulletin*, 189:114755, 2023.

[70] Romana Akhtar, Mohd Yaseen Sirwal, Khalid Hussain, Mudasir A Dar, Mohd Shahnawaz, and Zhu Daochen. Impact of plastic waste on the coral reefs: an overview. *Impact of Plastic Waste on the Marine Biota*, pages 239–256, 2022.

[71] Sarah C Gall and Richard C Thompson. The impact of debris on marine life. *Marine pollution bulletin*, 92(1-2):170–179, 2015.

[72] Prabhakar R Pawar, Sanket S Shirgaonkar, and Rahul B Patil. Plastic marine debris: Sources, distribution and impacts on coastal and ocean biodiversity. *PENCIL Publication of Biological Sciences*, 3(1):40–54, 2016.

[73] David R Bellwood, Morgan S Pratchett, Tiffany H Morrison, Georgina G Gurney, Terry P Hughes, Jorge G Álvarez-Romero, Jon C Day, Ruby Grantham, Alana Grech, Andrew S Hoey, et al. Coral reef conservation in the anthropocene: Confronting spatial mismatches and prioritizing functions. *Biological conservation*, 236:604–615, 2019.

[74] Miguel Carneiro and Rogélia Martins. Destructive fishing practices and their impact on the marine ecosystem. In *Life Below Water*, pages 295–304. Springer, 2022.

[75] OTEKENARI DAVID Elisha and MACLEAN JEBBIN Felix. Destruction of coastal ecosystems and the vicious cycle of poverty in niger delta region. *Journal of Global Agriculture and Ecology*, 11(2):7–24, 2021.

[76] Mark A Hixon. Reef fishes, seaweeds, and corals: a complex triangle. *Coral reefs in the Anthropocene*, pages 195–215, 2015.

[77] Peggy Fong and Valerie J Paul. Coral reef algae. *Coral reefs: an ecosystem in transition*, pages 241–272, 2011.

[78] John W McManus and Johanna F Polsenberg. Coral–algal phase shifts on coral reefs: ecological and environmental aspects. *Progress in Oceanography*, 60(2-4):263–279, 2004.

[79] Mallory M Rice, Leïla Ezzat, and Deron E Burkepile. Corallivory in the anthropocene: interactive effects of anthropogenic stressors and corallivory on coral reefs. *Frontiers in Marine Science*, 5:525, 2019.

[80] Ransom A Myers and C Andrea Ottensmeyer. Extinction risk in marine species. *Marine conservation biology: the science of maintaining the sea's biodiversity. Island Press, Washington, DC*, pages 58–79, 2005.

[81] Alan T White and Catherine A Courtney. Policy instruments for coral reef management and their effectiveness. *Economic valuation and policy priorities for sustainable management of coral reefs*, 141, 2004.

[82] James Evans Maragos. Impact of coastal construction on coral reefs in the us-affiliated pacific islands. *Coastal Management*, 21(4):235–269, 1993.

[83] Muhammad Salman Afzal, Furqan Tahir, and Sami G Al-Ghamdi. Recommendations and strategies to mitigate environmental implications of artificial island developments in the gulf. *Sustainability*, 14(9):5027, 2022.

[84] Paul LA Erftemeijer, Bernhard Riegl, Bert W Hoeksema, and Peter A Todd. Environmental impacts of dredging and other sediment disturbances on corals: a review. *Marine pollution bulletin*, 64(9):1737–1765, 2012.

[85] Hussein A El-Naggar. Human impacts on coral reef ecosystem. In *Natural resources management and biological sciences*. IntechOpen, 2020.

[86] John R Clark. *Coastal seas: the conservation challenge*. John Wiley & Sons, 2009.

[87] Nina Lincoff. Looking to hybrid species for the future of coral reefs. *Calif. L. Rev.*, 108:1597, 2020.

[88] Luis Malpica-Cruz, Stuart Fulton, Anastasia Quintana, Jose Alberto Zepeda-Domínguez, Blanca Quiroga-García, Lizbeth Tamayo, Jose Ángel Canto Noh, and Isabelle M Côté. Trying to collapse a population for conservation: commercial trade of a marine invasive species by artisanal fishers. *Reviews in Fish Biology and Fisheries*, 31(3):667–683, 2021.

[89] David W Souter and Olof Linden. The health and future of coral reef systems. *Ocean & Coastal Management*, 43(8-9):657–688, 2000.

[90] Magnus Nyström. Redundancy and response diversity of functional groups: implications for the resilience of coral reefs. *AMBIO: A Journal of the Human Environment*, 35(1):30–35, 2006.

[91] DA Westcott, CS Fletcher, Russ Babcock, and E Plaganyi-Lloyd. A strategy to link research and management of crown-of-thorns starfish on the great barrier reef: An integrated pest management approach. *Report to the National Environmental Science Programme*, 77, 2016.

[92] Alistair J Cheal, M Aaron MacNeil, Michael J Emslie, and Hugh Sweatman. The threat to coral reefs from more intense cyclones under climate change. *Global change biology*, 23(4):1511–1524, 2017.

[93] Bernhard Riegl. Extreme climatic events and coral reefs: how much short-term threat from global change? In *Geological approaches to coral reef ecology*, pages 315–341. Springer, 2007.

[94] Mireille L Harmelin-Vivien. The effects of storms and cyclones on coral reefs: a review. *Journal of Coastal Research*, pages 211–231, 1994.

[95] Drew Harvell, Eric Jordán-Dahlgren, Susan Merkel, Eugene Rosenberg, Laurie Raymundo, Garriet Smith, Ernesto Weil, and Bette Willis. Coral disease, environmental drivers, and the balance between coral and microbial associates. *Oceanography*, 20:172–195, 2007.

[96] Timothy R McClanahan. The near future of coral reefs. *Environmental conservation*, 29(4):460–483, 2002.

[97] Ernesto Weil. Coral reef diseases in the wider caribbean. In *Coral health and disease*, pages 35–68. Springer, 2004.

[98] Shinichi Sunagawa, Todd Z DeSantis, Yvette M Piceno, Eoin L Brodie, Michael K DeSalvo, Christian R Voolstra, Ernesto Weil, Gary L Andersen, and Monica Medina. Bacterial diversity and white plague disease-associated community changes in the caribbean coral montastraea faveolata. *The ISME journal*, 3(5):512–521, 2009.

[99] Juan A Sánchez, Santiago Herrera, Raúl Navas-Camacho, Alberto Rodríguez-Ramírez, Pilar Herron, Valeria Pizarro, Alison R Acosta, Paula A Castillo, Phanor Montoya, and Carlos Orozco. White plague-like coral disease in remote reefs of the western caribbean. *Revista de Biología Tropical*, 58:145–154, 2010.

[100] Arnfried Antonius. The 'band'diseases in coral reefs. In *Proc 4th int coral reef symp*, volume 2, pages 7–14, 1981.

[101] William B Gladfelter. White-band disease in acropora palmata: implications for the structure and growth of shallow reefs. *Bulletin of marine Science*, 32(2):639–643, 1982.

[102] Esther C Peters. Diseases of other invertebrate phyla: Porifera, cnidaria, ctenophora, annelida, echinodermata. In *Pathobiology of marine and estuarine organisms*, pages 393–449. CRC press, 2021.

[103] Klaus Rutzler, Deborah L Santavy, and Arnfried Antonius. The black band disease of atlantic reef corals. iii. distribution, ecology, and development. *Marine Ecology*, 4(4):329–358, 1983.

[104] Arnfried Antonius. Coral diseases in the indo-pacific: A first record. *Marine Ecology*, 6(3):197–218, 1985.

[105] Peter J Edmunds. Extent and effect of black band disease on a caribbean reef. *Coral Reefs*, 10:161–165, 1991.

[106] KG Kuta and LL Richardson. Abundance and distribution of black band disease on coral reefs in the northern florida keys. *Coral reefs*, 15:219–223, 1996.

[107] Susanne H Sokolow, Patrick Foley, Janet E Foley, Alan Hastings, and Laurie L Richardson. Editor's choice: Disease dynamics in marine metapopulations: modelling infectious diseases on coral reefs. *Journal of Applied Ecology*, 46(3):621–631, 2009.

[108] Richard G Carlton and Laurie L Richardson. Oxygen and sulfide dynamics in a horizontally migrating cyanobacterial mat: black band disease of corals. *FEMS Microbiology Ecology*, 18(2):155–162, 1995.

[109] LL Richardson, KG Kuta, S Schnell, and RG Carlton. Ecology of the black band disease microbial consortium. In *Proc 8th Int Coral Reef Symp*, volume 1, pages 597–600, 1997.

[110] Buddhadev Ranjit, Santosh Biswas, Joydeb Bhattacharyya, and Joydev Chattopadhyay. Dynamics of zooplankton-mediated disease outbreak in coral-reef. *Differential Equations and Dynamical Systems*, pages 1–29, 2023.

[111] James W Porter, Phillip Dustan, Walter C Jaap, Kathryn L Patterson, Vladimir Kosmynin, Ouida W Meier, Matthew E Patterson, and Mel Parsons. Patterns of spread of coral disease in the florida keys. *The ecology and etiology of newly emerging marine diseases*, pages 1–24, 2001.

[112] Amanda Shore and Jamie M Caldwell. Modes of coral disease transmission: how do diseases spread between individuals and among populations? *Marine Biology*, 166(4):45, 2019.

[113] Andrew W Bruckner, Robin J Bruckner, and Ernest H Williams Jr. Spread of a black-band disease epizootic through the coral reef system in st. ann's bay, jamaica. *Bulletin of Marine Science*, 61(3):919–928, 1997.

[114] Iliana B Baums, Claire B Paris, and Laurent M Chérubin. A bio-oceanographic filter to larval dispersal in a reef-building coral. *Limnology and Oceanography*, 51(5):1969–1981, 2006.

[115] Meir Sussman, Yossi Loya, Maoz Fine, and Eugene Rosenberg. The marine fireworm hermodice carunculata is a winter reservoir and spring-summer vector for the coral-bleaching pathogen vibrio shiloi. *Environmental Microbiology*, 5(4):250–255, 2003.

[116] SA Gignoux-Wolfsohn, Christopher J Marks, and Steven V Vollmer. White band disease transmission in the threatened coral, acropora cervicornis. *Scientific reports*, 2(1):804, 2012.

[117] Randi D Rotjan and Sara M Lewis. Impact of coral predators on tropical reefs. *Marine ecology progress series*, 367:73–91, 2008.

[118] Peter L Antonelli. Nonlinear allometric growth. i. perfectly cooperative systems. *Mathematical Modelling*, 4(4):367–372, 1983.

[119] Greta S Aeby and Deborah L Santavy. Factors affecting susceptibility of the coral montastraea faveolata to black-band disease. *Marine Ecology Progress Series*, 318:103–110, 2006.

[120] Julie C Blackwood and Alan Hastings. The effect of time delays on caribbean coral–algal interactions. *Journal of Theoretical Biology*, 273(1):37–43, 2011.

[121] Aaron Gonzales, Darryl Dela Cruz, and Siwen Shao. A mathematical model of coral reef response to predator-prey interactions, human control on crown of thorns starfish, and rises in temperature. 2022.

[122] Joydeb Bhattacharyya and Samares Pal. Microbial disease in coral reefs: An ecosystem in transition. *Discrete & Continuous Dynamical Systems-Series B*, 21(2), 2016.

[123] Peter J Mumby, Alan Hastings, and Helen J Edwards. Thresholds and the resilience of caribbean coral reefs. *Nature*, 450(7166):98–101, 2007.

[124] Julie C Blackwood, Alan Hastings, and Peter J Mumby. The effect of fishing on hysteresis in caribbean coral reefs. *Theoretical ecology*, 5:105–114, 2012.

[125] Julie C Blackwood, Connie Okasaki, Andre Archer, Eliza W Matt, Elizabeth Sherman, and Kathryn Montovan. Modeling alternative stable states in caribbean coral reefs. *Natural Resource Modeling*, 31(1):e12157, 2018.

[126] Xiong Li, Hao Wang, Zheng Zhang, and Alan Hastings. Mathematical analysis of coral reef models. *Journal of Mathematical Analysis and Applications*, 416(1):352–373, 2014.

[127] Haniyeh Fattahpour, Hamid RZ Zangeneh, and Hao Wang. Dynamics of coral reef models in the presence of parrotfish. *Natural Resource Modeling*, 32(2):e12202, 2019.

[128] Aniel Nieves-González, Claudia P Ruiz-Diaz, Carlos Toledo-Hernández, and Juan S Ramírez-Lugo. A mathematical model of the interactions between acropora cervicornis and its environment. *Ecological Modelling*, 406:7–22, 2019.

[129] Dana T Cook, Russell J Schmitt, Sally J Holbrook, and Holly V Moeller. Modeling the effects of selectively fishing key functional groups of herbivores on coral resilience. *Ecosphere*, 15(1):e4749, 2024.

[130] Arnfried Antonius. New observations on coral destruction in reefs. In *Tenth meeting of the association of Island Marine Laboratories of the Caribbean*, volume 10. University of Puerto Rico Mayaguez, Puerto Rico, 1973.

[131] WB Gladfelter. Population structure of acropora palmata on the windward forereef, buck island national monument: seasonal and catastrophic changes 1988–1989. *Ecological studies of Buck Island Reef National Monument, St. Croix, US Virgin Islands: a quantitative assessment of selected components of the coral reef ecosystem and establishment of long term monitoring sites. Part*, 1, 1991.

[132] Andrew W Bruckner and Bernhard Riegl. Yellow-band diseases. *Diseases of coral*, pages 376–386, 2015.

[133] Anthony Kodzo-Grey Venyo. Aspergillosis of the genito-urinary tract and kidney including: The penis. *Scrotum, Testis, Urinary Bladder, Ureter, Renal Pelvis, Vulva, Vagina, Uterus, Fallopian Tubes, the Ovaries, as well as the Kidney: A Review and Update., International Journal of Clinical Case Studies*, 2(3), 2023.

[134] Dana E Williams and Margaret W Miller. Coral disease outbreak: pattern, prevalence and transmission in acropora cervicornis. *Marine Ecology Progress Series*, 301:119–128, 2005.

[135] T Moriarty, W Leggat, Megan J Huggett, and TD Ainsworth. Coral disease causes, consequences, and risk within coral restoration. *Trends in Microbiology*, 28(10):793–807, 2020.

[136] Rebecca H Certner, Amanda M Dwyer, Mark R Patterson, and Steven V Vollmer. Zooplankton as a potential vector for white band disease transmission in the endangered coral, acropora cervicornis. *PeerJ*, 5:e3502, 2017.

[137] Thierry Work and Carol Meteyer. To understand coral disease, look at coral cells. *EcoHealth*, 11(4):610–618, 2014.

[138] Maggy M Nugues. Impact of a coral disease outbreak on coral communities in st. lucia: What and how much has been lost? *Marine Ecology Progress Series*, 229:61–71, 2002.

[139] Rebecca Vega Thurber, Laura D Mydlarz, Marilyn Brandt, Drew Harvell, Ernesto Weil, Laurie Raymundo, Bette L Willis, Stan Langevin, Allison M Tracy, Raechel Littman, et al. Deciphering coral disease dynamics: integrating host, microbiome, and the changing environment. *Frontiers in Ecology and Evolution*, 8:575927, 2020.

[140] Thierry M Work, Laurie L Richardson, Taylor L Reynolds, and Bette L Willis. Biomedical and veterinary science can increase our understanding of coral disease. *Journal of Experimental Marine Biology and Ecology*, 362(2):63–70, 2008.

[141] F Joseph Pollock, Pamela J Morris, Bette L Willis, and David G Bourne. The urgent need for robust coral disease diagnostics. *PLoS pathogens*, 7(10):e1002183, 2011.

[142] Susanne Sokolow. Effects of a changing climate on the dynamics of coral infectious disease: a review of the evidence. *Diseases of aquatic organisms*, 87(1-2):5–18, 2009.

[143] Joydeb Bhattacharyya and Samares Pal. Macroalgal allelopathy in the emergence of coral diseases. *Discrete & Continuous Dynamical Systems-B*, 22(3):741–762, 2017.

[144] Joydeb Bhattacharyya and Samares Pal. Hysteresis in coral reefs under macroalgal toxicity and overfishing. *Journal of biological physics*, 41:151–172, 2015.

[145] Elizabeth M Fisher, John E Fauth, Pamela Hallock, and Cheryl M Woodley. Lesion regeneration rates in reef-building corals montastraea spp. as indicators of colony condition. *Marine Ecology Progress Series*, 339:61–71, 2007.

[146] Jeroen AJM van de Water, Tracy D Ainsworth, William Leggat, David G Bourne, Bette L Willis, and Madeleine JH Van Oppen. The coral immune response facilitates protection against microbes during tissue regeneration. *Molecular Ecology*, 24(13):3390–3404, 2015.

[147] Claudia P Ruiz-Diaz, Carlos Toledo-Hernandez, Alex E Mercado-Molina, María-Eglée Pérez, and Alberto M Sabat. The role of coral colony health state in the recovery of lesions. *PeerJ*, 4:e1531, 2016.

[148] Yvonne Sadovy de Mitcheson and Patrick L Colin. *Reef fish spawning aggregations: biology, research and management*, volume 35. Springer Science & Business Media, 2011.

[149] Julianna J Renzi, Elizabeth C Shaver, Deron E Burkepile, and Brian R Silliman. The role of predators in coral disease dynamics. *Coral Reefs*, 41(2):405–422, 2022.

[150] KJ Nicolet, KM Chong-Seng, MS Pratchett, BL Willis, and MO Hoogenboom. Predation scars may influence host susceptibility to pathogens: evaluating the role of corallivores as vectors of coral disease. *Scientific reports*, 8(1):5258, 2018.

[151] Lawrence Perko. *Differential equations and dynamical systems*, volume 7. Springer Science & Business Media, 2013.

[152] Jonathan Levanoni, Amalia Rosner, Ziva Lapidot, Guy Paz, and Baruch Rinkevich. Coral tissue regeneration and growth is associated with the presence of stem-like cells. *Journal of Marine Science and Engineering*, 12(2):343, 2024.

[153] Ray Berkelmans and Madeleine JH Van Oppen. The role of zooxanthellae in the thermal tolerance of corals: a 'nugget of hope'for coral reefs in an era of climate change. *Proceedings of the Royal Society B: Biological Sciences*, 273(1599):2305–2312, 2006.

[154] Emma Korein, Maria Vega-Rodriguez, and Tania Metz Estrella. Developing recommendations for coral disease management in puerto rico using key informant interviews and participatory mapping. *Ocean & Coastal Management*, 236:106488, 2023.

[155] Madeleine JH Van Oppen, James K Oliver, Hollie M Putnam, and Ruth D Gates. Building coral reef resilience through assisted evolution. *Proceedings of the National Academy of Sciences*, 112(8):2307–2313, 2015.

[156] Cheryl J Briggs, Thomas C Adam, Sally J Holbrook, and Russell J Schmitt. Macroalgae size refuge from herbivory promotes alternative stable states on coral reefs. *PLoS One*, 13(9):e0202273, 2018.

[157] Stephen Ippolito, Vincent Naudot, and Erik G Noonburg. Alternative stable states, coral reefs, and smooth dynamics with a kick. *Bulletin of mathematical biology*, 78:413–435, 2016.

[158] Manuel González-Rivero, Laith Yakob, and Peter J Mumby. The role of sponge competition on coral reef alternative steady states. *Ecological Modelling*, 222(11):1847–1853, 2011.

[159] Toby Elmhirst, Sean R Connolly, and Terry P Hughes. Connectivity, regime shifts and the resilience of coral reefs. *Coral Reefs*, 28:949–957, 2009.

[160] Diego Lirman. Competition between macroalgae and corals: effects of herbivore exclusion and increased algal biomass on coral survivorship and growth. *Coral reefs*, 19:392–399, 2001.

[161] SAMARES PAL and JOYDEB BHATTACHARYYA. Catastrophic transitions in coral reef biome under invasion and overfishing. In *Mathematical Biology and Biological Physics*, pages 118–140. World Scientific, 2017.

[162] Steve J Box and Peter J Mumby. Effect of macroalgal competition on growth and survival of juvenile caribbean corals. *Marine Ecology Progress Series*, 342:139–149, 2007.

[163] Yanni Xiao and Lansun Chen. Modeling and analysis of a predator–prey model with disease in the prey. *Mathematical biosciences*, 171(1):59–82, 2001.

[164] Joseph H Connell. Diversity in tropical rain forests and coral reefs: high diversity of trees and corals is maintained only in a nonequilibrium state. *Science*, 199(4335):1302–1310, 1978.

[165] Stephen V Smith and RW Buddemeier. Global change and coral reef ecosystems. *Annual Review of Ecology and Systematics*, pages 89–118, 1992.

[166] Robert H Richmond. Coral reefs: present problems and future concerns resulting from anthropogenic disturbance. *American Zoologist*, 33(6):524–536, 1993.

[167] Clive R Wilkinson. Global change and coral reefs: impacts on reefs, economies and human cultures. *Global Change Biology*, 2(6):547–558, 1996.

[168] Alexander T Wolf and Maggy M Nugues. Synergistic effects of algal overgrowth and corallivory on caribbean reef-building corals. *Ecology*, 94(8):1667–1674, 2013.

[169] Esther C Peters. Diseases of coral reef organisms. *Coral reefs in the Anthropocene*, pages 147–178, 2015.

[170] Joleah B Lamb, Bette L Willis, Evan A Fiorenza, Courtney S Couch, Robert Howard, Douglas N Rader, James D True, Lisa A Kelly, Awaludinnoer Ahmad, Jamaluddin Jompa, et al. Plastic waste associated with disease on coral reefs. *Science*, 359(6374):460–462, 2018.

[171] Austin Greene, Megan J Donahue, Jamie M Caldwell, Scott F Heron, Erick Geiger, and Laurie J Raymundo. Coral disease time series highlight size-dependent risk and other drivers of white syndrome in a multi-species model. *Frontiers in Marine Science*, 7:601469, 2020.

[172] Andrew J Cole, Morgan S Pratchett, and Geoffrey P Jones. Diversity and functional importance of coral-feeding fishes on tropical coral reefs. *Fish and Fisheries*, 9(3):286–307, 2008.

[173] Sefano M Katz, F Joseph Pollock, David G Bourne, and Bette L Willis. Crown-of-thorns starfish predation and physical injuries promote brown band disease on corals. *Coral Reefs*, 33:705–716, 2014.

[174] KJ Nicolet, Mia O Hoogenboom, NM Gardiner, MS Pratchett, and BL Willis. The corallivorous invertebrate drupella aids in transmission of brown band disease on the great barrier reef. *Coral Reefs*, 32:585–595, 2013.

[175] Steven V Vollmer and David I Kline. Natural disease resistance in threatened staghorn corals. *Plos one*, 3(11):e3718, 2008.

[176] Laurie L Richardson. Coral diseases: what is really known? *Trends in ecology & evolution*, 13(11):438–443, 1998.

[177] William Ogilvy Kermack and Anderson G McKendrick. A contribution to the mathematical theory of epidemics. *Proceedings of the royal society of london. Series A, Containing papers of a mathematical and physical character*, 115(772):700–721, 1927.

[178] Roy M Anderson and Robert M May. Infectious diseases and population cycles of forest insects. *Science*, 210(4470):658–661, 1980.

[179] Norman MacDonald and Norman MacDonald. Logistic growth of a single species. *Time Lags in Biological Models*, pages 50–67, 1978.

[180] Xia Yang, Lansun Chen, and Jufang Chen. Permanence and positive periodic solution for the single-species nonautonomous delay diffusive models. *Computers & mathematics with applications*, 32(4):109–116, 1996.

[181] Jean Dieudonné. *Foundations of modern analysis*. Read Books Ltd, 2011.

[182] HI Freedman and V Sree Hari Rao. The trade-off between mutual interference and time lags in predator-prey systems. *Bulletin of Mathematical Biology*, 45(6):991–1004, 1983.

[183] LH Erbe, HI Freedman, and V Sree Hari Rao. Three-species food-chain models with mutual interference and time delays. *Mathematical Biosciences*, 80(1):57–80, 1986.

[184] Brian D Hassard, Nicholas D Kazarinoff, and Yieh-Hei Wan. *Theory and applications of Hopf bifurcation*, volume 41. CUP Archive, 1981.

[185] Joydeb Bhattacharyya and Samares Pal. Stage-structured cannibalism with delay in maturation and harvesting of an adult predator. *Journal of Biological Physics*, 39:37–65, 2013.

[186] Santosh Biswas, Sudip Samanta, and Joydev Chattopadhyay. Cannibalistic predator–prey model with disease in predator—a delay model. *International Journal of Bifurcation and Chaos*, 25(10):1550130, 2015.

[187] Santosh Biswas, Sudip Samanta, Qamar JA Khan, and Joydev Chattopadhyay. Effect of multiple delays on the dynamics of cannibalistic prey–predator system with disease in both populations. *International Journal of Biomathematics*, 10(04):1750049, 2017.

[188] Santosh Biswas, Bashir Ahmad, and Subhas Khajanchi. Exploring dynamical complexity of a cannibalistic eco-epidemiological model with multiple time delay. *Mathematical methods in the Applied Sciences*, 46(4):4184–4211, 2023.

[189] Surajit Das, PS Lyla, and S Ajmal Khan. Marine microbial diversity and ecology: importance and future perspectives. *Current science*, pages 1325–1335, 2006.

[190] RP Hedrick. Relationships of the host, pathogen, and environment: implications for diseases of cultured and wild fish populations. *Journal of Aquatic Animal Health*, 10(2):107–111, 1998.

[191] Michael J Sweet, Aldo Croquer, and John C Bythell. Experimental antibiotic treatment identifies potential pathogens of white band disease in the endangered caribbean coral acropora cervicornis. *Proceedings of the Royal Society B: Biological Sciences*, 281(1788):20140094, 2014.

[192] DL Gil-Agudelo, GW Smith, and E Weil. The white band disease type ii pathogen in puerto rico. *Revista de biologia tropical*, 54:59–67, 2006.

[193] Drew Harvell, Richard Aronson, Nancy Baron, Joseph Connell, Andrew Dobson, Steve Ellner, Leah Gerber, Kiho Kim, Armand Kuris, Hamish McCallum, et al. The rising tide of ocean diseases: unsolved problems and research priorities. *Frontiers in Ecology and the Environment*, 2(7):375–382, 2004.

[194] M Travis Maynard, Deanna M Kennedy, and S Amy Sommer. Team adaptation: A fifteen-year synthesis (1998–2013) and framework for how this literature needs to "adapt" going forward. *European Journal of Work and Organizational Psychology*, 24(5):652–677, 2015.

[195] Maggy M Nugues, Garriet W Smith, Ruben J Van Hooidonk, Maria I Seabra, and Rolf PM Bak. Algal contact as a trigger for coral disease. *Ecology letters*, 7(10):919–923, 2004.

[196] Michael J Sweet, John C Bythell, and Maggy M Nugues. Algae as reservoirs for coral pathogens. *PloS one*, 8(7):e69717, 2013.

[197] Katie L Barott, Alexander A Venn, Sidney O Perez, Sylvie Tambutté, and Martin Tresguerres. Coral host cells acidify symbiotic algal microenvironment to promote photosynthesis. *Proceedings of the National Academy of Sciences*, 112(2):607–612, 2015.

[198] Robert K Trench and Rudolf J Blank. Symbiodinium microadriaticum freudenthal, s. goreauii sp. nov., s. kawagutii sp. nov. and s. pilosum sp. nov.: Gymnodinioid dinoflagellate symbionts of marine invertebrates 1. *Journal of phycology*, 23(3):469–481, 1987.

[199] Yanni Xiao and Lansun Chen. Modeling and analysis of a predator–prey model with disease in the prey. *Mathematical biosciences*, 171(1):59–82, 2001.

[200] John Guckenheimer and Philip Holmes. *Nonlinear oscillations, dynamical systems, and bifurcations of vector fields*, volume 42. Springer Science & Business Media, 2013.

[201] Christos Douskos and Panagiotis Markellos. Complete coefficient criteria for five-dimensional hopf bifurcations, with an application to economic dynamics. *Journal of Nonlinear Dynamics*, 2015(1):278234, 2015.

[202] Peter J Mumby, Nicola L Foster, and Elizabeth A Glynn Fahy. Patch dynamics of coral reef macroalgae under chronic and acute disturbance. *Coral Reefs*, 24:681–692, 2005.

[203] Robert P Dickinson and Robert J Gelinas. Sensitivity analysis of ordinary differential equation systems—a direct method. *Journal of computational physics*, 21(2):123–143, 1976.

[204] Miriam Reverter, Nathalie Tapissier-Bontemps, David Lecchini, Bernard Banaigs, and Pierre Sasal. Biological and ecological roles of external fish mucus: a review. *Fishes*, 3(4):41, 2018.

[205] Sam HC Noonan, Geoffrey P Jones, and Morgan S Pratchett. Coral size, health and structural complexity: effects on the ecology of a coral reef damselfish. *Marine Ecology Progress Series*, 456:127–137, 2012.

[206] Maggy M Nugues, L Delvoye, and Rolf PM Bak. Coral defence against macroalgae: differential effects of mesenterial filaments on the green alga halimeda opuntia. *Marine Ecology Progress Series*, 278:103–114, 2004.

[207] A Kushmaro, Y Loya, M Fine, and E Rosenberg. Bacterial infection and coral bleaching. *Nature*, 380(6573):396–396, 1996.

[208] E Banin, Y Ben-Haim, M Fine, T Israely, and E Rosenberg. Virulence mechanisms of the coral bleaching pathogen vibrio shiloi. In *Proceedings of the Ninth International Coral Reef Symposium, Bali, 23-27 October 2000,*, volume 2, pages 1261–1266, 2002.

[209] Justin Mao-Jones, Kim B Ritchie, Laura E Jones, and Stephen P Ellner. How microbial community composition regulates coral disease development. *PLoS Biology*, 8(3):e1000345, 2010.

[210] Eugene Rosenberg, Omry Koren, Leah Reshef, Rotem Efrony, and Ilana Zilber-Rosenberg. The role of microorganisms in coral health, disease and evolution. *Nature Reviews Microbiology*, 5(5):355–362, 2007.

[211] Ehud Banin, Tomer Israely, Maoz Fine, Yossi Loya, and Eugene Rosenberg. Role of endosymbiotic zooxanthellae and coral mucus in the adhesion of the coral-bleaching pathogen vibrio shiloi to its host. *FEMS Microbiology letters*, 199(1):33–37, 2001.

[212] Michael E Hibbing, Clay Fuqua, Matthew R Parsek, and S Brook Peterson. Bacterial competition: surviving and thriving in the microbial jungle. *Nature reviews microbiology*, 8(1):15–25, 2010.

[213] Reed M Stubbendieck and Paul D Straight. Multifaceted interfaces of bacterial competition. *Journal of bacteriology*, 198(16):2145–2155, 2016.

[214] Pauline Wanjugi, GA Fox, and Valerie J Harwood. The interplay between predation, competition, and nutrient levels influences the survival of escherichia coli in aquatic environments. *Microbial ecology*, 72:526–537, 2016.

[215] Lotta-Riina Sundberg, Tarmo Ketola, Elina Laanto, Hanna Kinnula, Jaana KH Bamford, Reetta Penttinen, and Johanna Mappes. Intensive aquaculture selects for increased virulence and interference competition in bacteria. *Proceedings of the Royal Society B: Biological Sciences*, 283(1826):20153069, 2016.

[216] John C Ogden and Phillip S Lobel. The role of herbivorous fishes and urchins in coral reef communities. *Environmental biology of fishes*, 3:49–63, 1978.

[217] Alistair Cheal, Michael Emslie, Ian Miller, and Hugh Sweatman. The distribution of herbivorous fishes on the great barrier reef. *Marine Biology*, 159:1143–1154, 2012.

[218] Randi D Rotjan and Sara M Lewis. Parrotfish abundance and selective corallivory on a belizean coral reef. *Journal of experimental marine biology and ecology*, 335(2):292–301, 2006.

[219] Peter J Mumby. Herbivory versus corallivory: are parrotfish good or bad for caribbean coral reefs? *Coral Reefs*, 28(3):683–690, 2009.

[220] Darren J Coker, Shaun K Wilson, and Morgan S Pratchett. Importance of live coral habitat for reef fishes. *Reviews in Fish Biology and Fisheries*, 24:89–126, 2014.

[221] Barry Goldman, Frank Hamilton Talbot, OA Jones, and R Endean. Aspects of the ecology of coral reef fishes. *Biology and geology of coral reefs*, 3:125–154, 1976.

[222] Mohsen Kayal, Julie Vercelloni, Thierry Lison de Loma, Pauline Bosserelle, Yannick Chancerelle, Sylvie Geoffroy, Céline Stievenart, François Michonneau, Lucie Penin, Serge Planes, et al. Predator crown-of-thorns starfish (acanthaster planci) outbreak, mass mortality of corals, and cascading effects on reef fish and benthic communities. *PLoS One*, 2012.

[223] Lulu Wang, Zhen Jin, and Hao Wang. A switching model for the impact of toxins on the spread of infectious diseases. *Journal of Mathematical Biology*, 77:1093–1115, 2018.

[224] Arnab Chattopadhyay, Swarnendu Banerjee, Amit Samadder, and Sabyasachi Bhattacharya. Is toxicity a curse or blessing, or both?—searching answer from a disease-induced consumer-resource system. *Ecological Modelling*, 486:110534, 2023.

[225] Annick Dhooge, Willy Govaerts, and Yu A Kuznetsov. Matcont: a matlab package for numerical bifurcation analysis of odes. *ACM SIGSAM Bulletin*, 38(1):21–22, 2004.

[226] Richard B Aronson, William F Precht, Thaddeus JT Murdoch, and Martha L Robbart. Long-term persistence of coral assemblages on the flower garden banks, northwestern gulf of mexico: implications for science and management. *Gulf of Mexico Science*, 23(1):6, 2005.

[227] Curtis M Lively. The ecology of virulence. *Ecology Letters*, 9(10):1089–1095, 2006.

[228] Frank M Hilker and Kirsten Schmitz. Disease-induced stabilization of predator–prey oscillations. *Journal of Theoretical Biology*, 255(3):299–306, 2008.

[229] Michael Sieber, Horst Malchow, and Frank M Hilker. Disease-induced modification of prey competition in eco-epidemiological models. *Ecological complexity*, 18:74–82, 2014.

[230] Iulia Martina Bulai and Frank M Hilker. Eco-epidemiological interactions with predator interference and infection. *Theoretical Population Biology*, 130:191–202, 2019.

[231] Paul Van den Driessche and James Watmough. Further notes on the basic reproduction number. *Mathematical epidemiology*, pages 159–178, 2008.

[232] Pauline Van den Driessche. Reproduction numbers of infectious disease models. *Infectious disease modelling*, 2(3):288–303, 2017.

[233] Thomas J Goreau, James Cervino, Maya Goreau, Raymond Hayes, Marshall Hayes, Laurie Richardson, Garriet Smith, Kalli DeMeyer, Ivan Nagelkerken, Jaime Garzon-Ferrera, et al. Rapid spread of diseases in caribbean coral reefs. *Revista de biología tropical*, 46(S5):157–171, 1998.

[234] Bette L Willis, Cathie A Page, and Elizabeth A Dinsdale. Coral disease on the great barrier reef. In *Coral health and disease*, pages 69–104. Springer, 2004.

[235] A Halford, AJ Cheal, D Ryan, and D McB Williams. Resilience to large-scale disturbance in coral and fish assemblages on the great barrier reef. *Ecology*, 85(7):1892–1905, 2004.

[236] Laurie J Raymundo, Andrew R Halford, Aileen P Maypa, and Alexander M Kerr. Functionally diverse reef-fish communities ameliorate coral disease. *Proceedings of the National Academy of Sciences*, 106(40):17067–17070, 2009.

[237] Jordan M Casey, Tracy D Ainsworth, J Howard Choat, and Sean R Connolly. Farming behaviour of reef fishes increases the prevalence of coral disease associated microbes and black band disease. *Proceedings of the Royal Society B: Biological Sciences*, 281(1788):20141032, 2014.

[238] Andrew M Bate and Frank M Hilker. Complex dynamics in an eco-epidemiological model. *Bulletin of mathematical biology*, 75:2059–2078, 2013.

[239] Frank M Hilker, Michel Langlais, and Horst Malchow. The allee effect and infectious diseases: extinction, multistability, and the (dis-) appearance of oscillations. *The American Naturalist*, 173(1):72–88, 2009.

List of publications related to thesis

Published

i. **Buddhadev Ranjit**, Santosh Biswas, Joydeb Bhattacharyya, and Joydev Chattopadhyay. "Dynamics of Zooplankton-Mediated Disease Outbreak in Coral-reef." *Differential Equations and Dynamical Systems* **33**, 565–593 (2025).

ii. **Buddhadev Ranjit**, Arnab Chattopadhyay, Arindam Mandal, Santosh Biswas, and Joydev Chattopadhyay. "Beyond predation: Fish–coral interactions can tip the scales of coral disease." *Journal of Theoretical Biology* **599** (2025): 112031.

Communicated

i. **Buddhadev Ranjit**, Joydeb Chattopadhyay & Santosh Biswas, Coral Disease And Recovery Dynamics: A Mathematical Model Apporach.

ii. Santosh Biswas, **Buddhadev Ranjit**, Saddam Mollah, Joydev Chattopadhyay, Subhas Khajanchi & Bashir Ahmad, Effect of delay on coral reef ecosystem with disease presence in coral species .